



Swansea University
Prifysgol Abertawe



Swansea University E-Theses

Analysis of agrochemical compounds and related impurities by chromatographic-mass spectrometric methods.

Haggerty, Karen

How to cite:

Haggerty, Karen (2001) *Analysis of agrochemical compounds and related impurities by chromatographic-mass spectrometric methods..* thesis, Swansea University.
<http://cronfa.swan.ac.uk/Record/cronfa42684>

Use policy:

This item is brought to you by Swansea University. Any person downloading material is agreeing to abide by the terms of the repository licence: copies of full text items may be used or reproduced in any format or medium, without prior permission for personal research or study, educational or non-commercial purposes only. The copyright for any work remains with the original author unless otherwise specified. The full-text must not be sold in any format or medium without the formal permission of the copyright holder. Permission for multiple reproductions should be obtained from the original author.

Authors are personally responsible for adhering to copyright and publisher restrictions when uploading content to the repository.

Please link to the metadata record in the Swansea University repository, Cronfa (link given in the citation reference above.)

<http://www.swansea.ac.uk/library/researchsupport/ris-support/>

**ANALYSIS OF AGROCHEMICAL COMPOUNDS AND RELATED
IMPURITIES BY CHROMATOGRAPHIC–MASS SPECTROMETRIC
METHODS**

Karen Haggerty BSc. (Hons)

*A thesis submitted in fulfilment of the requirements for the degree of Doctor of
Philosophy in the University of Wales*

Mass Spectrometry Research Unit, University of Wales Swansea

June 2001



ProQuest Number: 10807453

All rights reserved

INFORMATION TO ALL USERS

The quality of this reproduction is dependent upon the quality of the copy submitted.

In the unlikely event that the author did not send a complete manuscript and there are missing pages, these will be noted. Also, if material had to be removed, a note will indicate the deletion.



ProQuest 10807453

Published by ProQuest LLC (2018). Copyright of the Dissertation is held by the Author.

All rights reserved.

This work is protected against unauthorized copying under Title 17, United States Code
Microform Edition © ProQuest LLC.

ProQuest LLC.
789 East Eisenhower Parkway
P.O. Box 1346
Ann Arbor, MI 48106 – 1346

DECLARATION

This work has not previously been accepted in substance for any degree and is not being concurrently submitted in candidature for any degree.

Signed (Candidate)

Date 15-FEB-02

STATEMENT 1

This thesis is the result of my own investigations, except where otherwise stated. Other sources are acknowledged by footnotes giving explicit references. A bibliography is appended.

Signed (Candidate)

Date 15-FEB-02

Signed (Supervisor)

Date

STATEMENT 2

I hereby give consent for my thesis, if accepted, to be available for photocopying and for inter-library loan, and for the title and summary to be made available to outside organisations.

Signed (Candidate)

Date 15-FEB-02

SUMMARY

Agrochemicals and pesticides are compounds of significant industrial and commercial importance. Over recent years, legislation has increased greatly and with this increased regulation, the necessity for trace impurity analysis of pesticides has grown. Modern chromatographic techniques with both UV and mass spectrometric detection have been used in the study of pesticidal compounds to separate and characterise impurities present at low levels. The use of these techniques is evaluated and suggestions for future work are outlined.

The use and analysis of the pesticidal study compounds are reviewed and the instrumental techniques of capillary electrophoresis (CE), mass spectrometry (MS) and high performance liquid chromatography (HPLC) are described.

The quaternary ammonium herbicide Paraquat is amongst the most widely used herbicidal products worldwide. The technique of capillary zone electrophoresis (CZE) was evaluated as a means of separating paraquat from a mixture of related impurity compounds. The preconcentration technique of transient capillary isotachopheresis (tCITP) was examined as a means of improving detection limits. Both CZE and tCITP were used successfully in the analysis of technical paraquat. CE-MS was performed with varying levels of success.

Flutriafol is a fungicidal compound widely used in the control of cereal diseases. HPLC methodology was developed for use in the separation of flutriafol from a mixture of related impurity compounds. The technique was successfully used in the analysis of a sample of production material with over 25 impurity peaks detected. HPLC-MS was performed and the use of SIM, SRM and CRM were investigated as a means of improving detection limits. HPLC-MS was used in the analysis of a production sample and over twenty peaks were detected in the total ion chromatogram (TIC). The mass spectral information obtained enabled the tentative identification of a number of impurities.

ACKNOWLEDGEMENTS

I would like to thank Professor Games for offering me a place in his group and introducing me to the fields of chromatography and mass spectrometry. I gratefully acknowledge the financial assistance of the EPSRC and Zeneca Agrochemicals and the funding provided by the BMSS and SCI, which enabled me to attend mass spectrometry conferences and broaden my knowledge of the subject.

My thanks also go to my colleagues at in the QC and ADG departments at Rhodia ChiRex for their encouragement and advice during the writing of this thesis.

Special thanks to my friends and colleagues in the MSRU, Cathy, Kate, Nadine, Siân, Alec, Gong, Qiu, Eileen and Brian for all their help during my time in Swansea.

Most of all I thank Michael and my parents, without their support and invaluable assistance I could not have completed this thesis.

For my parents.

Table of Contents

	Page
Table of Contents	i
List of Figures	vi
List of Tables	xv
List of Equations	xviii
Abbreviations	xix
Chapter 1 Pesticides	1
1.1 Introduction	2
1.2 Classification of pesticides	2
1.2.1 Non-systemic pesticides	2
1.2.2 Systemic pesticides	2
1.2.3 Herbicides	3
1.2.4 Fungicides	4
1.2.5 Insecticides	5
1.3 An historical overview of developments in pesticide science	5
1.4 Environmental concerns and the need for analysis	8
1.5 The study compounds	9
1.5.1 Paraquat	9
1.5.1.1 Mode of action	11
1.5.1.2 Herbicidal applications	12
1.5.1.3 Toxicology and the environment	12
1.5.1.4 Analysis	13
1.5.2 Flutriafol	16
1.5.2.1 Mode of action	17
1.5.2.2 Fungicidal applications	19
1.5.2.3 Toxicology and the environment	19
1.5.2.4 Analysis	20
References cited in Chapter 1	22

Chapter 2	Mass Spectrometry	30
2.1	Introduction	31
2.2	Ionisation techniques	31
2.2.1	Atmospheric pressure ionisation (API)	31
2.2.1.1	Electrospray ionisation (ESI)	32
2.2.1.2	Atmospheric pressure chemical ionisation (APCI)	35
2.3	Mass analysers	36
2.3.1	Quadrupole ion trap	37
2.3.2	Quadrupole mass analysers	39
2.4	Ion detection systems	41
2.4.1	Electron multipliers	41
2.4.1.1	Discrete dynode electron multipliers	42
2.4.1.2	Continuous dynode electron multipliers	42
2.5	The LCQ – instrumentation and operation	43
2.5.1	The API source	44
2.5.1.1	The ESI probe assembly	44
2.5.1.2	The APCI probe assembly	45
2.5.1.3	The API stack	46
2.5.1.4	Ion optics	47
2.5.2	The mass analyser	48
2.5.3	The ion detection system	49
2.6	Scan modes	51
2.6.1	Full scan MS	51
2.6.2	Full scan MS/MS	51
2.6.3	Full scan MS ⁿ	51
2.6.4	Selected ion monitoring (SIM)	52
2.6.5	Selected reaction monitoring (SRM)	52
2.6.6	Consecutive reaction monitoring (CRM)	53
2.6.7	ZoomScan™	53
	References cited in Chapter 2	54

Chapter 3	CE and CE-MS Studies of Paraquat and Related Impurities	56
3.1	Objective	57
3.2	Introduction	59
3.3	Electrophoretic theory	60
	3.3.1 Efficiency	64
	3.3.2 Resolution	67
3.4	Instrumentation	68
	3.4.1 Sample introduction	69
	3.4.1.1 Hydrodynamic injection	70
	3.4.1.2 Electrokinetic injection	71
	3.4.1.3 Other methods of injection	72
	3.4.2 Detection	73
	3.4.2.1 UV-visible absorbance detection	74
	3.4.2.2 Mass spectrometric detection	76
	3.4.2.2.1 Coaxial ESI interface	77
	3.4.2.3 Other methods of detection	78
3.5	Modes of capillary electrophoresis	80
	3.5.1 Capillary zone electrophoresis (CZE)	80
	3.5.1.1 Buffer selection	81
	3.5.1.2 Applications	82
	3.5.2 Capillary isotachopheresis (CITP)	83
	3.5.3 Capillary gel electrophoresis (CGE)	85
	3.5.4 Micellar electrokinetic capillary chromatography (MECC)	85
	3.5.5 Capillary isoelectric focussing (CIEF)	86
	3.5.6 Capillary electrochromatography (CEC)	87
3.6	Results and discussion	88
	3.6.1 CZE of paraquat and its impurities	88
	3.6.1.1 Variation of injection mode	94
	3.6.1.1.1 Hydrodynamic injection	94
	3.6.1.1.2 Electrokinetic injection	96
	3.6.1.2 Variation of buffer concentration	99
	3.6.1.3 Effect of applied voltage on the separation	105

3.6.1.4	Effect of organic modifier content on the separation	108
3.6.1.5	Limit of detection (LOD) and limit of quantitation (LOQ)	110
3.6.1.6	CZE of technical paraquat	111
3.6.2	tCITP of paraquat and impurities	114
3.6.2.1	Transient CITP	114
3.6.2.2	Effect of injection type and time on the separation	120
3.6.2.3	Effect of buffer concentration on the separation	123
3.6.2.4	Effect of capillary type on reproducibility and the separation	123
3.6.2.5	Linearity	129
3.6.2.6	Limit of detection (LOD) and limit of quantitation (LOQ)	130
3.6.2.7	tCITP of technical paraquat	131
3.6.3	CE-MS of paraquat and impurities	136
3.6.3.1	CZE-MS of paraquat and impurities	138
3.6.3.1.1	Variation of methanol content	146
3.6.3.1.2	Limit of detection (LOD) and limit of quantitation (LOQ)	155
3.6.3.1.3	CZE-MS of technical paraquat	156
3.6.3.2	tCITP-MS of paraquat and impurities	159
3.6.4	Conclusion	161
References cited in Chapter 3		167
Chapter 4	HPLC and HPLC-MS Studies of Flutriafol and Related Impurities	174
4.1	Objective	175
4.2	Introduction	177
4.3	Chromatographic theory	178
4.4	High performance liquid chromatography (HPLC)	182
4.5	Instrumentation	182
4.5.1	Mobile phase	184

4.5.2	Pumps	184
4.5.3	Sample injection	185
4.5.4	Columns	185
4.5.5	Detectors	186
4.5.5.1	UV-visible absorbance detection	187
4.5.5.2	Mass spectrometric detection	188
4.6	Column packings and mode of operation	191
4.6.1	Normal phase HPLC	191
4.6.2	Reversed-phase HPLC	192
4.6.3	Other modes of HPLC	193
4.7	Results and discussion	194
4.7.1	HPLC of flutriafol and related impurities	194
4.7.1.1	Effect of column length and particle size	202
4.7.1.2	Limit of detection (LOD) and limit of quantitation (LOQ)	206
4.7.1.3	Analysis of flutriafol technical material	207
4.7.2	HPLC-MS of flutriafol and related impurities	211
4.7.2.1	HPLC-APCI-MS	211
4.7.2.2	HPLC-ESI-MS	211
4.7.2.3	Comparison of ionisation modes	212
4.7.2.4	Limits of detection (LOD) for flutriafol and related impurities	219
4.7.2.5	Tandem Mass Spectrometry (MS ⁿ)	223
4.7.2.6	HPLC-MS of the seven component standard mixture	229
4.7.2.7	HPLC-MS of flutriafol technical material	233
4.8	Conclusion	243
	References cited in Chapter 4	248
Chapter 5	Experimental Details	251
5.1	Chapter 3	252
5.2	Chapter 4	255

List of Figures

	Page	
Chapter 1		
Figure 1.1	Worldwide pesticide sales by type 1960 - 1993	4
Figure 1.2	Growth in worldwide pesticide sales 1960 - 1993	7
Figure 1.3	Breakdown of new product costs from invention to launch	8
Figure 1.4	Structure of paraquat dichloride	9
Figure 1.5	Synthesis of paraquat	10
Figure 1.6	Electron delocalisation in paraquat	11
Figure 1.7	Structure of flutriafol	16
Figure 1.8	General formula of the triazole fungicides	16
Figure 1.9	General formulae of compounds used in the preparation of triazole fungicides	17
Figure 1.10	Schematic representation of the proposed mode of action of C-14 demethylation inhibitors	18
Chapter 2		
Figure 2.1	Schematic representation of the components of a mass spectrometer	30
Figure 2.2	Schematic representation of the electrospray ionisation process	33
Figure 2.3	Schematic representation of the essential features of an electrospray interface	34
Figure 2.4	Schematic representation of the APCI process in positive ion mode	36
Figure 2.5	Schematic representation of an ion trap mass analyser	37

Figure 2.6	Schematic representation of a quadrupole mass analyser	40
Figure 2.7	Schematic representation of a discrete dynode electron multiplier	42
Figure 2.8	Schematic representation of a continuous dynode electron multiplier	43
Figure 2.9	Cross sectional view of the Finnigan LCQ ESI probe assembly	45
Figure 2.10	Schematic representation of the Finnigan LCQ APCI probe assembly	46
Figure 2.11	Schematic representation of the Finnigan LCQ API stack	47
Figure 2.12	Cross sectional view of the Finnigan LCQ mass analyser	48
Figure 2.13	Schematic representation of the Finnigan LCQ ion detection system	50
Chapter 3		
Figure 3.1	Graphical representation of the trend in the use of CE for pesticide analysis 1981 –2000	57
Figure 3.2	Differential solute migration in capillary electrophoresis	61
Figure 3.3	Schematic representation of double layer formation in capillary electrophoresis	62
Figure 3.4	Schematic representation of the electroosmotic flow (EOF) profile generated in capillary electrophoresis	63
Figure 3.5	A two component electropherogram showing the definitions of various parameters	65
Figure 3.6	Instrumental set up of a capillary electrophoresis system	68
Figure 3.7	Schematic representation of a variable wavelength UV-Vis detector	75

Figure 3.8	Schematic representation of the coaxial electrospray interface for CE-MS developed by RD Smith et al	78
Figure 3.9	Electropherogram of a six component paraquat mixture at 30kV applied voltage, 20mM ammonium acetate buffer pH 3.7, 8 second pressure injection (CZE-UV)	89
Figure 3.10	Electropherogram of a six component paraquat mixture at 15kV applied voltage, 10mM sodium acetate buffer pH 4.0 with 100mM sodium chloride, 15 second voltage (10kV) injection (CZE-UV)	91
Figure 3.11	Cumulative efficiency of paraquat and impurities versus applied voltage and temperature for paraquat and impurities using 10mM sodium acetate buffer pH 4.0 with 100mM sodium chloride, 15 second voltage (10kV) injection	92
Figure 3.12	Resolution versus applied voltage and temperature for paraquat and impurities using 10mM sodium acetate buffer pH 4.0 with 100mM sodium chloride, 15 second voltage (10kV) injection	93
Figure 3.13	Electropherogram of a six component paraquat mixture using 30kV applied voltage, 20mM ammonium acetate buffer pH 3.7, 15 second pressure injection (CZE-UV)	94
Figure 3.14	Linearity of response for paraquat using pressure injections of varying lengths	95
Figure 3.15	Efficiency of paraquat versus hydrodynamic injection time	96
Figure 3.16	Electropherogram of a six component paraquat mixture using 30kV applied voltage, 20mM ammonium acetate buffer pH 3.7, 15 second voltage (10kV) injection (CZE-UV)	97
Figure 3.17	Linearity of response for paraquat using voltage (10kV) injections of varying lengths	98
Figure 3.18	Efficiency of paraquat versus electrokinetic injection time	99

Figure 3.19	Migration times of paraquat and impurities versus ammonium acetate buffer concentration	100
Figure 3.20	Cumulative efficiency of paraquat and impurities versus ammonium acetate buffer concentration	101
Figure 3.21	Resolution of paraquat and impurities versus ammonium acetate buffer concentration	103
Figure 3.22	Electropherogram of a six component paraquat mixture using 15kV applied voltage, 100mM ammonium acetate buffer pH 4.0, 10 second voltage (10kV) injection, 30°C (CZE-UV)	104
Figure 3.23	Migration times of paraquat and impurities versus applied voltage	105
Figure 3.24	Cumulative efficiency of paraquat and impurities versus applied voltage	106
Figure 3.25	Resolution of paraquat and impurities versus applied voltage	107
Figure 3.26	Migration times of paraquat and impurities versus percentage methanol content of buffer	108
Figure 3.27	Cumulative efficiency of paraquat and impurities versus percentage methanol content of buffer	109
Figure 3.28	Resolution of paraquat and impurities versus percentage methanol content of buffer	110
Figure 3.29	Electropherogram of a six component paraquat mixture using 20kV applied voltage, 100mM ammonium acetate buffer + 10% methanol, pH 4.0, 10 second voltage (10kV) injection, 30°C (CZE-UV)	111
Figure 3.30	Electropherogram of a sample of technical paraquat using 15kV applied voltage, 100mM ammonium acetate buffer + 10% methanol, pH 4.0, 10 second voltage (10kV) injection, 30°C (CZE-UV)	113

Figure 3.31	(a) Terminating Electrolyte: 100mM β -Alanine, 90 second pressure injection	118
	(b) Terminating Electrolyte: 100mM β -Alanine, 90 second voltage (10kV) injection	118
	(c) Terminating Electrolyte: 100mM Ammediol, 90 second voltage (10kV) injection	119
	(d) Terminating Electrolyte: 100mM Tris, 90 second voltage (10kV) injection	119
	(e) Terminating Electrolyte: 100mM Tetramethylammonium, 90 second pressure injection	120
	(f) Terminating Electrolyte: 100mM Diethylammonium, 90 second pressure injection	120
Figure 3.32	Cumulative efficiency of paraquat and impurities versus injection type and time	121
Figure 3.33	Effect of capillary type on migration time	125
Figure 3.34	Effect of capillary type on peak efficiency	128
Figure 3.35	Effect of capillary type on resolution	129
Figure 3.36	Linearity of response for each of the six study compounds	130
Figure 3.37	Electropherogram of a sample of technical paraquat using 15kV applied voltage, LE: 100mM ammonium acetate buffer, TE: 100mM β -Alanine pH 4.0, 90 second pressure injection, 30°C (tCITP-UV)	134
Figure 3.38	(a) Mass spectrum of paraquat obtained under CZE-MS conditions	140
	(b) Mass spectrum of 2,2-paraquat obtained under CZE-MS conditions	140
	(c) Mass spectrum of n-methyl pyridinium obtained under CZE-MS conditions	141
	(d) Mass spectrum of monoquat obtained under CZE-MS conditions	141

	(e) Mass spectrum of 4,4-bipyridyl obtained under CZE-MS conditions	142
	(f) Mass spectrum of 2,2-bipyridyl obtained under CZE-MS conditions	142
Figure 3.39	Proposed mechanism for the deprotonation of the paraquat [Cat] ²⁺ ion	144
Figure 3.40	Effect of methanol content of buffer on response	147
Figure 3.41	(a) TIE of a 50ppm six component paraquat standard using a 100mM ammonium acetate buffer containing 5% methanol and using a CE voltage of 20kV (CZE-MS)	148
	(b) Mass electropherograms of a 50ppm six component paraquat standard using a 100mM ammonium acetate buffer containing 5% methanol and using a CE voltage of 20kV (CZE-MS)	148
Figure 3.42	Migration times of paraquat and impurities versus methanol content of buffer	151
Figure 3.43	Cumulative efficiency of paraquat and impurities versus methanol content of buffer	151
Figure 3.44	Resolution of paraquat and impurities versus methanol content of buffer	152
Figure 3.45	(a) TIE of a six component paraquat mixture using 50mM ammonium acetate buffer containing 10% methanol and a CE voltage of 20kV	154
	(b) Mass electropherograms of a six component paraquat mixture using 50mM ammonium acetate buffer containing 10% methanol and a CE voltage of 20kV	154
Figure 3.46	(a) TIE for a sample of technical paraquat diluted by a factor of 100 obtained under CZE-MS conditions	157

	(b) Mass electropherograms for a sample of technical paraquat diluted by a factor of 100 obtained under CZE-MS conditions	157
Figure 3.47	Mass electropherograms of a six component paraquat mixture obtained using tCITP-MS conditions	160
Chapter 4		
Figure 4.1	A two component chromatogram showing the definitions of various parameters	178
Figure 4.2	Schematic representation of the essential components in an HPLC instrument	183
Figure 4.3	HPLC chromatogram of a seven component flutriafol standard mixture obtained using solvent system 9 (Table 4.4)	197
Figure 4.4	HPLC chromatogram of a seven component flutriafol standard mixture obtained using solvent system 8 (Table 4.4)	198
Figure 4.5	(a) HPLC chromatogram of a seven component flutriafol standard mixture obtained using gradient programme 1 (Table 4.6)	200
	(b) HPLC chromatogram of a seven component flutriafol standard mixture obtained using gradient programme 2 (Table 4.6)	201
	(c) HPLC chromatogram of a seven component flutriafol standard mixture obtained using gradient programme 3 (Table 4.6)	201
Figure 4.6	(a) HPLC chromatogram of a seven component flutriafol standard mixture obtained using a 10cm, 3 μ m Hypersil ODS column and gradient outlined in Table 4.8	205
	(b) HPLC chromatogram of a seven component flutriafol standard mixture obtained using a 10cm, 5 μ m Hypersil ODS column and gradient outlined in Table 4.8	206

Figure 4.7	HPLC chromatogram for a 20 μ l injection of a 2000ppm sample of technical flutriafol obtained using gradient programme 3 (Table 4.6)	208
Figure 4.8	(a) Mass spectrum of 2,2'-difluoro isomer obtained under HPLC-MS conditions in positive mode APCI	215
	(b) Mass spectrum of triazol-4-yl obtained under HPLC-MS conditions in positive mode APCI	215
	(c) Mass spectrum of flutriafol obtained under HPLC-MS conditions in positive mode APCI	216
	(d) Mass spectrum of methyl tertiary alcohol obtained under HPLC-MS conditions in positive mode APCI	216
	(e) Mass spectrum of 2,4'-difluorobenzophenone obtained under HPLC-MS conditions in positive mode APCI	217
	(f) Mass spectrum of bromoalkene (trans) obtained under HPLC-MS conditions in negative mode APCI	217
Figure 4.9	(a) Linearity of response for 2,2'-Difluoro Isomer in APCI positive mode	221
	(b) Linearity of response for Triazol-4-yl in APCI positive mode	221
	(c) Linearity of response for Flutriafol in APCI positive mode	222
	(d) Linearity of response for Methyl Tertiary Alcohol in APCI positive mode	222
Figure 4.10	(a) Proposed mechanism for the fragmentation of 2,2'-difluoro isomer	224
	(b) Proposed mechanism for the fragmentation of triazol-4-yl	225
	(c) Proposed mechanism for the fragmentation of flutriafol	226
	(d) Proposed mechanism for the fragmentation of methyl tertiary alcohol	227

Figure 4.11	(a) TIC for a seven component flutriafol standard mixture obtained under HPLC-MS conditions in positive mode APCI	230
	(b) Mass chromatograms for a seven component flutriafol standard mixture obtained under HPLC-MS conditions in positive mode APCI	231
Figure 4.12	(a) TIC for sample of flutriafol technical material obtained under HPLC-MS conditions in positive mode APCI	236
	(b) Mass chromatograms for a sample of flutriafol technical material obtained under HPLC-MS conditions in positive mode APCI	237-239

List of Tables

	Page
Chapter 3	
Table 3.1 Structures of paraquat and related impurities studied in Chapter 3	58
Table 3.2 Summary of methods used to reduce EOF in CE	64
Table 3.3 Comparison of the detection limits of some widely used CE detection techniques	79
Table 3.4 An overview of capillary electrophoresis modes	80
Table 3.5 Composition of paraquat standard mixture	90
Table 3.6 Data for Figures 3.11 and 3.12	92
Table 3.7 Repeatability of injection - data for paraquat using hydrodynamic sample introduction	95
Table 3.8 Repeatability of injection - data for paraquat using electrokinetic sample introduction	98
Table 3.9 Limits of detection and quantitation for each of the six study compounds using the tCITP method	112
Table 3.10 Migration times and tentative peak assignments for peaks detected in a sample of Technical Paraquat using CZE-UV	114
Table 3.11 Mobility data for cations used as leading and terminating electrolytes used in preliminary tCITP experiments	116
Table 3.12 Comparison of resolution data obtained using pressure and voltage injections	123
Table 3.13 Comparison of migration time reproducibility data obtained using different capillaries	126
Table 3.14 Comparison of peak area reproducibility data obtained using different capillaries	127

Table 3.15	Correlation coefficients for the data shown in Figure 3.36	131
Table 3.16	Limits of detection and quantitation for each of the six study compounds using the tCITP method	131
Table 3.17	Injection volumes calculated using ‘CE Expert’	132
Table 3.18	Migration times and tentative peak assignments for peaks detected in a sample of Technical Paraquat using tCITP-UV	134
Table 3.19	Approximate composition of Technical Paraquat sample	135
Table 3.20	Summary of CZE-MS data for each of the study compounds	143
Table 3.21	CZE-MS/MS data for paraquat and 2,2-paraquat	145
Table 3.22	Migration time, efficiency and resolution data for Figures 3.42, 3.43 and 3.44	150
Table 3.23	Limits of detection and quantitation for each of the six study compounds using CZE-MS in full scan mode	155
Table 3.24	Limits of detection and quantitation for each of the six study compounds using CZE-MS in single ion monitoring (SIM) mode	155
Table 3.25	Summary of CZE-MS data for Technical Paraquat sample	158
Chapter 4		
Table 4.1	Structures of flutriafol and related impurities studied in Chapter 4	176
Table 4.2	Composition of flutriafol standard mixture	195
Table 4.3	Summary of isocratic solvent compositions examined	196
Table 4.4	Comparison of resolution data obtained for isocratic solvent systems	197
Table 4.5	Key to peak assignments in sample chromatograms	198
Table 4.6	Summary of gradient elution programmes examined	199

Table 4.7	Comparison of resolution and efficiency data for gradient elution systems 1-3	200
Table 4.8	Gradient programmes used with 10cm Hypersil ODS columns	203
Table 4.9	Comparison of resolution and efficiency data obtained for each of the 10cm columns investigated	204
Table 4.10	Limits of detection and quantitation for each of the seven study compounds using HPLC with UV detection	207
Table 4.11	Area percent impurity profile of a sample of technical flutriafol	209
Table 4.12	Comparison of HPLC-APCI-MS and HPLC-ESI-MS	213
Table 4.13	Summary of HPLC-MS data for each of the study compounds	218
Table 4.14	Limits of detection (LOD) for flutriafol and related impurities by HPLC-MS	219
Table 4.15	Linear regression coefficients for data in Figures 4.9(a)-(d)	220
Table 4.16	Summary of collision energies required and fragments generated in MS ⁿ experiments	223
Table 4.17	Limits of detection (LOD) for flutriafol and related impurities by HPLC-MS using SRM and CRM	228
Table 4.18	Summary of mass spectral data obtained for flutriafol technical material in positive mode APCI	235

List of Equations

	Page	
Chapter 3		
Equation 3.1	Experimental determination of electrophoretic mobility	60
Equation 3.2	Electrophoretic mobility	60
Equation 3.3	Velocity of EOF	63
Equation 3.4	Column efficiency	65
Equation 3.5	Column efficiency	65
Equation 3.6	Resolution	67
Equation 3.7	Poiseuille's Equation	70
Equation 3.8	Determination of hydrostatic pressure	71
Equation 3.9	Determination of sample loading using electrophoretic injection	72
Equation 3.10	Beer-Lambert equation	74
Equation 3.11	Relationship between velocity and mobility	83
Equation 3.12	Theoretical efficiency as a function of applied voltage and electroosmotic mobility	102
Equation 3.13	Relationship between migration time and applied voltage	106
Equation 3.14	Calculation of limit of detection (LOD)	112
Equation 3.15	Calculation of limit of quantitation (LOQ)	112
Equation 3.16	Calculation of sample concentration ($\mu\text{g/ml}$)	135
Chapter 4		
Equation 4.1	Adjusted retention time	174
Equation 4.2	Capacity factor	174
Equation 4.3	Efficiency	180
Equation 4.4	Efficiency	180
Equation 4.5	Theoretical plate height	180
Equation 4.6	Chromatographic resolution	181

Abbreviations

22BP	2,2-Bipyridyl
22PQ	2,2-Paraquat
44BP	4,4-Bipyridyl
APCI	Atmospheric Pressure Chemical Ionisation
API	Atmospheric Pressure Ionisation
AU	Absorbance Unit
BIDS	Bath Information Data Service
CAD	Collisionally Activated Dissociation
ce	Collision Energy
CE	Capillary Electrophoresis
CEC	Capillary Electrochromatography
CE-MS	Capillary Electrophoresis – Mass Spectrometry
CF-FAB	Continuous Flow – Fast Atom Bombardment
CGE	Capillary Gel Electrophoresis
CI	Chemical Ionisation
CITP	Capillary Isotachophoresis
CLC	Capillary Liquid Chromatography
cmc	Critical Micelle Concentration
CRM	Continuous Reaction Monitoring
CZE	Capillary Zone Electrophoresis
DAD	Diode Array Detector
dc	Direct Current
DDT	Dichlorodiphenyltrichloroethane
DLI	Direct Liquid Introduction
DMI	Demethylation Inhibitor
DNA	Deoxyribonucleic Acid

EI	Electron Ionisation
EOF	Electroosmotic Flow
ESI	Electrospray Ionisation
FAB	Fast Atom Bombardment
FSCE	Free Solution Capillary Electrophoresis
GC	Gas Chromatography
GC-MS	Gas Chromatography – Mass Spectrometry
GPC	Gel Permeation Chromatography
HFBA	Heptafluorobutyric Acid
HPLC	High Performance Liquid Chromatography
HPLC-MS	High Performance Liquid Chromatography – Mass Spectrometry
i.d.	Internal diameter
IC	Ion Chromatography
IEC	Ion Exchange Chromatography
ITP	Isotachopheresis
IUPAC	International Union of Pure and Applied Chemistry
LC	Liquid Chromatography
LC-MS	Liquid Chromatography – Mass Spectrometry
LE	Leading Electrolyte
LOD	Limit of Detection
LOQ	Limit of Quantitation
m/z	Mass to charge ratio
MALDI	Matrix Assisted Laser Desorption Ionisation
mAU	Milliabsorbance Unit
MECC	Micellar Electrokinetic Capillary Chromatography
mM	Millimolar
MQ	Monoquat
MS	Mass Spectrometry
N/A	Not Applicable
NMP	N-Methyl Pyridinium

o.d.	Outer diameter
ODS	Octadecylsilica
PC	Paper Chromatography
PEEK	Polyetheretherketone
pI	Isoelectric Point
ppb	Parts Per Billion
ppm	Parts Per Million
PQ	Paraquat
PTFE	Polytetrafluoroethylene
RF	Radio Frequency
RI	Refractive Index
RRT	Relative Retention Time
RSD	Relative Standard Deviation
R _s	Resolution
RT	Retention Time
S/N	Signal to Noise Ratio
SDS	Sodium Dodecyl Sulphate
SIM	Single Ion Monitoring
SPE	Solid Phase Extraction
SRM	Single Reaction Monitoring
tCITP	Transient Capillary Isotachopheresis
TE	Terminating Electrolyte
TIC	Total Ion Chromatogram
TIE	Total Ion Electropherogram
TLC	Thin Layer Chromatography
TOF	Time Of Flight
TSP	Thermospray
UV	Ultra Violet
VWD	Variable Wavelength Detector

Chapter 1

Pesticides

1.1 – INTRODUCTION

A pesticide is any substance or mixture of substances intended to prevent, destroy, repel, attract or mitigate any pest [1]. Although the term encompasses a great number of classes of compounds, ranging from household disinfectants to the chemicals used to protect the hulls of ships from barnacles, this brief overview will discuss only the three major classes of pesticide; herbicides, fungicides and insecticides.

1.2 – CLASSIFICATION OF PESTICIDES

Pesticides are generally classified according to the type of organism they are intended to control and also according to their mode of action as systemic and non-systemic (contact) pesticides.

1.2.1 - Non-Systemic Pesticides

Non-systemic, also known as contact or surface, pesticides can be defined as those which act on contact with the surface of the organism and tend to remain at the point of application. Until the 1960s the majority of pesticides were non-systemic in their behaviour and although many are still widely used they suffer from the disadvantage of being open to the elements and as a consequence repeated application is necessary to maintain protection.

1.2.2 - Systemic Pesticides

Systemic pesticides act by penetrating the plant's tissues via the roots or the leaf cuticle and are translocated throughout the vascular system. Because the chemical comes into such close contact with the plant's tissues the selectivity of

toxicity is of vital importance as both host and pest are plants. Unlike contact pesticides they remain unaffected by weathering and are able to effectively maintain protection over long periods of time.

1.2.3 - Herbicides

Herbicides, more commonly known as weedkillers, are those pesticides used to control the growth of unwanted vegetation, primarily to allow more efficient growth in farmed areas, but also to clear weed growth from more urban areas such as pavements and railway lines. The original weedkillers were chemicals such as sulphuric acid and rock salt and were applied in huge doses killing all of the vegetation they came into contact with. More modern examples of these non-selective or total herbicides are the quaternary ammonium herbicides paraquat and diquat and the organophosphorus compound glyphosate, which produce the same total clearance effect but require significantly lower dosages of chemical and are considerably safer to use.

Although the total herbicides have their uses, their lack of selectivity renders them useless in the control of unwanted vegetation growing amongst desirable crop plants. In these areas selective herbicides are more appropriate.

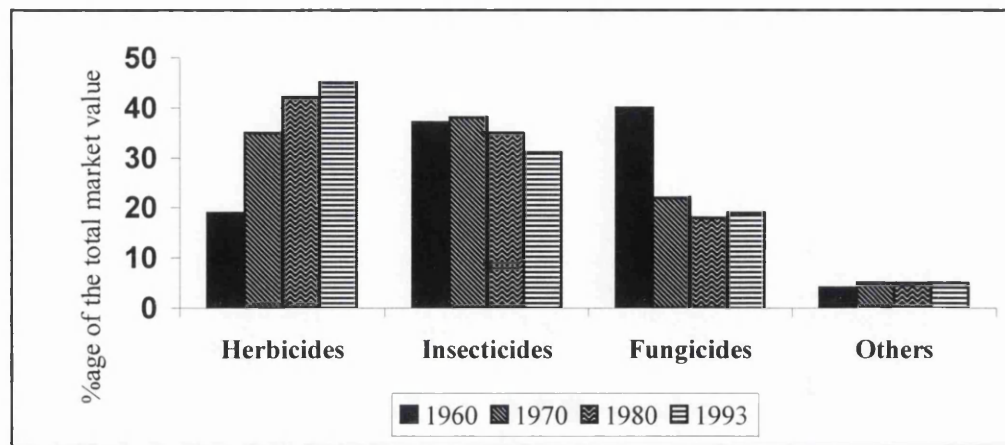


Figure 1.1 – Worldwide pesticide sales by type 1960 – 1993 [2]

It can be seen from Figure 1.1 that herbicide usage has increased significantly over the period shown, to a market value of \$11,590 million in 1993, and consequently represent economically and quantitatively the most important category of pesticide [2].

1.2.4 - Fungicides

Fungicides act to protect plants and seeds from fungal disease and can be classified as having either preventative or curative activity. Preventative fungicides are generally non-systemic in behaviour and are able to protect only the area of application; this type of chemical is typically used as a seed dressing to prevent infection prior to germination. The systemic curative fungicides are also known as plant chemotherapeutants and are comparable with the drugs used in the treatment of human diseases, indeed members of the sulphonamide class of compounds are effective in the treatment of infections in both mammals and plant life. The fungicide market today is dominated by these highly active and specific systemic chemicals, and in particular the members of the imidazole and triazole class of compounds. The triazole fungicides will be discussed further in Section 1.5.2.

1.2.5 - Insecticides

Insecticides are used primarily to control the spread of insect borne disease and to rid crop areas of infestation. The majority of modern insecticides are synthetic organic compounds that act on contact and are toxic to a wide range of species. Amongst the most important of these synthetic products are the pyrethroids which are synthetic analogues of the toxic agents found in one of the earliest natural insecticides, pyrethrum. With their high activity and potency they make up approximately one quarter of the world insecticide use today [3].

In 1993, the world insecticide market was worth approximately \$7,580 million, and it is estimated that half of the world use of insecticides is in developing countries, especially tropical regions [2].

1.3 - AN HISTORICAL OVERVIEW OF DEVELOPMENTS IN PESTICIDE SCIENCE [3]

Throughout history man has made use of the chemical substances available to him to protect his crops and other food supplies from attack by disease, pests and unwanted vegetation. The Ancient Greeks and the Romans are known to have made use of both sulphur and arsenic as insecticides, but it was not until the mid-19th century that scientists began to seriously research the possibilities of chemical crop protection. Some of the earliest pesticides, such as the insecticides rotenone and pyrethrum, were derived from natural sources and are the basis of products still in use today. However, many of the chemicals used as pesticides during the late 19th century and the early 20th century; such as compounds of arsenic and mercury; were highly toxic to many mammals (including man) as well as the target organisms.

It was not until the 1930s that the development of many of the major classes of synthetic pesticide that we recognise today took place. The Second World War and the years that followed saw many important advances in the field of pesticide science. With the majority of the work force serving in the armed forces an effective alternative to the labour intensive pre-war manual techniques was necessary to maintain adequate crop production levels, this led to the introduction of large-scale commercial manufacture of agrochemicals. Other notable advances made during this period were the development of the organophosphorus insecticides based largely on research into nerve gases carried out by Gerhard Schrader and research into the antibiotic properties of penicillin by Chain and Florey in 1940 led to the introduction of antibiotic based fungicides. It has been suggested that the discovery in 1939 of DDT (dichlorodiphenyltrichloroethane), with its insecticidal properties against the carriers of both malaria and typhus, assisted the Allied Forces in winning the war, enabling battles to be fought in areas where previously the risk of disease to the troops was too great.

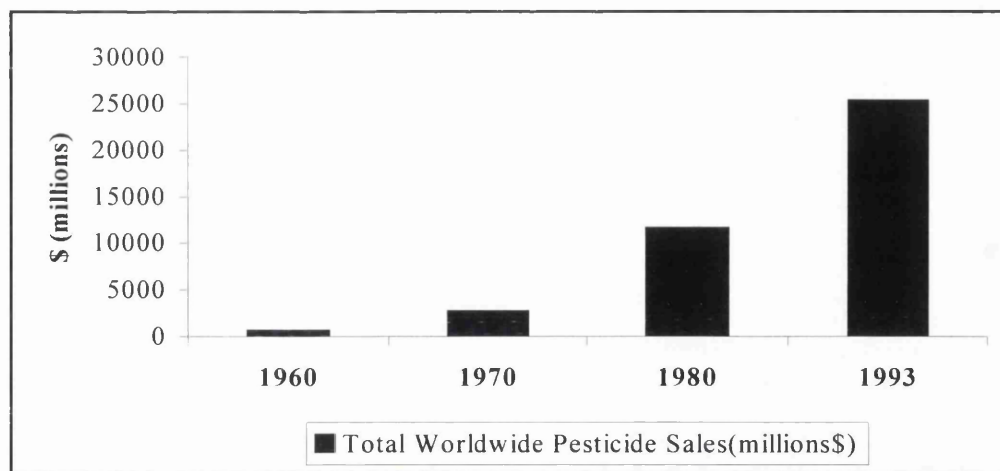


Figure 1.2 – Growth in Worldwide pesticide sales 1960 – 1993 [2]

In the latter part of the 20th Century the pesticide industry has continued to grow, see Figure 1.2, and significant developments, including the introduction of the triazole fungicides in the 1970s and the development of pesticidal products based on natural compounds extracted from microorganisms such as azoxystrobin and the spinosyns, are still being made but many of the products in use today were discovered over 35 years ago. With increased legislation over the toxicological and environmental safety of pesticides, the emphasis has been on the development of less persistent compounds with lower toxicity, greater potency and greater selectivity. As a consequence the costs involved in the development of new products have increased greatly, which in the 1970s led to a down turn in the introduction of significant new products. In order to justify increasingly high development costs those products that reach the market today generally have significant advantages over those already available in terms of higher selectivity and lower dosage.

1.4 - ENVIRONMENTAL CONCERNS AND THE NEED FOR ANALYSIS

Along with the undeniable benefits that pesticides have brought, their increased use has been accompanied by innumerable health scares, environmental problems and growing public distrust. The widely publicised and numerous problems surrounding the use of organochlorine insecticides such as DDT, in the 1950s [3] increased awareness of pesticide related pollution and highlighted the need for greater regulation of the production and use of agrochemicals. Legislation such as that laid down in the Food and Environmental Protection Act 1985 sets out the rigorous requirements for environmental and toxicological testing during the development of the chemical. Long term studies to determine the pesticide's effect on plant and animal life, and residue analysis on soil, water and crops are required in order to produce a comprehensive representation of the candidate pesticide's environmental behaviour. With these increasingly stringent regulations the cost involved in developing a new pesticide, over the 10 year period from invention to launch, will often exceed £50million, with the greatest proportion of this cost taken up by the toxicological, environmental and biological testing required for registration and approval, see Figure 1.3.

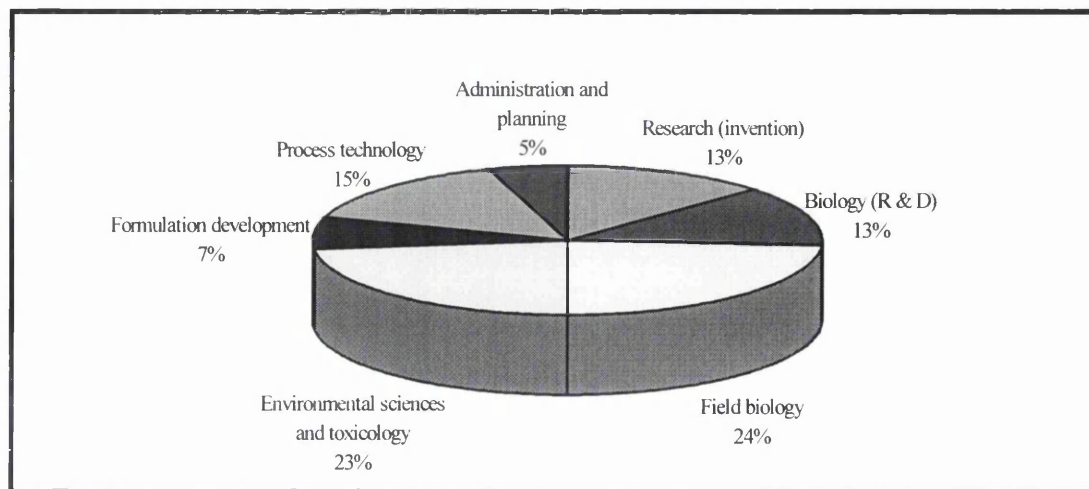


Figure 1.3 – Breakdown of new product costs from invention to launch [4]

In addition to the analysis required during the period of development the composition and impurity levels present in commercially available products must be determined and comply with approved specifications and environmental legislation. The levels of residues found in food, water and soil are highly regulated and continually monitored. Environmental monitoring and compositional analysis of pesticides are performed using a wide range of analytical techniques including the chromatographic methods that will be described in subsequent chapters.

1.5 – THE STUDY COMPOUNDS

The following sections discuss the compounds studied in the course of my work, describing their uses and summarising previously used methods of analysis.

1.5.1 – Paraquat

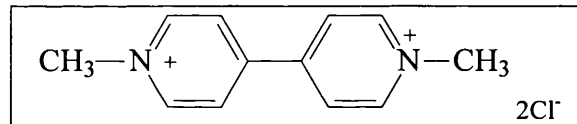


Figure 1.4 – Structure of paraquat dichloride

Paraquat, or 1,1'-dimethyl-4,4'-bipyridinium dichloride, was introduced by Imperial Chemical Industries Ltd. (ICI) in 1958 together with another bipyridinium herbicide, Diquat. Both paraquat and diquat were developed following research into quaternary ammonium compounds such as cetyltrimethyl ammonium bromide which had been observed to be effective desiccants of young plants [5]. It was discovered that ethylene dibromide and 2,2'-bipyridyl reacted to produce a compound with good herbicidal activity. At the time the composition of this product was unknown but was later discovered to be diquat dibromide. Further work in this area using related

compounds led to the development of paraquat and the less well known and less used morfamquat [6].

Paraquat is synthesised from pyridine in a free radical type reaction outlined in Figure 1.5. Pyridine is reacted with sodium in liquid ammonia to give 4,4'-tetrahydropyridyl, which then undergoes oxidation by air to produce 4,4'-bipyridyl. This is then reacted with methyl chloride in water to yield paraquat dichloride [7,3].

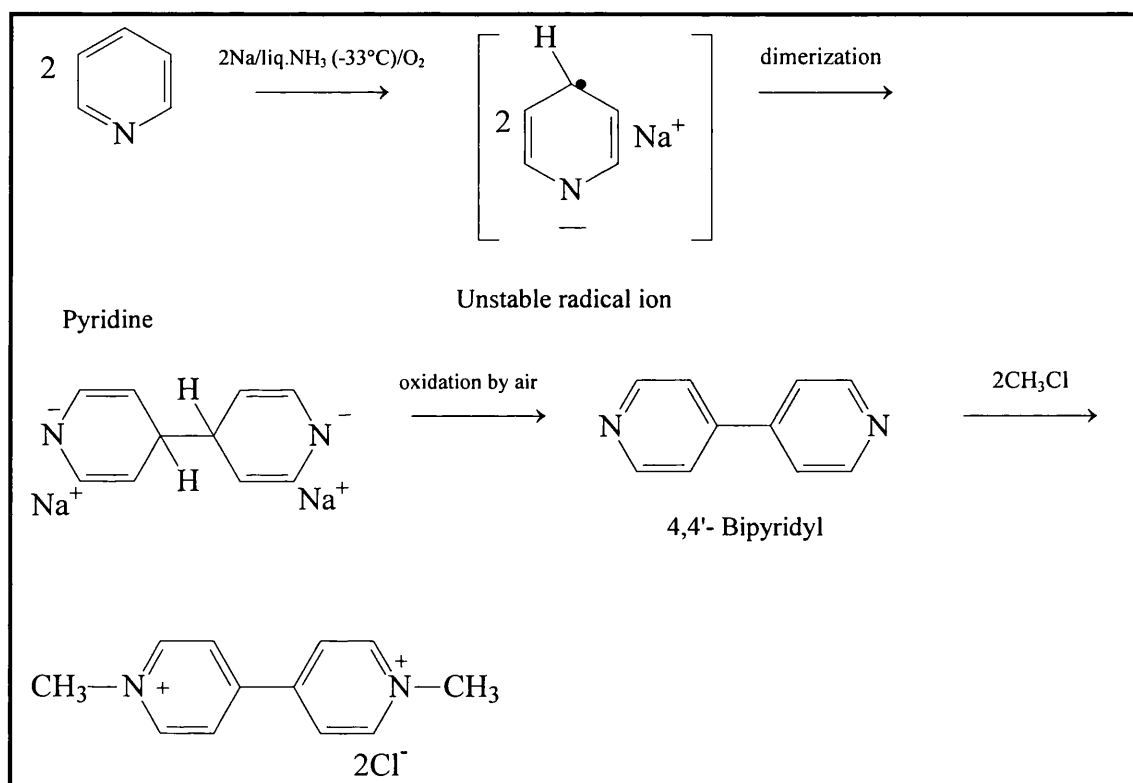


Figure 1.5 – Synthesis of paraquat

Paraquat is a non-selective, fast acting, contact herbicide which is absorbed by only the leaves it comes into contact with. As a cationic compound it is very readily exchanged with cations in soil colloids, becoming very strongly bound to the soil and resulting in the deactivation of the chemical on contact with the soil [6]. The

chemical is translocated throughout the plant resulting in the rapid desiccation of the foliage.

1.5.1.1 - Mode of Action

In the presence of sodium dithionite or zinc dust, paraquat is reduced to form highly coloured solutions containing radical cations stabilised by the delocalisation of the odd electron over all 12 nuclear carbon atoms resulting in the partial removal of the positive charges from the nitrogen.

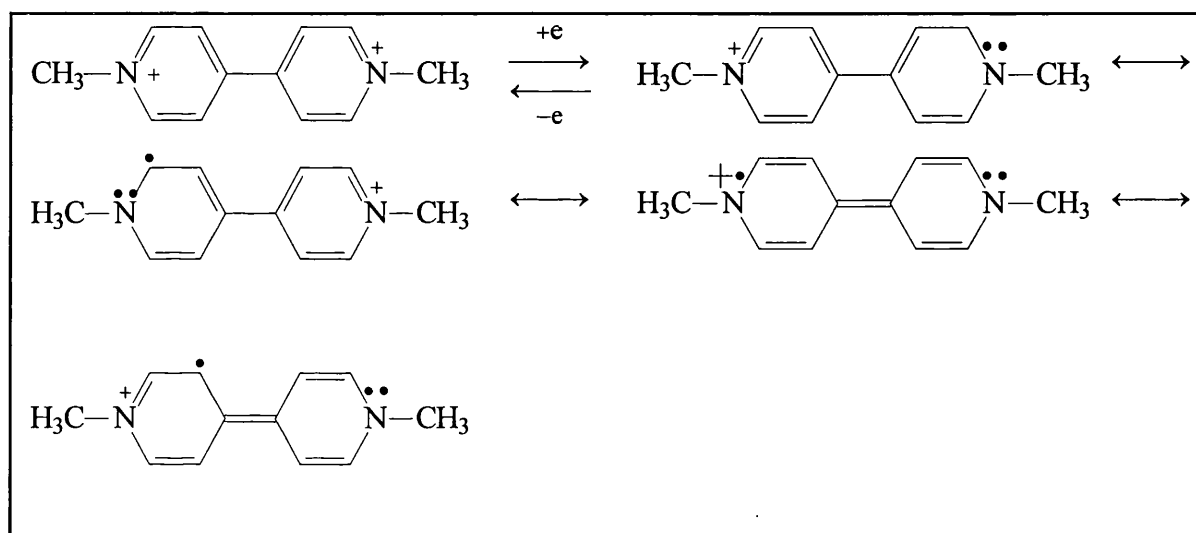
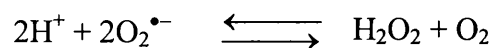
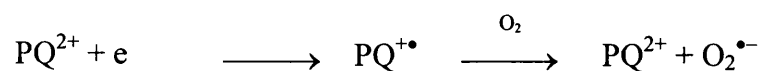


Figure 1.6 – Electron delocalisation in paraquat

This reduction has been demonstrated to occur in the chloroplasts of green plants during photosynthesis in the presence of both light and oxygen. Paraquat is rapidly reduced forming water-soluble free radicals, which are reoxidised to produce the reactive superoxide anion, $O_2^{\bullet-}$, which reacts to form hydrogen peroxide, H_2O_2 .



Evidence suggests that it is this hydrogen peroxide which is ultimately responsible for the death of the plant. It is highly nucleophilic and diffuses through the plant destroying membranes through a chain reaction known as lipid peroxidation.

1.5.1.2 - Herbicidal Applications

Paraquat is used to control grasses and broad-leaved weeds in numerous crop types, including citrus and apple orchards and banana and coffee plantations; [8,9] and is also effectively used in clearing areas of uncropped land, such as roadsides or industrial sites, of weeds. It has proved particularly useful in areas where soil erosion is a problem, the technique of 'Chemical Ploughing' eliminates the need for mechanical ploughing and consequently helps to preserve top soil. Paraquat is applied immediately prior to re-seeding, killing weeds and ensuring that the most fertile part of the soil is preserved and because it becomes inactive on contact with the soil the new crops are unaffected by root uptake or by soil and water contamination.

1.5.1.3 - Toxicology and the Environment

Obviously the fact that paraquat is used as a herbicide indicates that it is toxic to both terrestrial and aquatic vegetation, it is also highly toxic to mammals, including man and has in the past been linked with the rapid decline in the UK's hare population [3]. Although a large number of cases of paraquat poisoning have been reported these are largely due to the deliberate consumption of paraquat with suicidal intent or involve accidents or unsafe use by workers using the chemical [9,10].

As has been described previously, paraquat becomes inactive on contact with soil due to its binding properties. However, the continued accumulation of residues in the upper layers of the soil may have environmental implications and this has led to Germany restricting its use to only one application in every four years [9,11].

Although the World Health Organisation states that “Paraquat does not seem to present an environmental hazard” [9] and that it is “unlikely to pose a health hazard for the general population” [9] the number of accidental poisonings and high mammalian toxicity have led to several countries, including Sweden, Finland and Hungary, banning the use of paraquat [11]. Despite these potential environmental and toxicological problems the herbicidal product Gramoxone, where the active ingredient is paraquat, remains the second largest selling herbicidal product worldwide [11].

1.5.1.4 - Analysis

As legislation increases the need for the monitoring and analysis of paraquat levels in water, biological fluids, soil and agricultural products for environmental, forensic and clinical purposes continues to grow. Because of its toxicity, the use of paraquat has been restricted in a number of countries and limits have been set [9]. As a result a significant amount of research has been carried out in order to develop analytical methods for the determination of paraquat in a variety of matrices such as water [12-23], soil [13,15,24], biological fluids and tissues [15,25-32] and crops [15,33-40].

Initially analyses were performed using spectrophotometric methods [24,33] utilising the stable blue radical cation formed when paraquat is reduced in aqueous solution. Sample preparation has traditionally been time consuming and sensitivity low, although in recent years improvements have been made in these areas. Immunoassay [41], electrochemical [42] and TLC [44-46] methods have also been described and are reviewed in greater detail in LA Summers' book 'The Bipyridinium Herbicides'.

The development of gas chromatographic methods [25] led to improved sensitivity, but because paraquat is a non-volatile ionic compound the processes needed to volatilise the chemical, such as pyrolysis and derivatisation, render the technique extremely time consuming as well as causing poor reproducibility at low levels [47].

HPLC [16-23,27-32,34-40] has proved particularly useful and has the advantage of being rapid and sensitive although it is often difficult to achieve reproducible retention times and analyte responses due to the sorptive interactions experienced by the cationic species in solution [39]. This problem was overcome initially by making use of ion-exchange chromatography [27,48], but this technique has largely been replaced by ion-pair chromatography which has been effectively employed in the analysis of paraquat from a wide range of matrices with good recoveries and limits of detection as low as $0.1\mu\text{g/l}$ [23]. The compounds used as ion-pairing reagents in the majority of analyses are incompatible with mass spectrometric methods, which has limited the use of HPLC-MS in the determination of PQ. Barcelo et al [49] used ion-pair chromatography with post-column extraction

followed by thermospray mass spectrometry and Yoshida et al [50] performed HPLC-TSP-MS using a mobile phase of methanol, water and ammonium acetate but both methods suffer from poor chromatography and require large sample volumes to achieve the required sensitivities [21]. However, Marr and King's 1997 publication [21] describes an HPLC-ionspray tandem mass spectrometric method which successfully uses 10mM heptafluorobutyric acid (HFBA) as the ion-pair reagent. The addition of HFBA resulted in improved chromatography and the use of mass spectrometry provides increased specificity, selectivity and high sensitivities, the limit of detection for paraquat using this method is 5µg/l, significantly lower than for other published methods using mass spectrometry.

In recent years, interest in the use of capillary electrophoresis has increased and a number of papers describing CZE methods for the analysis of paraquat have been published [15,26,34,47,51-52]. CZE has the advantage of simplicity over the numerous other available methods, no derivatisation is necessary, it is quick, reproducible and can be used routinely. Comparison of the technique with ion-pair HPLC has been reported by Carneiro et al [47] and although CE gave good results, ion-pair chromatography offered greater sensitivity, especially in the analysis of 'real' samples. The use of mass spectrometric detection in conjunction with CE has been reported for the use of the determination and characterisation of paraquat and other quaternary ammonium herbicides [53-54] with both methods employing electrospray ionisation. Detection limits as low as 9µg/l have been reported and the use of this technique as a means of analysing paraquat and other quaternary ammonium herbicides in water appears to be promising.

1.5.2 – Flutriafol

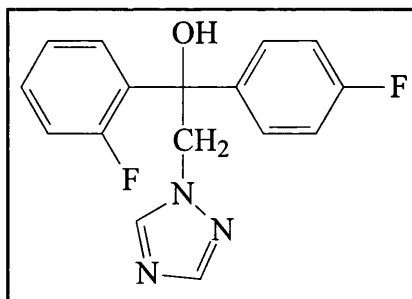


Figure 1.7 – Structure of flutriafol

Flutriafol, (chemical name (RS)-2,4'-difluoro- α -(1*H*-1,2,4-triazol-1-ylmethyl)benzhydryl alcohol) was developed by the ICI Plant Protection Division in 1983. It is one of the numerous triazole fungicides that have been introduced since their discovery in the late 1960s when it was observed that the 1-substituted 1,2,4-triazoles had good fungitoxicity.

Flutriafol is one of the triazole fungicides of the general formula shown below, where R₁ is alkyl, cycloalkyl or optionally substituted phenyl and R₂ is an optionally substituted phenyl, optionally substituted benzyl or an acid addition salt or metal complex thereof.

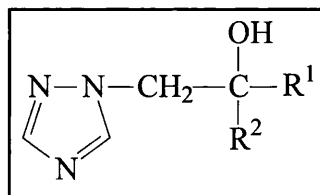


Figure 1.8 – General formula of the triazole fungicides

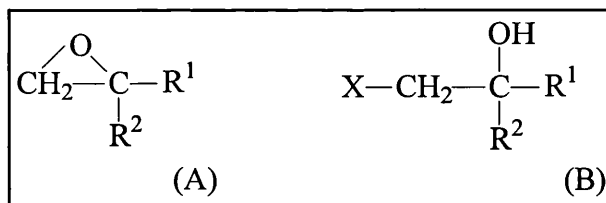


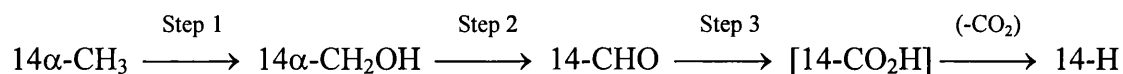
Figure 1.9 – General formulae of compounds used in the preparation of triazole fungicides

The preparation of these compounds is described in EP015756 [55]. Generally a compound of general formula (A) or (B), in which R1 and R2 are as previously defined and X is a halogen atom, is reacted with 1,2,4-triazole, either in the presence of an acid binding reagent or in the form of one of its alkali metal salts in a convenient solvent at a temperature between 20 and 100°C.

Isolation can be brought about by pouring the reaction mixture into water and recrystallising the solid formed from a convenient solvent.

1.5.2.1 – Mode of Action [3,56]

The triazole fungicides, along with the closely related imidazole fungicides, belong to a group of compounds known as C-14 demethylation inhibitors or DMIs. The synthesis of ergosterol, a steroidal compound crucial to the functioning of many fungi, requires the oxidative removal of a C-14 methyl group from another steroid, lanosterol, and its replacement with a hydrogen atom. A simplified outline of this process is shown below [3].



The demethylation process is catalysed by a specific form of the enzyme cytochrome P₄₅₀ and it is postulated that flutriafol and the other DMIs act by blocking the active site of this compound by co-ordinating with the porphyrin system within the enzyme, see Figure 1.10. Consequently, access of lanosterol and the oxygen molecules necessary for ergosterol biosynthesis is prevented. The inhibition of ergosterol production results in the production of defective lipoprotein membranes, either because of a shortage of ergosterol or as a result of the build up of the wrong type of lipid. Any specialist functioning of the membranes is prevented and results in the collapse of the fungal cell walls.

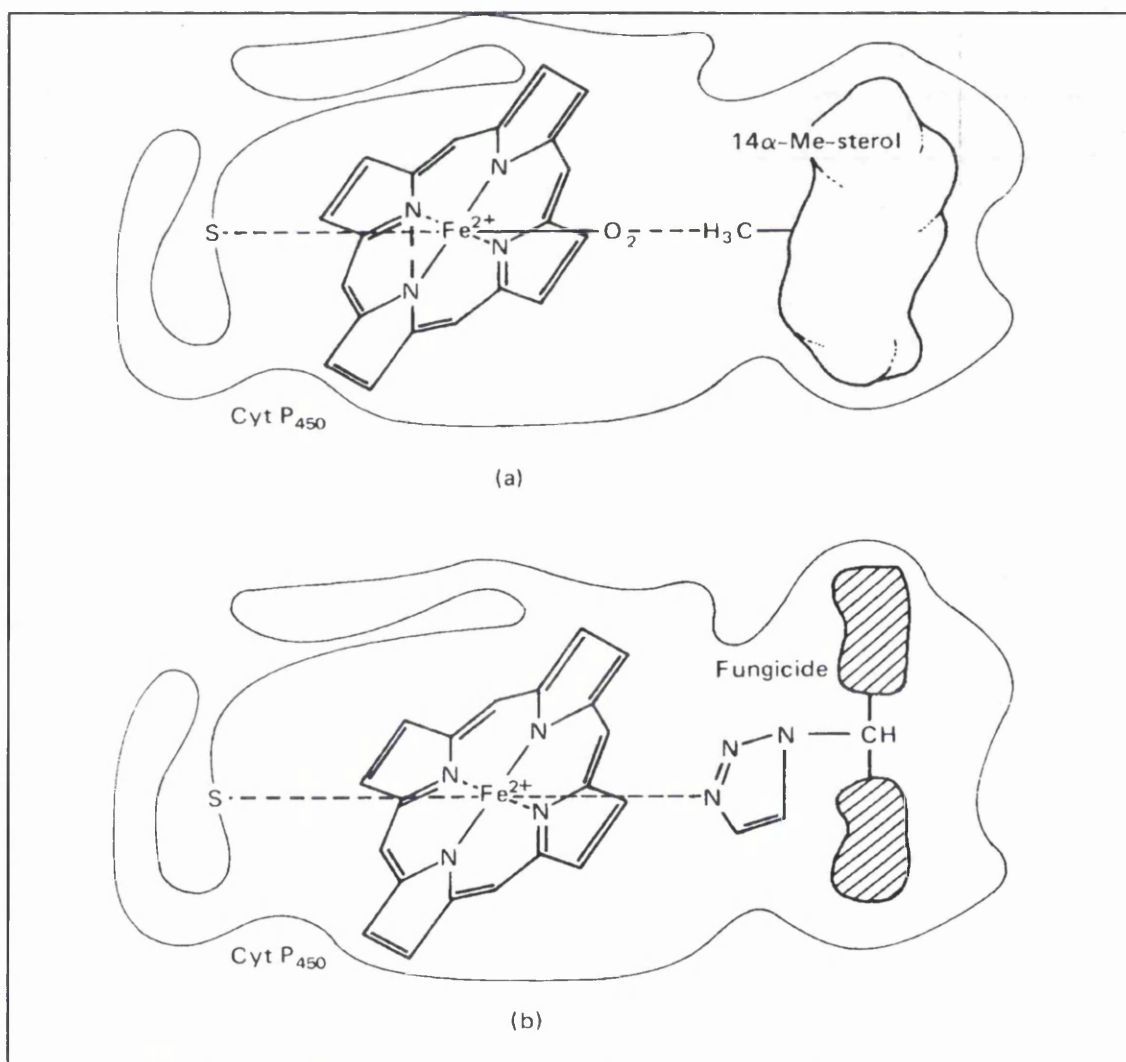


Figure 1.10 – Schematic representation of the proposed mode of action of C-14 demethylation inhibitors [56]

1.5.2.2 - Fungicidal Applications [3,8,57]

Flutriafol is a broad spectrum fungicide used largely in the control of both leaf and ear diseases, such as powdery mildews, rusts and smuts, in cereal crops, commercially available as Impact and Vincit. It is also widely used in formulations with other fungicidal compounds and as a non-mercurial seed dressing effective in the control of soil and seed borne diseases. Flutriafol is applied as a spray and is used to treat an area of 496,556 hectares of land in this country each year putting it amongst the 20 most widely used pesticides in the UK [58].

1.5.2.3 - Toxicology and the Environment [3,56]

In general the use of fungicides does not appear to cause much environmental damage, and the introduction of systemic fungicides such as flutriafol which are absorbed and translocated within the plant leaving no harmful residues should reduce the possibility of environmental contamination from fungicidal use. Mammalian toxicity is relatively low and after several years of use, no detrimental effects have been observed on birds, animals, or even soil microorganisms. Flutriafol and the other DMIs are highly potent with application rates less than one-tenth of those of conventional non-systemic fungicides. One other significant environmental advantage of flutriafol is its use as a seed dressing, the previously widely used and highly toxic organomercury compounds have largely been replaced by flutriafol and the other DMIs. One of the less desirable results of the introduction of systemic fungicides is the increase in the development of resistant fungal strains, fortunately in the case of flutriafol and the other triazole DMIs the risk is relatively low and to date very few cases have been reported. Risk can be further minimised by formulating systemic compounds with more traditional surface fungicides.

1.5.2.4 – Analysis

Although flutriafol is amongst the numerous pesticide residues it is deemed necessary to measure in several countries, literature searches on the subject of the analysis of flutriafol using a number of different search engines resulted in only a very limited number of publications being found. Even when searches were expanded to encompass the analysis of triazole fungicides in general, the resulting number of references produced remained small. The following paragraphs aim to summarise the analytical methodology utilised within these papers.

Work carried out by Bolygó and Atreya in 1991 [59] describes the use of an SPE method for the trace enrichment of flutriafol and 11 other pesticides, including several other triazole compounds, from large volumes of water. Determination of flutriafol was performed using gas chromatography and GC-MS. Comparison of SPE with the more time consuming traditionally used technique of liquid-liquid extraction proved SPE to be more efficient with higher recoveries and greater sensitivity with a limit of determination of 0.03µg/l.

The 1995 publication by Balinova [60] also describes the use of SPE, again using C18 cartridges to extract flutriafol and 16 other fungicides from water samples. Determination in this case was carried out using the technique of bioautography in which the fungicides are separated by thin layer chromatography followed by the application of suspensions of fungal spores as spray reagents. Although the technique has the advantage of not requiring complex or costly instrumentation the need to incubate, or develop, the plates for 48 hours makes rapid analysis an

impossibility. It is however highly sensitive and applicable to a wide range of compounds, making it a useful screening technique.

REFERENCES CITED IN CHAPTER 1

1. www.epa.gov/pesticides/whatis.htm
2. Trace Determination of Pesticides and Their Degradation Products in Water. Damia Barcelo and Marie-Claire Hennion. Elsevier. 1997.
3. Agrochemicals Preparation and Mode of Action. RJ Cremlyn. John Wiley & Sons. 1991
4. Agrochemicals – Benefits and Risks. David Evans. *Chemistry in Britain*, **34**, (1998), 20-23
5. Diquat and Paraquat – New Agricultural Tools. WR Boon. *Chemistry and Industry* May 8, (1965), 782-788
6. The Bipyridinium Herbicides. LA Summers. Academic Press. 1980.
7. Pesticides Process Encyclopaedia Chemical Technology Review No. 81. Marshall Sittig. Noyes Data Corp. 1977
8. The Pesticide Manual, 11th Edition. Editor CDS Tomlin. British Crop Protection Council. 1997
9. Paraquat Health and Safety Guide. World Health Organisation, Geneva. 1991.
10. The Paraquat Report. Paul Brennan and Richard Sutherland. A Side Effects Report. 1983.
11. www.pan-uk.org/actives/paraquat.htm
12. Influence of organic matter and surfactants on solid-phase extraction of diquat, paraquat and difenzoquat from waters. M Ibáñez, Y Picó, J Mañes, *J.Chromatogr. A* **727**, (1996), 245-252
13. Isotachophoresis of cationic herbicides in waters and soils. Z Stránský, *J. Chromatogr.* **320**, (1985), 219-231

14. On-line isotachophoretic sample pretreatment in ultratrace determination of paraquat and diquat in water by capillary electrophoresis. D Kaniansky, F Iványi and FI Onuska, *Anal. Chem.* **66**, (1994), 1817-1824
15. Simultaneous determination of diquat and paraquat residues in various matrices by capillary zone electrophoresis with diode array detection. T Pérez-Ruiz, C. Martínez-Lozano, A Sanz, V Tomás, *Chromatographia* **43**, (1996), 468-472
16. Anomalies in the high-performance liquid chromatographic determination of diquat in water samples. DR Lauren and MP Agnew, *J.Chromatogr.* **303**, (1984), 206-210
17. High-sensitivity high-performance liquid chromatographic analysis of diquat and paraquat with confirmation. VA Simon and A Taylor, *J.Chromatogr.* **479**, (1989), 153-158
18. Rapid method for extraction and reverse phase liquid chromatographic determination of paraquat residues in water. Ijaz Ahmad, *J. Assoc. Off. Anal. Chem.* **66**, (1983), 663-666
19. Determination of diquat and paraquat in water using high-performance liquid chromatography with confirmation by liquid-chromatography-particle beam mass spectrometry. I Kambhampati, KS Roinestad, TG Hartman, JD Rosen, EK Fukuda, RL Lippincott, RT Rosen, *J.Chromatogr. A* **688**, (1994), 67-73
20. On-line liquid chromatographic trace enrichment and high-performance liquid chromatographic determination of diquat, paraquat and difenzoquat in water. M Ibáñez, Y Picó, J Mañes, *J.Chromatogr. A* **728**, (1996), 325-331
21. A simple high-performance liquid chromatography/ion spray tandem mass spectrometry method for the direct determination of paraquat and diquat in water. JC Marr and JB King, *Rapid Commun. Mass Spectrom.* **11**, (1997), 479-483

22. Comparison of immunoassay to high-pressure liquid chromatography and gas-chromatography-mass spectrometry analysis of pesticides in surface water. MI Selim, C Achutan, JM Starr, T Jiang and BS Young. Chapter 19, *Immunochemical Technology for Environmental Applications*, American Chemical Society, 1997.
23. On-line determination of bipyridilium herbicides in water by HPLC. M Ibáñez, Y Picó, J Mañes, *Chromatographia* **45**, (1997), 402-407
24. Colorimetric determination of paraquat residues in soil and water. JD Pope Jr and JE Benner, *J. Assoc. Off. Anal. Chem.* **57**, (1974), 202-204
25. Determination of the herbicides paraquat and diquat in blood and urine by gas chromatography. S Kawase, S Kanno and S Ukai, *J. Chromatogr.* **283**, (1984), 231-240
26. Simultaneous determination of paraquat and diquat in serum using capillary electrophoresis. M Tomita, T Okuyama and Y Nigo, *Biomed. Chromatogr.* **6**, (1992), 91-94
27. The analysis of paraquat in urine by high-speed liquid chromatography. A Pryde and FJ Darby, *J. Chromatogr.* **115**, (1975), 107-116
28. High-performance liquid chromatography of paraquat and diquat in urine with rapid sample preparation involving ion-pair extraction on disposable cartridges of octadecyl-silica. R Gill, SC Qua and AC Moffat, *J. Chromatogr.* **255**, (1983), 483-490
29. Determination of paraquat in tissue using ion-pair chromatography in conjunction with spectrophotometry. Tsung-Li Kuo, *Forensic Science International* **33**, (1987), 177-185

30. Determination of paraquat in rat brain by high-performance liquid chromatography. MT Carasantini and G Nisticò, *J. Chromatogr.* **643**, (1993), 419-425
31. Simultaneous determination of paraquat and diquat in human tissues by high-performance liquid chromatography. S Ito, T Nagata, K Kudo, K Kimura and T Imamura, *J. Chromatogr.* **617**, (1993), 119-123
32. Liquid Chromatographic method for simultaneous determination of paraquat and diquat in plasma, urine and vitreous humour. I Sánchez Sellero, A Cruz, P Fernández and M López-Rivadulla, *J. Liq. Chrom. & Rel. Technol.* **19**, (1996), 2009-2024
33. Spectrophotometric method for the determination of paraquat in water, grain and plant materials. P Shivare and VK Gupta, *Analyst* **116**, (1991), 391-393
34. Simultaneous determination of residues of paraquat and diquat in potatoes using high-performance capillary electrophoresis with ultraviolet detection. YY Wigfield, KA McCormack and R Grant, *J. Agric. Food Chem.* **41**, (1993), 2315-2318
35. Determination of paraquat in sunflower seeds by reversed-phase high-performance liquid chromatography. DC Paschal, LL Needham, ZJ Rollen and JA Liddle, *J. Chromatogr.* **177**, (1979), 85-90
36. Reverse-phase liquid chromatographic determination of paraquat and diquat in agricultural products. T Nagayama, T Maki, K Kan, M Iida and T Nishima, *J. Assoc. Off. Anal. Chem.* **70**, (1987), 1008-1011
37. Analytical method for the simultaneous determination of diquat and paraquat residues in potatoes by high-pressure liquid chromatography. BL Worobey, *Pestic. Sci.* **18**, (1987), 245-257

38. Liquid chromatographic method for determination of diquat and paraquat herbicides in potatoes: collaborative study. BL Worobey, *J. of AOAC Int.* **76**, (1993), 881-887
39. Liquid chromatographic determination of paraquat and diquat in crops using a silica column with aqueous ionic mobile phase. TM Chichila and SM Walters, *J. Assoc. Off. Anal. Chem.* **74**, (1991), 961-967
40. Determination of paraquat and diquat in low-moisture food crops using silica column cleanup and liquid chromatography with UV detection. TMP Chichila and DM Gilvydis, *J. of AOAC Int.* **76**, (1993), 1323-1328
41. Enzyme-linked immunosorbent assay for paraquat and its application to exposure analysis. J Van Emon, B Hammock and JN Seiber, *Anal. Chem.* **58**, (1986), 1866-1873
42. Liquid membrane ion-selective electrodes for diquat and paraquat. GJ Moody, RK Owusu and JDR Thomas, *Analyst* **112**, (1987), 121-127
43. Ion-pairing reagents in ion-selective electrodes for diquat, paraquat and 4,4'-dipyridinium dications. GJ Moody, RK Owusu and JDR Thomas, *Analyst* **112**, (1987), 1347-1353
44. A rapid method of thin-layer chromatography to aid the identification of quaternary nitrogen drugs. HD Crone and EM Smith, *J. Chromatogr.* **77**, (1973), 234-236
45. Thin-layer chromatography and spot test of paraquat-contaminated marihuana. NH Choulis, *J. Chromatogr.* **168**, (1979), 562
46. Sequential thin-layer chromatography of paraquat and related compounds. MB Abou-Donia and AA Komeil, *J. Chromatogr.* **152**, (1978), 585-588

47. Comparison of capillary electrophoresis and reversed-phase ion-pair high-performance liquid chromatography for the determination of paraquat, diquat and difenzoquat. MC Carneiro, L Puignou and MT Galceran, *J. Chromatogr. A* **669**, (1994), 217-224
48. Analysis of paraquat formulations by liquid chromatography. Y Kawano, J Audino and M Edlund, *J. Chromatogr.* **115**, (1975), 289-292
49. Determination of quaternary amine pesticides by thermospray mass spectrometry. D Barceló, G Durand and RJ Vreeken, *J. Chromatogr.* **647**, (1993), 271-277
50. Determination of paraquat and diquat by liquid chromatography-thermospray mass spectrometry. M Yoshida, T Watabiki, T Tokiyasu and N Ishida, *J. Chromatogr.* **628**, (1993), 235-239
51. Capillary zone electrophoresis of two cationic herbicides, paraquat and diquat. J Cai and Z El Rassi, *J. Liq. Chrom.* **15**, (1992), 1193-1200
52. Capillary electrophoresis of quaternary ammonium ion herbicides: paraquat, diquat and difenzoquat. MT Galceran, MC Carneiro and L Puignou, *Chromatographia* **39**, (1994), 581-586
53. Determination of quaternary ammonium herbicides by capillary electrophoresis/mass spectrometry. E Moyano, DE Games and MT Galceran, *Rapid Commun. Mass Spectrom.* **10**, (1996), 1379-1385
54. Capillary electrophoresis-electrospray mass spectra of the herbicides paraquat and diquat. X Song and WL Budde, *J. Am. Soc. Mass Spectrom.* **7**, (1996), 981-986
55. Triazole compounds, a process for preparing them, their use as plant fungicides and fungicidal compositions containing them. KP Parry, PA Worthington and WG Rathmell, *European Patent 0015756*, (1983)

56. The Biochemistry and Uses of Pesticides 2nd Edition. Kenneth A. Hassall. Macmillan Press Ltd. (1990) 335-343
57. www.zenecaag.com
58. www.environment.detr.gov.uk/pesticidestax/19.htm
59. Solid-phase extraction for multi-residue analysis of some triazole and pyrimidine pesticides in water. Elek Bolygó and Naresh C Atreya, *Fresenius J. Anal. Chem.* **339**, (1991), 423-430
60. Extension of the bioautograph technique for multiresidue determination of fungicide residues in plants and water. Anna Balinova, *Anal. Chim. Acta* **311**, (1995), 423-427

Chapter 2

Mass Spectrometry

2.1 - INTRODUCTION

The term mass spectrometer can be used to describe any instrument that measures the abundance of ions based on their m/z values [1]. Whilst a number of different types of mass spectrometer are available each comprises the same basic components and performs the same functions:

- Sample inlet
Converts sample molecules into gaseous ions
(Note: the inlet system and ion source are often combined to form a single component)
- Ionisation source
- Mass analyser
Separates ions according to their mass-to-charge ratio (m/z)
- Ion detection system
Detects ions and measures their mass and abundance

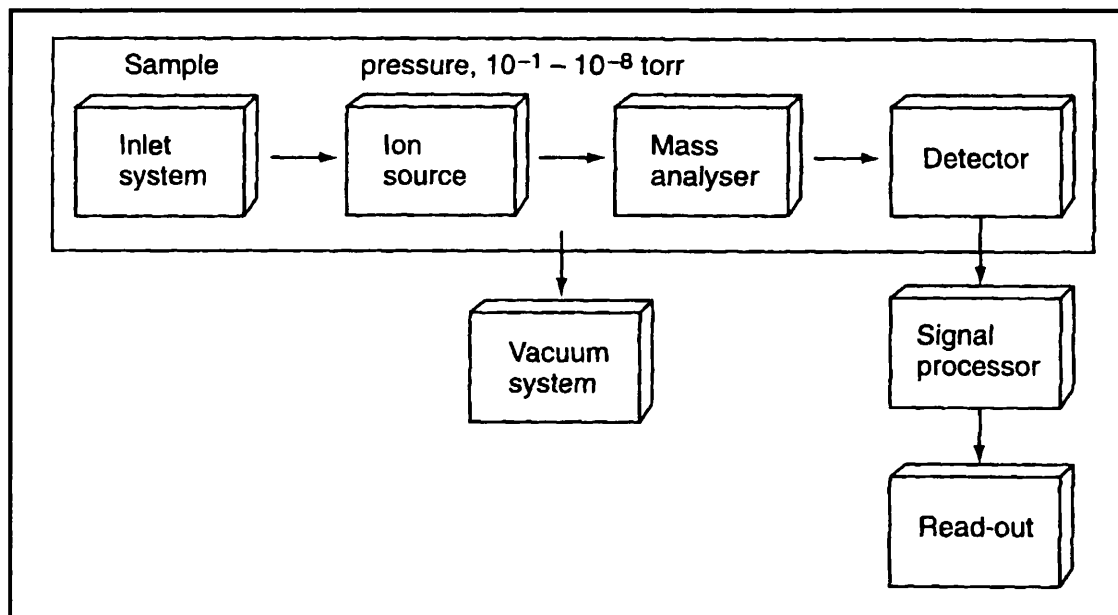


Figure 2.1 – Schematic representation of the components of a mass spectrometer [2]

Also fundamental to the operation of mass spectrometers is the requirement for a vacuum system to maintain the low pressures necessary in the mass analyser and detector to prevent losses in efficiency as a result of unwanted collisions.

Since its introduction in the early 20th Century the technique of mass spectrometry has developed to become one of the most powerful and widely used analytical techniques available.

2.2 - IONISATION TECHNIQUES

A number of different techniques are currently used in the formation of sample ions, amongst the most commonly used are Electron Ionisation (EI), Chemical Ionisation (CI), Thermospray (TSP), Fast Atom Bombardment (FAB), Matrix Assisted Laser Desorption (MALDI), Electrospray (ESI) and Atmospheric Pressure Chemical Ionisation (APCI). The following sections discuss only the atmospheric pressure ionisation methods, ESI and APCI. Detailed descriptions of the other techniques can be found elsewhere [2-7].

2.2.1 - Atmospheric Pressure Ionisation (API)

The term API is used to describe those ionisation processes performed at atmospheric pressure as opposed to those such as EI and CI which are performed at reduced pressures [1]. The most common examples of API sources are ESI and APCI.

2.2.1.1 - Electrospray Ionisation (ESI) [3–9]

The work that forms the basis of electrospray was reported by Dole [10] in 1968, but it was not until the 1980s that the first true electrospray interface for mass spectrometry was developed by Fenn and co-workers [11]. The technique is widely used in the interfacing of chromatographic separations with mass spectrometry and has a wide range of application [12].

The process of ESI results in the transfer of sample ions from solution into the gas phase. This is generally accomplished by forcing the sample solution through a fine capillary or narrow bore needle to which a high potential, typically 3–5kV, has been applied. When the solution reaches the end of this tube the electric field results in the almost instantaneous formation of a fine spray of charged droplets. Often a nebulising gas, typically N₂, is used to enhance this process and assist in the process of desolvation. The solvent from these charged droplets evaporates constantly increasing the surface charge density until it reaches a critical point known as the Rayleigh Stability Limit. At this point the number of electrostatic charges on the surface becomes so large relative to the droplet size that the electrostatic repulsion is greater than the surface tension holding the droplet together consequently an explosion occurs resulting in the production of a number of smaller droplets. This process repeats many times until the analyte ion escapes the droplet (ion desorption) or all the solvent has evaporated leaving the ion in the gas phase (ion evaporation). A schematic representation of the process of electrospray ion formation is shown in Figure 2.2.

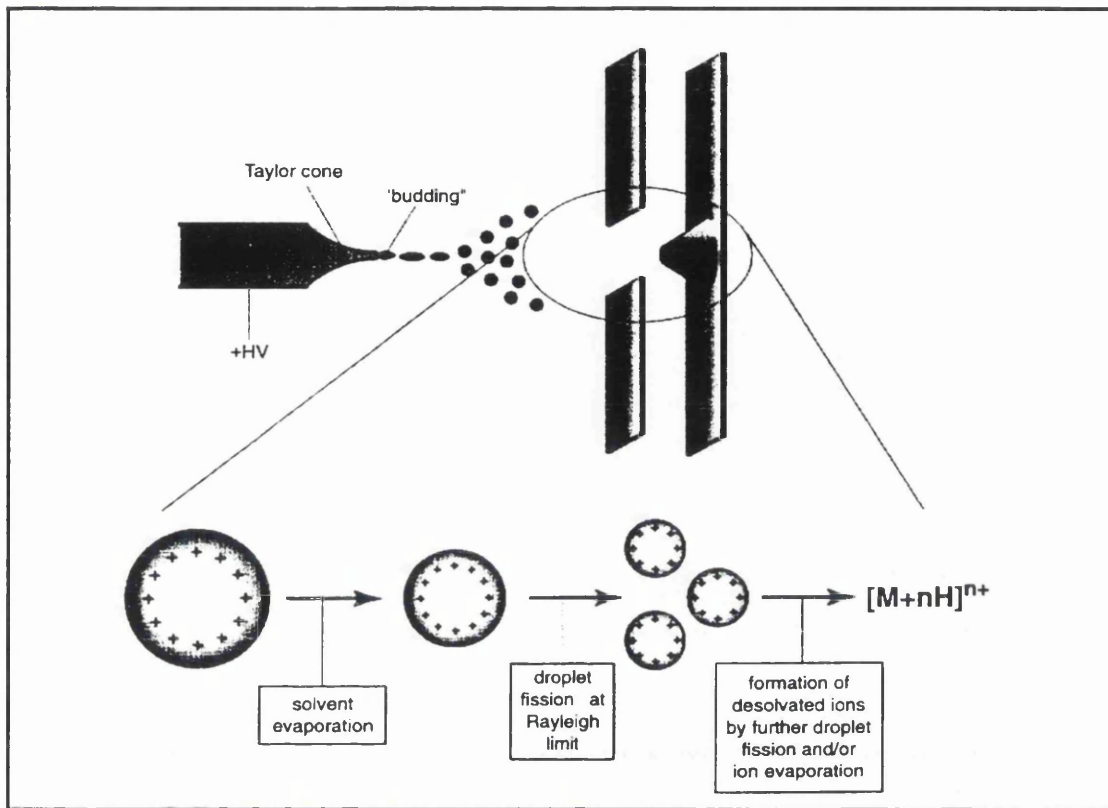


Figure 2.2 – Schematic representation of the electrospray ionisation process [9]

Following their formation the ions are extracted via a sampling orifice, a heated capillary in the Finnigan LCQ, initially into two evacuated regions containing a nozzle and skimmer where the sample ions are further separated and focused. The ions are then finally passed into the mass analyser.

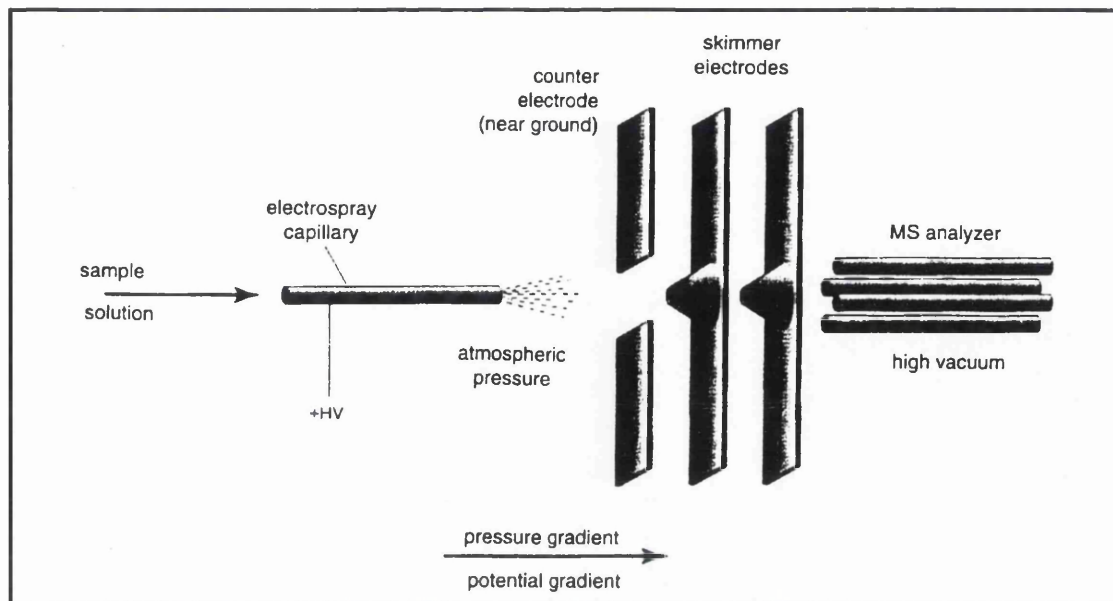


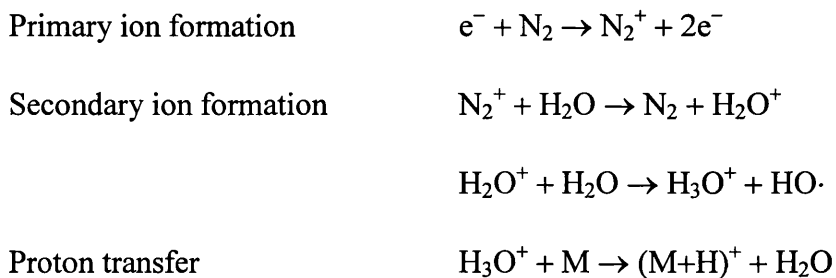
Figure 2.3 – Schematic representation of the essential features of an electrospray interface [9]

Many of the ions formed in the ESI process are of the form $(M+nX)^{n+}$ in the positive ion mode where X is a cation such as Na^+ , K^+ or NH_4^+ . However, the majority of ions are formed as a result of proton transfer giving rise to ions of the form $(M+n\text{H})^{n+}$ and $(M-n\text{H})^{n+}$, with those molecules with many sites capable of being protonated and deprotonated forming multiply charged ($n > 1$) quasi-molecular ions. Whilst these ions give little structural information they provide accurate molecular mass information and the presence of multiply charged ions allows the study of molecules with masses higher than the limit of the mass analyser. This phenomenon enables the analysis of high molecular weight biological macromolecules with relative molecular masses up to 300000 to be studied using relatively inexpensive quadrupole mass spectrometers.

2.2.1.2 - Atmospheric Pressure Chemical Ionisation (APCI) [1,3,6,8,12]

APCI, is an ionisation technique which uses gas phase ion-molecule reactions at atmospheric pressure. Like ESI it is a 'soft' ionisation technique but the high temperatures involved mean that it is not as soft a technique as ESI.

The sample liquid is directly introduced into a pneumatically assisted nebuliser where a stream of gas, typically air or N₂, converts it into a fine spray of small droplets. The droplets then pass through a heated tube, the vaporiser, where temperatures of 400-600°C result in the vaporisation of the solvent and sample. Located near the exit of this vaporiser tube is a needle to which a high voltage has been applied resulting in the creation of a corona discharge. As the mixture of sample, solvent and nitrogen gas leave the vaporiser and pass through this area a series of chemical reactions involving the nitrogen gas and solvent molecules results in the formation of reagent ions. These reagent ions then react with sample molecules, resulting in the formation of sample ions. Typical processes taking place in positive-ion mode APCI are shown below and illustrated in Figure 2.4.



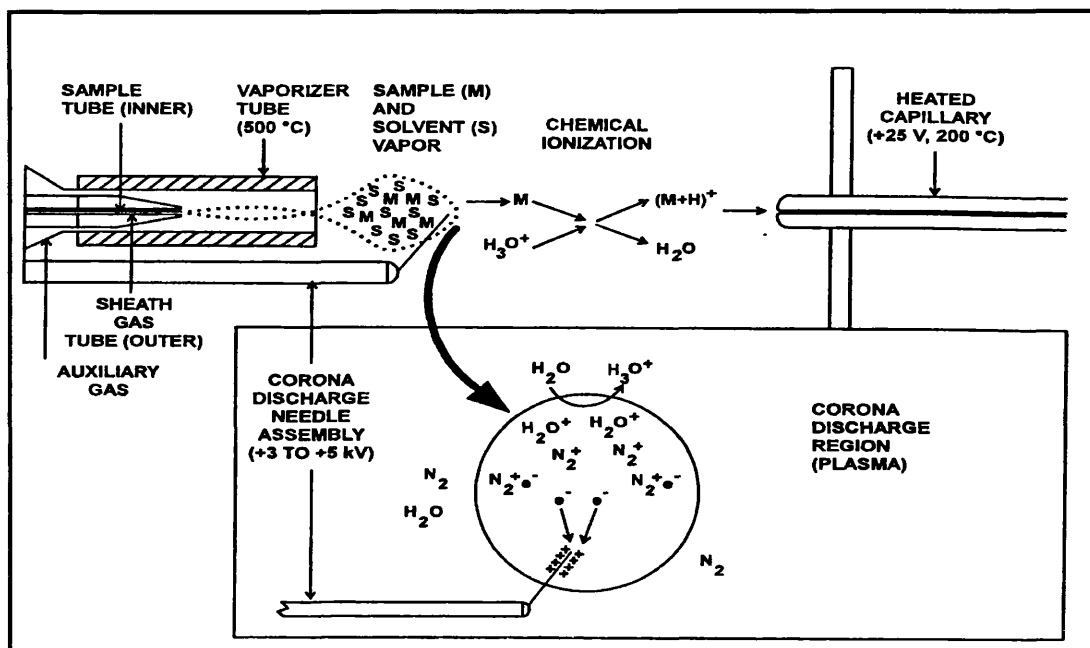


Figure 2.4 – Schematic representation of the APCI process in positive ion mode [8]

The ions are then directed towards the sampling orifice by the flow of sheath and auxiliary gases where they are focused toward the high vacuum region of the mass analyser.

2.3 - MASS ANALYSERS

Several methods of separating ions with different mass-to-charge ratios are available. The early instruments employed magnetic or electrostatic fields as a means of mass analysis and while such instruments are still available more recently developed analysers such as quadrupole mass filters, quadrupole ion traps and time of flight (TOF) analysers are more widely used. The following sections will discuss quadrupole ion traps and quadrupole mass filters only, more detailed accounts of other mass analysers can be found elsewhere [3-7].

2.3.1 - Quadrupole Ion Trap [1,2,4,6,7,8,13]

An ion trap is a device in which gaseous ions can be formed and confined for extended periods by electric and/or magnetic fields. As the site for mass analysis it is responsible for the storage, isolation, collision-induced dissociation and ejection of ions. A schematic representation of an ion trap is shown in Figure 2.5.

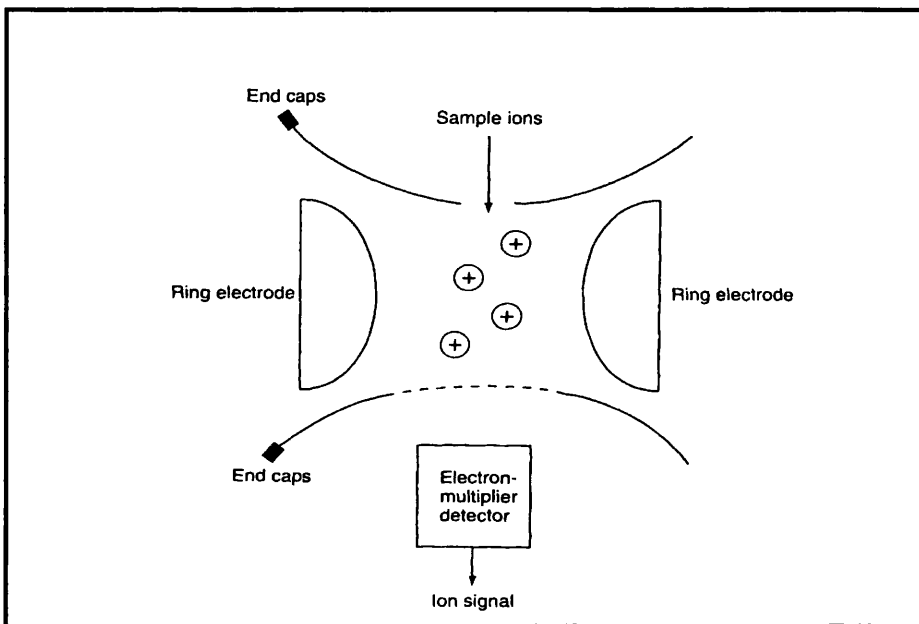


Figure 2.5 – Schematic representation of an ion trap mass analyser [2]

The principal components of the ion trap are three stainless steel electrodes; a central doughnut shaped ring electrode and a pair of end-cap electrodes located at the entrance and the exit of the trap forming a cavity in which mass analysis occurs. Each end-cap electrode has a small aperture in its centre through which the ions generated in the source are first introduced into the analyser cavity and then ejected into the ion detection system.

Each of the stages of ion trap operation, injection, trapping and ejection is achieved by the application of various voltages to the ring and end-cap electrodes and are summarised below.

- Injection – samples are drawn into the cavity of the ion trap as a result of the application of a dc offset voltage to the mass analyser electrodes. This is known as the mass analyser dc offset voltage and is -10V in positive ion mode and $+10\text{V}$ in negative ion mode.
- Trapping – the process of trapping the ions is brought about by the application of an ac voltage of constant frequency (0.76MHz) and variable amplitude (0 to 8500 V) to the ring electrode. This is known as the ring electrode RF voltage and results in the generation of a three-dimensional quadrupole field within the cavity of the analyser. This time varying field drives the ionic motion in both the axial (towards the end-caps) and radial (from the ring electrode to the centre) directions. For an ion to remain trapped, these oscillations must be stable.
- Ejection – when the amplitude of the ring electrode RF voltage is low, all ions above a minimum m/z are trapped, this is referred to as the storage voltage. During the process of ejection (also known as ‘scan-out’) a mass dependent instability is produced causing ions to be ejected from the mass analyser in the axial direction. The ring electrode RF voltage is ramped at a constant rate and as it increases ions of increasing m/z

values become unstable in the axial direction resulting in their ejection from the trap via the exit end-cap. The voltage at which an ion is ejected from the trap is known as its resonance voltage.

Helium can be introduced into the mass analyser where it is used as a damping gas, reducing the kinetic energy of the ions, slowing them down and allowing them to be focused in the centre of the cavity increasing the resolution and the sensitivity of the system. In addition, it is used as a collision activation partner during the collision induced dissociation steps of SRM, CRM or MSⁿ analyses.

Ion trap mass spectrometers are rugged, compact and typically less expensive than sector or quadrupole instruments. These factors, in addition to the ability of the more sophisticated ion traps to perform MSⁿ experiments without the need for two linked analysers, make the ion trap a particularly versatile instrument which continues to grow in popularity.

2.3.2 - Quadrupole mass analysers [1,2,4-7]

Quadrupole mass analysers, otherwise known as quadrupole mass filters, are by far the most commonly employed mass analyser in use today, having the advantage of being more compact, less expensive and more rugged than magnetic sector instruments. This type of mass analyser separates ions based on oscillations of ions in an electric field.

A quadrupole consists of a set of four metal rods either circular or preferably hyperbolic in cross-section, precisely straight and parallel and arranged equidistantly

around a central, imaginary axis. A schematic representation of a quadrupole analyser is shown in Figure 2.6.

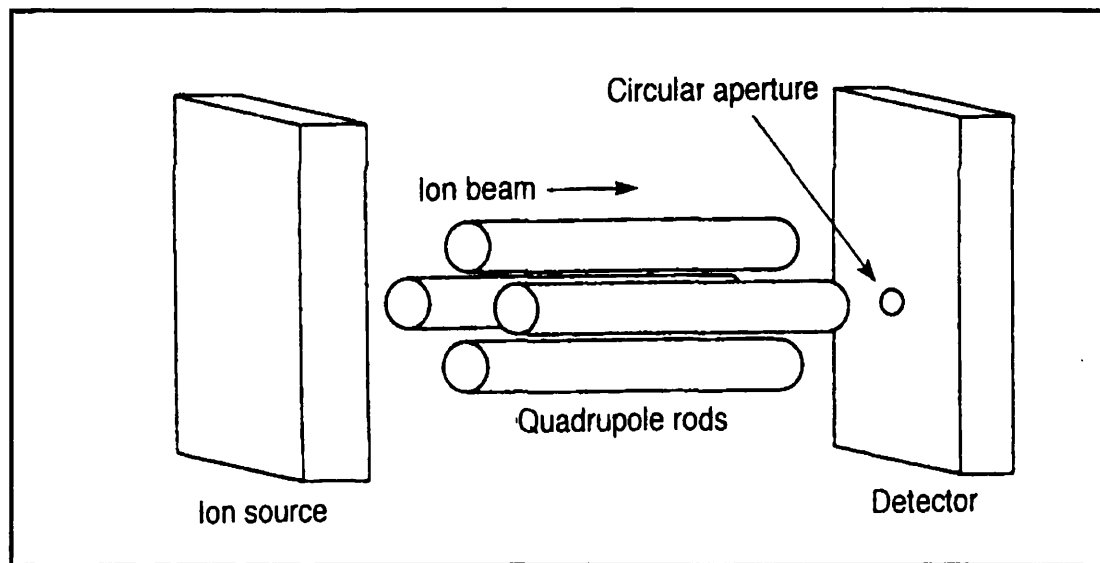


Figure 2.6 – Schematic representation of a quadrupole mass analyser [2]

Diagonally opposite pairs of rods are connected electrically, with one pair attached to the positive terminal of a variable dc source and the other to the negative terminal. In addition, variable RF ac voltages are also applied to each pair of rods.

Ions are extracted from the ion source and accelerated into the central space that constitutes the quadrupole field along the longitudinal axis in the direction of the detector. For any given amplitude of a fixed ratio of RF and dc voltages, ions of only a single m/z value will produce stable oscillations and be successfully transmitted through the quadrupole. All other ions will experience unstable oscillations resulting in collision with the rods where they are neutralised and ejected from the quadrupole. A scan is obtained by increasing the magnitude of the RF and dc voltages such that ions of the next m/z ratio are transmitted and those of the original m/z become unstable until all m/z ratios over a specified range have been transmitted. When the scan is complete the voltages are discharged and set to zero and the process is

repeated. Changes in voltage can be made very quickly and accurately enabling an entire scan to be performed in a fraction of a second.

2.4 - ION DETECTION SYSTEMS [2-8]

Once the beam of separated ions leaves the mass analyser it must then be detected and transformed into a usable signal by a detector. Several different types of detector are available, which may be classified in either of two categories. The direct measurement detectors, such as the photographic plate and the Faraday cup, monitor directly the ions arriving at the detector. This class of detector is essential in the measurement of highly precise isotopic ratios but suffer from limited sensitivity. The second classification, the multiplier detectors such as the electron multiplier, photon multiplier and array type detectors, use electron multiplication to increase the intensity of the signal. Whilst they do not offer the precision of detection of the Faraday cup they allow greater sensitivity and a fast response making them particularly applicable to rapid scanning techniques.

The electron multiplier is at present the detector of choice for most routine experiments and is the arrangement employed in the Finnigan LCQ. The following section describes the operation of the electron multiplier detector while detailed discussion of the other types of detector can be found elsewhere [2,4,5,6,7].

2.4.1 - Electron Multipliers

Electron multipliers can be either discrete or continuous dynode multipliers, both use the principle of secondary-electron emission to effect amplification.

2.4.1.1 - Discrete dynode electron multipliers

The discrete-dynode electron multiplier consists of a series of conversion dynodes with copper-beryllium surfaces held at successively higher voltages. The ion beam from the mass analyser is focused onto the first conversion dynode resulting in the emission of a number of electrons directly proportional to the number of bombarding ions. These secondary electrons are accelerated and focused onto a second dynode again resulting in the emission of electrons. This process is typically repeated several times, resulting in the amplification of the signal. A schematic representation of a discrete dynode electron multiplier is shown in Figure 2.7.

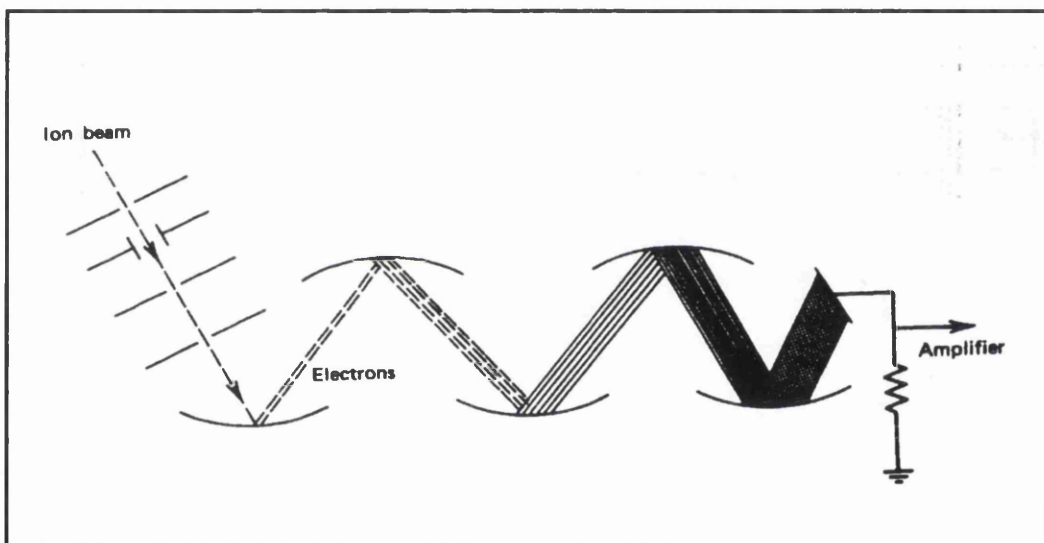


Figure 2.7 – Schematic representation of a discrete dynode electron multiplier [4]

2.4.1.2 - Continuous dynode electron multipliers

The continuous dynode is a cornucopia shaped device made from glass and heavily doped with lead. A schematic representation of a continuous dynode electron multiplier is shown in Figure 2.8.

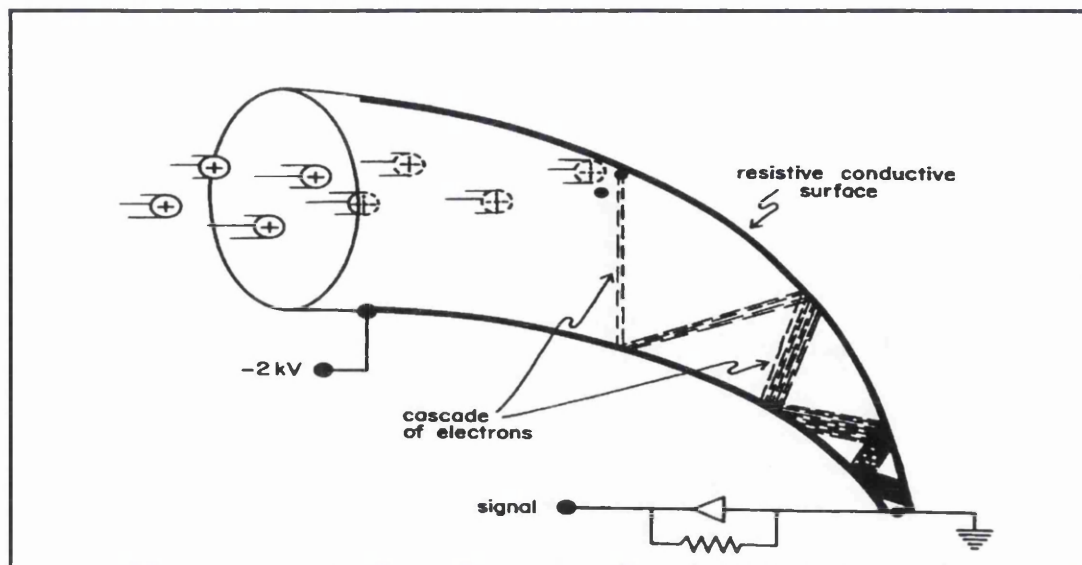


Figure 2.8 – Schematic representation of a continuous dynode electron multiplier [4]

A voltage of up to 2kV is applied across the detector providing an electrical gradient along its length. Ions strike the inner surface of the tube resulting in the emission of a stream of electrons which are attracted along the positive electrical gradient further into the detector. These secondary electrons continue to collide with the wall of the dynode, ejecting more electrons with each impact resulting in the rapid amplification of the signal which is detected at a grounded plate at the end of the cornucopia.

2.5 - THE LCQ –INSTRUMENTATION AND OPERATION [8]

The mass spectrometer used to perform the work discussed in the chapters that follow was the Finnigan LCQ, a benchtop quadrupole ion-trap instrument with MS^n capabilities. The basic principles discussed in the previous sections are generally applicable to the operation of this instrument, but what follows is a more specific description of the operation of the LCQ.

2.5.1 - The API Source

In addition to generating ions the API source also serves as the interface between the LC or CE and the mass spectrometer. It consists of an API stack held under vacuum to which one of two available probe assemblies (ESI or APCI) are attached depending on the mode of ionisation required.

2.5.1.1 - The ESI probe assembly

The ESI probe is able to accommodate sample flow rates of 1-1000 μ l/min without the need for splitting, although sensitivity is generally enhanced if splitting is performed. Where very low flow rates are involved, such as in the case of CE-MS, a sheath liquid can be introduced via a syringe pump to enhance and stabilise the ESI process. A schematic representation of the LCQ ESI probe assembly is shown in Figure 2.9.

The sample is introduced via a short length of 100 μ m id fused silica capillary that extends to the end of the ESI needle, to which a large voltage is applied. As the sample leaves the capillary it is nebulised into a fine aerosol of charged droplets by the coaxial flow of nitrogen gas provided via the sheath and auxiliary gas inlets.

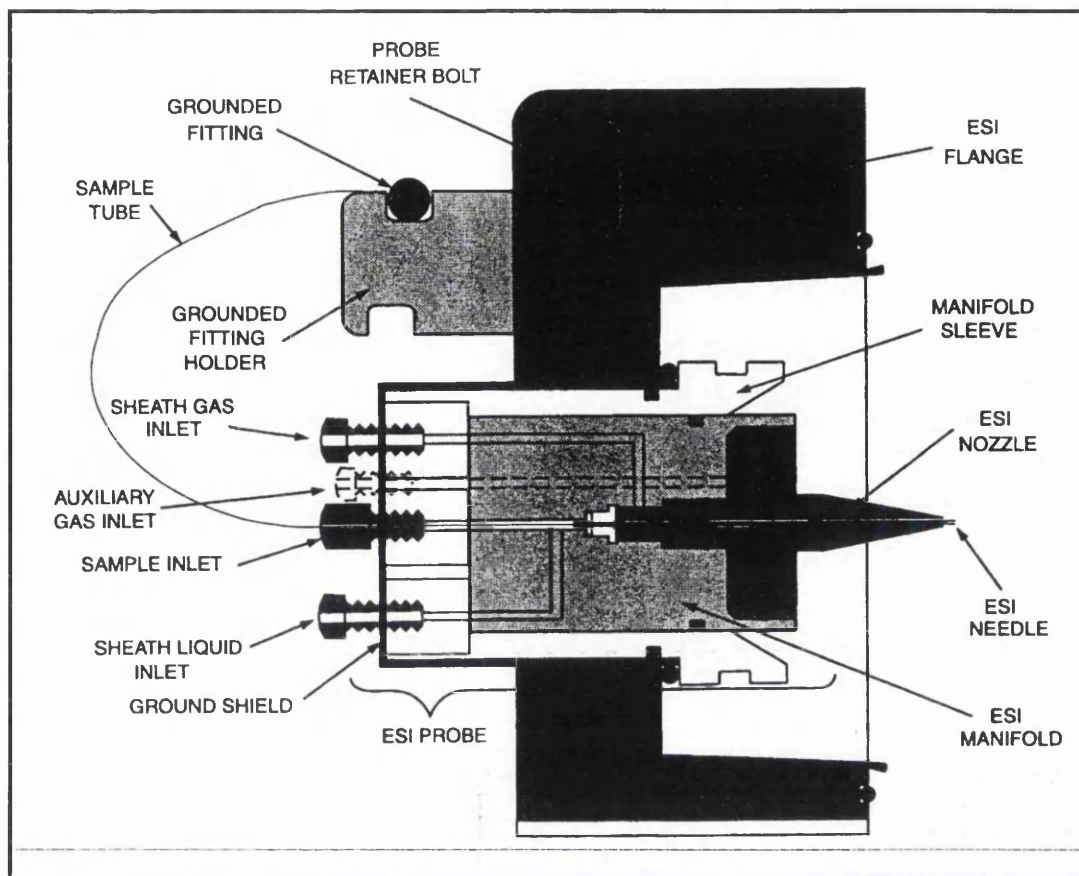


Figure 2.9 – Cross sectional view of the Finnigan LCQ ESI probe assembly [8]

2.5.1.2 - The APCI probe assembly

The APCI probe is able to accommodate sample flow rates of 200-2000 $\mu\text{l}/\text{min}$. With the assistance of the sheath and auxiliary gases the sample is sprayed from the nozzle as a mist of droplets. These droplets enter the vaporiser where they are flash vaporised at temperatures of up to 600°C. This vapour is swept towards the corona needle by the sheath and auxiliary gases where ionisation occurs. A schematic representation of the APCI probe assembly is shown in Figure 2.10.

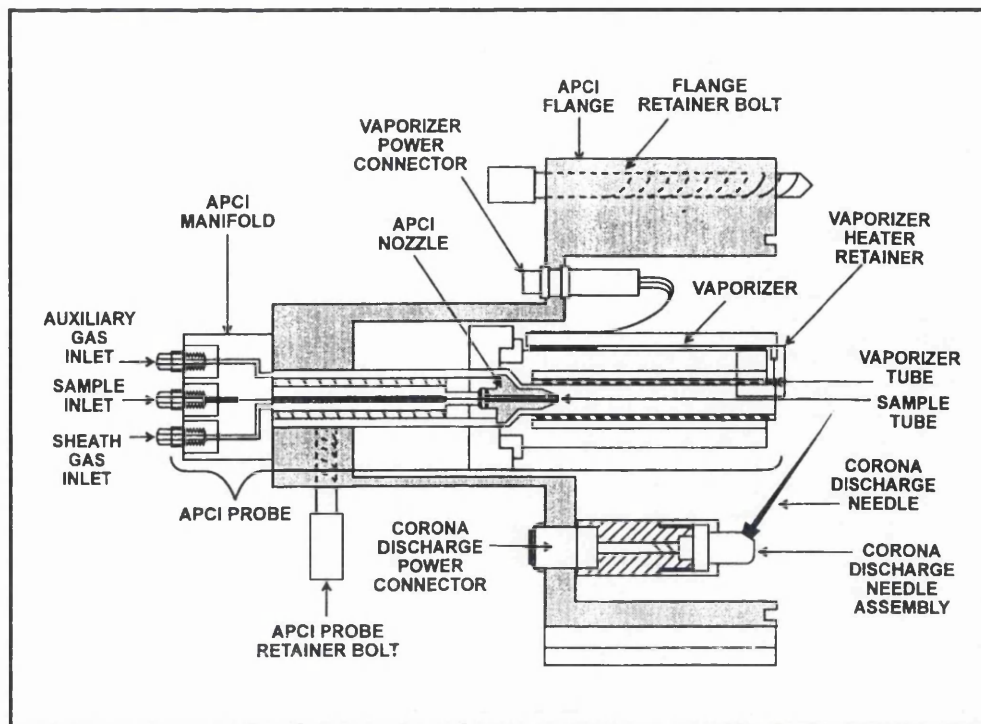


Figure 2.10 – Schematic representation of the Finnigan LCQ APCI probe assembly

[8]

2.5.1.3 - The API stack

The API stack is the section of the source held under vacuum and is responsible for further focusing the ions. The principal components in the API stack are the heated capillary, the tube lens and the skimmer; a diagram of the API stack is shown in Figure 2.11

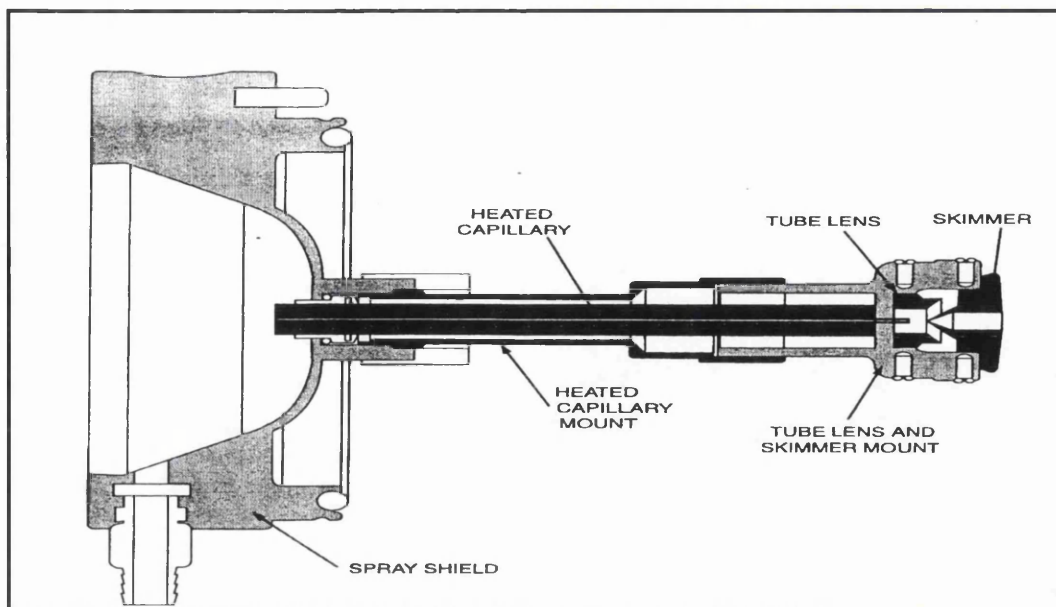


Figure 2.11 – Schematic representation of the Finnigan LCQ API stack [8]

Ions generated by the ESI or APCI source are drawn into the heated capillary where they are exposed to temperatures of up to 300°C. These high temperatures assist in the further desolvation of the ions. As the ions pass from atmospheric pressure into the vacuum region the decreasing pressure gradient and a potential of $\pm 25\text{V}$ applied to the tube lens assist in focusing the ions towards the skimmer region of the stack. The skimmer is at ground potential and acts as a vacuum baffle between the capillary-skimmer region, which is maintained at a pressure of 1 Torr, and the lower pressure region found in the first octapole of the ion optics, which is evacuated to 10^{-3} Torr.

2.5.1.4 - Ion optics

After passing through the skimmer, the beam of ions enters a region of lenses and octapoles which further focus the ions and transmit the ions from the source to the mass analyser. The optics consists primarily of two octapoles separated by the interoctapole lens. An RF voltage and dc voltage are applied to the octapole rods

generating an electric field that guides the ions along the axis of the octapole. The interoctapole lens further focuses the ion beam.

2.5.2 - The Mass Analyser

A diagram of the ion trap mass analyser is shown in Figure 2.12. Ions enter the cavity of the mass analyser via an aperture in the entrance end-cap electrode. In this cavity the ions are subjected to a range of different RF, dc and ac voltages depending on the scan mode selected. These applied voltages bring about the storage, isolation and ejection of the ions. Helium gas also enters the cavity through a nipple on the exit end-cap electrode and acts as a damping gas significantly enhancing the sensitivity and mass spectral resolution. When the appropriate voltage is applied ions are ejected from the trap via the exit end-cap electrode.

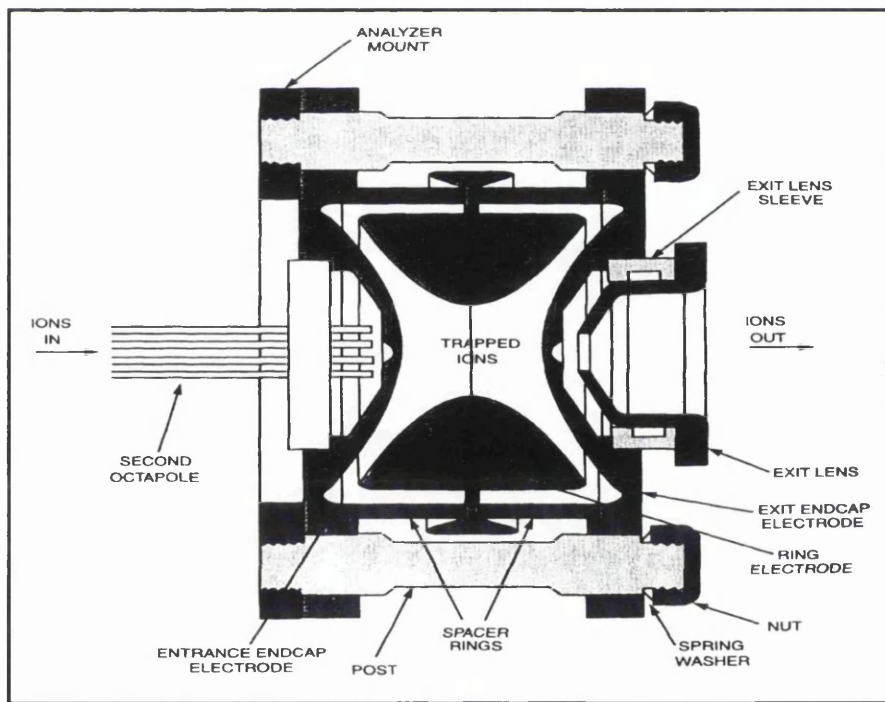


Figure 2.12 – Cross sectional view of the Finnigan LCQ mass analyser [8]

2.5.3 - The Ion Detection System

The LCQ is equipped with an off-axis ion detection system comprising a conversion dynode and an electron multiplier and is located to the rear of the mass analyser. Ions are ejected from the mass analyser and focused onto the surface of the conversion dynode positioned at right angles to the ion beam. A potential of +15kV for negative ion detection or -15kV for positive ion detection is applied to the dynode. When the ions strike the surface of the dynode one or more secondary particles are produced, these are focused by the curved surface and accelerated by a voltage gradient into the electron multiplier.

The electron multiplier is mounted on the top cover plate of the vacuum manifold adjacent to the mass analyser. Its principal components are an anode and a cathode to which a voltage of +2.5kV is applied. The secondary particles generated by the conversion dynode strike the inner wall of the cathode resulting in the ejection of electrons. These ejected electrons are drawn further into the cathode and continue to strike the inner surface of the cathode resulting in the emission of more electrons. This cascade of electrons is collected at the anode located at the exit end of the cathode. The current collected at the anode is proportional to the number of secondary particles striking the cathode and is converted to a voltage by the electrometer and recorded by the data system. A schematic representation of the ion detection system is shown in Figure 2.13.

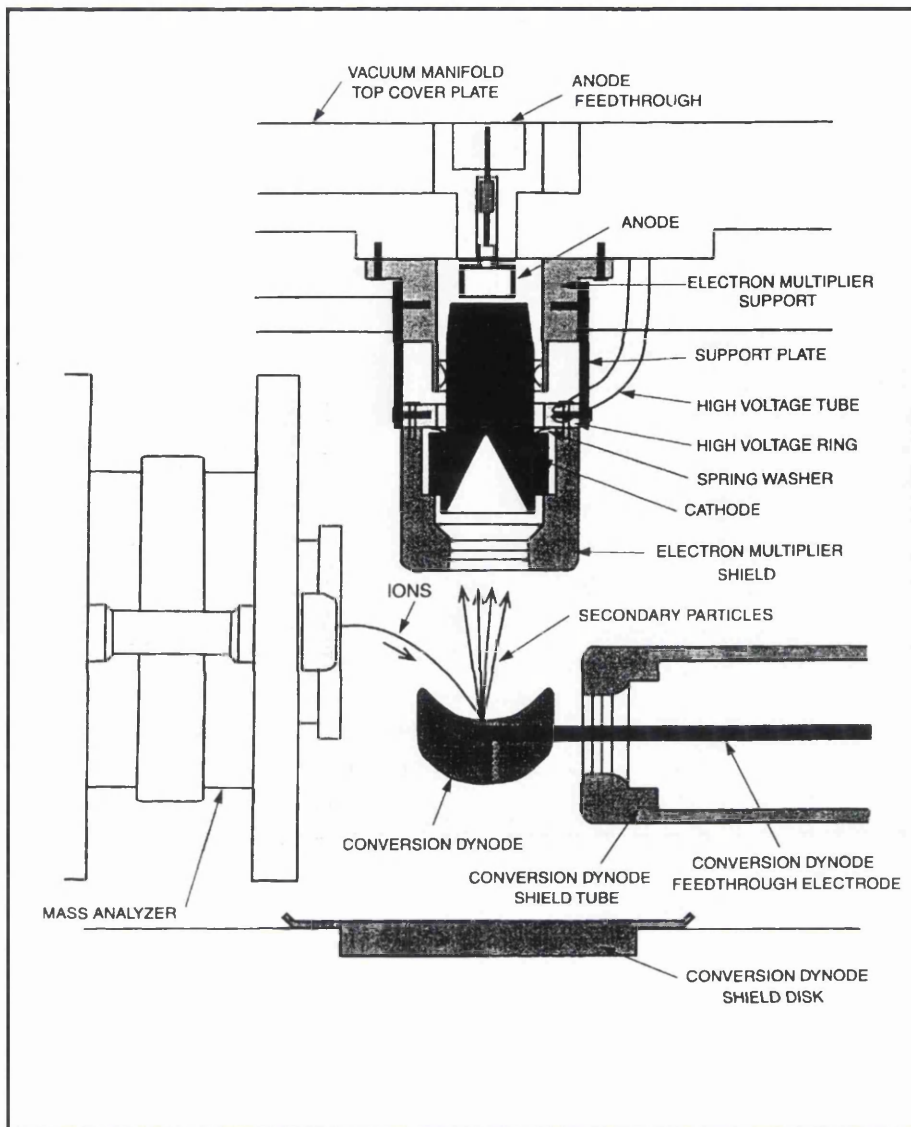


Figure 2.13 – Schematic representation of the Finnigan LCQ ion detection system

[8]

2.6 - SCAN MODES [8]

A number of different scan modes are available with the LCQ each with specific areas of application. The following sections give a brief overview of each of the modes of operation.

2.6.1 - Full scan MS

Full scan MS mode uses a single stage of mass analysis with no fragmentation taking place. The mass analyser is scanned over a selected m/z range without interruption to produce a full mass spectrum of each analyte. This mode is particularly useful in the determination of the molecular weights of unknown compounds.

2.6.2 - Full scan MS/MS

Full scan MS/MS uses two stages of mass analysis and results in the production of a product ion mass spectrum for a single selected precursor ion. Ions generated by the source are introduced into the mass analyser and stored. Ions of one selected m/z are isolated while all other ions are ejected; the selected ions are then excited and undergo collisions with the helium gas present in the trap. These collisions result in fragmentation of the precursor ions and the resultant product ions are sequentially scanned out of the mass analyser, detected and recorded. Information regarding the structure of an analyte may be obtained through this mode.

2.6.3 - Full scan MSⁿ

MSⁿ allows up to ten stages of mass analysis to be performed; as in MS/MS precursor ions of a single specified m/z are isolated in the trap and involved in

collisions with helium causing them to fragment and produce product ions. In the second stage product ions of one selected m/z ratio are selected to become the ‘new’ precursor ions, while all other ions are ejected from the trap. These ‘new’ precursor ions are excited and undergo collisions to produce further product ions which are then stored in the trap. This process can be repeated up to seven more times until the product ions of interest are produced. At the n th stage of mass analysis, the final product ions are sequentially scanned out of the mass analyser to produce a product ion mass spectrum.

2.6.4 - Selected ion monitoring (SIM)

In SIM a single stage of mass analysis is used to monitor only a single specified ion. Ions of the selected m/z are stored in the mass analyser while all other ions are ejected. The selected ions are then scanned out of the ion trap to produce a SIM mass spectrum. This mode of operation is particularly useful in trace analysis where a small amount of a known target compound is present in a complex mixture. As only specific ions are monitored, detection limits can be improved and analysis times can be reduced.

2.6.5 - Selected reaction monitoring (SRM)

SRM uses two stages of mass analysis to monitor precursor ion and product ion pairs. Like SIM this technique offers rapid analysis times and is particularly useful in trace analysis. However, because SRM monitors a pair of ions the specificity obtained is much greater than that possible with SIM. SRM is achieved by first isolating the selected precursor ion in the analyser and ejecting all other ions from the trap, these precursor ions are then excited and undergo collisions with the

helium gas present within the trap, resulting in the formation of one or more product ions. Of these product ions a single m/z is selected and isolated before being scanned out of the analyser to produce an SRM product ion mass spectrum.

2.6.6 - Consecutive reaction monitoring (CRM)

CRM is the multi-stage analogue of SIM and SRM in which a multi-step reaction path is monitored. The first two stages of mass analysis again involve the isolation and fragmentation of a selected precursor ion followed by the selection and isolation of a single product ion. This selected product ion undergoes collisions to produce further product ions and the process is repeated up to seven more times until the selected n th product ion is isolated and scanned out to produce a CRM final product ion mass spectrum. Specificity can be further increased with the use of CRM but suffers from decreasing sensitivity as the number of reactions monitored increases.

2.6.7 - ZoomScan™

ZoomScan is a high-resolution scan mode that allows the determination of the charge state and molecular weight of an ion when only the m/z ratio is known. This is achieved by evaluation of the differences between ^{12}C and ^{13}C isotopic peaks for a specified ion.

REFERENCES CITED IN CHAPTER 2

1. Mass Spectrometry Desk Reference. O. David Sparkman. Global View Publishing. (2000).
2. Mass Spectrometry: Analytical Chemistry by Open Learning. James Barker. John Wiley and Sons. (1999).
3. Principles of Instrumental Analysis. Douglas A. Skoog and James J. Leary. Saunders College Publishing. (1992).
4. Introduction to Mass Spectrometry. J. Throck Watson. Lippincott-Raven. (1997).
5. Mass Spectrometry – Principles and Applications. E De Hoffmann, J Charette and V Stroobant. John Wiley and Sons. (1986)
6. Mass Spectrometry for Chemists and Biochemists. Robert A.W. Johnstone and Malcolm E. Rose. Cambridge University Press. (1996).
7. Back To Basics CD-ROM. Micromass. (2000).
8. Finnigan MAT: LCQ MS Detector Operator's and Service Manual.
9. Electrospray: Principles and Practice. Simon J Gaskell. *J. Mass Spectrom.* **32**, (1997), 677-688
10. Molecular Beams of Macroions. M Dole, RL Hines, RC Mack, RC Mobley, LD Ferguson and MB Alice. *J. Chem. Phys.* **49**, (1968), 2240-2249
11. Electrospray interface for liquid chromatographs and mass spectrometers. CM Whitehouse, RN Dreyer, M Yamashita, JB Fenn. *Anal. Chem.* **57**, (1985), 675-679
12. Atmospheric-pressure-ionization mass spectrometry. II. Applications in pharmacy, biochemistry and general chemistry. AP Bruins. *Trends in Analytical Chemistry* **13**, (1994), 81-90

13. An Introduction to Quadrupole Ion Trap Mass Spectrometry. Raymond A March. *J. Mass Spectrom.* **32**, (1997), 351-369

Chapter 3

CE and CE-MS Studies of Paraquat and Related Impurities

3.1 - OBJECTIVE

As has been previously discussed in Section 1.4, growing concern for the environment and the resulting increase in legislation has emphasised the need for improved characterisation and detection of low level impurities. The analysis of paraquat has been reported widely, largely in combination with other quaternary ammonium herbicides and this is detailed in Section 1.5.1.4. No reports describing the analysis of paraquat and its impurities were found. The use of CE as an analytical technique continues to grow, and has shown significant growth in the area of pesticide analysis over recent years [1]. A graphical illustration of the increase in the number of publications in this area can be seen in Figure 3.1. The data represented in this graph was obtained from a BIDS literature search covering the years 1981 to 2000 using the keywords '*capillary electrophoresis*' and '*pesticide*'.

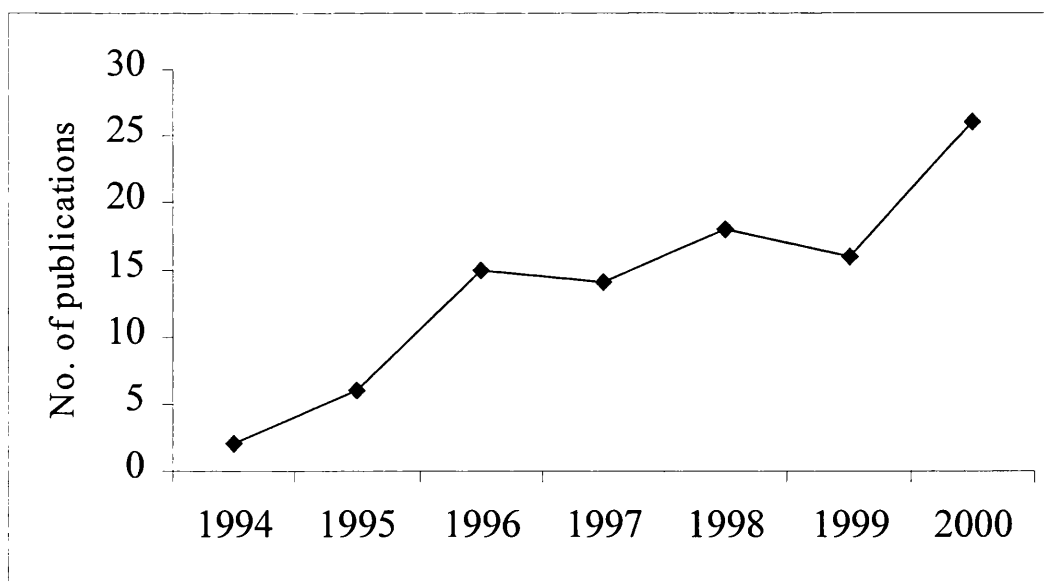


Figure 3.1 – Graphical representation of the trend in the use of CE for pesticide analysis 1981 – 2000

The purpose of this study is to evaluate the use of capillary electrophoresis and its related techniques in improving the separation and determination of paraquat and its impurities. The structures of the study compounds are shown in Table 3.1.

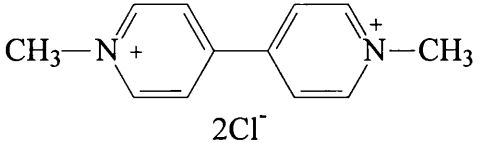
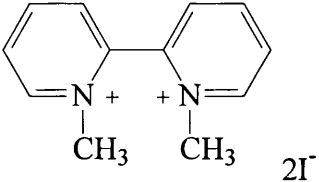
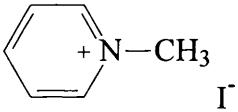
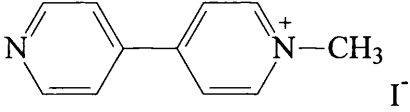
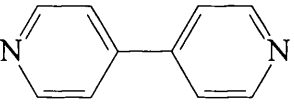
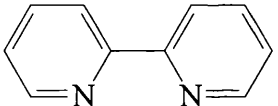
Structure	Abbreviation	Compound name
	PQ	Paraquat Dichloride
	22PQ	2,2'-Paraquat Di-iodide
	NMP	N-Methyl Pyridinium Iodide
	MQ	Monoquat Iodide
	44BP	4,4'-Bipyridyl
	22BP	2,2'-Bipyridyl

Table 3.1 – Structures of paraquat and related impurities studied in Chapter 3

3.2 – INTRODUCTION [2-8]

Electrophoresis can be simply described as the migration of charged substances in solutions under the influence of an applied electric field. The technique has been used to perform separations for over a century with the earliest experiments being carried out using glass U-tubes filled with gel-like substances. The use of solid support materials such as cellulose, paper and silica gel was introduced in the 1930s and although this technique is still widely used in the analysis of biological macromolecules using slabs of polyacrylamide gel it is labour intensive, difficult to automate and produces low efficiency separations. Throughout the 1960s and 70s, further improvements were made with developments by Hjerten in 1967 [9] and Mikkers in 1979 [10], but it was not until the early 1980s that the major breakthrough was made. It is widely acknowledged that the work of Jorgenson and Lukacs [11-12] was the first work to demonstrate the potential of the technique we know today as capillary electrophoresis. The years that followed saw a huge growth in research in the field of CE with several major developments and numerous improvements to performance and detection being made [13]. Just 20 years after its development CE is a well established and widely used technique. The combination of the separation mechanism of electrophoresis with the automation possibilities of HPLC has produced a powerful analytical technique used in the analysis of amino acids, peptides and proteins, pesticides, pharmaceuticals, organic acids, inorganic ions and even whole cells and virus particles.

3.3 - ELECTROPHORETIC THEORY [2-6]

Electrophoretic separations are based on the different migration velocities of charged species as they migrate through a buffer under the influence of an electric field. The relationship between these parameters is described by the equation below:

$$\mu_{ep} = \frac{v_{ep}}{E} = \frac{L_d / t_m}{V / L_t}$$

Equation 3.1

Where μ_{ep} = apparent electrophoretic mobility
 v_{ep} = electrophoretic velocity
 E = applied electric field
 L_d = length of capillary to detector
 t_m = migration time
 L_t = total length of capillary
 V = applied voltage

Electrophoretic mobility can also be expressed as follows:

$$\mu_{ep} = \frac{q}{6\pi\eta r}$$

Equation 3.2

Where q = net charge on the ion
 η = buffer viscosity
 r = stokes radius of the ion

Electrophoretic mobility is dependent on the ion shape but for the above equations, it is assumed that the ions are spherical and do not interact with other ions in the solution. From Equation 3.2, it is evident that those species with high charge-to-size ratios will have high electrophoretic mobilities and will therefore, for a given electric field and buffer system, have a high velocity.

The above formulae are useful only in determining the apparent mobility. In order to calculate the effective mobility the phenomenon of electroosmotic flow (EOF) must be taken into consideration. EOF is the bulk flow of liquid through an electric field and is of fundamental importance in CE as it is this phenomenon which allows both anionic and cationic species to be separated and analysed simultaneously. Were it not for EOF charged species would only migrate in the direction of the electrode with the opposite charge to itself, while neutral species with zero electrophoretic mobility would remain stationary. With the presence of the EOF (and under normal conditions), cationic species migrate the fastest, followed by the neutrals and finally the anions. Although the anions are attracted to the anode, the magnitude of the EOF still carries them towards the cathode. The process of this differential solute migration on the basis of size and charge is shown schematically in Figure 3.2.

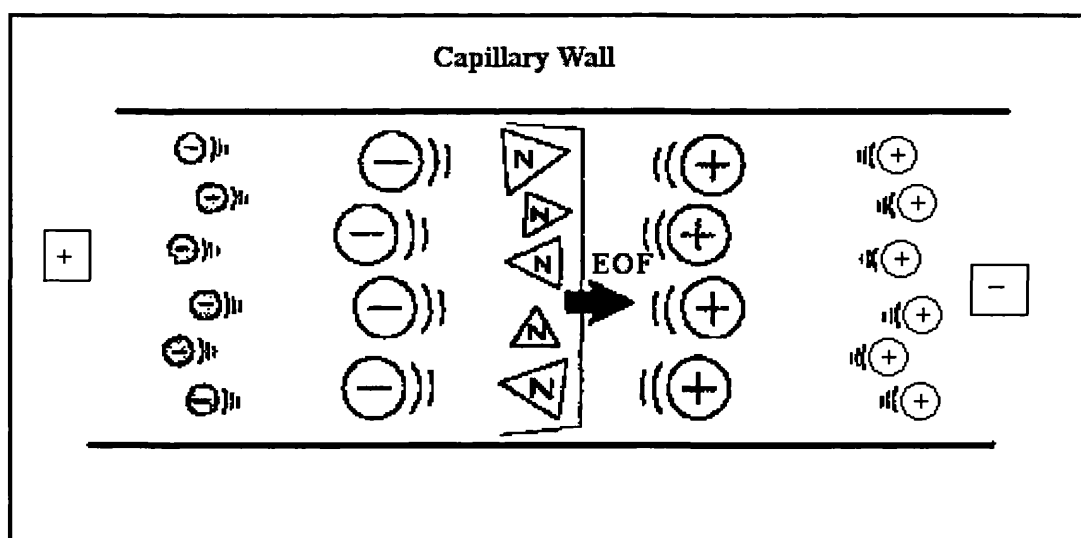


Figure 3.2 - Differential solute migration in capillary electrophoresis

EOF results from the charge that is produced on the inner walls of the capillary in the presence of buffer. Under aqueous conditions and at pH levels greater than 2, the surface silanol (Si-OH) groups found on the internal walls of the

fused silica capillary become ionised to produce anionic silanoate (Si-O^-) groups. Cations from the buffer are absorbed onto the negatively charged capillary surface by electrostatic attractions, balancing the surface charge and creating an electrical double layer. Between the inner and outer layers a potential difference is generated, this is known as the zeta potential, ξ .

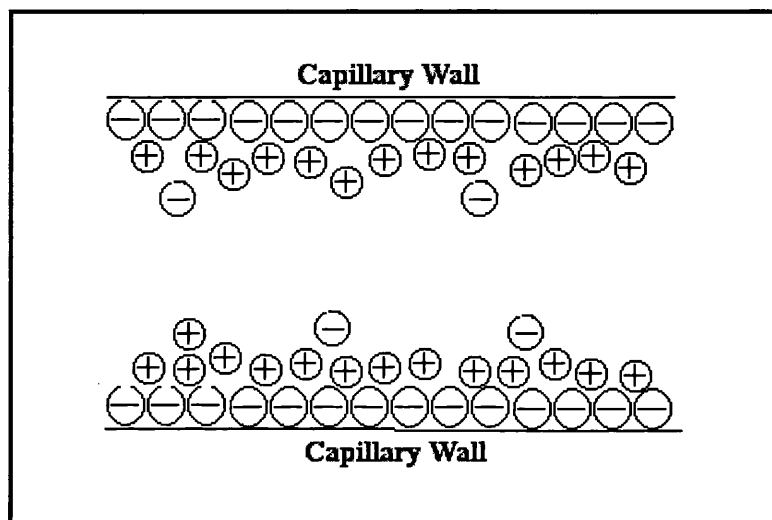


Figure 3.3 - Schematic representation of double layer formation in capillary electrophoresis

In the presence of an applied electric field the cations in the outer layer are attracted towards the negative electrode and because these cations have solvation spheres the bulk of the solution is dragged behind them producing the flat flow profile shown in Figure 3.4.

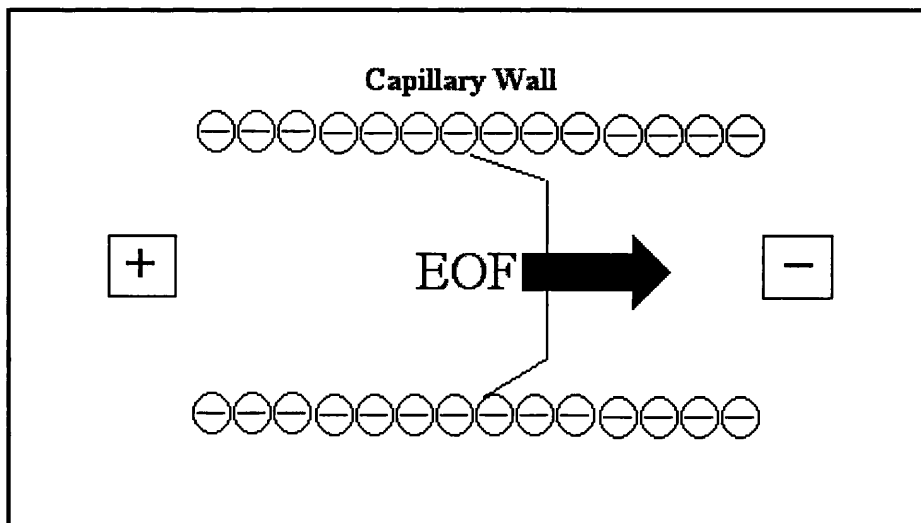


Figure 3.4 - Schematic representation of the electroosmotic flow (EOF) profile generated in capillary electrophoresis

This flat profile is unique to EOF and unlike the hydrodynamic flow produced by an external pump, as in HPLC, the flow is almost uniform throughout the capillary. Consequently EOF does not contribute to band broadening and results in greater efficiency.

The EOF can be defined as:

$$v_{eo} = \left[\frac{\varepsilon\xi}{4\pi\eta} \right] \times E$$

Equation 3.3

Where

- v_{eo} = velocity of EOF
- ε = dielectric constant
- ξ = zeta potential at the capillary wall
- η = buffer viscosity
- E = applied electric field

In order to calculate the EOF a neutral marker, such as methanol or acetone, can be injected and the time taken to reach the detector measured. While the EOF is for the most part beneficial, for certain modes of CE, such as CIEF, CITP and CGE it is necessary to suppress the EOF. Fundamentally, control of EOF requires alteration of the capillary surface charge or the buffer viscosity. Several manufacturers now produce bonded capillaries coated with phases that claim to reduce or eliminate EOF altogether; these coated capillaries also have the added advantage of reducing solute-wall interactions and therefore offer improved efficiency [14-16]. EOF reduction may be accomplished in a number of other ways, several of which are summarised in Table 3.2.

• Decrease electric field	Results in a decrease in efficiency and resolution and increases analysis times
• Decrease buffer pH	Protonates silanol groups and results in a decreased zeta potential
• Decrease operating temperature	Increases buffer viscosity ∴ decreases EOF
• Increase buffer concentration	Results in double-layer decompression and decreased zeta potential
• Addition of organic modifier to buffer	Changes zeta potential and viscosity

Table 3.2 – Summary of methods used to reduce EOF in CE

3.3.1 - Efficiency

The term efficiency describes the ability of a system to separate analytes and is dependent on dispersion effects which cause the broadening of analyte zones. The combination of the flat flow profile generated by the EOF and the absence of a stationary phase help to make the technique of capillary electrophoresis the most

efficient of the chromatographic methods. As with the other chromatographic techniques the efficiency of a CE system can be measured in terms of the number of theoretical plates, N , achieved by the capillary. Experimentally, N can be calculated from an electropherogram, see Figure 3.5, using either of the following equations:

$$N = 16 \times \left[\frac{t}{w} \right]^2$$

Equation 3.4

$$N = 5.54 \times \left[\frac{t}{w/2} \right]^2$$

Equation 3.5

Where t = migration time of the component
 w = temporal peak width at the base line
 $w/2$ = temporal peak width at half the peak height

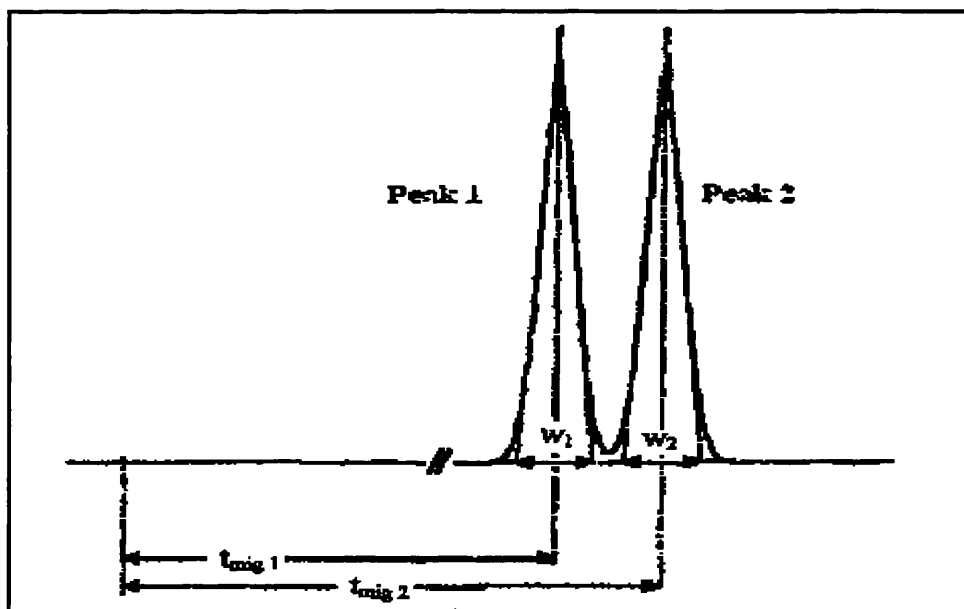


Figure 3.5 - A two component electropherogram showing the definitions of various parameters

Although plate numbers as high as 10^6m^{-1} have been recorded for open tubular systems, CE separations are still susceptible to band broadening resulting from a number of different factors.

- Joule Heating

The phenomenon of Joule heating arises when a current is passed along a capillary. As a consequence of this heat generation the temperature within the capillary increases. As the heat is dissipated, a temperature gradient is generated across the capillary with the temperature at the centre of the capillary being higher than the temperature at the walls. Consequently, the viscosity of the buffer at the centre of the capillary will be lower than at the walls producing a flow profile resembling hydrodynamic flow and resulting in band broadening. This factor can be minimised by the use of narrow bore (25 - 100 μm) capillaries, which allow the heat generated to be more readily dissipated.

Ineffective heat dissipation is also a problem, if the heat is not removed at a rate equal to its production the temperature will rise. The use of narrow bore capillaries assists in this process but the incorporation of cooling systems into CE instruments is the most effective means of heat removal and temperature control.

- Adsorption

Solute-wall interactions are detrimental to the CE separation, resulting in moderate cases in band broadening and peak tailing and in more extreme cases the total adsorption of the analyte may occur. The primary causes of adsorption are the ionic interactions between cationic solutes and the negatively charged capillary wall and hydrophobic interactions. Many approaches have been employed in overcoming this problem. Amongst the simplest of these is to select a buffer pH such that the analyte and the capillary wall have the same charge, i.e.

< 2 to 3 or > 9 to 10. Increasing the concentration of the buffer also decreases adsorption by reducing the effective surface charge. The use of capillary coatings is a particularly useful method of decreasing solute-wall interactions. By coating the silica walls with buffer additives, such as hydrophilic polymers or detergents, the charge on the wall can be reversed or eliminated and as a result decreases adsorption.

- Sample Injection Width

The injection width of the sample is the most important extrinsic contribution to band broadening. If the plug length is greater than the dispersion caused by diffusion both efficiency and resolution will suffer. The practical limit of injection length is less than 1 to 2% of the total capillary length; however, typical conditions often require longer injection lengths to achieve the desired detection limits. Several methods are available which allow the use of increased injection times and hence improved detection limits while maintaining peak efficiency.

3.3.2 Resolution

Resolution is the term used to describe the degree of separation of one sample component from another and can be determined directly from the electropherogram using the following equation:

$$R_s = \frac{2(t_{m2} - t_{m1})}{(w_1 + w_2)}$$

Equation 3.6

A resolution of 1.0 corresponds to a peak overlap of about 4% with higher R_s values representing progressively smaller overlaps. Resolution values of greater than 1.2 are desirable, with a value of 1.5 representing an almost complete separation.

3.4 – INSTRUMENTATION [2-7]

In order to perform capillary electrophoresis, a system comprising five basic components is required:

- Inlet and outlet vials
- Anode and cathode electrodes with a high voltage power supply
- Capillary
- Injection system
- Detector attached to a data handling system

In general, commercially available instruments often have additional features such as autosamplers and thermostatted capillary compartments.

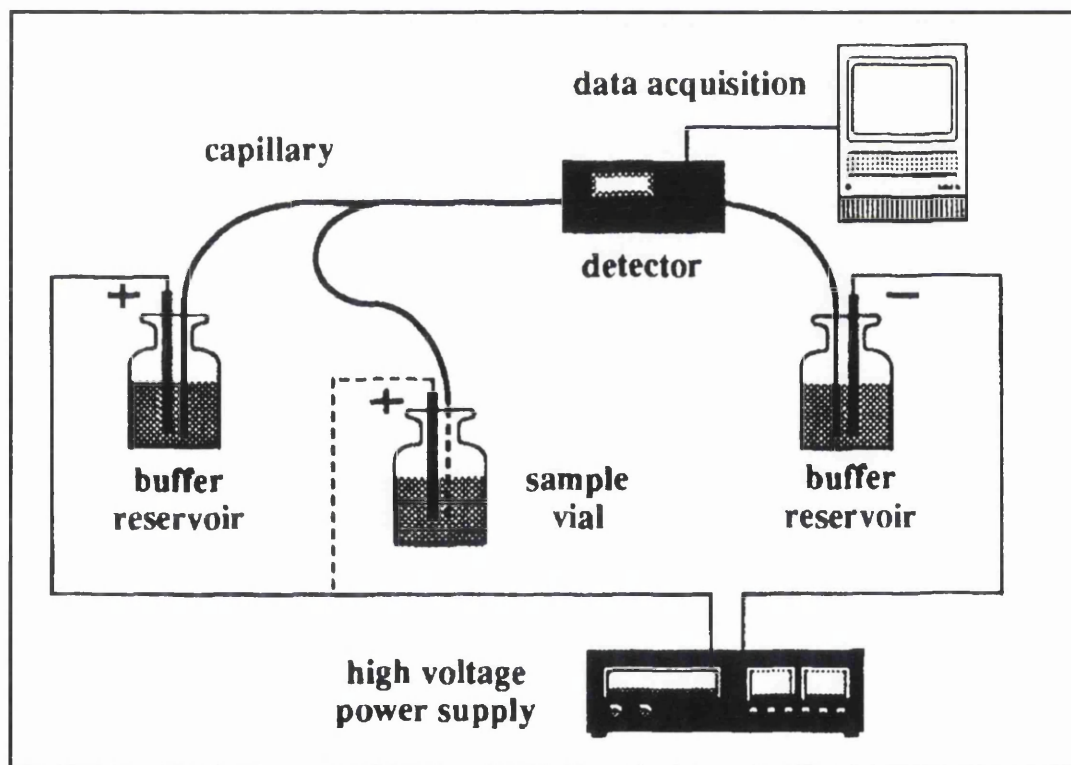


Figure 3.6 - Instrumental set up of a capillary electrophoresis system

The paragraph below describes the basic set-up and operation of a simple instrument comprising the five listed components; in addition, sample introduction and methods of detection are discussed further in sections 3.4.1 and 3.4.2.

A diagram of the basic set-up is depicted in Figure 3.6. The capillary is typically fused silica of between 25 and 200 μm internal diameter, and up to a metre in length, coated externally with polyimide to improve strength and robustness. A small section of this coating must be removed in order to provide a UV transparent window for detection. The capillary is filled with electrolyte, generally an aqueous buffer, and placed between two electrolyte reservoirs. One end of the capillary is moved into the sample vial and the sample is introduced either by electromigration or by hydrodynamic flow. The capillary is returned to the inlet buffer reservoir and a voltage of up to 30kV is applied between the anode and cathode. As the separated sample zones migrate through the capillary they pass the optical window and detection takes place. Output from the detector is sent to the data system and displayed as an electropherogram.

3.4.1 - Sample Introduction

Sample loading is a major consideration in CE, in order to maintain highly efficient separations band broadening must be avoided. Theory suggests that the sample should be injected in as small a volume as possible, generally in the range of 5-50nl. However, in practice the sample plug length is of greater importance than the actual volume and should generally be less than 1% of the total length of the capillary. In order to achieve optimum resolution and peak shape sample overloading should be avoided with the concentration of the injected sample

approximately 100 times less than that of the electrolyte. Reproducibility of sample injection has been greatly improved with the advent of automated CE systems allowing small sample volumes to be introduced with acceptable standard deviations. Several injection systems have been developed but the two most widely used techniques, and those present in the majority of commercially available instruments, are hydrodynamic injection and electrokinetic injection.

3.4.1.1 - Hydrodynamic Injection

Hydrodynamic sample introduction is achieved by applying a pressure difference along the length of the capillary and can be performed by one of three methods:

- applying a high pressure to the inlet end
- applying a vacuum at the outlet end
- using gravity to generate a hydrostatic pressure.

The volume of sample introduced via the high pressure and vacuum modes of injection can be determined using Poiseuille's equation for liquid flow in a circular tube:

$$V_i = \frac{\Delta p \cdot \pi \cdot r^4 \cdot t}{8 \eta \times L_T}$$

Equation 3.7

Where V_i = injection volume
 Δp = pressure difference
 r = inner radius of capillary
 t = injection time
 η = viscosity
 L_T = total capillary length

It can be seen from Equation 3.7 that variation of the injection time and/or the pressure difference will result in a change in injection volume. In practice the duration of the injection must be kept as short as possible in order to minimise the effect of siphoning. Providing that the variables in equation 3.7 remain constant this technique will produce reproducible injection volumes with an RSD of between 2-3% [7].

If siphoning is used to generate a hydrostatic pressure injection the pressure difference can be defined as:

$$\Delta p = \rho \cdot g \cdot \Delta h$$

Equation 3.8

Where ρ = density of sample solution
 g = gravitational acceleration
 Δh = height difference between liquid levels of vials

In this case, the sample volume is dependent on injection time and on the difference in heights of the sample and buffer vials. This technique suffers from poor reproducibility with an RSD of approximately 10% where manual injections are performed, but can be improved to 2% or better with the use of automated systems [7].

3.4.1.2 - Electrokinetic Injection

Electrokinetic injection is achieved by applying a voltage between the sample vial and the outlet for a short time. This results in sample being introduced onto the capillary by electroosmotic flow and electrophoretic migration. Unlike

hydrodynamic injection, which displays no bias in sample loading, the quantity of each analyte introduced is dependent on its electrophoretic mobility with those species with high mobilities being loaded to a greater extent than those with lower mobilities. The amount of each component, i , injected can be determined by the following equation:

$$Q_i = \frac{(\mu_i + \mu_{eo}) \cdot \pi \cdot r^2 \cdot V \cdot c_i \cdot t}{L_T}$$

Equation 3.9

Where

- Q_i = amount of species i introduced into the capillary
- V = voltage
- μ_i = electrophoretic mobility
- μ_{eo} = electroosmotic mobility
- r = inner radius of capillary
- c_i = concentration of species i
- t = injection time
- L_T = total capillary length

Although electrokinetic injection is the simplest to perform it suffers from the problem of sample bias and the resulting detrimental effect on reproducibility, consequently hydrodynamic sample introduction is the preferred technique. In spite of its disadvantages, electrokinetic injection is used extensively, particularly in capillary gel electrophoresis and where very viscous samples are under analysis.

3.4.1.3 - Other Methods of Injection

Other sample introduction techniques developed include rotary type systems similar to those used in HPLC, split flow syringe injectors and microinjector devices. Although all of these techniques have numerous advantages over the aforementioned methods of injection, including fixed reproducible injection volumes, all require

Chapter 3 CE and CE-MS Studies of Paracetamol and Related Impurities 15

elaborate constructions to prevent sample overloading and the introduction of dead volumes. The popularity of these techniques may increase if significant advances in miniaturisation are made as such systems may lead to improvements in separation efficiencies.

3.4.2 - Detection

The development of a highly sensitive, universal, low cost detection system remains the greatest technical problem in CE. The most important requirements are:

- small volume detection cell
- small contribution to peak width
- high sensitivity
- large dynamic range
- fast detector response
- good resistance against temperature changes
- reliable and convenient ease of use
- selective detection
- non-selective detection

Obviously there is no perfect detector which fulfils all these requirements, consequently a variety of detection techniques are currently used in CE each with its own advantages and area of application. The following sections will concentrate on the two techniques used throughout the course of my work, UV-VIS Absorbance and Mass Spectrometry. In addition, a further section will give a brief overview of other widely used methods of detection.

3.4.2.1 - UV-Visible Absorbance Detection

In spite of its low sensitivity in comparison with other techniques, detection by UV-VIS absorbance remains the most widely used method of detection in CE. The technique is based on the absorbance of UV or visible light described by the Beer-Lambert Law, see Equation 3.10. In addition to its ease of use, it is sensitive to a wide range of compounds and functional groups.

$$A = \epsilon \cdot c \cdot l$$

Equation 3.10

Where A = absorbance
 ϵ = molar absorptivity
 c = concentration
 l = cell path length

An optical window is created in the fused silica by removing a small area of the polyimide coating; this is typically performed by burning, etching or scratching. Because detection takes place ‘on-capillary’ band broadening is avoided and consequently high efficiencies are maintained. Unfortunately, the short path length available (i.e. the internal diameter of the capillary) greatly limits the achievable levels of sample detection. Attempts have been made to improve sensitivity by extending the path length. The use of modified capillaries such as extended light path bubble capillaries [17] and Tsuda’s rectangular capillaries [18] is described in greater detail elsewhere [2-7]

The majority of commercially available instruments use modified HPLC UV-VIS detectors typically employing high intensity deuterium lamps with either a filter system or monochromator used to select the desired wavelength. A schematic

diagram of a detection system similar to that employed in the instrument used during the course of my studies, the Beckman P/ACE 2200, is shown in Figure 3.7.

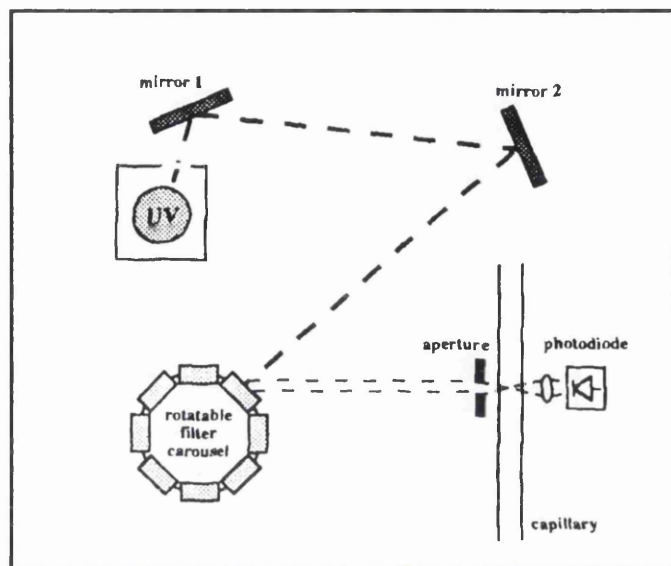


Figure 3.7 - Schematic representation of a variable wavelength UV-Vis detector [2]

The detection system shown is typical of what is known as a Variable Wavelength Detector or VWD. The beam of light is focused by a pair of mirrors onto a filter where a specific wavelength is isolated. The beam is then directed through the detection cell of the capillary and on to a photodiode which produces an electrical response proportional to the intensity of transmitted light.

An alternative to the single beam VWD type detector is the Diode Array Detector or DAD. This technique utilises a system of lenses to focus light into the detection cell; the transmitted light is then dispersed by a polychromator before falling onto the photodiode-array. This arrangement of several diodes allows detection over a whole wavelength range within a single run, which is highly advantageous when developing new methods.

3.4.2.2 - Mass Spectrometric Detection [2,19-22]

The use of mass spectrometry as a means of detection is desirable for a number of reasons, but foremost is its ability, as a 'universal' detector, to detect all samples within the mass range of the instrument. In addition, the technique also provides both good sensitivity and selectivity, particularly when used in SIM mode. The combination of the high efficiency separation of CE and the capability of mass spectrometry to identify unknown compounds is potentially a very powerful technique. Consequently, an enormous amount of research has been carried out in the field of CE-MS interfacing.

In developing an interface for CE-MS several factors must be considered:

- in the absence of a buffer vial at the interface end of the capillary an electrical connection must be achieved in some other way;
- buffer composition must be considered, the presence of non-volatile components present in many commonly used CE buffers can result in contamination of the interface and ion source;
- the low flow rates generated in CE, typically in the range 0.01-0.1 μ l/min are too low for stable operation of most ion sources which generally require flows of 2-5 μ l/min.

The majority of CE-MS work performed to date has employed either electrospray (ESI) [23-28] or continuous-flow fast atom bombardment (CF-FAB) [29-30] as the ionisation technique and in general three main approaches to interfacing have emerged. The first is the liquid junction type interface, in which the CE capillary is connected, via a tee-junction, to a transfer line which is itself coupled

to the mass spectrometer. In this case, a make-up flow of running buffer is added at the liquid junction. The co-axial type interface employs a sheath capillary through which the capillary is threaded and is surrounded by a flow of sheath liquid which provides the electric contact at the cathode end of the CE capillary. The most recently developed type of interface involves no make up liquid and maintains the electrical circuit by means of a metal-coated CE tip. The development of these 'sheathless' interfaces has resulted in significant improvements in sensitivity and as a consequence this is likely to be an area of focus in the coming years.

The section below discusses in detail the Coaxial Electrospray interface, further discussion of the other interfaces can be found elsewhere [2,5,19-22,29,30].

3.4.2.2.1 - Coaxial ESI Interface

The very first on-line combination of CE with MS was performed by Olivares et al in the late 1980s. This first interface was based on an LC-MS interface and electrical contact was provided initially via a single needle [23] and later by metallising the capillary terminus [24]. The performance of this interface was hampered by the flow rates obtained and subsequently this metal contact was replaced with a thin sheath of flowing liquid in the first true coaxial interface developed by the same research group [25]. This interface, shown in Figure 3.8, overcame many of the limitations of the previous approaches and resulted in significant improvements in performance.

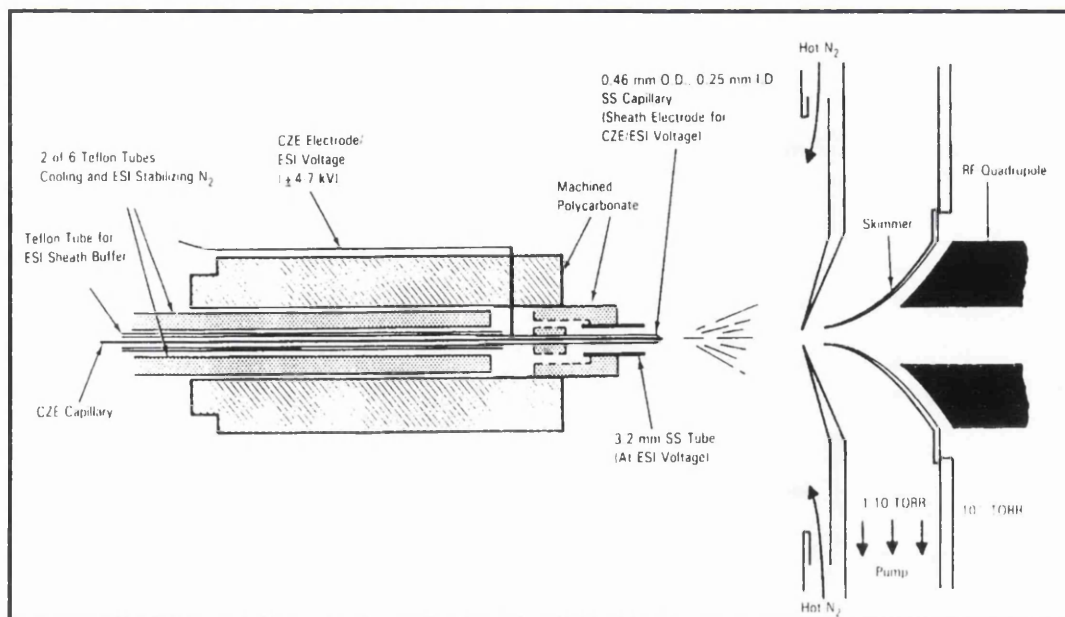


Figure 3.8 - Schematic representation of the coaxial electrospray interface for CE-MS developed by RD Smith et al [25]

The sheath liquid is typically an organic solvent such as methanol, acetonitrile or isopropanol containing a small percentage of acidic modifier. As this sheath liquid constitutes the great majority of the electrosprayed liquid, its selection is often crucial. While an optimised sheath flow composition can promote ionisation and improve sensitivity the ‘wrong’ sheath liquid can alter migration order and decrease separation performance [31].

The majority of applications developed in recent years have made use of this type of interface, reflecting its ease of operation in comparison with the other configurations.

3.4.2.3 - Other Methods of Detection

Apart from the methods of detection described in the previous sections the most commonly used and commercially available technique is fluorescence

detection, which is highly sensitive and particularly useful in the analysis of peptides and proteins, but suffers from the need for sample derivatisation. The use of lasers can increase the sensitivity of this technique even further, though obviously the cost is rather prohibitive.

Other less common methods of detection include electrochemical techniques based on amperometry, potentiometry and conductivity. Radioactivity, refractive index and chemiluminescence have also been used. Although each of these techniques is highly sensitive and each has its own area of application as yet none is commercially available and consequently are not widely used. Table 3.3 shows the limits of detection for the previously described detection techniques as well as those less commonly used. More detailed discussion of the detection techniques mentioned in this section can be found elsewhere [2,5,7,8,13].

Detection Method	Detection Limits	
	Absolute amount [mol]	Concentration [mol/l]
UV absorption	$10^{-15} - 10^{-13}$	$10^{-7} - 10^{-4}$
Indirect UV absorption	$10^{-16} - 10^{-13}$	$10^{-8} - 10^{-4}$
Fluorescence	$10^{-18} - 10^{-13}$	$10^{-9} - 10^{-4}$
Laser-induced fluorescence	$10^{-21} - 10^{-17}$	$10^{-13} - 10^{-7}$
Indirect fluorescence	$10^{-16} - 10^{-14}$	$10^{-7} - 10^{-5}$
Amperometry	$10^{-16} - 10^{-14}$	$10^{-8} - 10^{-6}$
Conductometry	$10^{-18} - 10^{-16}$	$10^{-7} - 10^{-5}$
Potentiometry	10^{-19}	10^{-8}
Mass Spectrometry	10^{-17}	10^{-8}
On-line radioactivity measurements	$10^{-18} - 10^{-16}$	$10^{-10} - 10^{-8}$

Table 3.3 – Comparison of the detection limits of some widely used CE detection techniques [7]

3.5 - MODES OF CAPILLARY ELECTROPHORESIS [2-8,13]

In the 20 years since the technique of CE was first introduced a number of different modes of operation have been developed, these are detailed in Table 3.4 below.

Mode	Separation Principle
Capillary zone electrophoresis (CZE)	Based on solute electrophoretic mobility
Capillary isotachopheresis (CITP)	Based on solute electrophoretic mobility between leading and terminating electrolytes
Capillary gel electrophoresis (CGE)	Based on differences in solute size
Micellar electrokinetic capillary chromatography (MECC)	Based on solute electrophoretic mobility and interaction with surfactant micelles
Capillary isoelectric focusing (CIEF)	Based on solute isoelectric points
Capillary electrochromatography (CEC)	Based on solute electrophoretic mobility and interaction with stationary phase

Table 3.4 – An overview of capillary electrophoresis modes

In general each of the techniques listed above can be performed using a standard commercially available CE instrument with changes in buffer composition or capillary type being made where necessary.

3.5.1 - Capillary Zone Electrophoresis (CZE)

The simplest and most widely used of the techniques is CZE, also known as Free Solution Capillary Electrophoresis (FSCE). In addition to its simplicity, the ability of the technique to separate both cations and anions in a single run along with its applicability to a wide range of compound types makes this a particularly valuable and versatile analytical technique.

The procedures and principles involved in this technique have been described previously in Sections 3.3 and 3.4. The capillary is filled with buffer identical to that contained in the inlet and outlet buffer vials, a small volume of sample is introduced and a voltage is applied. The electric field results in the migration of the sample through the capillary with each component being separated into a discrete zone based on its electrophoretic mobility. Variations in buffer composition, ionic strength and pH result in changes in electrophoretic mobilities affecting both efficiency and selectivity significantly, consequently buffer selection is of fundamental importance to the CZE separation.

3.5.1.1 Buffer selection

When choosing a buffer system for CZE, several factors must be considered:

- pH

The selected electrolyte must possess a high buffering capacity over as wide a pH range as possible, typically buffer capacity is limited to a range of two pH units centred around the pK_a value of the electrolyte. Amongst the most commonly used buffer systems are phosphates, which as polybasic compounds have the advantage of having multiple pK_a values and are therefore useful over a greater pH range.

The net charge on any particular analyte ion is dependent on the degree of ionisation produced by the pK_a of the acid or base and the pH of the buffer solution. Consequently in the case of weak acids and bases where pH can strongly influence the net charge, and therefore the mobility, of the species, changes in buffer pH are particularly effective in altering the selectivity of the

separation. Typically, the pH selected should be at least two units above or below the pK_a of the analyte species to ensure complete ionisation.

- Ionic strength and buffer concentration

Typically, buffer concentration is between 50 and 100mM but varies depending on the application. An increase in the ionic strength of the buffer results in an increase of buffer cations at the capillary surface. This results in a decrease in the zeta potential and consequently results in a decreased EOF.

- Buffer additives

A number of different types of additives or modifiers are used in CZE to make changes to the nature of the separation system. Amongst the most commonly used additives are organic solvents which alter the polarity and viscosity of the electrolyte system, consequently the EOF and electrophoretic mobilities of the analyte species are altered. The addition of organic solvents has the additional advantage of acting as a solubilising agent for those species which have low solubilities in aqueous solutions. Other commonly used additives include chiral selectors such as the cyclodextrins which allow the separation of chiral compounds, an area of analysis of increasing importance.

3.5.1.2 - Applications

CZE is particularly useful in the separation and analysis of biological molecules such as peptides and proteins with particular success in peptide mapping. The technique has also proved valuable in the analysis of inorganic ions and organic acids which have previously been separated by ion chromatography.

3.5.2 - Capillary Isotachophoresis (CITP)

CITP is a 'moving boundary' technique, which until 1981 was the most widely used instrumental CE technique [4]. One of the main disadvantages of CITP is that only anions or cations can be separated in a single run. CITP makes use of a discontinuous buffer system, consisting of a leading electrolyte (LE) and a terminating electrolyte (TE). These buffers are selected on the basis of their mobilities and in the case of a cation separation the cations of the LE (cathode vial) must have mobilities higher than the analyte cations and those of the TE (anode vial) must have a lower mobility.

The sample is introduced onto the capillary which is filled with leading electrolyte and sandwiched between LE and TE. When the voltage is applied the analyte cation with the highest mobility will migrate faster, moving away from the lower mobility sample cations resulting first in mixed sample zones either side of the original sample plug and then in fully separated discrete sample zones containing only one cationic species. At this point, a steady state equilibrium has been reached and no further separations occur, leaving the sample bands to migrate through the capillary at the same velocity as the leading cation. The relationship between velocity and mobility can be described by Equation 3.11.

$$v = \mu \cdot E$$

Equation 3.11

Where

- v = velocity
- μ = ion mobility
- E = electric field strength

Chapter 5 CZE and CE-MS Studies of Paraquat and Related Impurities 84

The electric field is self-correcting in order to maintain constant velocity throughout the sample zones and varies from zone to zone with the lowest field strength being found in the zone of highest mobility cations. This phenomenon of self-correction maintains the integrity of the focused single analyte sample zones and consequently results in highly efficient separations.

In general, CITP separations are monitored using a conductivity detector. A stepwise output known as an isotachopherogram is produced, with the step length used for quantitation of the analyte. Conventional UV detection can be used in conjunction with spacer compounds to produce a more familiar electropherogram output. These spacer compounds are non-absorbing species with mobilities that fall in between the mobilities of two peaks which need to be resolved. In practice however the selection and use of spacer compounds is far from straightforward, particularly when a complex mixture is under analysis.

Despite having the advantage of generating highly efficient separations, CITP is not widely used largely because of the problems of detection and the necessity for spacer compounds. The technique is however being increasingly used as a preconcentration technique prior to CZE [32-36]. Several groups have reported the coupling of the two techniques and improvements in detection limits by factors of between 200 and 1000 have been observed. Further, more detailed discussion of coupled column and single capillary CZE-CITP can be found elsewhere [2,37]

3.5.3 - Capillary Gel Electrophoresis (CGE)

CGE combines the traditional technique of slab gel electrophoresis with the automated, instrumental capabilities of CE. The separation mechanism employed is identical to that used in slab gel electrophoresis and is based on the electrophoretic migration of charged species through a suitable polymer which acts as a molecular sieve separating the analytes on the basis of their molecular sizes. The technique is particularly applicable to those compounds, such as oligonucleotides, SDS proteins and DNA restriction fragments, which vary in size but not in size-charge ratios and as a consequence are not well separated by CZE. Capillaries filled with different types of gel media are now commercially available and the technique is widely used in the separation and analysis of biological compounds and has proved particularly important in DNA analysis and sequencing and has been utilised in the American Human Genome Project. A more detailed discussion of CGE can be found elsewhere [2-8.13]

3.5.4 - Micellar Electrokinetic Capillary Chromatography (MECC)

MECC was developed in 1984 by Terabe and co-workers [38] and, as the name suggests, combines aspects of both chromatography and electrophoresis. The technique's unique ability to separate neutral species in addition to improving selectivity in the analysis of charged analytes has made it the most commonly used mode of CE after CZE. The separation is achieved by the use of surfactants in the running buffer, which at levels greater than the critical micelle concentration (cmc) form aggregates known as micelles. These micelles form a pseudophase into which analyte molecules are partitioned, this partitioning is the basis of the separation.

Chapter 5 CE and CIE MS Studies of Paracetamol and Related Impurities 88

The most commonly used surfactant in MECC is sodium dodecyl sulphate (SDS) which forms anionic micelles which migrate in the direction of the anode against the direction of the EOF, consequently the overall migration velocity of the micelles is slowed compared to the bulk flow of solvent. When an analyte molecule is associated with the micellar pseudophase its overall migration velocity is slowed and when a neutral molecule is associated with the bulk phase, its migration velocity is equal to that of the EOF. Consequently, those species with a greater affinity for the micelle migrate more slowly than those associated with the bulk phase.

As in CZE, selectivity can be manipulated with variations in buffer concentration and pH, or with the addition of organic or chiral modifiers. In addition to these variables, changes in surfactant structure or type can be used in the optimisation of MECC separations. As has been previously mentioned MECC is a particularly versatile technique by virtue of its ability to separate both neutral and charged species, this has led to its use in a wide variety of applications including pharmaceuticals, vitamins and amino acids. Further discussion of MECC and micellar theory can be found elsewhere [2-8,13].

3.5.5 - Capillary Isoelectric Focussing (CIEF)

CIEF is based on the separation of sample components due to their different isoelectric points (pI). The pI is the pH at which an ampholyte has zero net charge, existing mainly as a zwitterion and will not migrate in an electric field. The capillary is filled with a mixture of sample and carrier ampholytes resulting in the formation of a pH gradient, where the pH is low at the anode and high at the cathode. On application of an electric field the sample species migrate through the gradient to

Chapter 5 CE and CE-MS Studies of Paracetamol and Related Impurities 87

their pI where they become focused into very sharp zones. When this focusing step is complete a steady state is reached and no current flows, at this point mobilisation of the focused zones takes place. Mobilisation of the focused zones past the detector window can be achieved with the addition of a salt to one of the reservoirs or by applying a pressure to one end of the capillary.

The technique is limited to the analysis of amphoteric species and is used almost exclusively to separate proteins and polypeptides. This technique is discussed in greater detail elsewhere [2-8,13].

3.5.6 - Capillary Electrochromatography (CEC) [39]

The technique of CEC has been a relatively recent development combining aspects of both CE and HPLC to produce highly efficient separations. A silica capillary is packed with a conventional HPLC stationary phase; C8 and C18 are the most commonly used, although the particles used are generally much smaller. Unlike HPLC, which is pressure driven, CEC uses an electric field to drive the flow. Analyte species are separated primarily as a result of their partitioning between the stationary phase and the mobile phase. This technique has grown rapidly in recent years and has proved useful in a variety of fields of application. Further discussion of this technique can be found elsewhere [2,13,39].

3.6 - RESULTS AND DISCUSSION

The objective of this study was to investigate the use of CZE in separating the impurities found in technical paraquat, see Table 3.1, and to assess the technique in combination with a mass spectrometric detector as a means of determination.

In addition, the technique of tCITP as a method of preconcentration was studied as a means of improving the detection limits of the impurities.

3.6.1 - CZE OF PARAQUAT AND ITS IMPURITIES

A method for the CZE separation of paraquat and the five impurities shown in Table 3.1 was provided by Zeneca Agrochemicals [40] and it was intended that this method would be developed for use on-line with a mass spectrometric detector.

Operating Conditions

Capillary:	57cm × 50µm i.d. fused silica capillary (50cm to detector)
Buffer:	20mM Ammonium Acetate (Acetic Acid) buffer, pH 3.7
Injection Mode:	Pressure
Injection Time:	8 seconds
Applied Voltage:	30kV
Temperature:	30°C
Detection:	UV @ 254nm
Run Time:	8 minutes

Initial work performed using this method was carried out over a period of several weeks with no success whatsoever. No separation was achieved and only a few 'lumps' in the baseline were observed, an example of the electropherograms obtained under these conditions is shown in Figure 3.9. Variations in injection mode

and time, buffer concentration, buffer pH and applied voltage were all attempted, but again with no success.

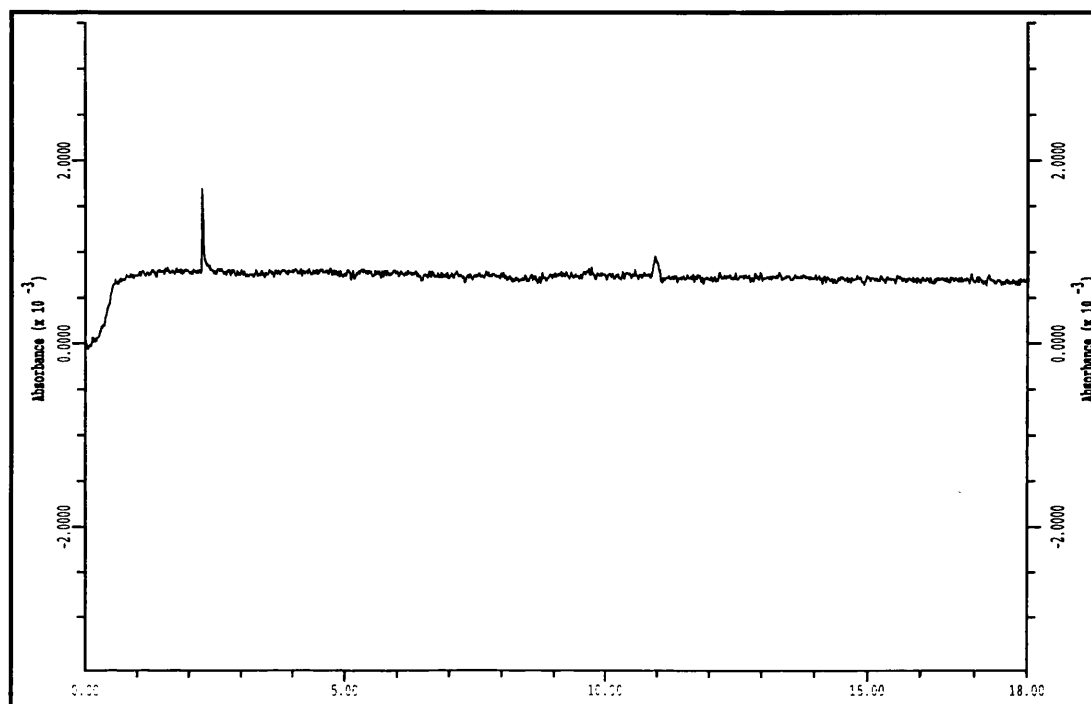


Figure 3.9 - Electropherogram of a six component paraquat mixture at 30kV applied voltage, 20mM ammonium acetate buffer pH 3.7, 8 second pressure injection

At this stage in the study and after discussion with Dr. Encarna Moyano, who has been involved with several publications in the field of quaternary ammonium herbicide analysis [41-42], it was decided to follow an alternative method published by other members of Dr Moyano's research group [43]. The 1994 publication by Galceran et al describes the CE separation of paraquat and two other quaternary ammonium herbicides, diquat and difenzoquat, and makes use of low ionic strength buffers modified with alkali metal chloride. Based on the published methodology and on Dr Moyano's recommendations [44] the conditions detailed below were used in a series of experiments to assess the utility of the literature conditions.

Operating Conditions

Capillary:	57cm × 50µm i.d. fused silica capillary (50cm to detector)
Buffer:	10mM Sodium Acetate (Acetic Acid) buffer, pH 4.0 made up with 100mM Sodium Chloride
Injection Mode:	Voltage (10kV)
Injection Time:	15 seconds
Applied Voltage:	15kV
Temperature:	30°C
Detection:	UV @ 254nm
Run Time:	15 minutes

These preliminary experiments were performed using dilutions of a standard mixture, the composition of which is detailed in Table 3.5.

Paraquat	5mg/ml
2,2-Bipyridyl	0.5mg/ml
2,2-Paraquat	0.05mg/ml
Monoquat	0.05mg/ml
4,4-Bipyridyl	0.005mg/ml
N-Methyl pyridinium ion	0.005mg/ml

Table 3.5 – Composition of paraquat standard mixture

An electropherogram containing six well resolved peaks was obtained and can be seen in Figure 3.10. Although no individual standards were available for peak identification purposes at this stage, the peaks were tentatively identified on the basis of their size/charge ratios.

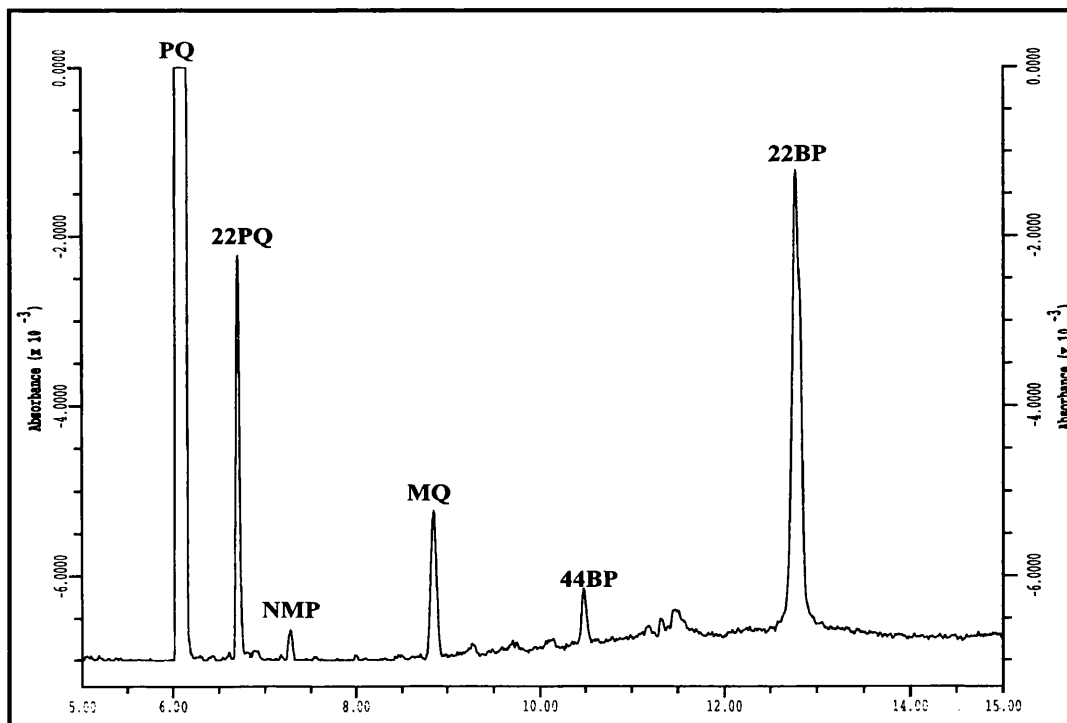


Figure 3.10 - Electropherogram of a six component paraquat mixture at 15kV applied voltage, 10mM sodium acetate buffer pH 4.0 with 100mM sodium chloride, 15 second voltage (10kV) injection

Persistent problems with current errors were experienced, largely as a result of droplets of moisture collecting on the vial caps and causing discharge and resulting in an unstable current. By decreasing the operating temperature by 5°C to 25°C this problem was largely avoided. Further slight adjustments to the method were made in order to optimise the operating conditions for the study compounds. It was observed that increasing the applied voltage to 20kV had the effect of decreasing migration times and consequently decreasing the analysis time while still retaining separation integrity. See Table 3.6 and Figures 3.11 and 3.12.

	Applied Voltage: 15kV Temperature: 30°C		Applied Voltage: 15kV Temperature: 25°C		Applied Voltage: 20kV Temperature: 25°C	
	RESOLUTION	EFFICIENCY (plates/metre)	RESOLUTION	EFFICIENCY (plates/metre)	RESOLUTION	EFFICIENCY (plates/metre)
PQ	N/A	19582	N/A	27701	N/A	19645
2,2-PQ	3.41 PQ/22PQ	36901	4.46 PQ/22PQ	50729	3.84 PQ/22PQ	40507
NMP	4.91 22PQ/NMP	67808	5.03 22PQ/NMP	73720	4.71 22PQ/NMP	68765
MQ	11.31 NMP/MQ	39800	10.98 NMP/MQ	39221	9.35 NMP/MQ	25331
4,4-BP	7.80 MQ/44BP	68345	10.19 MQ/44BP	86099	7.80 MQ/44BP	70365
2,2-BP	12.33 44BP/22BP	28128	8.70 44BP/22BP	17943	10.99 44BP/22BP	31204

Table 3.6 – Data for Figures 3.11 and 3.12

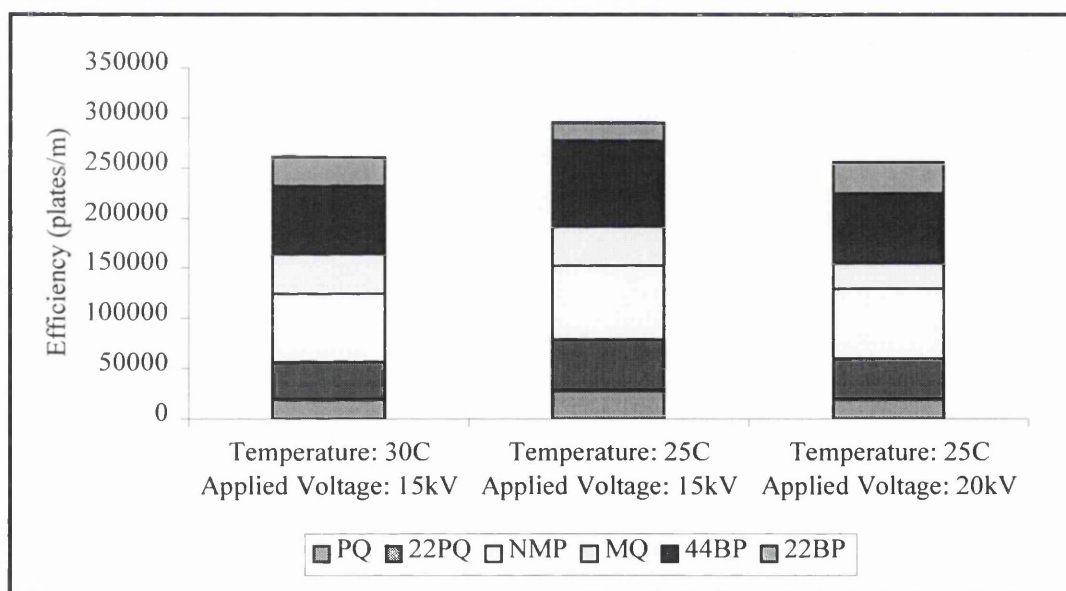


Figure 3.11 – Cumulative efficiency of paraquat and impurities versus applied voltage and temperature for paraquat and impurities using 10mM sodium acetate buffer pH 4.0 with 100mM sodium chloride, 15 second voltage (10kV) injection

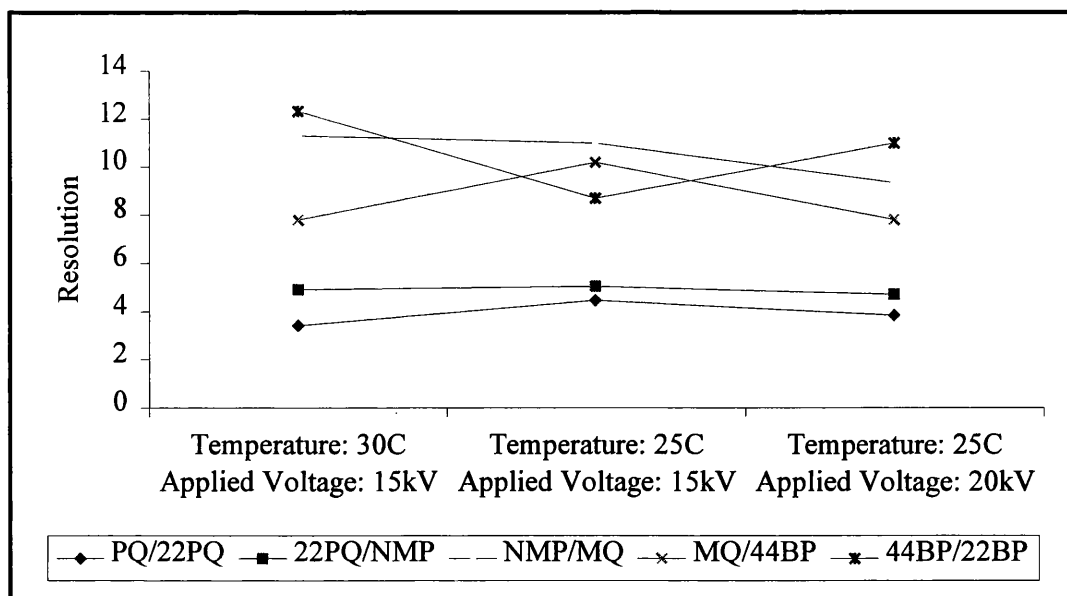


Figure 3.12 - Resolution versus applied voltage and temperature for paraquat and impurities using 10mM sodium acetate buffer pH 4.0 with 100mM sodium chloride, 15 second voltage (10kV) injection

Although this method was initially relatively successful and produced baseline separation of all six components within 10 minutes, only a limited amount of further work was performed (including the successful separation of a sample of technical paraquat). The failure of the method to consistently generate a good separation with reproducible migration times coupled with the possible lack of compatibility of the buffer with mass spectrometric detection meant that there was little point in persevering with these conditions. It should be noted, however, that it is thought that the use of non-volatile buffers in CE-MS may not be as harmful as it is in LC-MS because of the dilution of the capillary effluent in the liquid-junction or coaxial coupling [41].

3.6.1.1 – Variation of injection mode

Further experiments using variations of the original Zeneca operating conditions were performed and the effect of injection mode and injection time was assessed.

3.6.1.1.1 - Hydrodynamic Injection

As experienced in the original experiments, the analyses performed using the pressure injection suggested in the method supplied by Zeneca were again unsuccessful and generated electropherograms showing only two very small peaks, see Figure 3.13 below.

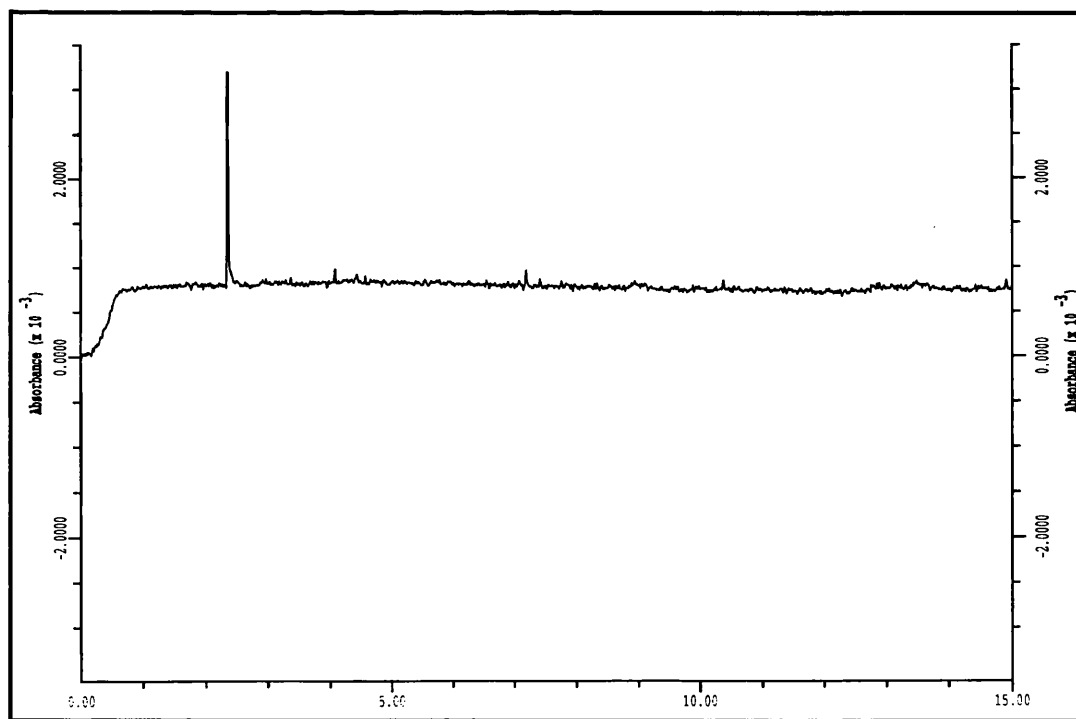


Figure 3.13 - Electropherogram of a six component paraquat mixture at 30kV applied voltage, 20mM ammonium acetate buffer pH 3.7, 15 second pressure injection

The use of injection times greater than the suggested 8 seconds was also investigated, again with no success. Figure 3.14 below shows the average peak area of the paraquat peak plotted against injection time.

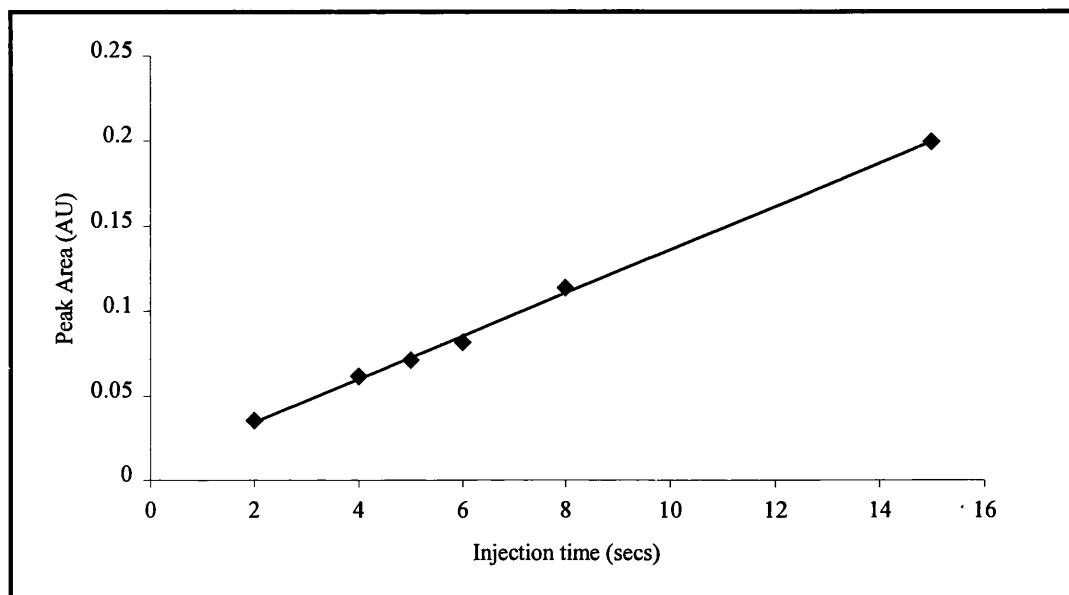


Figure 3.14 - Linearity of response for paraquat using pressure injections of varying lengths

The response was found to be linear, with a correlation coefficient of 0.998, over the range of injection times used.

The reproducibility of the response for each injection time was also investigated with repeat injections performed for each injection time. The %RSD was calculated for each data point, these results are tabulated below.

	Injection Time (seconds)					
	2	4	5	6	8	15
Mean Peak Area	0.03542	0.06154	0.07116	0.08148	0.11356	0.19939
%RSD	8.18	4.09	3.09	1.65	3.88	3.83

Table 3.7 – Repeatability data for paraquat using hydrodynamic sample introduction

As expected, the reproducibility of the peak response was improved slightly with increasing injection time, peak efficiency was however lowered, see Figure 3.15. The shorter injection times resulted in sharper and more efficient peaks as the very narrow analyte zone is less affected by dispersion processes.

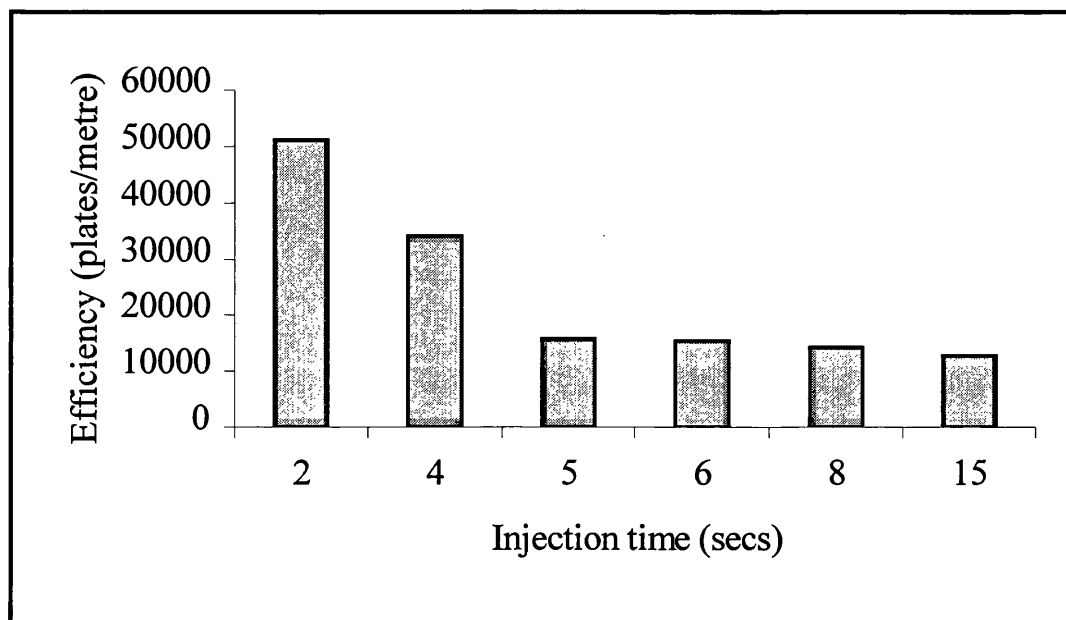


Figure 3.15 - Efficiency of paraquat versus hydrodynamic injection time

3.6.1.1.2 - Electrokinetic Injection

Those separations performed using electrokinetic injections, however, produced more promising results with several small peaks clearly visible alongside the paraquat peak at 2.2 minutes at all of the injection times employed. In the electropherograms generated when 15 second injections were used all five impurity peaks were visible above the baseline noise as can be seen in Figure 3.16.

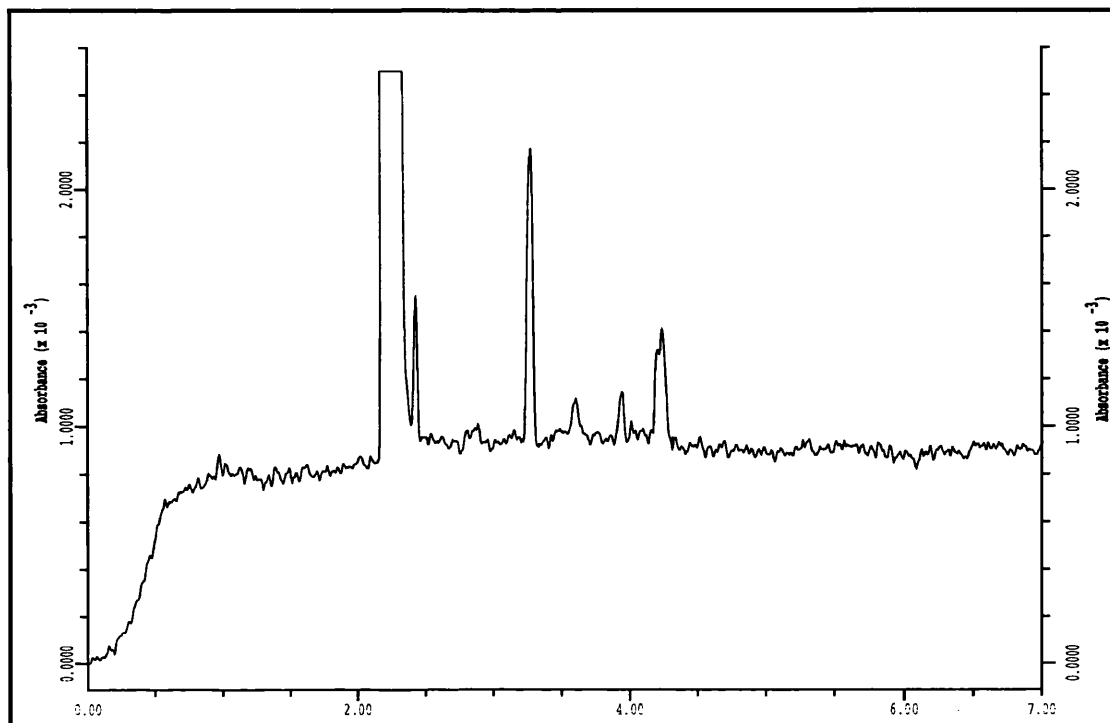


Figure 3.16 - Electropherogram of a six component paraquat mixture at 30kV applied voltage, 20mM ammonium acetate buffer pH 3.7, 15 second voltage (10kV) injection

The variation of injection times was again studied for comparison, and although other sample components were detected, only the details for paraquat are displayed below for direct comparison with the results obtained with hydrodynamic injections.

Plotting of the peak response against injection time again demonstrated the linearity of the technique over the range used with a correlation coefficient of 0.994, see Figure 3.17.

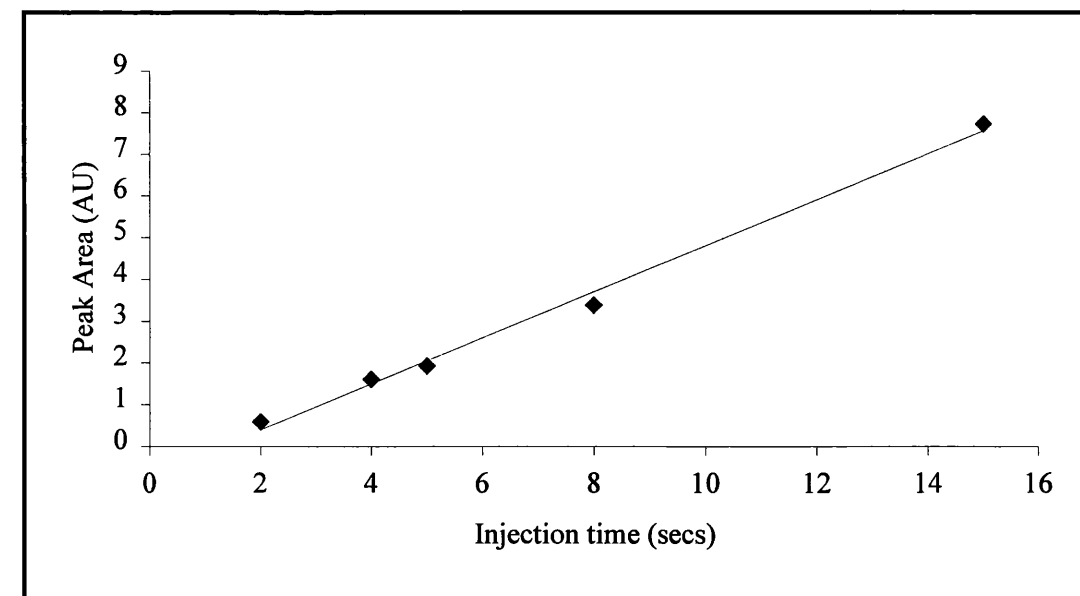


Figure 3.17 - Linearity of response for paraquat using voltage (10kV) injections of varying lengths

As with hydrodynamic injection, increases in injection time resulted in improved reproducibility but lowered peak efficiency, see Table 3.8 and Figure 3.18.

	Injection Time (seconds)				
	2	4	5	8	15
Mean Peak Area	0.59058	1.60203	1.93032	3.38351	7.72417
%RSD	6.71	12.20	2.79	3.01	2.77

Table 3.8 - Repeatability of injection - data for paraquat using electrokinetic sample introduction

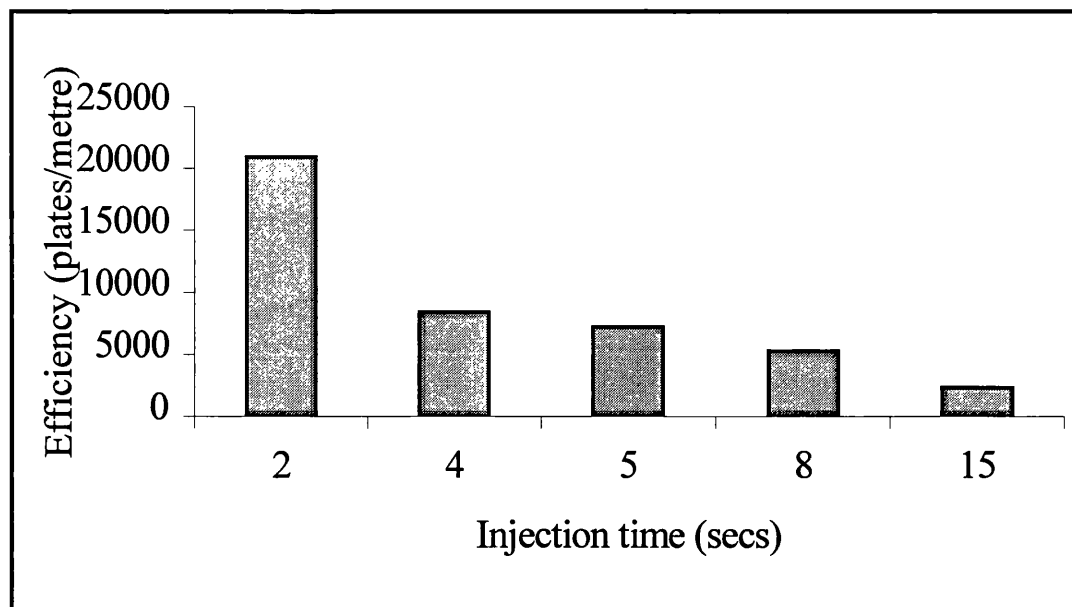


Figure 3.18 - Efficiency of paraquat versus electrokinetic injection time

Although hydrodynamic sample introduction is generally used in preference to electrokinetic injection as it offers greater reproducibility and does not discriminate between sample components of differing mobilities, in this case the use of electrokinetic injection was preferred. While the peaks produced using pressure injection were sharper and more efficient than those achieved with electrokinetic sample introduction the fact that it consistently failed to produce anything other than a single peak meant that there was little point in continuing to use it.

3.6.1.2 - Variation of buffer concentration

With a view to improving the resolution and efficiency of the separation, the effect of increasing the buffer concentration was investigated. Since no general rule can be applied to the effect of increased buffer concentration [2] it is particularly important to study the impact of ionic strength on the separation.

Figure 3.19 demonstrates that the migration times of paraquat and the five related impurities generally increase with increasing buffer concentrations. Although the effect is less pronounced between 150mM and 200mM where the migration times for each of the six compounds virtually plateau.

Typically, an increase in the ionic strength of the CE electrolyte results in a decrease in the zeta potential at the capillary surface which itself results in a lowering of the EOF. Increases in buffer concentration can also result in temperature increases and viscosity changes, which may themselves influence the EOF and mobilities of the analytes. The effect of variations in ionic strength on the CE separation of both a mixture of benzoic acid derivatives [2] and a mixture of carboxylic acids [7] has been reported. In each case, whilst the EOF is only slightly decreased with the increased buffer concentration the migration times of the analytes are significantly increased.

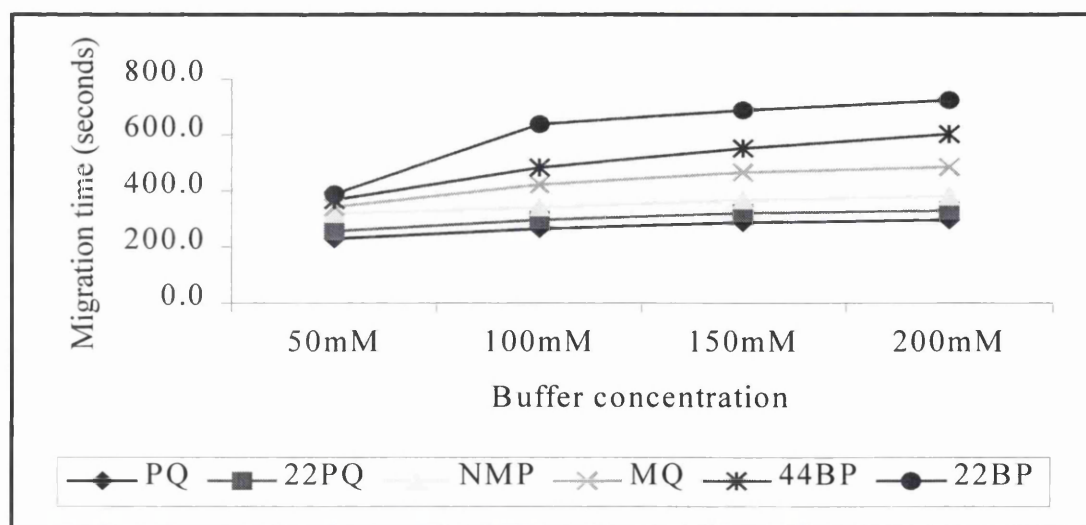


Figure 3.19 - Migration times of paraquat and impurities versus ammonium acetate buffer concentration

Efficiency

Figure 3.20 shows a plot of peak efficiencies, in terms of theoretical plate numbers, calculated using Equation 3.4, for each of the six compounds run at progressively higher buffer concentrations in the range 50 – 200mM. It can be seen that as the buffer concentration increases so the efficiency for each component is decreased.

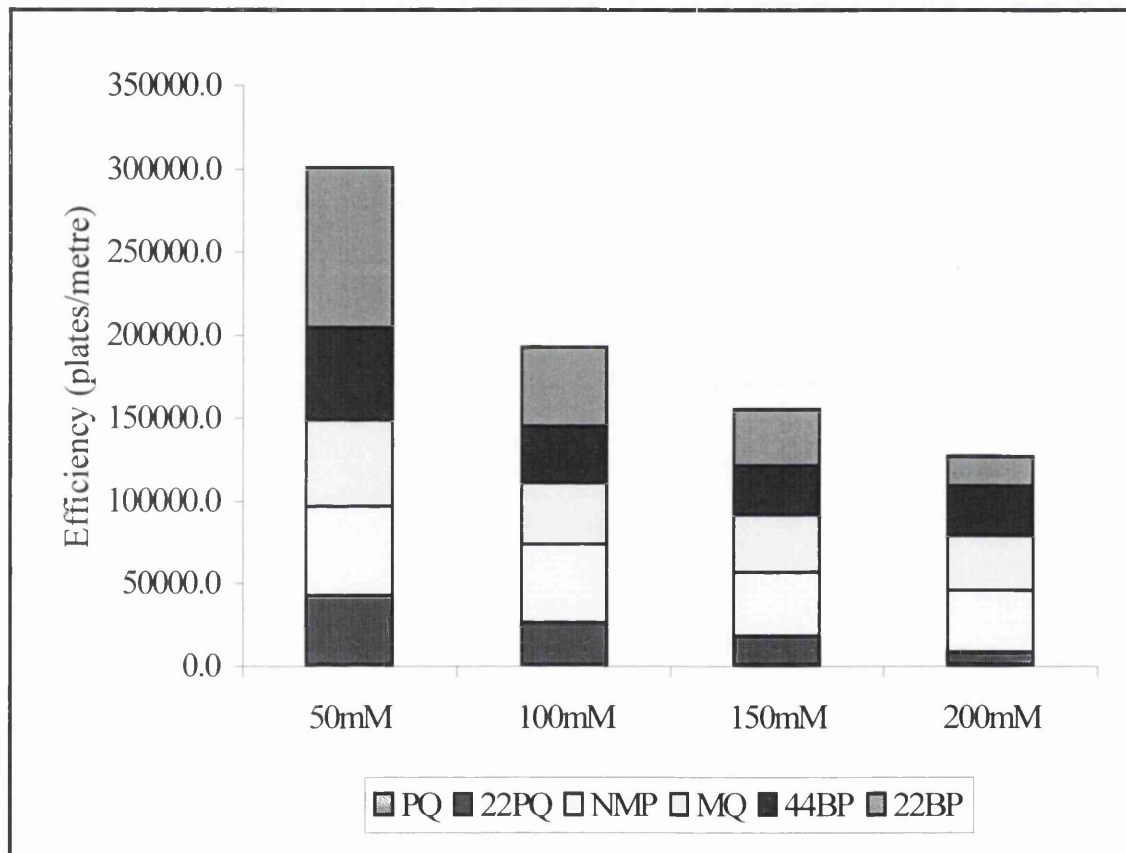


Figure 3.20 – Cumulative efficiency of paraquat and impurities versus ammonium acetate buffer concentration

$$N = \frac{(\mu + \mu_{eo}) \cdot V}{2 \cdot D}$$

Equation 3.12

Where	N	=	number of theoretical plates
	μ	=	electrophoretic mobility
	μ_{eo}	=	electroosmotic mobility
	V	=	applied voltage
	D	=	diffusion coefficient

The above equation expresses the theoretical efficiency as a function of applied voltage and electroosmotic mobility. Equation 3.12 indicates that peak efficiency will be increased with an increase in electroosmotic mobility. Consequently, as the ionic strength is increased and the zeta potential at the capillary surface is decreased the electroosmotic mobility of the analytes will decrease resulting in a decrease in peak efficiency.

Resolution

It can be seen from Figure 3.21 that in general the resolution of the six compounds increases with an increase in the concentration of the CE buffer. So, while the lower buffer concentrations offer shorter analysis times and sharper, more efficient peaks, the resolution in the critical separation of paraquat and 2,2-paraquat is slightly lower than that achieved in the separations using 150mM and 200mM buffers where almost baseline resolution is obtained. The other components are all so well separated over the range of buffer concentrations that the differences are of less importance.

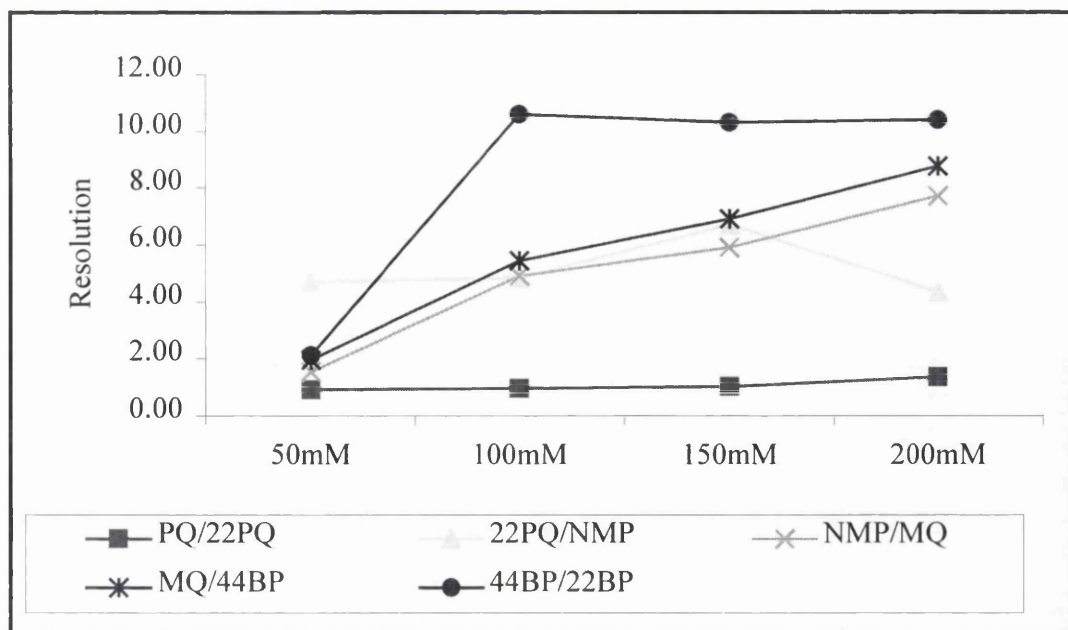


Figure 3.21 - Resolution of paraquat and impurities versus ammonium acetate buffer concentration

With the lower buffer concentrations offering the most rapid analysis times and most efficient peaks and the higher concentrations providing slightly better resolution in the separation of PQ and 22PQ the 100mM buffer appeared to offer a compromise between the two extremes. Separation, including almost baseline resolution of paraquat and 2,2-paraquat (Resolution = 0.97), was achieved within 11 minutes and peak shape was on the whole good. It was also observed that at the higher buffer concentrations peak shape deteriorated and greater tailing and splitting was apparent. Consequently the conditions outlined below were used in the initial online CZE-MS experiments detailed in Section 3.6.3.1 and in subsequent offline CZE experiments.

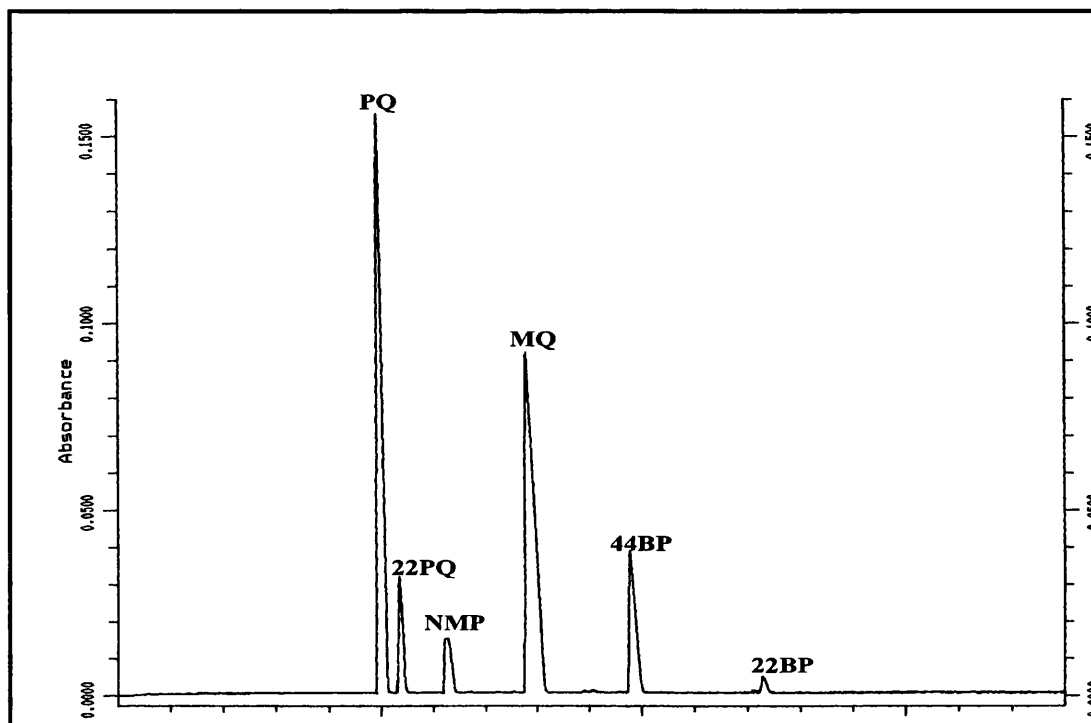


Figure 3.22 - Electropherogram of a six component paraquat mixture at 15kV applied voltage, 100mM ammonium acetate buffer pH 4.0, 10 second voltage (10kV) injection, 30°C

Operating Conditions

Capillary:	57cm × 50 μ m i.d. fused silica capillary (50cm to detector)
Buffer:	100mM Ammonium Acetate (Acetic Acid) buffer, pH 4.0
Injection Mode:	Voltage (10kV)
Injection Time:	10 seconds
Applied Voltage:	15kV
Temperature:	30°C
Detection:	UV @ 254nm
Run Time:	15 minutes

Research has shown that water is a poor solvent for electrospray as it does not allow efficient droplet charging [45], in terms of electrospray compatibility, the ideal CZE buffer would be volatile and contain a significant amount of organic solvent. Consequently the use of methanol as a buffer additive and its effect on the separation

were investigated. Experiments were performed using 50 and 100mM ammonium acetate buffers, pH adjusted to 4.0 and containing 0, 10 or 20% methanol and run under the previously discussed operating conditions. The effect of varying the applied voltage was also studied.

3.6.1.3 - Effect of applied voltage on the separation

The graphical data presented in this section is specifically that obtained using the 100mM ammonium acetate buffer containing 10% methanol, but is representative of the results achieved at each of the buffer concentrations and each percentage of methanol.

Migration Time

Figure 3.23 demonstrates that the migration time of each of the six sample components decreases as the applied voltage is increased.

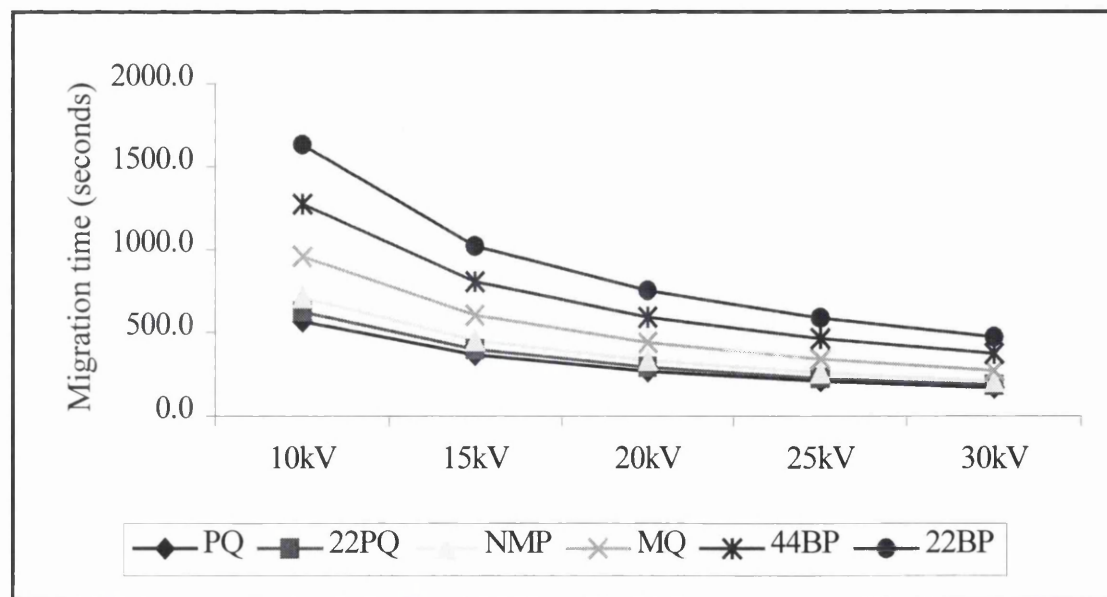


Figure 3.23 - Migration times of paraquat and impurities versus applied voltage

This pattern of response is in agreement with Equation 3.13 shown below, this is a rearrangement of Equation 3.1 which indicates that the shortest analysis times will be achieved with the use of the highest applied voltages.

$$t_m = \frac{L_d \cdot L_t}{\mu_{ep} \cdot V}$$

Equation 3.13

Efficiency

From Equation 3.12 it would appear that the highest efficiencies would be obtained with the use of the highest possible applied voltages. However, theoretical plate numbers are proportional to the voltage only for the lower values as in practice the phenomenon of joule heating results in a reduction in efficiency at higher voltages. From Figure 3.24, it can be seen that there exists an optimum applied voltage, 20kV, at which point the peak efficiency reaches a maximum.

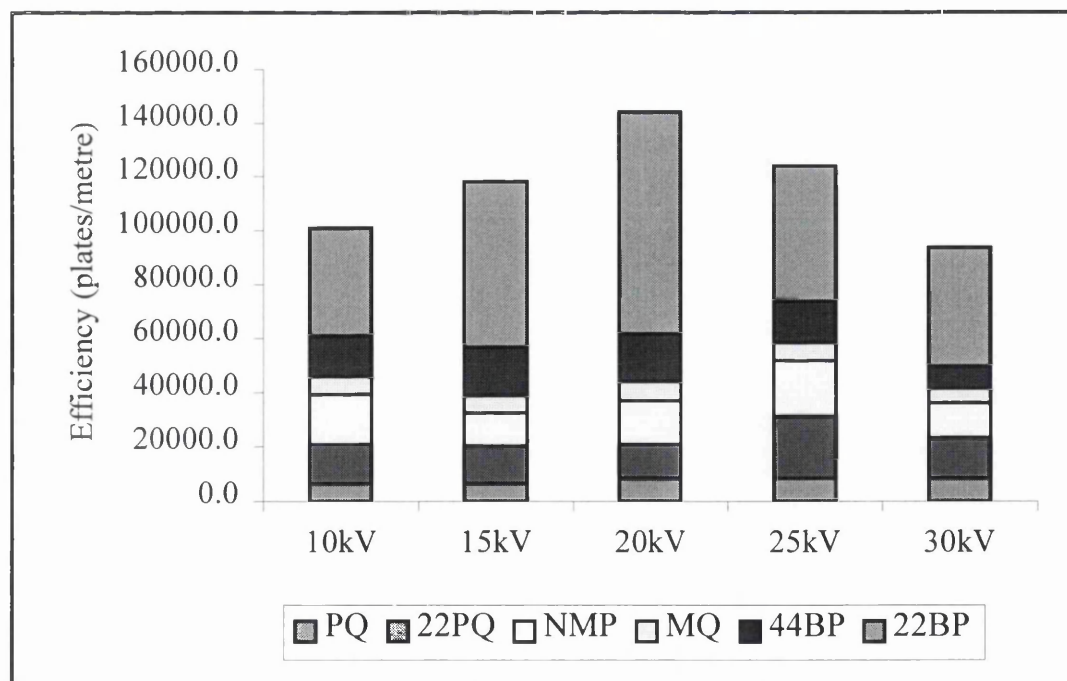


Figure 3.24 - Cumulative efficiency of paraquat and impurities versus applied voltage

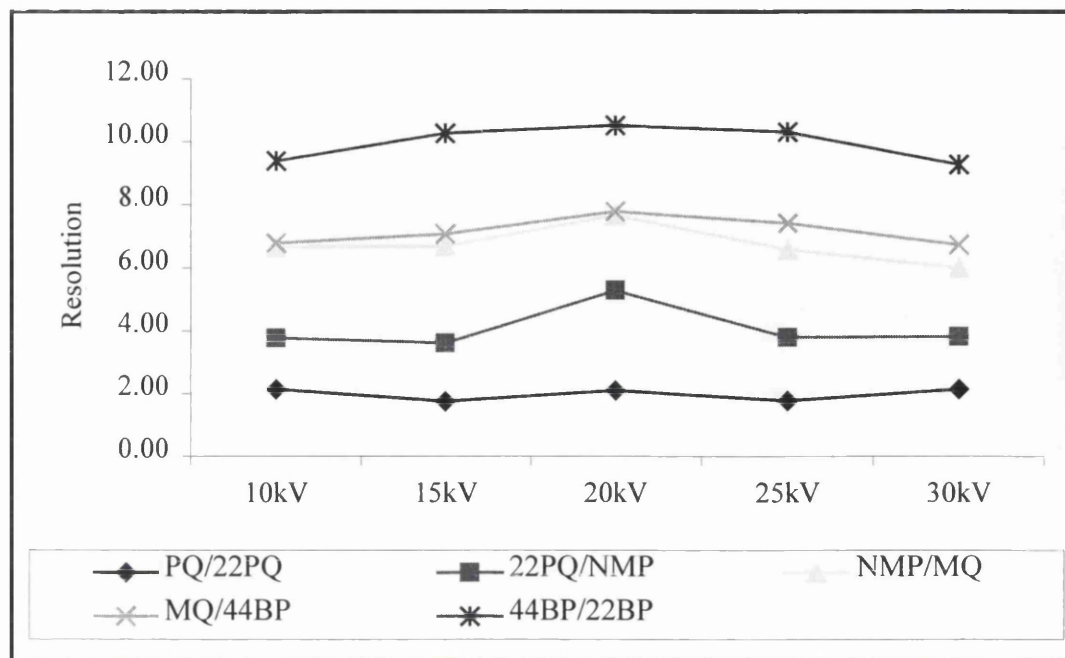


Figure 3.25 - Resolution of paraquat and impurities versus applied voltage

As it has been shown that efficiency increases to a maximum at 20kV and then drops off, so it follows that the resolution should follow the same pattern as the two factors are related. Figure 3.25 illustrates that this is indeed the case, with the resolution of each pair of compounds showing a general increase up to 20kV and decreasing thereafter. Baseline resolution is obtained for each pair of components.

3.6.1.4 - Effect of organic modifier content on the separation

Migration Time

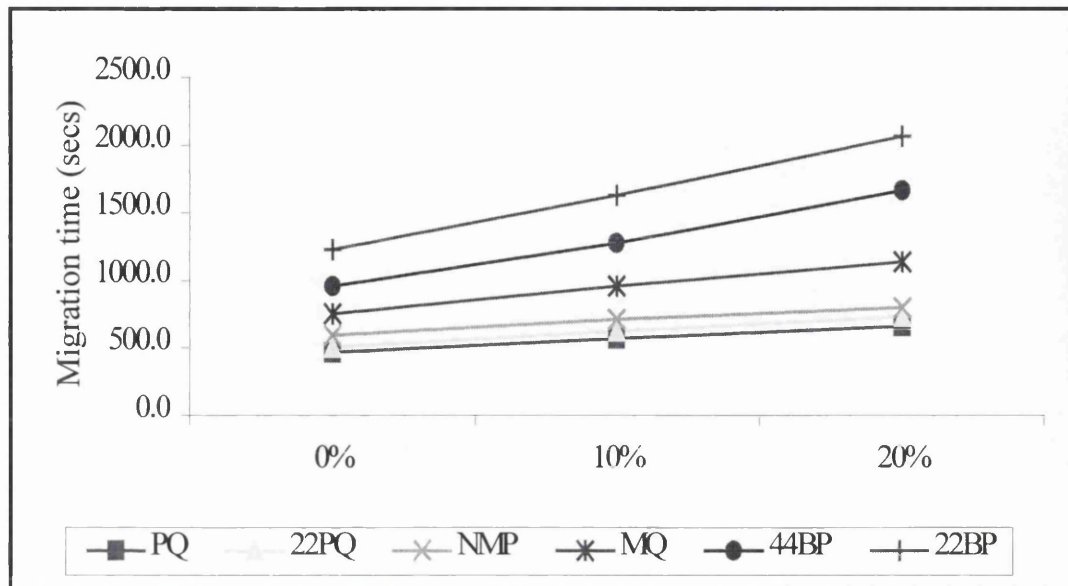


Figure 3.26 - Migration times of paraquat and impurities versus percentage methanol content of buffer

The data displayed in Figure 3.26 is specifically that obtained with the use of the 100mM ammonium acetate buffer with an applied voltage of 10kV, but is representative of the data pattern obtained at each of the applied voltages.

In general the addition of organic solvents to the CE buffer electrolyte alters the polarity and viscosity of the buffer system and as a consequence results in changes in the EOF and the electrophoretic mobility of the analytes. In this case, the addition of methanol has resulted in a reduction in the EOF and in the mobilities of the analyte species leading to increased migration times and an overall increase in analysis time. This behaviour is comparable with the pattern of results observed in studies reported by Fujiwara and Honda [46].

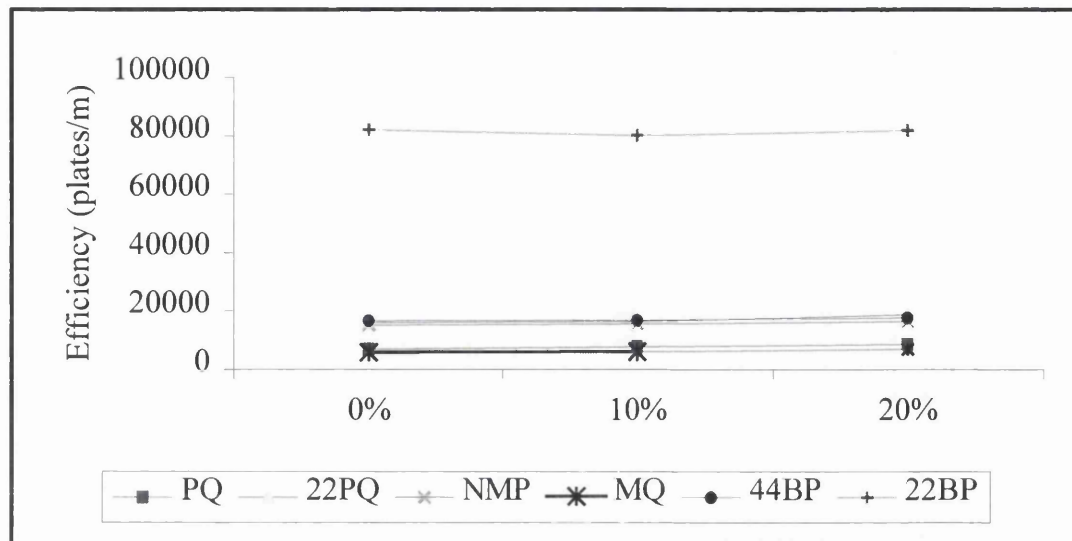


Figure 3.27 - Efficiency of paraquat and impurities versus percentage methanol content of buffer

Figure 3.27 above shows that the efficiency for each of the sample components remains almost constant, but is in general increased as the percentage of methanol in the buffer is increased. Although the data above is specifically that obtained from the runs performed at 20kV it is representative of the data obtained at each of the other voltages used.

The migration time data obtained would appear to indicate that the increased solvent content brings about a reduction in the EOF and analyte mobility, which should result in an increase in efficiency. This trend is confirmed by the efficiency data shown in Figure 3.27.

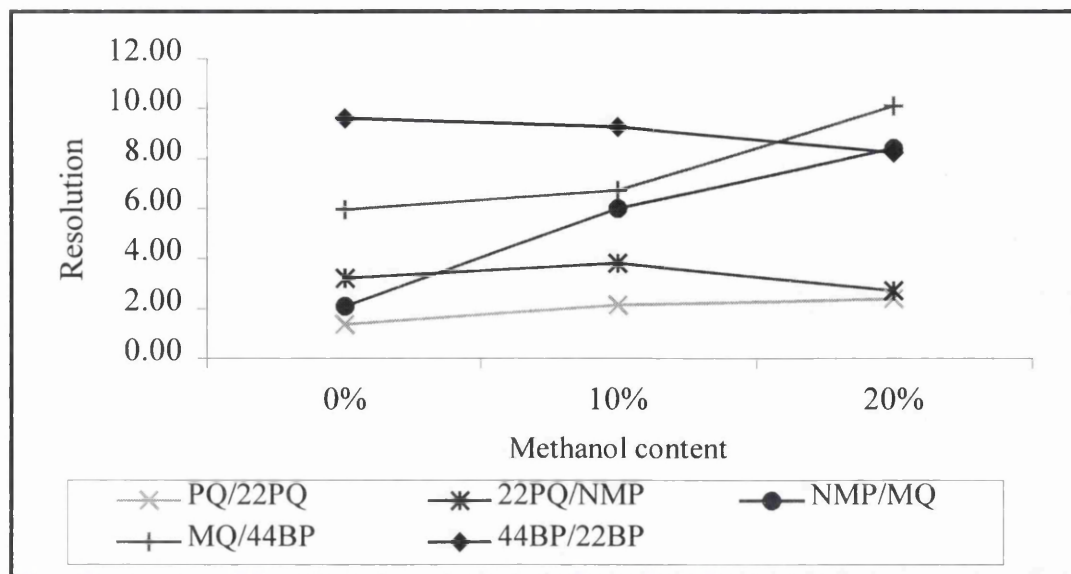


Figure 3.28 – Resolution of paraquat and impurities versus percentage methanol content of buffer

Figure 3.28 illustrates the trend in resolution over the range of methanol percentages. Although the above data is specifically that from the runs performed at 20kV the trends observed are representative of those obtained at each of the applied voltages used. In general resolution shows an upward trend, increasing as the percentage of methanol increases, this is in agreement with the increasing efficiencies reported in the previous section. The exceptions to this general trend are the separations of 2,2-paraquat and n-methyl pyridinium and 4,4-bipyridyl and 2,2-bipyridyl. The resolutions for each of these separations increase as the methanol content of the buffer is increased from 0% to 10% methanol but then drop as the methanol content is increased to 20%. In each case, the resolution obtained was far greater than is necessary for adequate baseline separation so this reduction in resolution is not critical but the reason for these anomalies are not fully understood.

An example of the separation achieved using a 100mM ammonium acetate buffer containing 10% methanol and an applied voltage of 20kV is shown below in Figure 3.29. It can be seen that each of the six components is well resolved and peak shape is good.

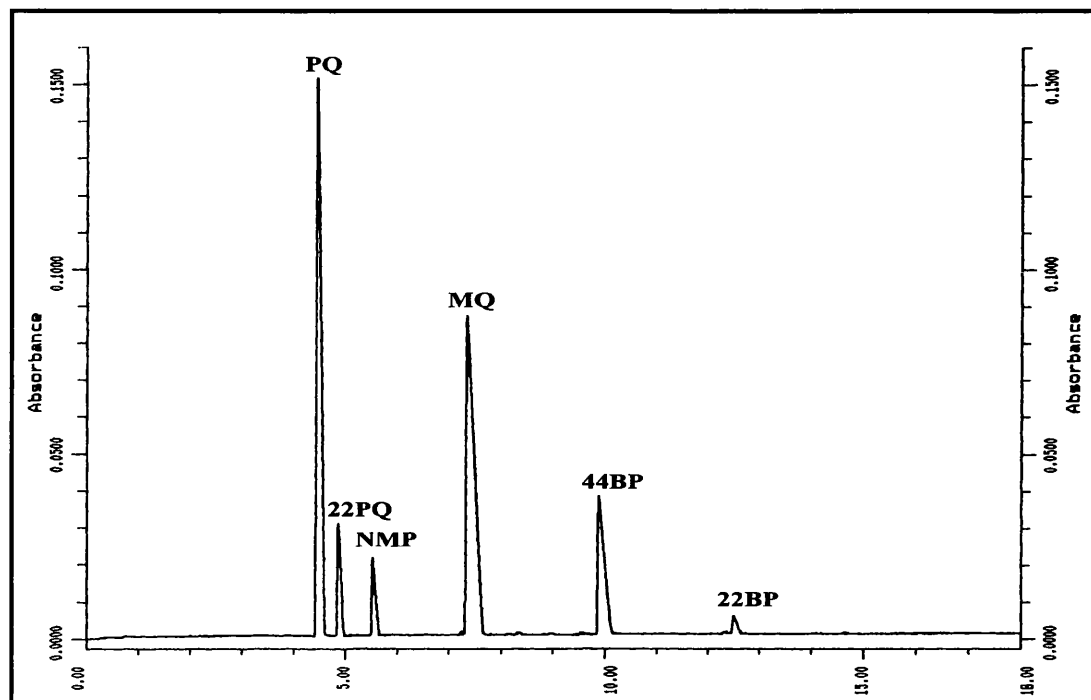


Figure 3.29 - Electropherogram of a six component paraquat mixture at 20kV applied voltage, 100mM ammonium acetate buffer + 10% methanol, pH 4.0, 10 second voltage (10kV) injection, 30°C

3.6.1.5 - Limit of detection (LOD) and limit of quantitation (LOQ)

The limit of detection (LOD) of a chromatographic method can be defined as 3:1 signal-to-noise ratio and the limit of quantitation (LOQ) as 10 times the signal-to-noise ratio [47]. The LOD and LOQ for each of the six study compounds using the CZE conditions previously described were determined. The baseline noise from an electropherogram showing the separation of all six components at known

concentrations, was expanded, measured and determined to be equivalent to 0.1mAU. The height of each of the sample peaks was measured and converted into mAU. Using the equations below the LOD and LOQ for each component was determined.

$$\text{LOD} = \frac{3 \times \text{noise}}{\text{signal}} \times \text{Concentration of component}$$

Equation 3.14

$$\text{LOQ} = \frac{10 \times \text{noise}}{\text{signal}} \times \text{Concentration of component}$$

Equation 3.15

	LOD (ppb)	LOQ (ppb)
PQ	211	704
22PQ	1200	4000
NMP	2143	7143
MQ	366	1220
44BP	682	2273
22BP	5000	16667

Table 3.9 - Limits of detection and quantitation for each of the six study compounds using the tCITP method

3.6.1.6 – CZE of technical paraquat

After successfully performing separations on standard mixtures of the six study compounds, the methodology developed was used to attempt the separation of a sample of technical paraquat. The CE operating conditions used are detailed overleaf.

Operating Conditions

Capillary:	57cm × 50 μ m i.d. fused silica capillary (50cm to detector)
Buffer	100mM Ammonium Acetate buffer, pH 4.0 10% Methanol
Injection Mode:	Voltage (10kV)
Injection Time:	10 seconds
Applied Voltage:	15kV
Temperature:	25°C
Run Time:	15 minutes
Detection:	UV @ 254nm

In order to prevent overloading of the capillary and detector with the high level of paraquat present in the sample the technical paraquat was diluted with water prior to analysis. An example of the electropherograms obtained for the analysis of the technical paraquat diluted by a factor of 200 in water is shown in Figure 3.30.

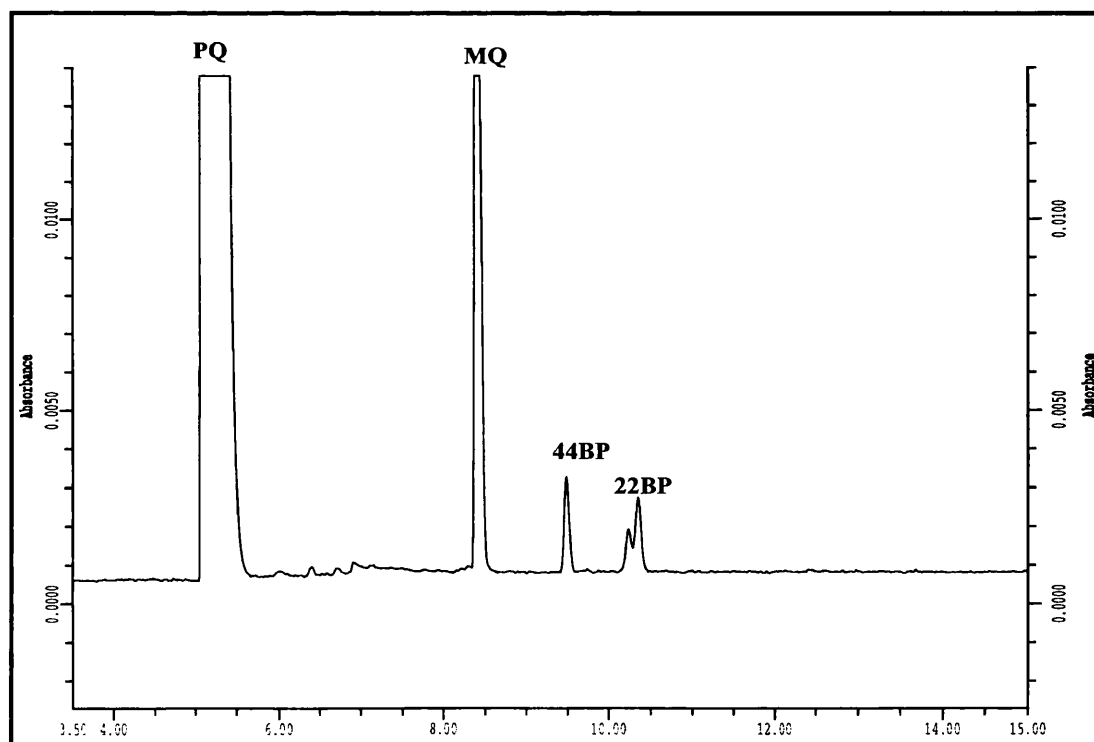


Figure 3.30 - Electropherogram of a sample of technical paraquat at 15kV applied voltage, 100mM ammonium acetate buffer + 10% methanol, pH 4.0, 10 second voltage (10kV) injection, 30°C

It can be seen that in addition to the paraquat peak at t_{mig} 5.09 minutes, 3-4 other peaks are clearly visible above the baseline noise. These peaks have been tentatively assigned as follows, based on the migration times obtained in the analyses of standard mixtures.

t_{mig} (minutes)	Peak Assignment (tentative)
5.09	Paraquat
8.39	Monoquat
9.46	4,4-Bipyridyl
10.24/10.35	2,2-Bipyridyl

Table 3.10 – Migration times and tentative peak assignments for peaks detected in a sample of Technical Paraquat using CZE-UV

No peak corresponding to 2,2-paraquat was observed but it was unclear whether this meant that no 2,2-paraquat was present in the sample or that the very large and overloaded paraquat peak was masking a smaller 2,2-paraquat peak. A small ‘lumpy’ peak was observed in the baseline at a time corresponding with the migration time of n-methyl pyridinium. However, peak shape was poor and it was not clearly visible above the baseline noise in that region of the electropherogram, so it was unclear whether it was due to n-methyl pyridinium. It was hoped that subsequent CZE-MS experiments would confirm the identity of each these peaks and assist in the identification of any impurities present at lower levels or not detected by UV.

3.6.2 – tCITP OF PARAQUAT AND ITS IMPURITIES

With a view to improving the detection limits for the trace components, the technique of transient capillary isotachopheresis (tCITP) was assessed. As discussed in Section 3.5.2 CITP has traditionally been used as a means of separation but has more recently been employed as a preconcentration step prior to CZE. This was initially achieved by the coupling of two instruments or two capillaries but more recently preconcentration (CITP) and separation (CZE) have been achieved in a single capillary [37,48]. This technique has become known as transient capillary isotachopheresis or tCITP [49,50] and has been successfully used in the analysis of proteins, peptides and small ionic compounds. Transient CITP has also been used in combination with electrospray mass spectrometry to improve the detection of protein samples over conventional CZE [51].

3.6.2.1 – Transient CITP

In tCITP rather than sandwiching the sample between leading and terminating electrolyte as in traditional CITP the sample is dissolved in the leading electrolyte (LE) and injected onto a capillary filled with low mobility terminating electrolyte (TE). At the beginning of the separation, analytes are isotachophoretically concentrated between the leading electrolyte and the terminating electrolyte. However, because the leading electrolyte is itself preceded by terminating electrolyte the ions of the LE migrate away from the sample. The analyte ions then separate zone electrophoretically in the terminating electrolyte. Like CITP, it is a technique capable of analysing much larger sample volumes than CZE as the analyte bands are concentrated and focused between the high mobility electrolyte and the low mobility electrolyte.

As with conventional ITP the selection of the leading and terminating electrolyte is fundamental to the success of the technique. As the study compounds are cationic (or neutral), the buffers selected must contain cations with higher (LE) and lower (TE) mobilities than the analytes. After consulting tables of mobility data it was observed that the ammonium cation has the highest recorded mobility and as it had already been used successfully in the CZE experiments it was decided to continue with ammonium acetate as the leading electrolyte. A range of cations with lower mobilities were selected; β -Alanine, Ammediol, Tris, Tetramethylammonium, Triethylammonium and Diethylammonium, and these were used as the terminating electrolyte in the initial studies performed with a view to developing a successful tCITP method. Since no literature regarding the mobilities of the study compounds was available, the cations chosen as potential terminating electrolyte were selected so that they covered a relatively wide mobility range.

Cation	Mobility ($\times 10^{-9} \text{ m}^2 \text{ V}^{-1} \text{ s}^{-1}$)
Ammonium	+72.2
β -Alanine	+37.5
Ammediol	+27.7
Tris	+26.9
Tetramethylammonium	+42.6
Triethylammonium	+30.6
Diethylammonium	+34.1

Table 3.11 – Mobility data for cations used as leading and terminating electrolytes used in preliminary tCITP experiments [52]

Following the procedure outlined in several papers by Frantisek Foret, Toni Thompson et al [59,51] and Christine Schwer [50], samples were prepared and diluted in the leading electrolyte. The samples were introduced onto the capillary filled with terminating electrolyte before the separation voltage was applied. For the initial work the experimental conditions employed were as outlined below, with terminating electrolyte and injection mode and time all being varied in order to assess the optimal conditions.

Operating Conditions

Capillary:	57cm × 50 μ m i.d. fused silica capillary (50cm to detector)
Leading Electrolyte:	100mM Ammonium Acetate buffer, pH 4.0
Terminating Electrolyte:	Varied
Injection Mode:	Varied
Injection Time:	Varied
Applied Voltage:	15kV
Temperature:	30°C
Detection:	UV @ 254nm

Each of the buffers used as TE was prepared in 100mM concentration and adjusted to pH 4.0 with glacial acetic acid.

Comparison of the electropherograms obtained for each of the terminating electrolytes showed on the whole that the majority of the buffer systems suffered from poor peak shape, poor resolution and missing peaks. By far the most successful separation, in terms of resolution, peak shape and the number of components detected above the baseline noise, was achieved when using β -alanine as the terminating electrolyte. Examples of the electropherograms obtained in these experiments can be seen in Figures 3.31(a) – (f).

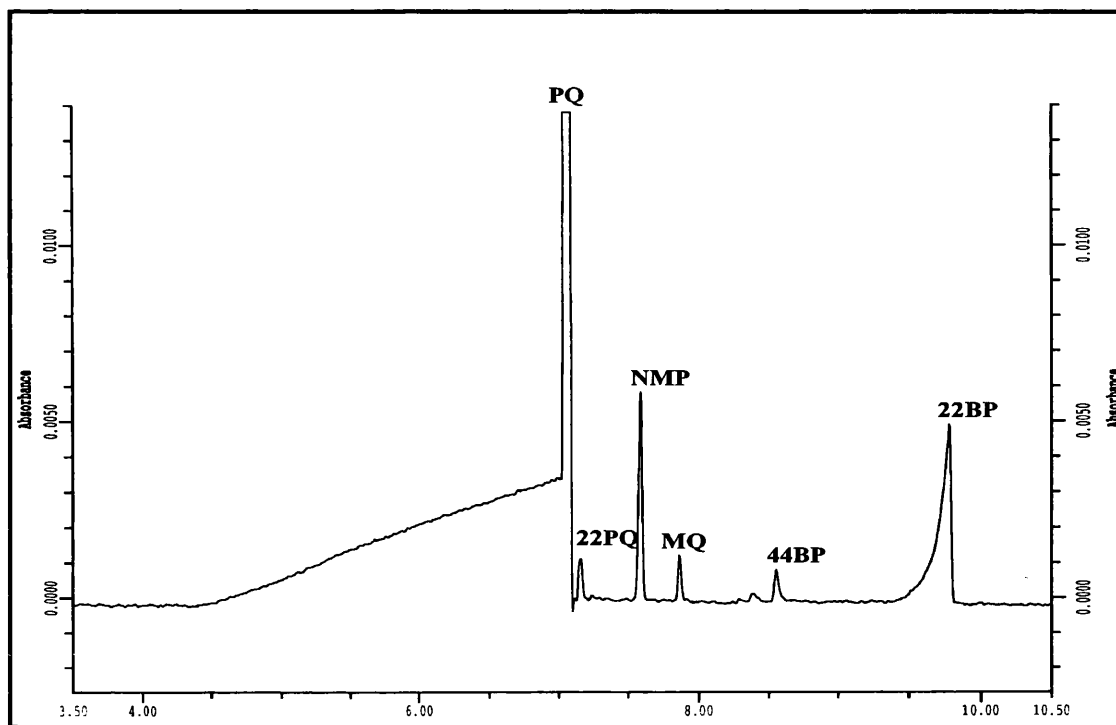


Figure 3.31(a) – Terminating Electrolyte: 100mM β -Alanine, 90 second pressure injection

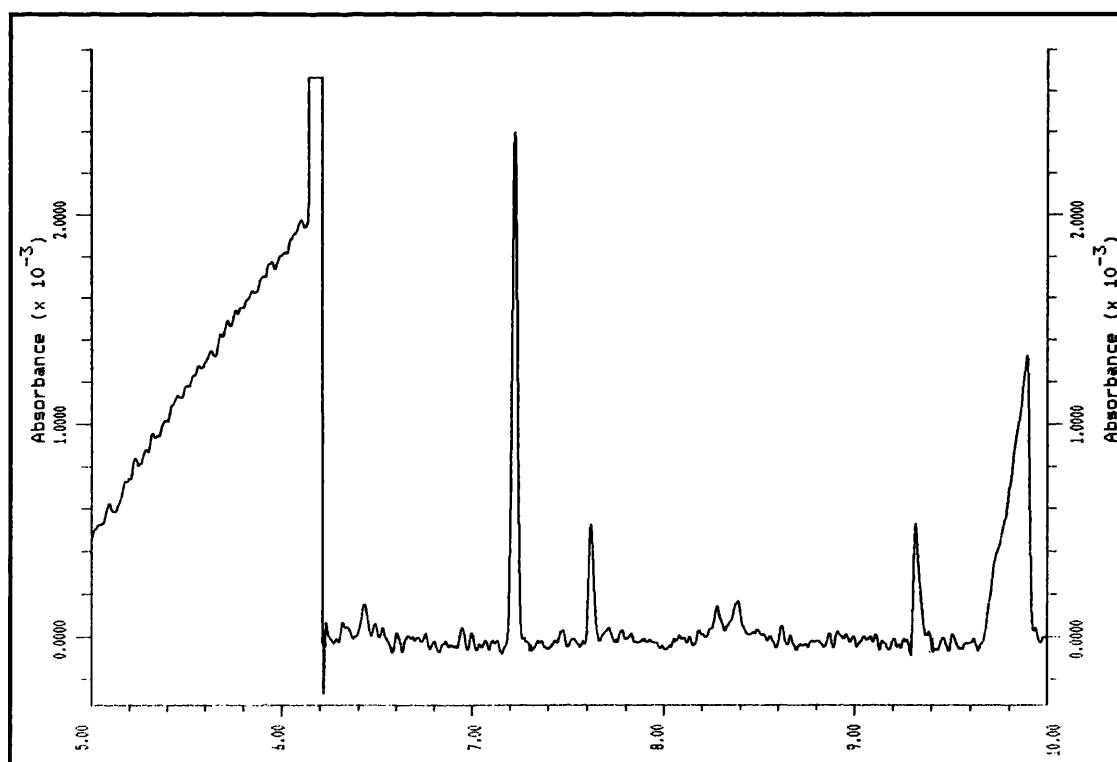


Figure 3.31(b) – Terminating Electrolyte: 100mM β -Alanine, 90 second voltage (10kV) injection

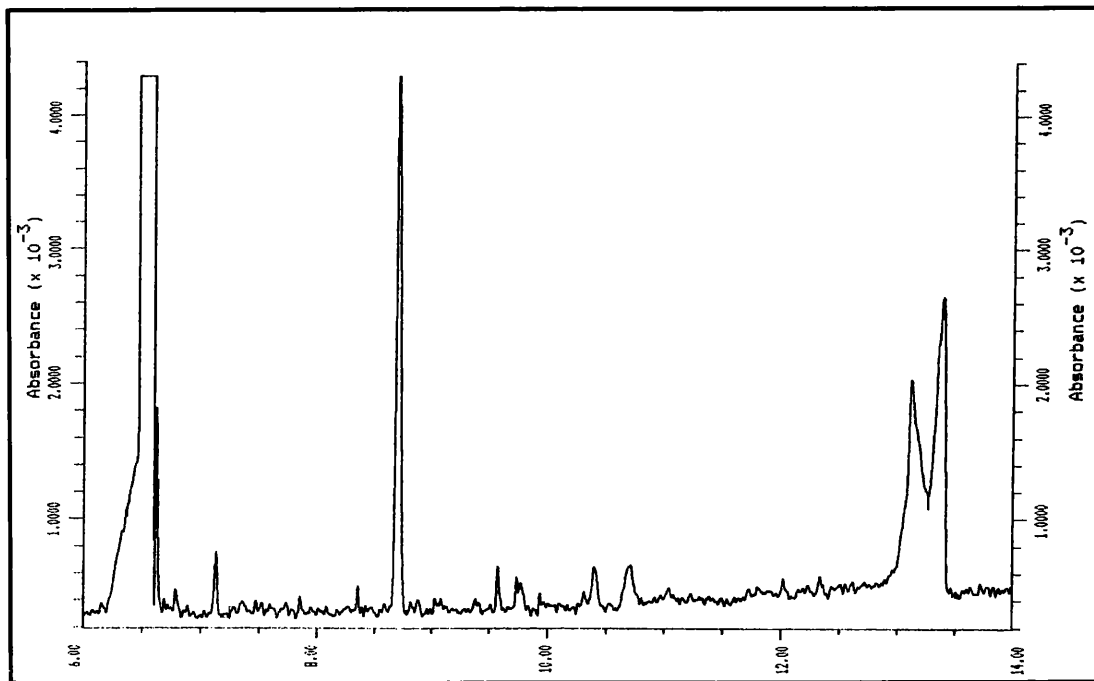


Figure 3.31(c) – Terminating Electrolyte: 100mM Ammediol, 90 second voltage (10kV) injection

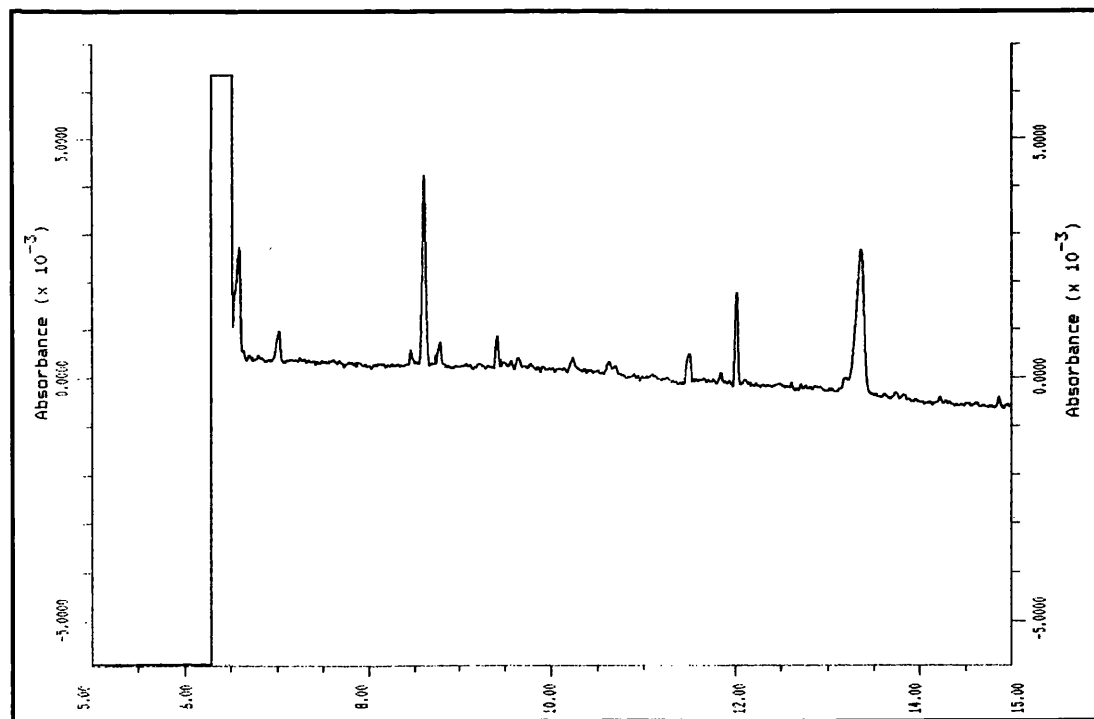


Figure 3.31(d) – Terminating Electrolyte: 100mM Tris, 90 second voltage (10kV) injection

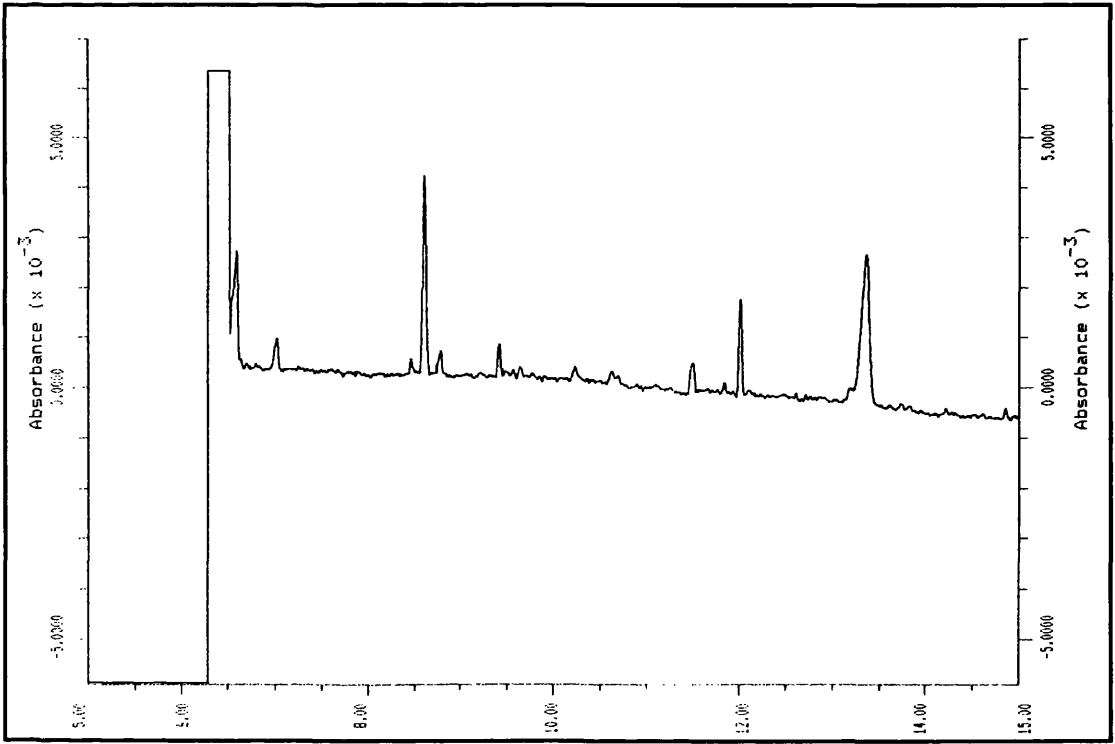


Figure 3.31(e) - Terminating Electrolyte: 100mM Tetramethylammonium, 90 second pressure injection

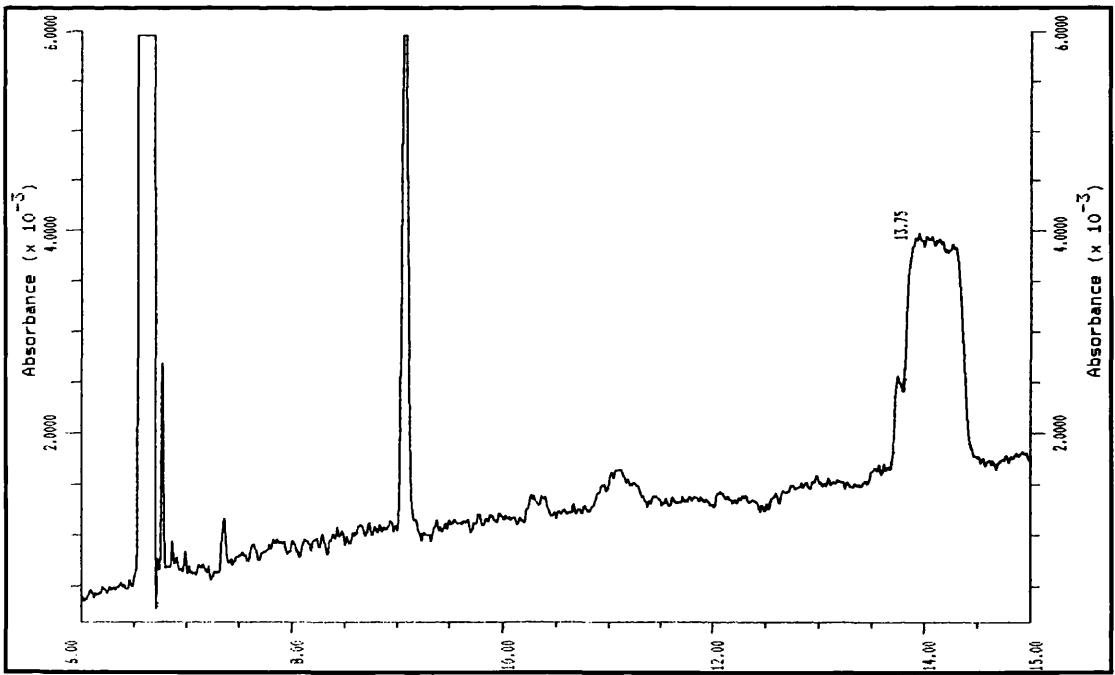


Figure 3.31(f) - Terminating Electrolyte: 100mM Diethylammonium, 90 second pressure injection

3.6.2.2 - Effect of injection type and time on separation

Having selected β -alanine as being the most successful of the terminating electrolytes studied, the effect of varying the injection time and the influence of the mode of injection on the separation achieved under these conditions was assessed.

Efficiency

Comparison of the cumulative calculated peak efficiencies obtained for each mode of injection can be seen in Figure 3.32.

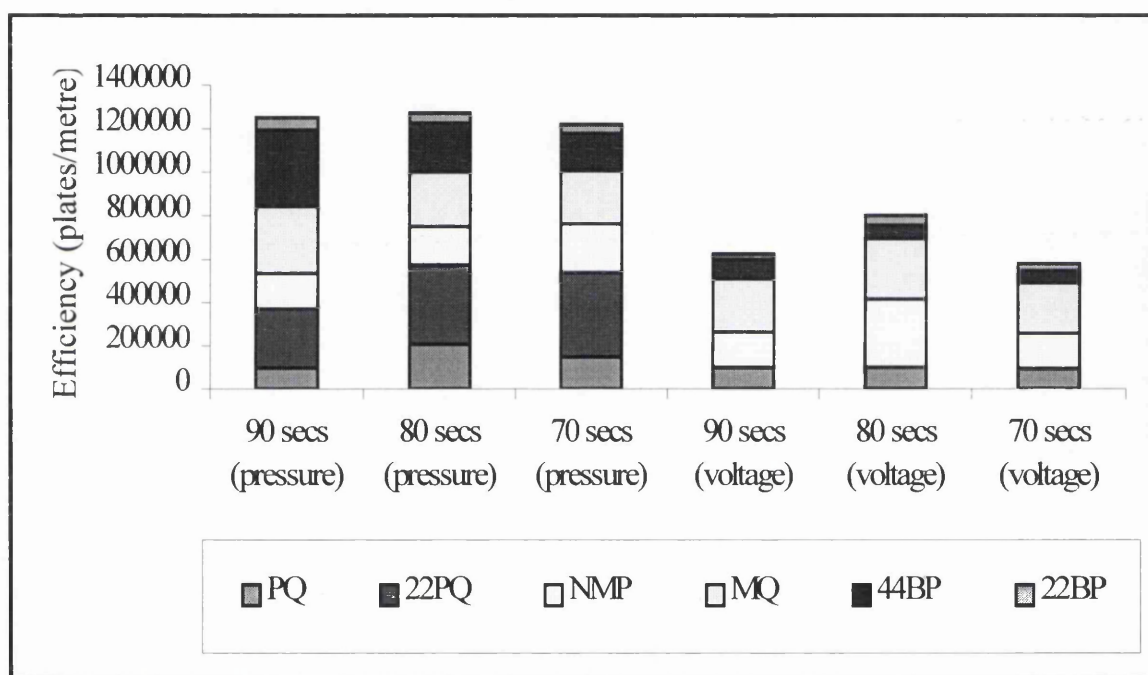


Figure 3.32 – Cumulative efficiency of paraquat and impurities versus injection type and time

It should be noted, however, that the 2,2-paraquat peak was not observed in the electropherograms from the experiments that used voltage injection, which accounts in some way for the great differences in cumulative efficiency between the two injection modes. It should also be noted that due to the significant ramping on

the paraquat peak the figure calculated for the peak efficiency can only be regarded as an estimate at best.

It was observed that the peak efficiencies achieved for the first four (three in the case of the voltage injection experiments) component peaks were, in general, similar in magnitude for each injection mode. With the exception of the overloaded paraquat peak each of these peaks is sharp and symmetrical. Differences in the 4,4-bipyridyl peak shape and efficiency are more apparent. The peak shape achieved with the use of hydrodynamic injection is again sharp and symmetrical, while those in the electrokinetic injection experiments are significantly wider than the preceding peaks, resulting in the relatively poor calculated peak efficiencies observed. Poor peak shape is observed for the 2,2-bipyridyl peak for each of the modes of injection. The peak width is at least twice that of the 2,2PQ, NMP and MQ peaks in each case, and unlike these peaks the 2,2BP peak exhibits significant fronting. This would appear to indicate that the 2,2-bipyridyl is not being focussed at the front of the column as well as the other analytes, possibly as a result of insufficient differences between the mobilities of the analyte and the terminating electrolyte.

Resolution calculations were also performed for comparison; the data generated is shown below in Table 3.12. No data is given for those separations involving 2,2-paraquat for the voltage injection experiments as the component was not detected and is most probably unresolved from the large paraquat peak.

	90 Second injection		80 Second injection		70 Second injection	
	Pressure	Voltage	Pressure	Voltage	Pressure	Voltage
PQ/22PQ	0.54	-	1.76	-	1.50	-
22PQ/NMP	3.86	-	6.17	-	7.75	-
NMP/MQ	2.93	8.85	1.87	7.24	5.05	5.80
MQ/44BP	10.09	24.51	10.23	17.42	10.81	15.97
44BP/22BP	9.31	3.61	9.81	2.19	8.94	2.09

Table 3.12 – Comparison of resolution data obtained using pressure and voltage injections

However, although the separation and peak shape under these conditions was otherwise good, the high concentration of paraquat in the standard mix resulted in very severe ramping/fronting on the peak most probably as a result of overloading but could possibly be due to buffer system incompatibility. Although the objective of this work was to enhance the detection of the trace impurities and the appearance of the paraquat peak was of less importance in these separations further work was performed with a view to improving the resolution and peak shape. Experiments were repeated using 150, 50 and 20mM β -alanine (pH 4.0) as terminating electrolyte.

3.6.2.3 – Effect of buffer concentration on the separation

The six component mixture was prepared in a solution of ammonium acetate buffer with its concentration corresponding with that of the terminating electrolyte being used in each case, either 20, 50 or 150mM. The sample was injected onto the capillary using hydrodynamic injection for 50, 60, 70, 80 or 90 seconds.

None of the alternative buffer concentrations resulted in any improvement in the paraquat peak shape. In addition, comparison of the separations achieved under each set of conditions with the results previously obtained with the use of 100mM electrolytes showed that the use of both the higher and lower buffer concentrations had a detrimental effect on the separation.

3.6.2.4 – Effect of capillary type on reproducibility and the separation

During the course of these studies some problems were experienced with between-run reproducibility with migration times varying significantly between repeat analyses performed on different days. It was proposed that one possible reason for these differences in migration times was the adsorption of the analyte species to the capillary walls [14,15,53]. With a view to eliminating this adsorption and hopefully improving reproducibility the use of specialist coated and deactivated CE capillaries was investigated. The two capillaries used were the Supelco CElect Neutral Hydrophilic P150 and the MicroSolv CE Deactivated Fused Silica capillary. According to the sales literature the inert, biocompatible polymer bonded to the capillary surface of the Supelco product would reduce sample-to-column wall interactions and reduce the EOF resulting in more efficient and more reproducible

Chapter 3 CE and CE-MS Studies of Pesticides and Related Impurities 123

separations [54]. The MicroSolv capillary also promised to reduce the wall adsorption effect produced by active silanol sites and suppress EOF with the result of improved resolution [55].

In order to assess the utility of the capillaries and their claims regarding improvements in reproducibility a brief study was carried out. A number of repeat injections of both individual standards and mixed standards were performed on each of the two coated capillaries and on the standard fused silica capillary on two days approximately 1 month apart.

Migration Time

Figure 3.33 illustrates that each of the specialist capillaries exhibits lower migration times for each of the six sample components.

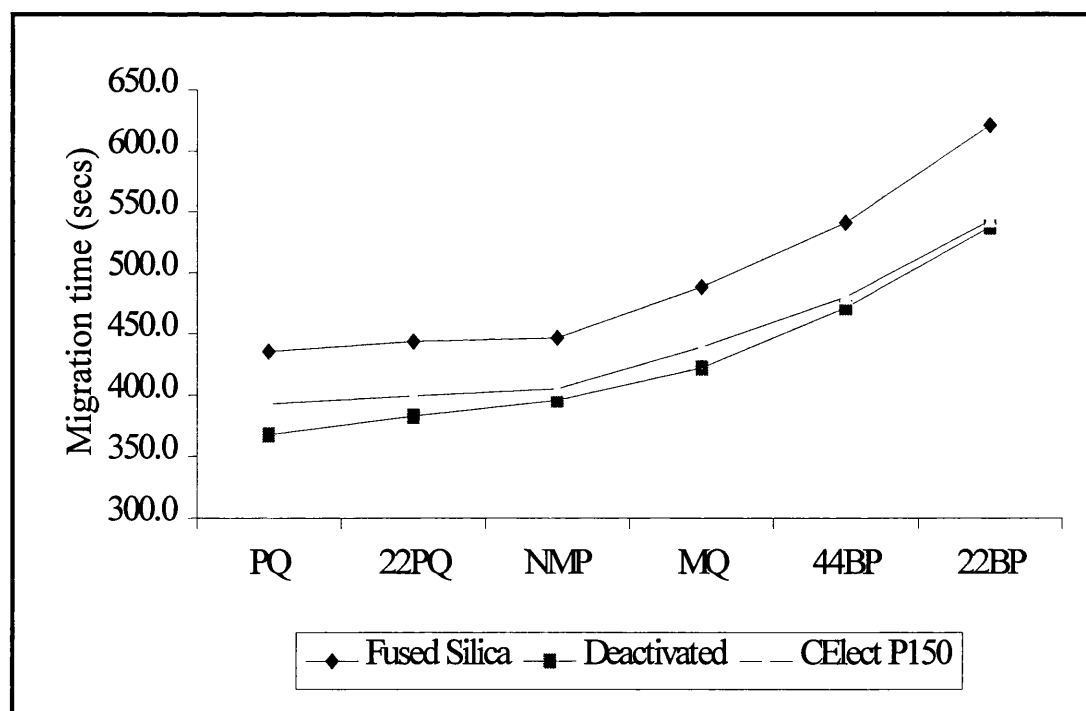


Figure 3.33 – Effect of capillary type on migration time

	Within Run %RSD			Between Run %RSD		
	Fused Silica	Deactivated	CElectP150	Fused Silica	Deactivated	CElectP150
PQ	2.39	4.97	1.47	3.82	5.67	3.13
22PQ	2.27	0.67	1.77	4.06	1.87	3.33
NMP	2.01	5.33	1.79	3.97	3.89	2.78
MQ	2.07	5.10	1.88	4.88	3.66	3.39
44BP	2.61	5.14	1.63	5.14	3.64	3.97
22BP	4.30	5.52	1.94	6.62	3.94	4.77

Table 3.13 – Comparison of migration time reproducibility data obtained using different capillaries

The results displayed in Table 3.13 demonstrate that in general the reproducibility of the migration times obtained when using the CElect-P150 column is better, both within run and between run, than either the fused silica capillary or the MicroSolv deactivated capillary. An improvement in comparison with the standard fused silica capillary was expected, but the results obtained using the deactivated capillary were generally poor by comparison.

Chapter 3 GC and GC-MS Studies of Puriquin and Related Impurities 127

Peak Area Reproducibility

	Within Run %RSD			Between Run %RSD		
	Fused Silica	Deactivated	CElectP150	Fused Silica	Deactivated	CElectP150
PQ/22PQ	1.34	0.76	0.43	3.58	4.98	31.72
22PQ/NMP	0.44	1.61	0.43	5.01	3.91	28.98
NMP/MQ	0.54	1.16	0.72	4.35	1.61	29.72
MQ/44BP	0.35	1.37	0.89	4.47	3.45	30.10
44BP/22BP	0.41	1.15	0.52	5.13	5.04	28.37

Table 3.14 – Comparison of peak area reproducibility data obtained using different capillaries

The comparison of peak area reproducibility data is less straightforward as any error involved with the injection technique would also have an effect on peak area in addition to any capillary adsorption effects. The data shown in Table 3.14 is fairly inconclusive and it is difficult to draw any firm conclusions from it. In the experiments performed on all three capillaries the peak area increased steadily throughout. This was particularly noticeable with the CElect P-150 capillary where the average areas for each component on day 2 were approximately double the areas on day 1. With this limited study it would be rash to make any definitive statements regarding the benefits to peak area reproducibility of using specialist capillaries, but based on the data obtained there would appear to be little advantage.

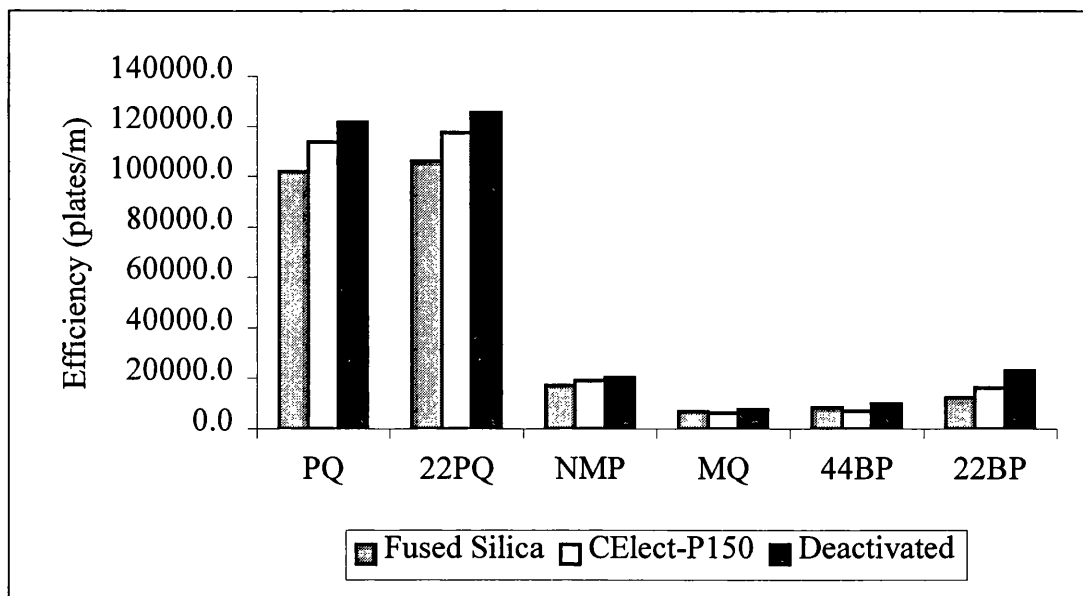


Figure 3.34 – Effect of capillary type on peak efficiency

Figure 3.34 illustrates the effect of capillary type on the peak efficiencies obtained for each of the six study compounds. It can be seen that, in general, the efficiencies achieved with the use of the deactivated capillary and the CElect P-150 capillary are higher than those generated with either the standard fused silica capillaries. Both specialist capillaries produced the improved efficiencies as advertised in the sales literature and based on this limited series of experiments their use would appear to be advantageous.

Resolution

It can be seen from Figure 3.35 that, with one exception, the resolution values achieved using both of the specialist capillaries are greater than those obtained with the standard fused silica capillary. The results mirror the pattern seen with the peak efficiencies and again support the claims of the manufacturers. The average migration times obtained for each of the capillaries indicated that the EOF was

suppressed to the greatest extent in the MicroSolv CE Deactivated capillary. The figures calculated for both efficiency and resolution would appear to confirm this as both sets of data for this capillary were better than those obtained for either of the other capillaries.

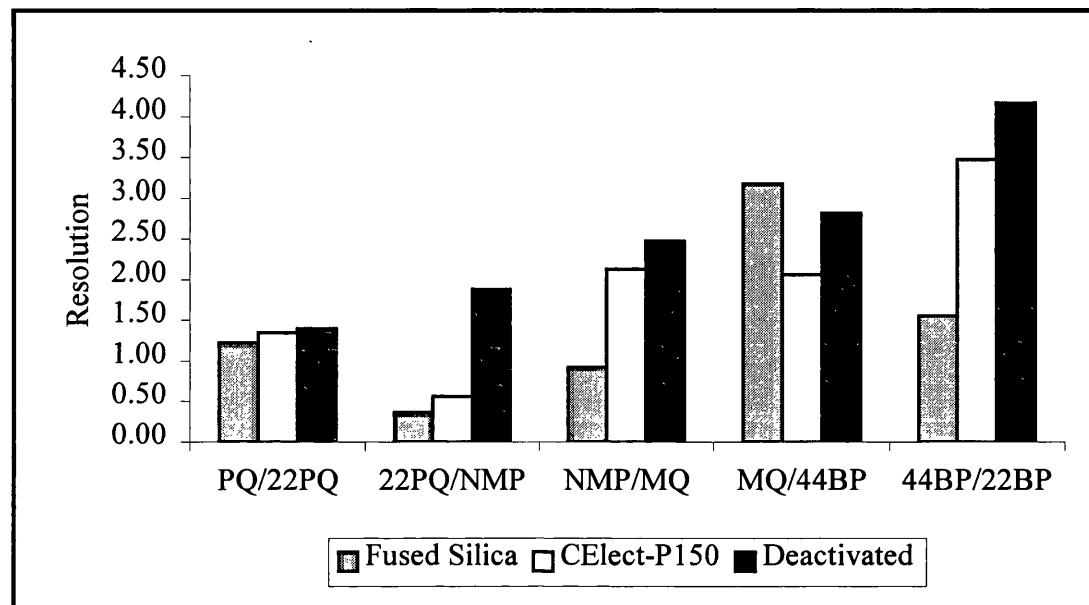


Figure 3.35 – Effect of capillary type on resolution

While it would appear that the specialist capillaries do offer some advantages over the standard fused silica typically used, based on the data generated in this limited study the benefits to this specific separation would appear to be limited. The problem, which prompted the investigation of these alternative capillary types, was the poor reproducibility of migration times, and although both specialist capillaries produced some improvement in this area the cost of these capillaries in comparison with the standard fused silica was rather prohibitive. Consequently, the majority of the subsequent work, including the on-line CE-MS experiments, was performed using the standard fused silica capillary.

3.6.2.5 – Linearity

In order to investigate the linearity of the tCITP method a series of standards in the range 0.1ppm to 100ppm were produced for each of the six study compounds. The data obtained from the replicate injections of progressively more dilute standards was plotted in order to determine the linearity of response of the method over the concentration range 0.1 to 100ppm. Regression calculations performed for the linearity plot of each compound produced R^2 values of greater than 0.9990 in each case, thus demonstrating that the method is linear for each of the six study compounds over the range 0.1 to 100ppm.

The linearity graphs produced for each compound are shown in Figure 3.36. Table 3.15 shows the correlation coefficients determined for each of the six compounds.

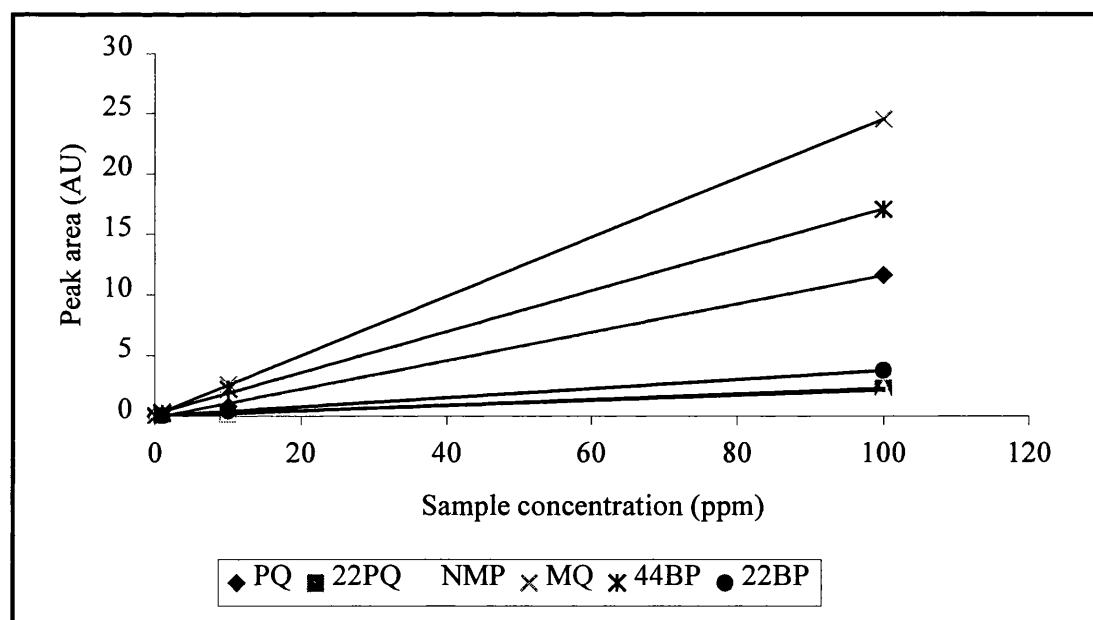


Figure 3.36 – Linearity of response for each of the six study compounds

	Correlation Coefficient (R²)
PQ	0.9992
22PQ	1.0000
NMP	0.9998
MQ	1.0000
44BP	0.9991
22BP	0.9995

Table 3.15 – Correlation coefficients for the data shown in Figure 3.36

3.6.2.6 - Limit of detection (LOD) and limit of quantitation (LOQ)

The LOD and LOQ for each of the six study compounds was determined using Equations 3.14 and 3.15.

	LOD (ppb)	LOQ (ppb)
PQ	2.5	8.2
22PQ	225.0	750.0
NMP	29.6	98.8
MQ	14.3	47.7
44BP	32.7	108.9
22BP	540.9	1803.1

Table 3.16 – Limits of detection and quantitation for each of the six study compounds using the tCITP method

Comparison of the LOD and LOQ achieved using tCITP with those previously obtained using CZE and shown in Table 3.9 shows that, improvements in detection limits by factors of between 5.3 and 84.4 were achieved with the use of the preconcentration technique. The variation in the level of improvement achieved for each of the compounds may be due to any differences in sample loading resulting from the use of electrokinetic injection in the original CZE experiments.

Use of the Beckman ‘CE Expert’ [56] application enabled the calculation of additional information relating to the theoretical volume of analyte injected at the calculated limit of detection under the experimental conditions detailed.

Compound	Volume Injected (nl)	Analyte Injected (pg)	Analyte Injected (fmol)
Paraquat	104	0.26	1.41
2,2-Paraquat	104	23.52	126.5
N-Methyl Pyridinium	104	3.10	32.93
Monoquat	104	1.50	8.75
4,4-Bipyridyl	104	3.42	21.92
2,2-Bipyridyl	104	56.56	362.5

Table 3.17 – Injection volumes calculated using ‘CE Expert’

The figures calculated and displayed in Table 3.17 are based on theoretical principles and should be regarded as approximations and are included for information only.

3.6.2.7 – tCITP of technical paraquat

After successfully performing the transient capillary isotachophoretic separation on standard mixtures of paraquat and the other five compounds the operating conditions detailed below were used in the analysis of the technical paraquat sample. In the previously performed CZE analysis only paraquat and three of the five known impurities were detected in the sample diluted by a factor of 200 in water, it was hoped that tCITP would improve on this.

As with the CZE experiments the technical paraquat sample was diluted prior to analysis, in this case the sample was diluted with the leading electrolyte, 100mM ammonium acetate buffer and adjusted to pH 4.0.

Operating Conditions

Capillary:	57cm × 50 μ m i.d. fused silica capillary (50cm to detector)
Leading Electrolyte:	100mM Ammonium Acetate buffer, pH 4.0
Terminating Electrolyte:	100mM β -Alanine, pH 4.0
Applied Voltage:	15kV
Injection Mode:	Pressure
Injection Time:	90 seconds
Temperature:	30°C
Detection:	UV @ 254nm

Samples diluted by factors of up to 4000 were injected. In addition to the peak resulting from the paraquat, six additional peaks are observed in the electropherogram of the sample diluted by 1000, shown in Figure 3.37.

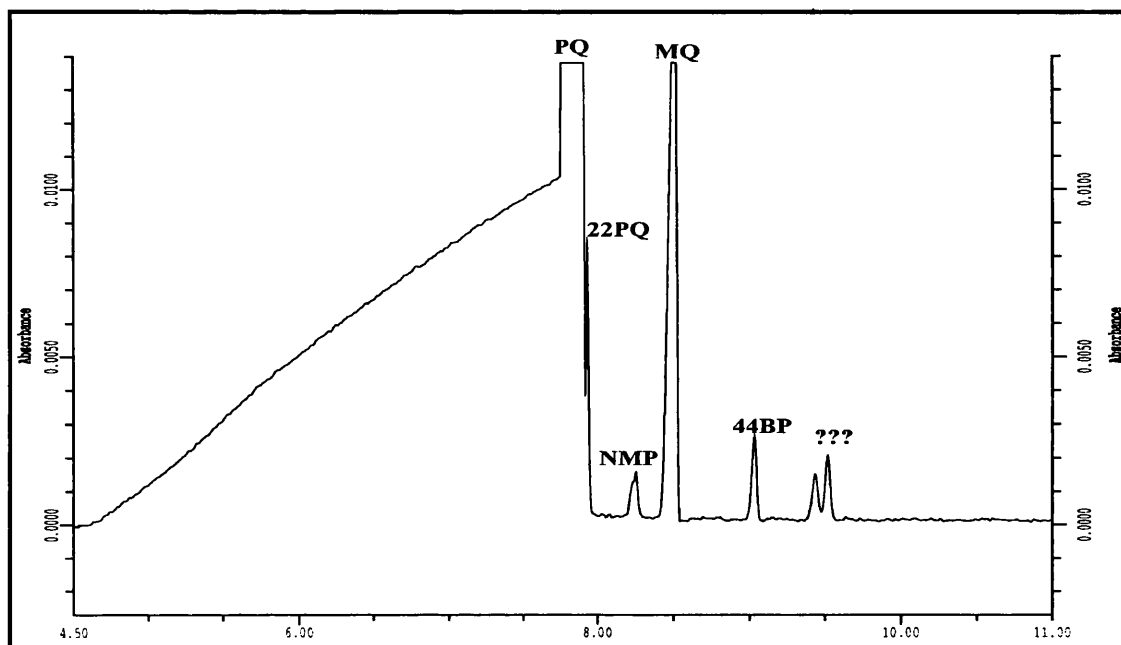


Figure 3.37 - Electropherogram of a sample of technical paraquat using 15kV applied voltage, LE: 100mM ammonium acetate buffer, TE: 100mM β -Alanine pH 4.0, 90 second pressure injection, 30°C (tCITP-UV)

Comparison of the relative retention times of the peaks obtained in this separation of the technical sample with those of the standard mixture of the six study compounds allowed the identification of four out of the six impurity peaks, see Table 3.18.

Standard Mixture		Technical Sample		
Component	RRT	Peak	RRT	Peak Assignment
PQ	1.00	1	1.00	PQ
22PQ	1.01	2	1.01	22PQ
NMP	1.04	3	1.05	NMP
MQ	1.07	4	1.08	MQ
44BP	1.14	5	1.15	44BP
22BP	1.28	6	1.20	?
		7	1.21	?

Table 3.18 - Migration times and tentative peak assignments for peaks detected in a sample of Technical Paraquat using tCITP-UV

It is possible that one of the remaining unidentified peaks at RRT 1.20 or 1.21 may be due to 2,2-bipyridyl. Had spiking experiments been performed at this point this could have been clarified, but it was anticipated that on-line tCITP-MS studies would assist in the identification of each of these unknown components.

Use of the linear calibration graphs produced from the data generated in the linearity study allows the quantitation of each of the identified impurities in the sample of technical paraquat. Using the equation below, Equation 3.16, the concentration of each of the components in $\mu\text{g/ml}$ was calculated.

$$\text{Concentration } (\mu\text{g/ml}) = \frac{\text{Peak Area Sample}}{\text{Peak Area Std}} \times \text{Conc}^n \text{ Standard } (\mu\text{g/ml}) \times 1000$$

Equation 3.16

As the standards were not prepared with the intention of using them for quantitation the results tabulated below in Table 3.19 can only be viewed as approximations.

Peak	Peak Area	Concentration ($\mu\text{g/ml}$)	Concentration (%w/v)
PQ	42.58311	367127.4	36.71
22PQ	0.16707	7335.7	0.73
NMP	0.07109	3272.8	0.33
MQ	1.07697	4394.4	0.44
44BP	0.11984	704.0	0.07
UNKNOWN 1	0.07307	—	—
UNKNOWN 2	0.09398	—	—

Table 3.19 – Approximate composition of Technical Paraquat sample

3.6.3 – CE-MS OF PARAQUAT AND IMPURITIES

The mass spectrometer used in the experiments described in the section was the Finnigan LCQ ion trap which has been described in detail in Section 2.5. In order to perform CE-MS using the LCQ and the Beckman P/ACE 2200 CE instrument certain modifications were made to both the CE instrument and the Finnigan ESI interface. A brief overview of these modifications is given below and a more detailed account of the interfacing the Beckman CE with a Finnigan ESI source can be found elsewhere [57].

Modifications to the Beckman P/ACE 2200

- A small hole was cut into the right hand side of the plexi-glass safety lid in order to allow the outlet end of the capillary to extend across to the mass spectrometer.
- Any outlet vials were removed from the inner autosampler carousel as the electrical contact at the outlet was achieved via the flow of sheath liquid.
- The spring loaded lever arm normally used in controlling the position of the outlet buffer vial was removed in order to prevent the possibility of the capillary being snapped as it moves during the normal operation of the CE instrument.
- The capillary was taped to the base of the CE detector unit in order to prevent it from being caught by the vials as they rotated.
- The capillary cartridge was prepared with the minimum length of 20cm between the inlet and the UV detector window and with at least 50 – 60cm length of capillary after the UV window to reach the ESI interface of the LCQ.

- The distance between the two instruments was kept to a minimum in order to maintain chromatographic efficiency and limit accidental contact with the capillary exposed to high voltages.
- The polyimide coating from the tip of the fused silica capillary was removed prior to use to prevent any possible contamination of the source.
- The Beckman P/ACE 2200 was positioned on a hydraulic trolley with variable height facility. This allowed the CE to be positioned such that the inlet buffer vial was at the same height as the capillary inlet on the ESI source in order to minimise the effect of siphoning.
- An earth lead was attached between the CE and the mass spectrometer for reasons of safety.
- The fault detection system circuit present in the electronics of the instrument was disabled. In normal operation this circuit detects any imbalance in current between the two high voltage electrodes and immediately shuts down the instrument in order to prevent damage to the electronic circuitry of the instrument which may result from current leaks or arcing. A switch was fitted into the circuit so that this safety feature could be disabled during on-line operation.

Modifications to the Finnigan ESI interface

- A wider bore electrospray needle was used in order to accommodate the outer diameter of the CE capillary. Consequently, a wider bore nozzle piece is also required to allow the positioning of the ESI needle.

- Sheath liquid is introduced at a rate of 3–5 $\mu\text{l}/\text{min}$ by means of the syringe pump incorporated into the front cover of the LCQ. The sheath liquid enters the source through the sheath liquid inlet and through the ESI needle surrounding the CE capillary. It was found that particular attention should be paid to the needle seal housing the electrospray needle. If this needle seal was damaged in any way or the needle was not correctly sealed, the sheath liquid was able to leak into the surrounding probe assembly causing discharge and resulting in an unstable ESI spray. This problem was controlled to some extent with the use of a small amount of PTFE tape wrapped around the needle seal to improve the seal.
- In order to achieve the low sheath gas flows often desirable in CE-MS, i.e. less than 20 units, the ‘sheath gas flow protect’ option in the diagnostics set-up of the LCQ operating system was deselected.
- In order to maintain the stability of the electrical contact necessary for the initialisation and sample injection on the CE instrument it was necessary to wait until the sample had been injected and the separation voltage had been reached before setting the mass spectrometer to scan.

3.6.3.1 – CZE-MS of paraquat and impurities

Prior to analysis the LCQ was tuned and calibrated using a mixture of caffeine, MRFA and Ultramark 1621 as recommended by the manufacturer [58]. In order to optimise the mass spectrometer operating conditions for the analysis of paraquat a 100ppm solution of paraquat was infused via the Beckman CE instrument using the high pressure rinse feature. The LCQ Tune Program was used to

Chapter 3 CE and CE-MS Studies of Purified and Related Impurities 159

automatically tune the instrument and adjust each of the electrospray parameters to give the optimum signal from the electrospray – MS system.

The conditions initially used were as detailed below:

CE operating conditions

Capillary:	Approximately 70cm × 50 μ m fused silica
Buffer:	100mM Ammonium acetate, pH 4.0
Applied Voltage:	15kV
Injection:	10 second (10kV)

Mass spectrometer operating conditions

Electrospray Voltage:	+4.5kV
Spray Current:	1.07 μ A
Capillary Temperature:	200°C
Capillary Voltage:	26.00
Tube Lens Offset:	-10.00
Sheath Gas Flow Rate:	50 arbitrary units
Auxiliary Gas Flow Rate:	0 arbitrary units
Sheath Liquid:	Methanol/10mM Acetic Acid (9:1)
Sheath Liquid Flow Rate:	3 μ l/min

Once the mass spectrometer conditions were optimised, the previously developed CE methodology, summarised above, was applied to the species under investigation. Each of the individual standards was injected and scanned over the range 50 - 200 m/z units in order to acquire mass spectral data for each compound and to determine the on-line migration time for each compound. The results of these initial on-line experiments are summarised Table 3.20, and CE-MS spectra for each compound are shown in Figures 3.38(a)-(f). The numbers in parentheses refer to relative abundances and a tentative identification of the fragment ion species is also given.

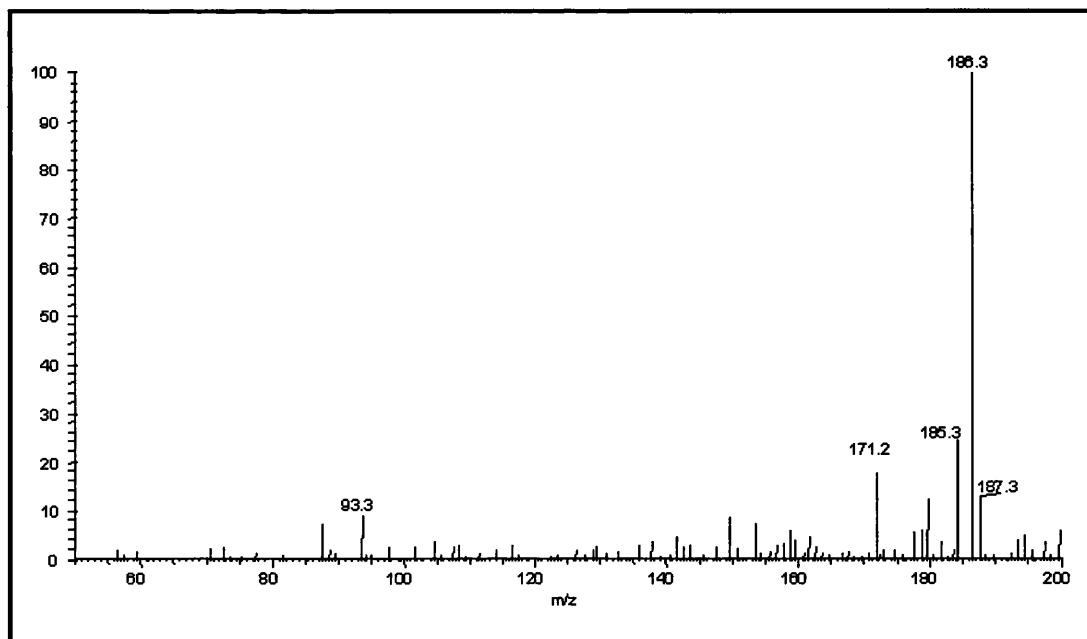


Figure 3.38(a) – Mass spectrum of Paraquat under CZE-MS conditions

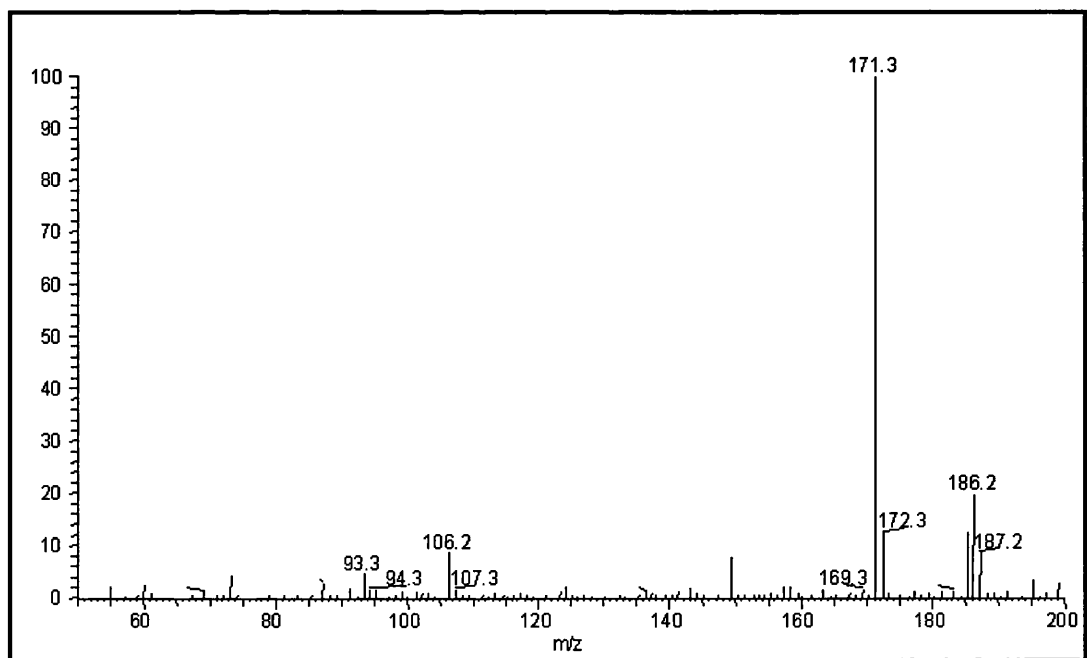


Figure 3.38(b) – Mass spectrum of 2,2-Paraquat under CZE-MS conditions

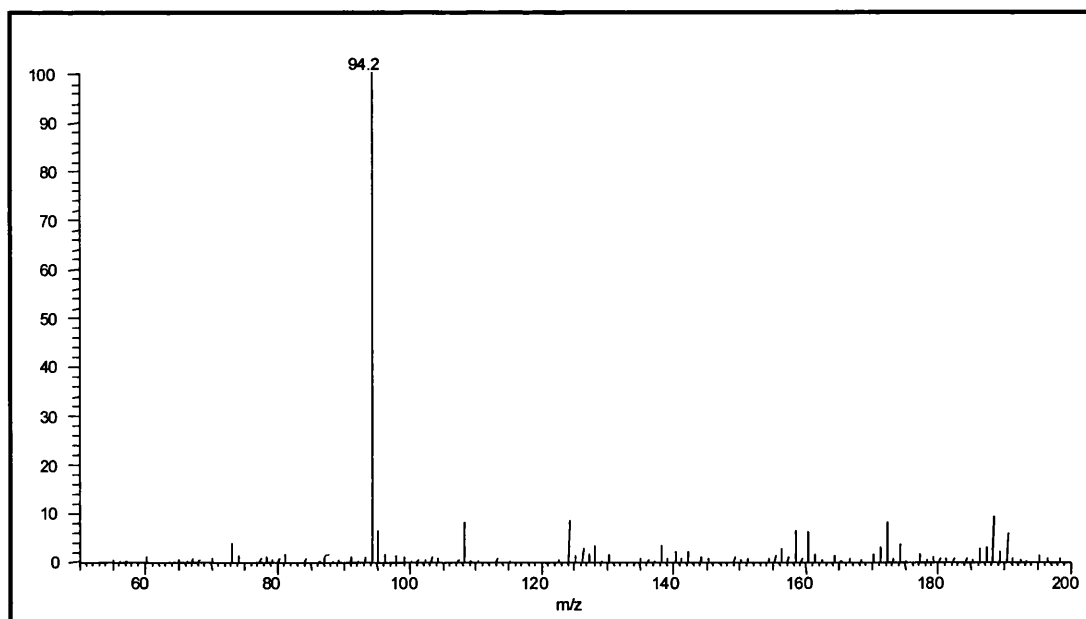


Figure 3.38(c) – Mass spectrum of n-Methyl Pyridinium under CZE-MS conditions

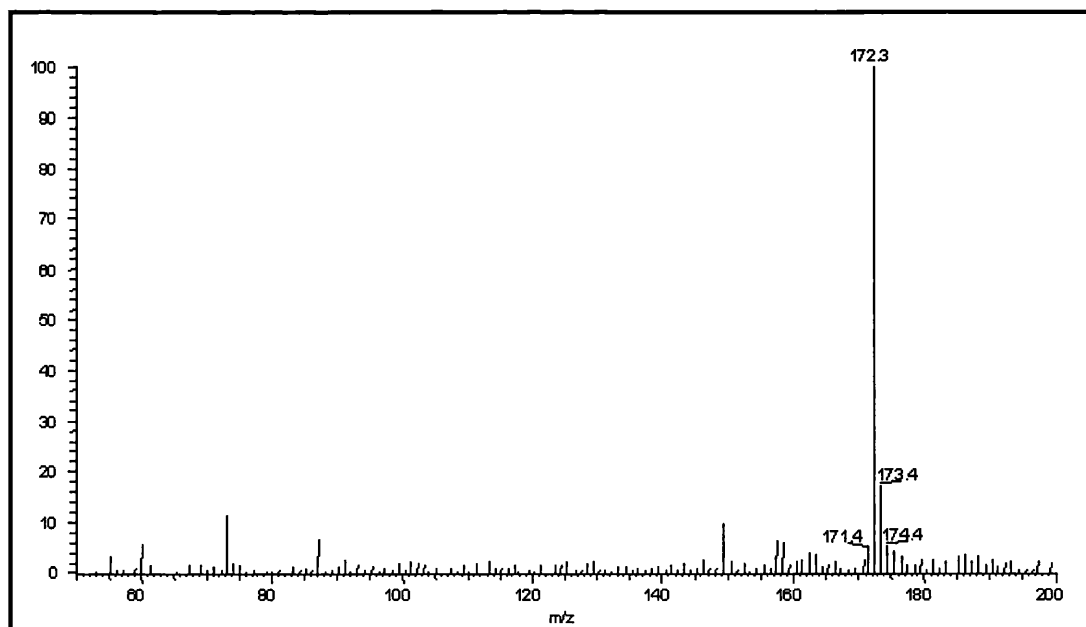


Figure 3.38(d) – Mass spectrum of Monoquat under CZE-MS conditions

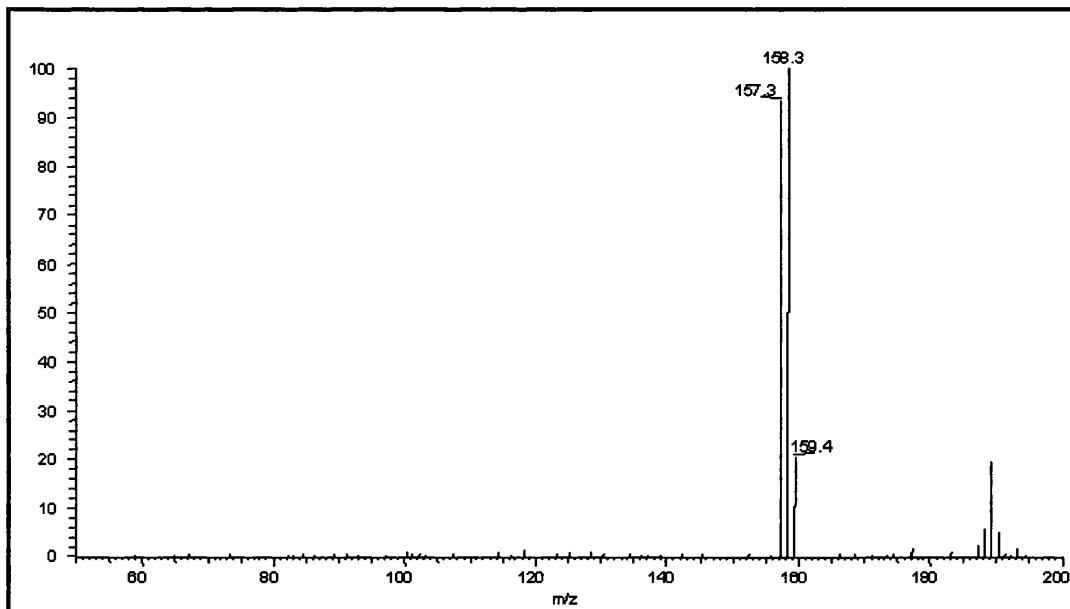


Figure 3.38(e) – Mass spectrum of 4,4-Bipyridyl under CZE-MS conditions

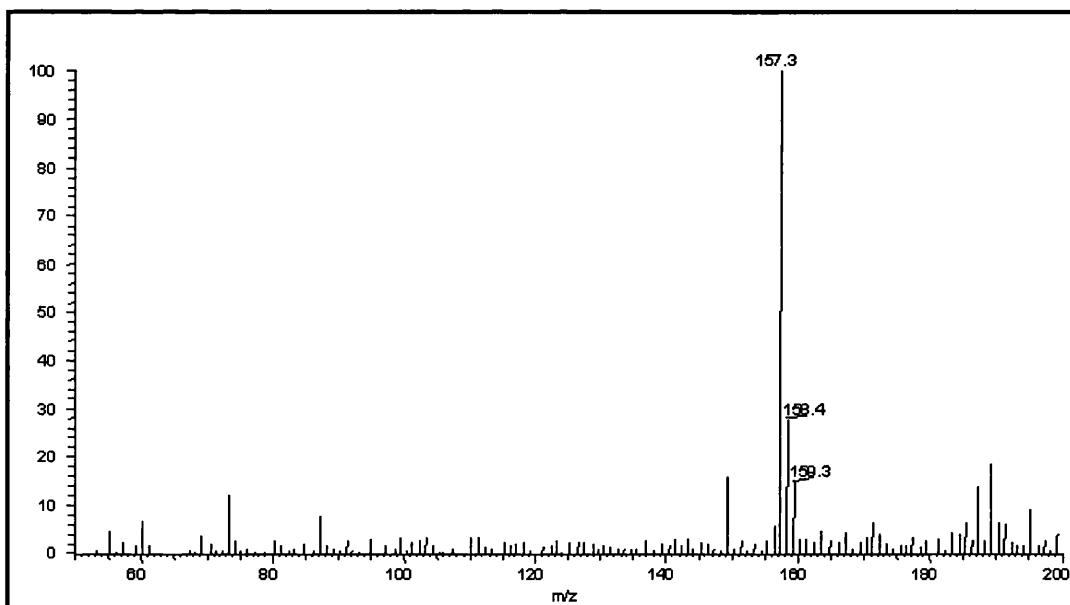


Figure 3.38(f) – Mass spectrum of 2,2-Bipyridyl under CZE-MS conditions

Analyte	M_r	Ion Observed	Species
Paraquat ion (PQ)	186	186 ₍₁₀₀₎ 185 ₍₂₆₎ 171 ₍₂₀₎ 93 ₍₁₂₎	[Cat] ^{+•} [Cat-H] ⁺ [Cat-CH ₃] ⁺ [Cat] ²⁺ or [Cat-C ₅ H ₄ NCH ₃] ⁺
2,2-Paraquat ion (22PQ)	186	171 ₍₁₀₀₎ 186 ₍₂₂₎ 185 ₍₁₁₎ 106 ₍₁₀₎ 93 ₍₆₎	[Cat-CH ₃] ⁺ [Cat] ^{+•} [Cat-H] ⁺ [Cat-H-C ₅ H ₃ NH ₂] ⁺ [Cat] ²⁺ or [Cat-C ₅ H ₄ NCH ₃] ⁺
N-methyl pyridinium ion (NMP)	94	94 ₍₁₀₀₎	[Cat] ⁺
Monoquat ion (MQ)	171	172 ₍₁₀₀₎	[Cat+1] ⁺
4,4-Bipyridyl (44BP)	156	158 ₍₁₀₀₎ 157 ₍₉₇₎	[M+2] ⁺ [M+H] ⁺
2,2-Bipyridyl (22BP)	156	157 ₍₁₀₀₎ 158 ₍₂₂₎	[M+H] ⁺ [M+2] ⁺

Table 3.20 – Summary of CZE-MS data for each of the study compounds

The major ions obtained for paraquat are comparable with those reported by Song and Budde [59] and Moyano et al [41] using CE-MS. The ion at m/z 93 has been confirmed as being doubly charged in nature, identifying it as the doubly charged di-cation [Cat]²⁺ rather than a fragment ion corresponding to half of the m/z 186 base ion. In (CAD) MS/MS experiments performed by Moyano et al the precursor ion of m/z 186 did not produce any fragment ions with m/z 93, while fragment ions with m/z values greater than 93 were obtained when (CAD) MS/MS was carried out using m/z 93 as the precursor ion. It is postulated by Song and Budde that the ion at m/z 185 is formed by the deprotonation of the m/z 93 [Cat]²⁺ ion i.e. [Cat²⁺-H]⁺. A mechanism has been proposed for this deprotonation, whereby ammonia removes a proton from the doubly charged molecular ion of

paraquat during desolvation of charged electrospray droplets or in the gas phase. The ammonium ion present in the CE buffer is in equilibrium with ammonia and protonated water in aqueous solution, consequently, ammonia is on hand to remove an acidic proton from one of paraquat's methyl groups. Alternatively, proton transfer from the ammonium ion to the acetate anion may occur, this is illustrated in Figure 3.39.

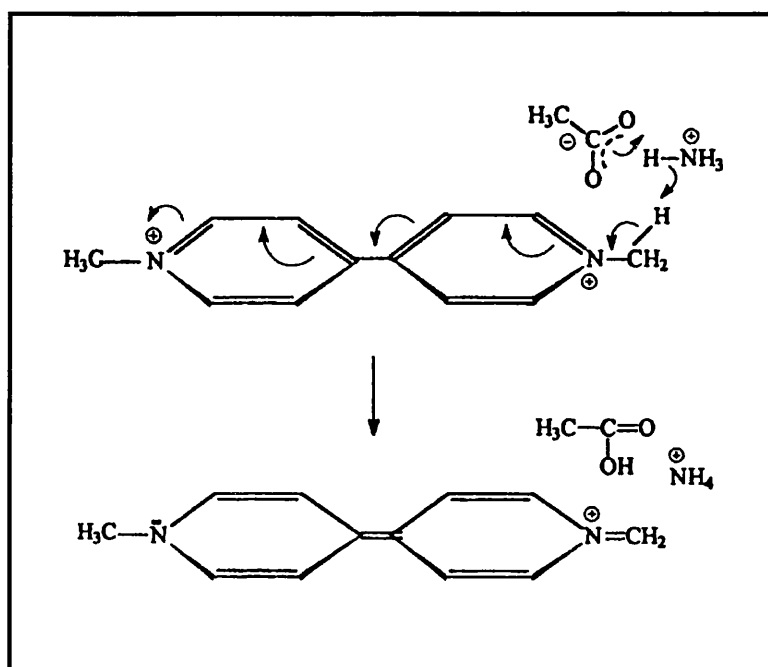


Figure 3.39 – Proposed mechanism for the deprotonation of the paraquat $[\text{Cat}]^{2+}$ ion [59]

The mass spectrum of the positional isomer of paraquat, 2,2-paraquat, also shows the molecular ion at m/z 186 but in this case it is much less intense. The base peak is found at m/z 171, and most probably results from the loss of a methyl group i.e. $[\text{Cat}-\text{CH}_3]^+$. A small peak at m/z 106, not present in the paraquat mass spectrum, is also observed, corresponding to a loss of 80 this has been tentatively assigned as $[\text{Cat}-\text{H}-\text{C}_5\text{H}_3\text{NH}_2]^+$ but the rearrangement and fragmentation processes

that may bring about this loss are not known. These differences in fragmentation are most probably due to differences between the stabilities of each of the compounds. While paraquat experiences para-directed charge stabilisation this is not the case in 2,2'-paraquat and the charge on the ring is less readily stabilised. In addition, the methyl groups in 2,2'-paraquat are in close proximity and as a result of these steric effects the loss of the methyl group is more favourable.

Both n-methyl pyridinium and monoquat showed little fragmentation with the most abundant ions being assigned to the $[\text{Cat}]^+$ or $[\text{Cat}_+1]^+$ ions. The most abundant peaks in the 2,2-bipyridyl and 4,4-bipyridyl mass spectra again correspond to the molecular ion.

MS/MS experiments were also performed at this point, but with limited success. Those experiments performed on monoquat, n-methyl pyridinium, 4,4-bipyridyl and 2,2-bipyridyl generated no useful results. Collision energies were either too low and did not result in any fragmentation or were too high and no ions were detected. A minimal amount of MS/MS information was obtained for paraquat and 2,2'-paraquat and this is tabulated below in Table 3.21.

Analyte	Precursor Ion m/z	%ce	Product Ion m/z
PQ	186 $[\text{Cat}]^{+\bullet}$	12	171 $[\text{Cat}-\text{CH}_3]^+$
	93 $[\text{Cat}]^{2+}$	8	171 $[\text{Cat}-\text{CH}_3]^+$
22PQ	186 $[\text{Cat}]^{+\bullet}$	13	171 $[\text{Cat}-\text{CH}_3]^+$

Table 3.21 – CZE-MS/MS data for paraquat and 2,2'-paraquat

Chapter 3 – CE and CE-MS Studies of Paraquat and Related Impurities 145

Both MS/MS experiments for paraquat and 2,2-paraquat using m/z 186 as the precursor ion generated product ions with m/z 171 corresponding to the loss of a methyl group. When m/z 93 was used as the precursor ion, in the case of paraquat, product ions with m/z greater than the precursor ions (m/z 171) were generated. This reflects the results reported by Moyano et al and as discussed previously confirms that the identity of the ion at m/z is [Cat]²⁺ rather than being the result of fragmentation of the m/z 186 [Cat]⁺ ion. MS³ experiments were attempted on both paraquat and 2,2-paraquat but were not successful and generated no useful data.

3.6.3.1.1 – Variation of methanol content

After performing these preliminary experiments to confirm the masses of interest and the online migration times of each of the study compounds the separation of a mixture of the six compounds was attempted using the experimental conditions as detailed above. These initial experiments were relatively unsuccessful and with a view to improving the stability and reproducibility of the separation, the use of buffers containing a percentage of methanol was investigated. As has been previously discussed, the use of significant amounts of organic solvents in CE buffers is desirable in terms of electrospray compatibility and enhances droplet charging. The use of methanol containing CE buffers has been investigated in offline experiments and although migration times were increased, efficient separations with fully resolved peaks were still obtained. Comparison of the response obtained for each of the six compounds using 100mM ammonium acetate buffers containing 5, 10 and 20 % methanol is illustrated in Figure 3.40.

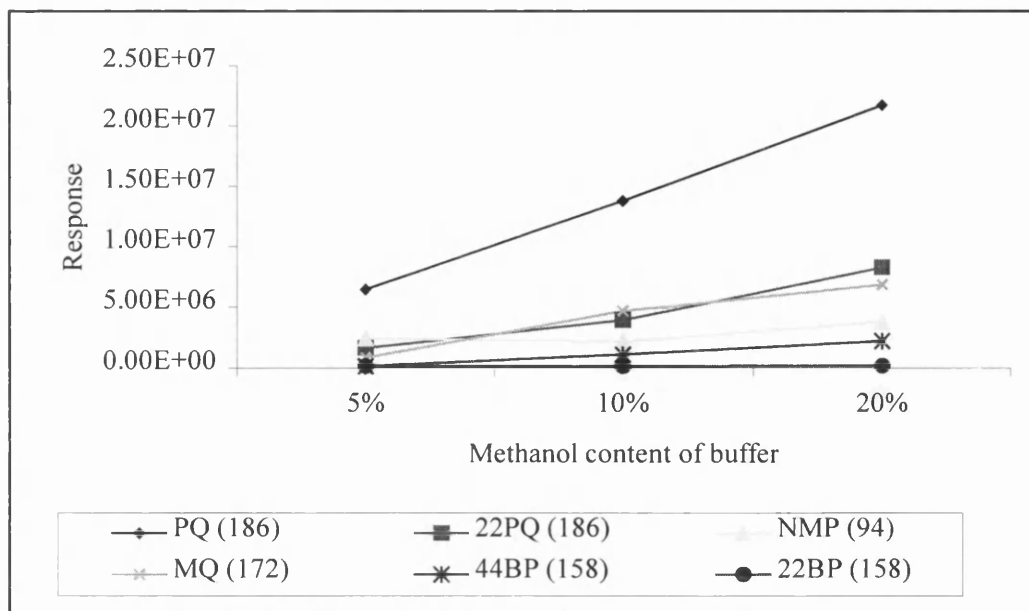


Figure 3.40 – Effect of methanol content of buffer on response

It can be seen from the data illustrated in Figure 3.40 that in general the response obtained for the base ion of each of the six study compounds is increased with the increase in methanol content of the buffer. This would appear to confirm that the electrospray efficiency is increased by the addition of an organic solvent modifier to the CE buffer. It was also observed in this series of experiments that the base ion for 2,2-paraquat had changed from m/z 171, as it had been in the initial experiments, to m/z 186. The reasons for this difference are not fully understood, but may also be the result of the increased stability of the electrospray resulting from the presence of methanol in the buffer system.

An example of the mass electropherograms obtained for the separation of a 50ppm mixture of the six study compounds using 100mM ammonium acetate buffer containing 5% methanol are shown in Figures 3.41(a) and (b).

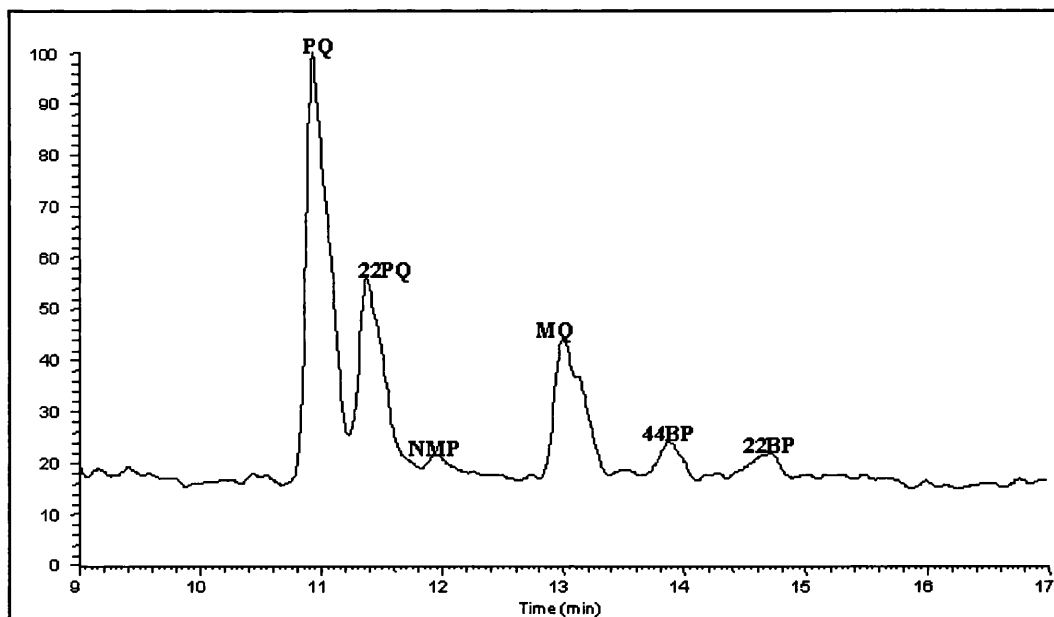


Figure 3.41(a) – TIE of a 50ppm six component paraquat standard using a 100mM ammonium acetate buffer containing 5% methanol and using a CE voltage of 20kV (CZE-MS)

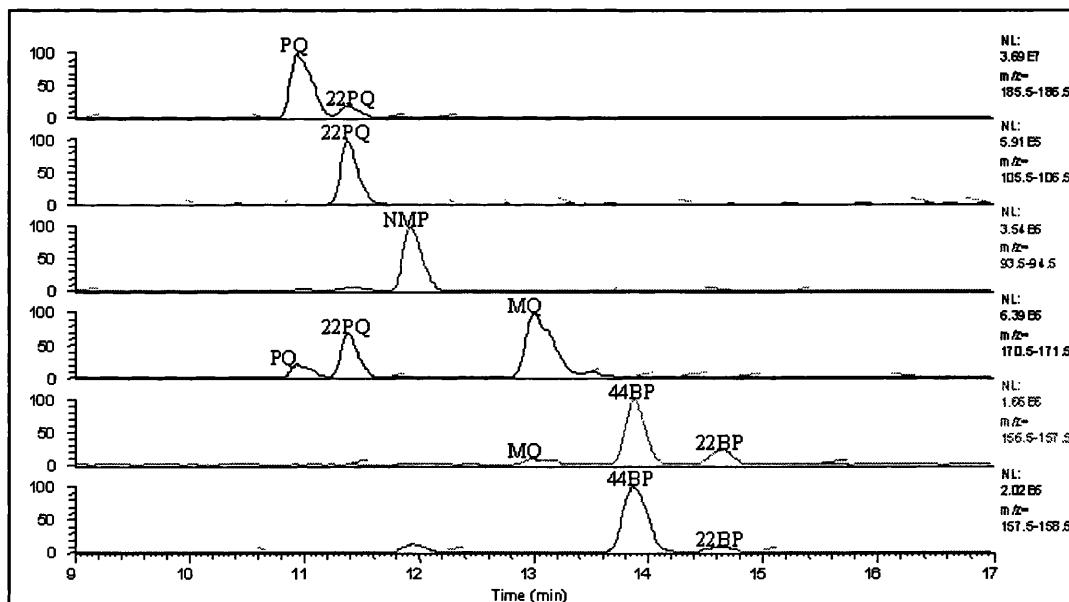


Figure 3.41(b) – Mass electropherograms of a 50ppm six component paraquat standard using a 100mM ammonium acetate buffer containing 5% methanol and using a CE voltage of 20kV (CZE-MS)

Chapter 3 CZE and CE-MS Studies of Paracetamol and Related Impurities 119

It can be seen that all six components are visible in the total ion electropherogram (TIE) and that separation is complete in less than 15 minutes. The lengthiest separation time obtained when using the buffer containing 20% methanol was around 25 minutes. Separation integrity was maintained with each of the three different buffer compositions, with near to baseline resolution, or better, obtained for each component. Comparisons of the peak shapes obtained in these on-line experiments with those achieved during the off-line CZE studies are less favourable. The peak shapes obtained on-line and visible in the total ion electropherogram are relatively poor in comparison with the sharp, efficient peaks produced in the CZE experiments, this would suggest a significant degree of band broadening at the CE-MS interface. Calculated values for the efficiency and resolution of each of the six component peaks are shown in Table 3.22.

		PQ	22PQ	NMP	MQ	44BP	22BP
100mM Ammonium Acetate + 5% Methanol	t_{mig} (secs)	655.8	682.2	716.4	780.0	832.8	882.6
	Efficiency	10750.3	11633.3	5371.3	9388.5	11510.1	5342.6
	Resolution	N/A	PQ/22PQ 1.04	22PQ/NMP 1.06	NMP/MQ 1.78	MQ/44BP 1.67	44BP/22BP 1.26
100mM Ammonium Acetate + 10% Methanol	t_{mig} (secs)	834.6	879.0	930.6	1059.6	1165.8	1257.6
	Efficiency	11507.9	12764.9	14307.6	7514.1	17196.7	15811.6
	Resolution	N/A	PQ/22PQ 1.43	22PQ/NMP 1.66	NMP/MQ 3.22	MQ/44BP 2.51	44BP/22BP 2.43
100mM Ammonium Acetate + 20% Methanol	t_{mig} (secs)	982.2	1038.6	1077.6	1268.4	1423.8	1519.2
	Efficiency	14435.3	28694.5	17375.6	17686.6	22285.8	19425.7
	Resolution	N/A	PQ/22PQ 1.97	22PQ/NMP 1.36	NMP/MQ 5.39	MQ/44BP 4.07	44BP/22BP 2.33

Table 3.22 – Migration time, efficiency and resolution data for Figures 3.42, 3.43 and 3.44

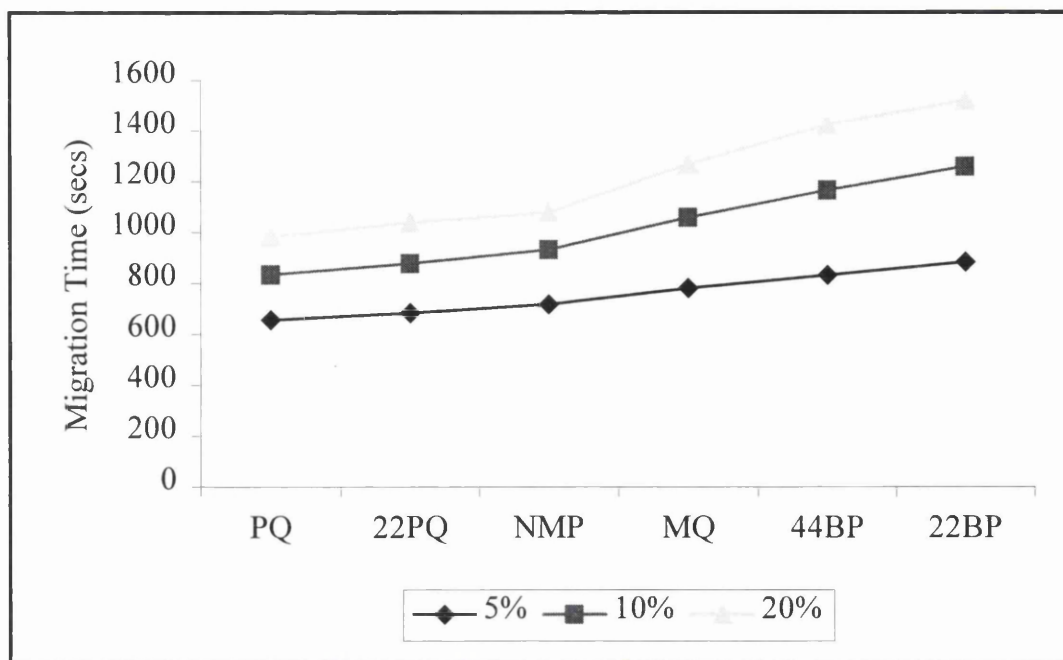


Figure 3.42 – Migration times of paraquat and impurities versus methanol content of buffer

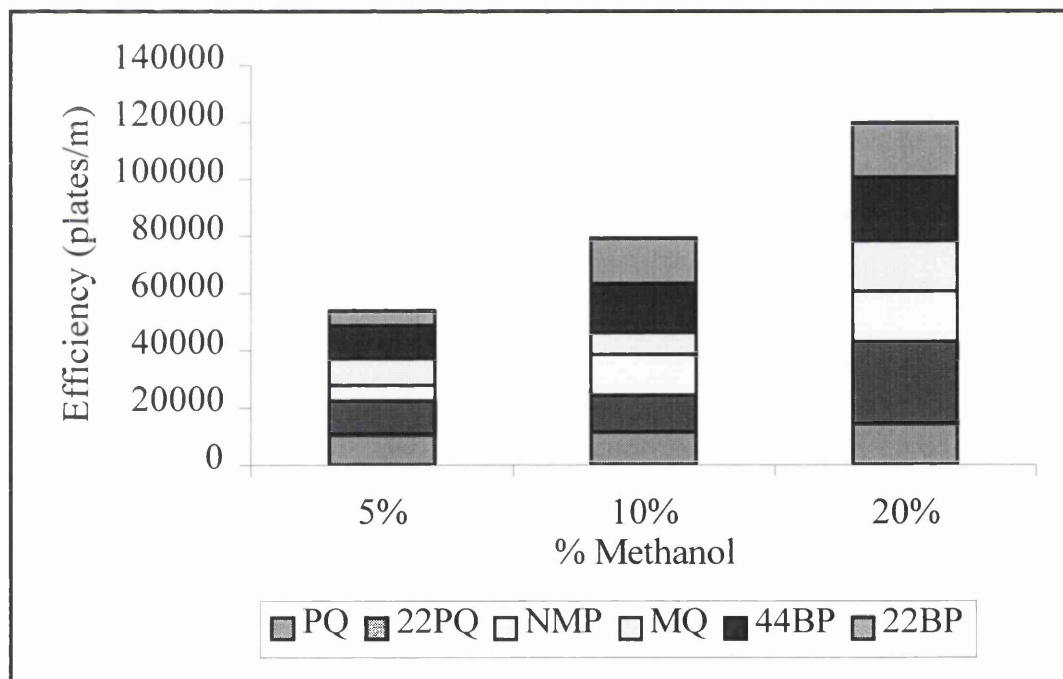


Figure 3.43 – Cumulative efficiency of paraquat and impurities versus methanol content of buffer

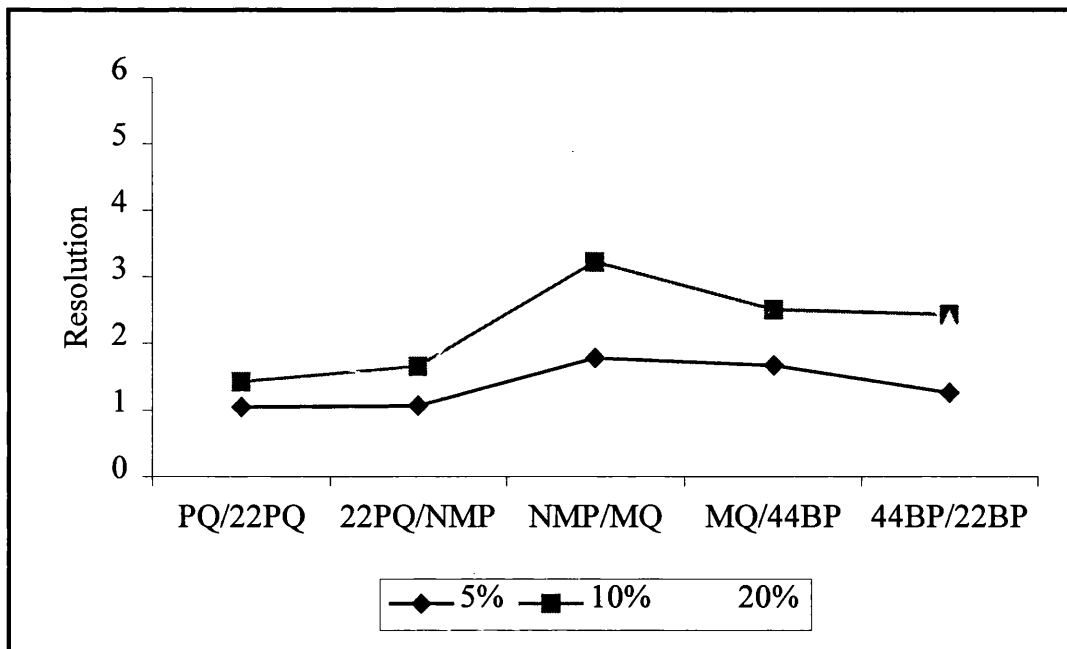


Figure 3.44 - Resolution of paraquat and impurities versus methanol content of buffer

The figures obtained indicated a general increase in efficiency and resolution with increasing methanol content. This reflected the trend obtained in off-line experiments, although the possibly anomalous drop in resolution at 20% methanol seen in off-line studies was not observed here. While the optimum off-line CZE conditions were obtained using 100mM ammonium acetate buffers, the use of high concentration buffers in on-line CE-MS is often less desirable as unfavourable currents resulting in discharge at higher applied voltages can be generated. Although this problem is less significant at the relatively low applied voltage, 15kV, being used in these experiments, some problems with discharging had been experienced. Although these had been largely due to leakage of sheath liquid inside the ESI probe a study of the use of lower concentration buffer was undertaken, with a view to minimising the risk of unstable electrospray and discharging. Experiments using

50mM ammonium acetate buffers containing 10% and 20% methanol modifier were performed at different CE separation voltages and the results obtained were compared with the data from the experiments previously performed using 100mM ammonium acetate buffers.

The on-line separations obtained using the 50mM buffers and increased applied voltages were, in general, poor in comparison with those achieved in the previous experiments using 100mM ammonium acetate with significant decreases in resolution observed. The exception to this observation was the separation achieved using the 50mM ammonium acetate buffer containing 10% methanol, and an applied voltage of 20kV. An example of the mass electropherograms obtained in this series of experiments is shown in Figure 3.45. It can be seen that each of the six study compounds is visible in the total ion electropherogram and peak shape, resolution and efficiency are comparable with those obtained in the experiments using the 100mM buffer with 10% methanol. These conditions also have the advantage of producing separations that were complete in less than 12 minutes.

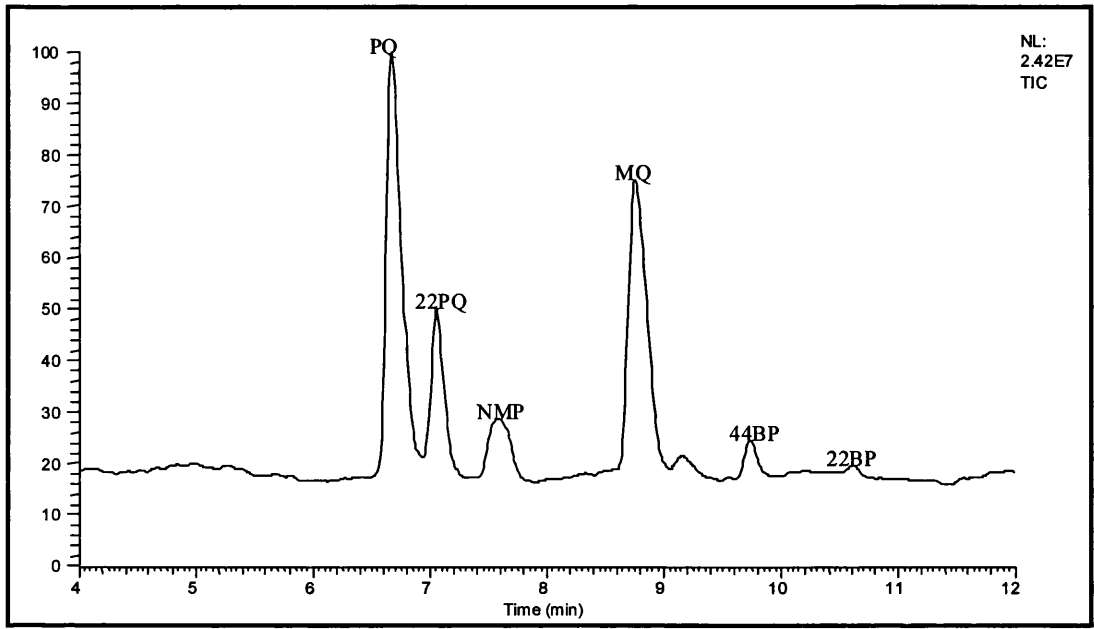


Figure 3.45(a) – TIE of a six component paraquat mixture using 50mM ammonium acetate buffer containing 10% methanol and a CE voltage of 20kV

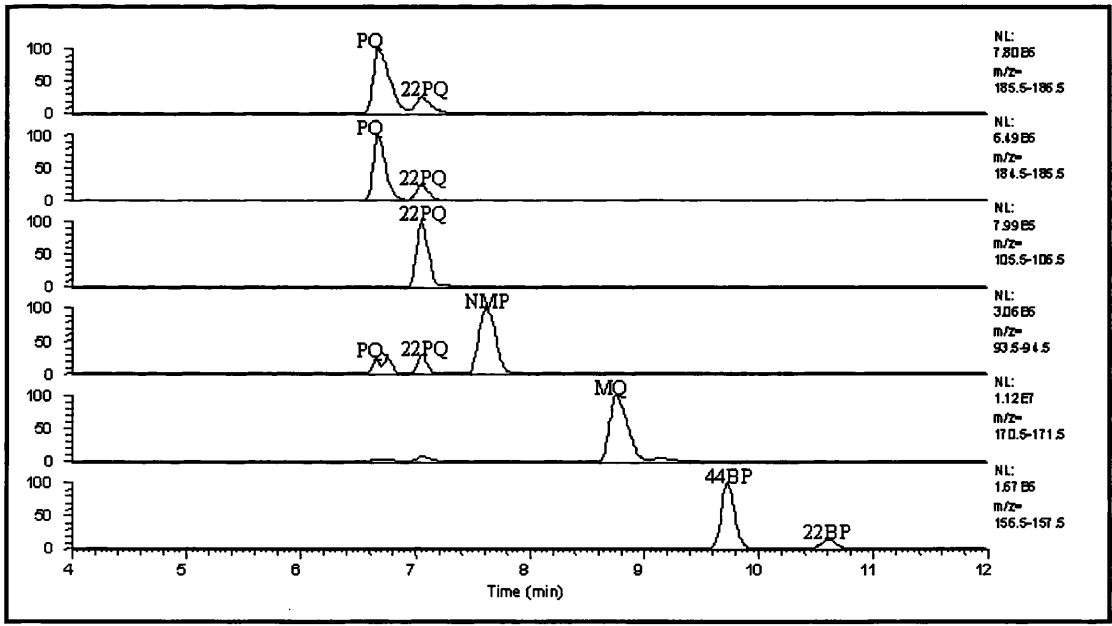


Figure 3.45(b) – Mass electropherograms of a six component paraquat mixture using 50mM ammonium acetate buffer containing 10% methanol and a CE voltage of 20kV

3.6.3.1.2 - Limit of detection (LOD) and limit of quantitation (LOQ)

The LOD and LOQ for each of the six study compounds were again determined using Equations 3.14 and 3.15 for both the full scan and single ion monitoring experiments. The details of each are shown in Tables 3.23 and 3.24.

	LOD (ppb)	LOQ (ppb)
PQ	540	1800
22PQ	2180	7270
NMP	2610	8700
MQ	680	2260
44BP	3430	11430
22BP	10000	33330

Table 3.23 – Limits of detection and quantitation for each of the six study compounds using CZE-MS in full scan mode

	LOD (ppb)	LOQ (ppb)
PQ	60	190
22PQ	200	660
NMP	280	920
MQ	350	1190
44BP	500	1670
22BP	2140	7140

Table 3.24 – Limits of detection and quantitation for each of the six study compounds using CZE-MS in single ion monitoring (SIM) mode

The detection limits achieved using CZE-MS in full scan mode showed no improvement over those obtained in the off-line experiments with UV detection. Although the values calculated are of similar orders of magnitude for each of the six compounds, the detection limits are in each case lower for the CZE-MS experiments.

This is probably the result of signal suppression due to the relatively large amount of ammonium acetate buffer entering the source.

The use of single ion monitoring (SIM) resulted in improvements in LOD for each of the sample components, ranging from a twofold improvement for monoquat to improvements by factors of about 10 for paraquat, 2,2-paraquat and n-methyl pyridinium.

3.6.3.1.3 – CZE-MS of technical paraquat

Using the previously described conditions, the on-line analysis of a sample of technical paraquat was attempted. Off-line CZE experiments had provided detected several peaks, including paraquat, monoquat and 4,4-bipyridyl, in addition to unknown component peaks. It was hoped that the CZE-MS experiments would offer improved sensitivity in addition to assisting in the identification of these unknowns and confirm the identities of the peaks detected by UV. These experiments were limited in their success and rather disappointing in comparison with the off-line experiments. Examples typical of the TIE and mass electropherograms obtained for the technical paraquat sample are shown in Figures 3.46(a) and (b).

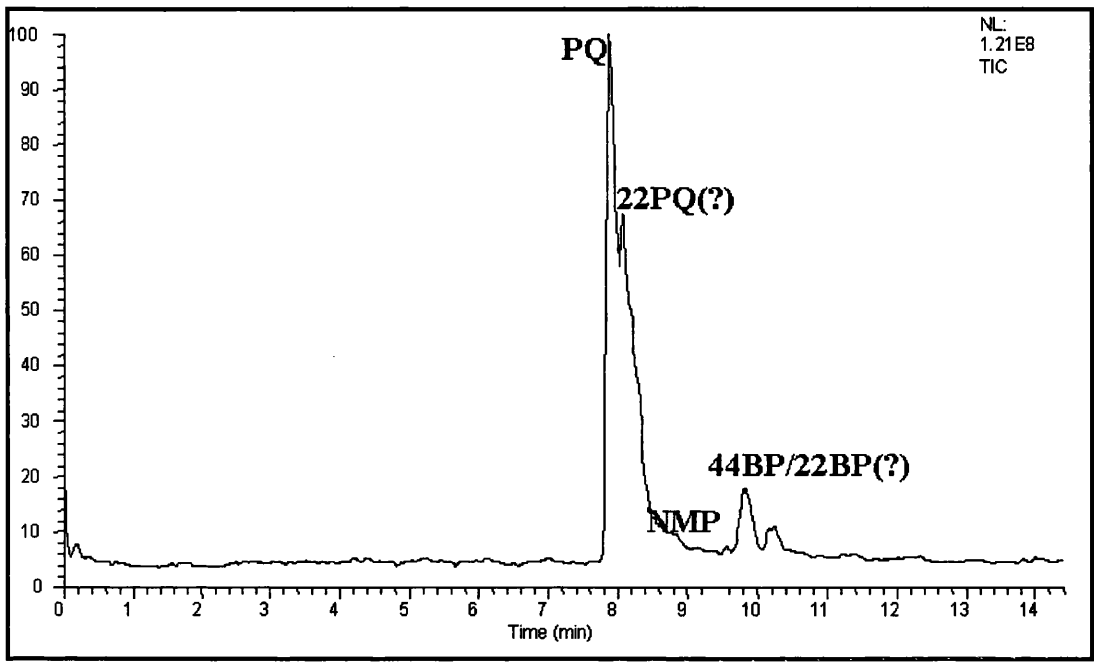


Figure 3.46(a) – TIE for a sample of technical paraquat diluted by a factor of 100 obtained under CZE-MS conditions

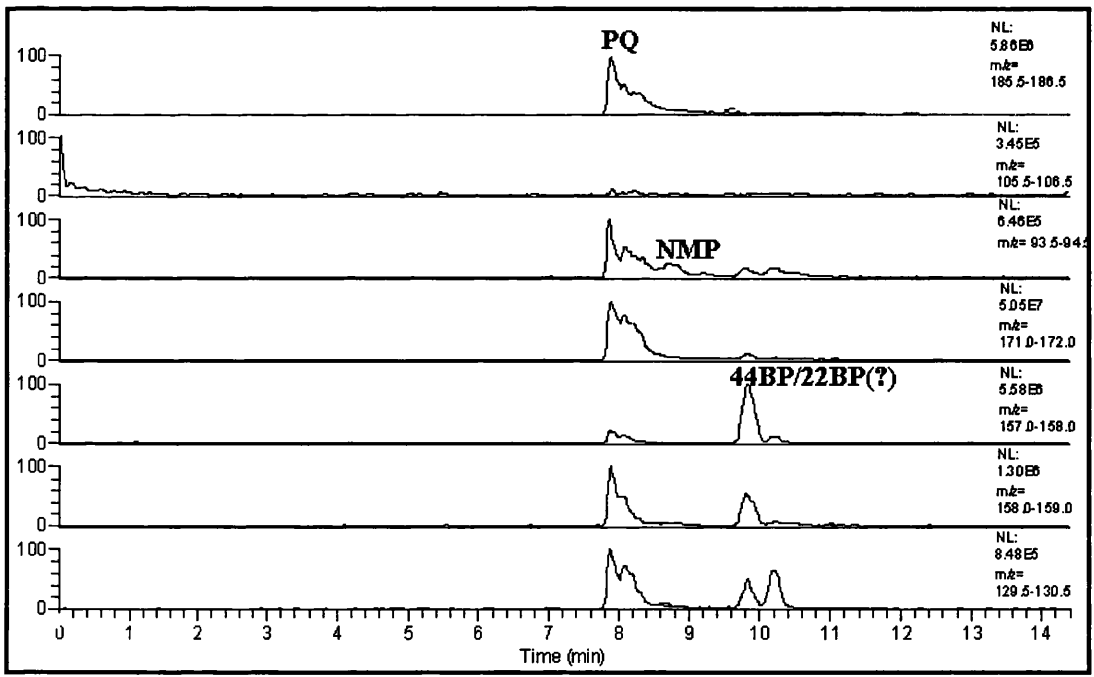


Figure 3.46(b) – Mass electropherograms for a sample of technical paraquat diluted by a factor of 100 obtained under CZE-MS conditions

Only three peaks are clearly visible in the total ion electropherogram, with one further possible peak present as a shoulder on the main paraquat peak. Examination of the individual ion electropherograms for the known ions of interest and the mass spectra for each of the peaks observed in the TIE allowed tentative identification of each of the impurity peaks. Table 3.25 summarises these results.

t_{mig} (mins)	m/z	Tentative Peak Assignment
7.9	186, 185, 171, 93	PQ
8.1	186, 185, 171, 93	22PQ (?)
8.8	171, 94	NMP
9.8	157	22BP/44BP(?)
10.2	157, 155, 130	

Table 3.25 – Summary of CZE-MS data for Technical Paraquat sample

Peak identification was hampered by the swamping of the peaks in close proximity to the paraquat peak with ions associated with the paraquat as a result of its very high concentration in the sample. Further dilution of the sample failed to overcome this problem.

3.6.3.2 - tCITP-MS of Paraquat and Impurities

Following the CZE-MS experiments attempts were made to transfer the tCITP methodology that had been successfully used in off-line analyses for use on-line with mass spectrometric detection. Initial experiments were performed using the operating conditions detailed below.

CE operating conditions

Capillary	Approximately 70cm \times 50 μ m fused silica
LE	50mM β -Alanine, 0% Methanol, pH 4.0
TE	50mM Ammonium Acetate, 0% Methanol, pH 4.0
Applied voltage	20kV
Injection	90 second pressure injection

Mass spectrometer operating conditions

Electrospray Voltage	+4.5kV
Spray Current	1.07 μ A
Capillary Temperature	200°C
Capillary Voltage	26.00
Tube Lens Offset	-10.00
Sheath Gas Flow Rate	50 arbitrary units
Auxiliary Gas Flow Rate	0 arbitrary units
Sheath Liquid	Methanol/10mM Acetic Acid (9:1)
Sheath Liquid Flow Rate	3 μ l/min

The results obtained in these initial experiments were rather disappointing in comparison with the separations achieved in the off-line tCITP experiments. Sensitivity was relatively poor and only the paraquat peak was visible in the total ion electropherogram. Although the peaks observed in the individual ion mass electropherograms were sharp, as they had been in the off-line electropherograms,

resolution was lost and peaks corresponding to 2,2-paraquat and n-methyl pyridinium were not visible.

Attempts were made to improve resolution by increasing the buffer concentration and increasing the percentage of methanol present in the buffer with limited success. With the use of 100mM ammonium acetate buffer with 20% methanol pH adjusted to 4.0 the peak corresponding to the n-methyl pyridinium ion was observed separated from the first peak. The paraquat and 2,2-paraquat peaks, however, remained unresolved. The loss of separation observed may result from incompatibilities between the CE buffer system and the sheath liquid [31]. A limited amount of work was performed with variations in sheath liquid composition but again with little success. An example of the mass electropherograms obtained using tCITP-MS is shown in Figure 3.47.

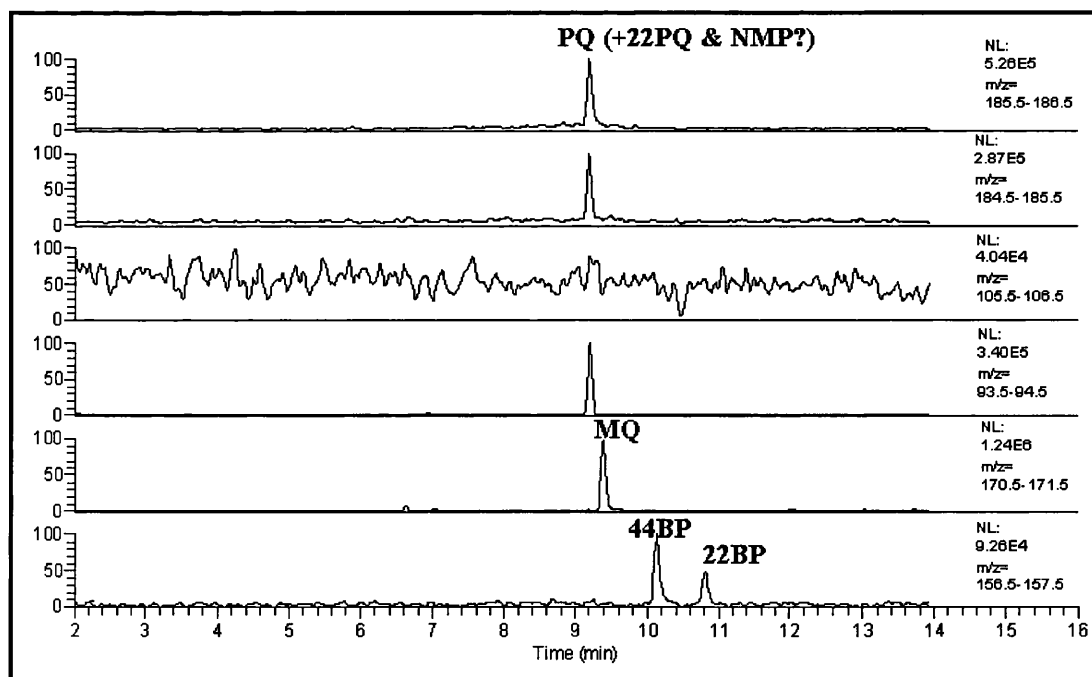


Figure 3.47 – Mass electropherograms of a six component paraquat mixture obtained using tCITP-MS conditions

3.6.4 – CONCLUSION

The analysis of the herbicide paraquat and five related impurities by capillary electrophoresis has been successfully performed and is reported in this chapter. Capillary electrophoresis has several advantages over HPLC and the other analytical techniques previously used in the analysis of paraquat; analysis times are relatively short and the minimal sample and buffer volumes necessary eliminate the problem of solvent disposal and literally hundreds of analyses can be performed from the microlitre sample volumes typically consumed for a single HPLC injection.

The six study compounds were successfully separated using conditions adapted from literature methodology used for the separation of paraquat and two other quaternary ammonium herbicides. The method made use of a low ionic strength ammonium acetate buffer made up with 100mM sodium chloride and produced well resolved efficient peaks in an analysis time of less than 15 minutes. These conditions were also successfully used in the analysis of a sample of technical paraquat. However, the presence of sodium chloride in this buffer system limited its use to offline CZE analysis as the range of electrolytes suitable for use in the interfacing of capillary electrophoresis with mass spectrometry is limited to volatile buffers. Consequently, an alternative method utilising a higher concentration of ammonium acetate and containing no sodium chloride was developed. The hydrodynamic and electrokinetic modes of injection were examined in detail in order to determine the optimum injection conditions. Although hydrodynamic injection is generally the preferred mode of sample introduction, it failed to produce anything more than a single analyte peak over a range of injection times. By comparison, electrokinetic sample introduction was more successful and all six of the study

compounds were detected. This greater sensitivity may be the result of sample stacking and field amplification effects produced when samples prepared in water (or low concentration buffer) are introduced electrokinetically onto a capillary filled with a higher concentration buffer with greater conductivity [60].

Variation of buffer concentration and applied voltage were examined and the effect of these variables on analyte migration times, peak efficiencies and resolution was reported and found to comply with the fundamentals of electrophoretic and electroosmotic theory. Any deviations from theory were mainly accounted for by the phenomenon of Joule heating.

With a view to improving the electrospray compatibility of the buffer system in preparation for its interfacing with the mass spectrometer the effect of the addition of an organic additive, in this case methanol, to the buffer was examined. Although the analyte migration times were increased in the presence of methanol, analysis times remained less than 15 minutes in the majority of cases. Peak efficiencies and resolution were observed to be improved with levels of methanol up to 10%.

Limits of detection of between 211ppb for paraquat and 5000ppb for 22-bipyridyl were achieved using off-line CZE with UV detection at 254nm. Attempts were made to further improve on these detection limits by making use of the technique of Transient Capillary Isotachopheresis (tCITP) which allows larger sample volumes to be introduced onto the capillary without inducing band broadening. Ammonium acetate which had been previously used in the CZE experiments was used as the leading electrolyte (LE) while a range of compounds

Chapter 5 CZE and CE MS Studies of Paraquat and Related Impurities 169

were initially used as the terminating electrolyte (TE) in the system before settling on β -alanine. Electrolyte concentrations and injection mode were studied in order to determine the optimum conditions for the separation. The limits of detection for each of the six study compounds were improved by factors of between 5.3 and 84.4.

During the course of the CZE and tCITP studies some problems were experienced with analyte migration times varying significantly between repeat analyses performed on different days. With a view to improving the reproducibility of the analyte migration times the use of specialist coated capillaries was studied and compared with the standard fused capillaries typically used. Two commercially available coated capillaries were studied both of which claimed to reduce adsorption of analyte to the capillary walls, reduce the EOF, and as a consequence improve the reproducibility and efficiency of the separation. Some improvements in migration time and peak area reproducibility and peak efficiencies were observed with each of the coated capillaries. However, as the study did not demonstrate a significant benefit over the standard fused silica capillaries for the separation of the six study compounds and the cost of the specialist capillaries was comparatively high they were not used in any subsequent work.

Both the off-line CZE and tCITP methods developed using the standard mixture of the six study compounds were used in the analysis of a sample of technical Paraquat. Using the CZE methodology, three of the impurities were detected in a sample diluted by a factor of 200. The paraquat peak itself was overloaded and in addition to the three known impurities, other small peaks were observed but peak shape was poor and they were not clearly visible above the

Chapter 5 CE and CE-MS Studies of Paraquat and Related Impurities 107

baseline noise. Transient CITP was more successful and peaks corresponding to four out of the five known impurities were detected in the sample diluted by up to 1000 times in addition to two unknown components. The linearity graphs prepared using the dilutions of each individual standard were used in determining approximate quantitation data for the sample.

While each of the off-line CE methods developed were successful in terms of the separation and limits of detection achieved in the analysis of standard mixtures both methods suffered when interfaced with the mass spectrometer. CZE-MS was moderately successful, separation integrity was maintained and the detection limits achieved were comparable with those obtained with UV detection, with improvements resulting from the use of single ion monitoring. Transient CITP-MS was rather less successful and resulted in poor separation efficiency.

Further work should be concentrated primarily in several areas; improving the on-line tCITP-MS method, improving or employing an alternative CE-MS interface, performing a more extensive study into the utility of coated capillaries and assessing the methodology developed for use in quantitative analysis and in the analysis of paraquat in different environmental sample matrices.

Although the transient CITP method was very effective in off-line experiments with UV detection the results obtained when interfacing of the method with the mass spectrometric detector was performed were very disappointing. Further work to improve the interfacing of the tCITP-MS method should be performed in order to fully assess the potential of this technique as a method of

determining trace impurities in paraquat. One possible area to make improvements is in the selection of an alternative sheath liquid for the tCITP-MS interface. It has been demonstrated that as sample and electrolyte ions exit the CE capillary at the electrospray interface counterions from the sheath liquid simultaneously enter the capillary and migrate towards the injection end, producing a moving ionic boundary as a result. While this phenomenon enables the use of non-volatile buffer ions, such as phosphates, it also results in changes in migration order and losses in resolution. A study of different sheath liquid compositions may assist in the improvement of the separation.

One of the major difficulties experienced during these studies was maintaining an effective seal at the sheath liquid inlet of the electrospray source, which led to frequent problems with leakages of sheath liquid and resulted in current errors and discharging. Use of the new low flow ionisation techniques of micro- and nano-electrospray [61-63] may go some way to resolving this problem and this area should be investigated. The limits of detection achieved in the CZE-MS experiments were relatively poor in comparison with those achieved in the off-line experiments with UV detection, again this could be improved with the use of an alternative interfacing arrangement. The presence of high concentrations of electrolyte ions entering the mass spectrometer has the effect of suppressing ionisation. Consequently, the use of an off-axis electrospray source, such as the Micromass Z-Spray combined inlet and ion source, which reduce the amount of buffer entering the source may have a beneficial effect on the sensitivity of the technique.

Chapter 5 GC and GC-MS Studies of Paraquat and Related Impurities 100

As has been previously mentioned some variation of analyte migration times was experienced with analyses performed on different days. A study of two commercially available coated capillaries was inconclusive although some improvements were observed the study was too limited to draw any firm conclusions regarding the utility of their use in this separation. A more extensive study including a wider range of capillaries carried out over a longer period of time could be beneficial, if a suitable capillary is found it would improve the reproducibility and robustness of the method.

Further work should include the analysis of environmental samples, such as soil, crops and water, spiked with paraquat to assess the usefulness of the methods developed in the analysis of paraquat in a variety of sample matrices. The growth in environmental legislation has increased the need for the quantitation of pesticides and related impurities. The developed methodology should therefore be assessed for their use as quantitative analytical methods.

REFERENCES CITED IN CHAPTER 3

1. Analysis of agrochemicals by capillary electrophoresis. F Menzinger, P Schmitt-Kopplin, D Freitag and A Kettrup, *J Chromatogr. A* **891**, (2000), 45-67
2. Capillary Electrophoresis: Principles and Practice. R Kuhn and S Hoffstetter-Kuhn. Springer-Verlag (1993)
3. High Performance Capillary Electrophoresis – An Introduction. Dr. David N Heiger. Hewlett-Packard (1992)
4. Introduction to Capillary Electrophoresis, Beckman Primer. Beckman Instruments Inc. (1994)
5. Capillary Electrophoresis Theory and Practice. Ed. Patrick Camilleri. CRC Press (1998)
6. An Introduction to Capillary Electrophoresis. Bio-Rad Laboratories (1994).
7. Capillary Electrophoresis: Methods and Scope. Heinz Engelhardt, Wolfgang Beck, Jörg Kohr and Thomas Schmitt. *Angew. Chem. Int. Ed Engl.* **32**, (1993), 629-649
8. Capillary Electrophoresis. Andrew G Ewing, Ross A Wallingford and Teresa M Olefirowicz. *Anal. Chem.* **61**, (1989), 292A-303A
9. Free Zone Electrophoresis. S Hjerten. *Chromatogr. Rev.* **9**, (1967), 122
10. Concentration Distributions in Free Zone Electrophoresis. FEP Mikkers, FM Everaerts and TPEM Verheggen. *J. Chromatogr.* **169**, (1979), 11-20
11. Zone Electrophoresis in Open-Tubular Glass Capillaries. James W Jorgenson and Krynn DeArman Lukacs. *Anal. Chem.* **53**, (1981), 1298-1302
12. High Resolution Separations Based on Electrophoresis and Electroosmosis. James W Jorgenson and Krynn DeArman Lukacs. *J. Chromatogr.* **218**, (1981), 209-216

- Chapter 11 CE and CE-MS Studies by Fritzsche and Related Experiments 109
13. Trends in Capillary Electrophoresis: 1997. Qing Yang, Kus Hidajat and Sam FY Li. *J. Chromatogr. Sci.* **35**, (1997), 358-373
 14. Coated versus fused-silica capillaries for the separation of inorganic and organic cations by capillary zone electrophoresis. Hannah Burt, David M Lewis and Kelvin N Tapley. *J. Chromatogr. A* **736**, (1996), 265-272
 15. Effects of surface coatings on CE separations of pharmaceutically active compounds. Mingxian Huang, Mark Bigelow and Michael Byers. *LC.GC Int.* **9**, (1996), 658-664
 16. Manipulation of electroosmotic flow in capillary electrophoresis. Xian-Wei Yao, Dan Wu and Fred E Regnier. *J. Chromatogr.* **636**, (1993), 21-29
 17. Evaluation of extended light path capillaries for use in capillary electrophoresis with laser-induced fluorescence detection. Roderic O Cole, Donna L Hiller, Craig A Chwojdak and Michael J Sepaniak. *J. Chromatogr. A* **736**, (1996), 239-245
 18. Rectangular Capillaries for Capillary Zone Electrophoresis. T Tsuda, JV Sweedler and RN Zare. *Anal. Chem.* **62**, (1990), 2149-2152
 19. Capillary electrophoresis-mass spectrometry. Jianyi Cai and Jack Henion. *J. Chromatogr. A* **703**, (1995), 667-692
 20. Capillary electrophoresis-mass spectrometry. WMA Niessen, UR Tjaden and J van der Greef. *J. Chromatogr.* **636**, (1993), 3-19
 21. Recent advances in capillary electrophoresis/electrospray/mass spectrometry. J Fred Banks. *Electrophoresis* **18**, (1997), 2255-2266
 22. Mass Spectrometry for Chemists and Biochemists. Robert AW Johnstone and Malcolm E Rose. Cambridge University Press (1996)

23. On-line Mass Spectrometric Detection for Capillary Zone Electrophoresis. Jose A Olivares, Nhung T Nguyen, Clement R Yonker and Richard D Smith. *Anal. Chem.* **59**, (1987), 1230-132
24. Capillary Zone Electrophoresis-Mass Spectrometry Using an Electrospray Ionisation Source. Richard D Smith, Jose A Olivares, Nhung T Nguyen and Harold R Udseth. *Anal. Chem.* **60**, (1988), 436-441
25. Improved Electrospray Ionisation Interface for Capillary Zone Electrophoresis-Mass Spectrometry. Richard D Smith, Charles J Barinaga and Harold R Udseth, *Anal. Chem.* **60**, (1988), 1948-1952
26. Comparison of buffer systems and interface designs for capillary electrophoresis-mass spectrometry. JH Wahl and RD Smith. *J. Cap. Elec.* **1**, (1994), 62-71
27. A CE/ESI-MS Interface for Stable, Low-Flow Operation. Daniel P Kirby, Jacqueline M Thorne, Wolfgang K Götzinger and Barry L Karger. *Anal. Chem.* **68**, (1996), 4451-4457
28. A New High-performance Interface for Capillary Electrophoresis/Electrospray Ionization Mass Spectrometry. Joanne C Severs, Amy C Harms and Richard D Smith. *Rapid Commun. Mass Spectrom.* **10**, (1996), 1175-1178
29. Coupling Capillary Zone Electrophoresis and Continuous-Flow Fast Atom Bombardment Mass Spectrometry for the Analysis of Peptide Mixtures. RM Caprioli, WT Moore, M Martin, BB DaGue, K Wilson and S Moring. *J. Chromatogr.* **480**, (1989), 247-257
30. Coupling of Capillary Zone Electrophoresis and Capillary Liquid Chromatography with Coaxial Continuous-Flow Fast Atom Bombardment Tandem Sector Mass Spectrometry. MA Moseley, LJ Deterding, KB Tomer and JW Jorgenson. *J. Chromatogr.* **480**, (1989), 197-209

31. Liquid Sheath Effects on the Separation of Proteins in Capillary Electrophoresis/Electrospray Mass Spectrometry. Frantisek Foret, Toni J Thompson, Paul Vouros, Barry L Karger, Petr Gebauer and Petr Bocek. *Anal. Chem.* **66**, (1994), 4450-4458
32. On-Line Coupling of Isotachophoresis with Capillary Zone Electrophoresis. D Kaniansky and J Marak. *J. Chromatogr.* **498**, (1990), 191-204
33. Capillary Zone Electrophoresis of Dilute Samples with Isotachophoretic Preconcentration. V Dolnik, KA Cobb and M Novotny. *J. Microcol. Sep.* **2**, (1990) 127-131
34. On-Line Isotachophoretic Sample Preconcentration for Enhancement of Zone Detectability in Capillary Zone Electrophoresis. F Foret, V Sustacek and P Bocek. *J. Microcol. Sep.* **2**, (1990), 229-233
35. Isotachophoresis as an on-line concentration pretreatment technique in capillary electrophoresis. DS Stegehuis, H Irth, UR Tjaden and J van der Greef. *J. Chromatogr.* **538**, (1991), 393-402
36. Analyte focusing in capillary electrophoresis using on-line isotachophoresis. DS Stegehuis, UR Tjaden and J van der Greef. *J. Chromatogr.* **591**, (1992), 341-349
37. Single Capillary Isotachophoresis-Zone Electrophoresis: Current Practice and Prospects, A Review. Martin Mazereeuw, Ubbo R Tjaden and Nico J Reinhoud. *J. Chromatogr. Sci.* **33**, (1995), 686-697
38. Electrokinetic Separations with Micellar Solutions and Open-Tubular Capillaries. S Terabe, K Otsuka, K Ichikama, A Tsuchiya and T Ando. *Anal. Chem.* **56**, (1984), 111-113

39. Capillary ElectroChromatography. Norman Smith. Beckman Coulter Inc. (1999)
40. Susan Crosland, Zeneca Agrochemicals, personal communication
41. Determination of Quaternary Ammonium Herbicides by Capillary Electrophoresis/Mass Spectrometry. E Moyano, DE Games and MT Galceran. *Rapid Commun. Mass Spectrom.* **10**, (1996), 1379-1385
42. On-Line Ion-Pair Solid-Phase Extraction-Liquid Chromatography-Mass Spectrometry for the Analysis of Quaternary Ammonium Herbicides. R Castro, E Moyano and MT Galceran. *J. Chromatogr. A* **869**, (2000), 441-449
43. Capillary Electrophoresis of Quaternary Ammonium Ion Herbicides: Paraquat, Diquat and Difenzoquat. MT Galceran, MC Carneiro and L Puignou. *Chromatographia* **39**, (1994), 581-586
44. E Moyano, personal communication
45. Effect of Solvent on Dynamic Range and Sensitivity in Pneumatically-assisted Electrospray (Ion Spray) Mass Spectrometry. Risto Kostianen and Andries P Bruins. *Rapid Commun. Mass Spectrom.* **10**, (1996), 1393-1399
46. Effect of Addition of Organic Solvent on the Separation of Positional Isomers in High-Voltage Capillary Zone Electrophoresis. Shigeru Fujiwara and Susumu Honda. *Anal. Chem.* **59**, (1987), 487-490
47. ICH Harmonised Tripartite Guidance. Notes for guidance on the validation of analytical procedures: methodology (CPMP/ICH/281/95). The European Agency for the Evaluation of Medicinal Products, ICH, UK (1996)
48. Strategy for setting up single-capillary isotachopheresis-zone electrophoresis. NJ Reinhoud, UR Tjaden and J van der Greef. *J. Chromatogr. A* **653**, (1993), 303-312

49. On-column transient and coupled column isotachophoretic preconcentration of protein samples in capillary zone electrophoresis. Frantisek Foret, Eva Szoko and Barry L Karger. *J. Chromatogr.* **608**, (1992), 3-12
50. Sensitivity enhancement in capillary zone electrophoresis using discontinuous buffer systems. Christine Schwer. Beckman Application Note, (1993), 12-15.
51. Capillary Electrophoresis/Electrospray Ionization Mass Spectrometry: Improvement of Protein Detection Limits Using On-Column Transient Isotachophoretic Sample Preconcentration. Toni J Thompson, Frantisek Foret, Paul Vouros and Barry L Karger. *Anal. Chem.* **65**, (1993), 900-906
52. Measurement of Mobilities and Dissociation Constants by Capillary Isotachophoresis. Jan Pospichal, Petr Gebauer and Petr Bocek. *Chem. Rev.* **89**, (1989), 419-430
53. Some variables affecting reproducibility in capillary electrophoresis. Zakariya K Shihabi and Mark E Hinsdale. *Electrophoresis* **16**, (1995), 2159-2163
54. Supelco Chromatography Products Catalogue.
55. MicroSolv Sales Literature.
56. CE Expert version 1.0. Harry Whatley. Beckman Instruments Inc. (1997).
57. JC Severs PhD Thesis, University of Wales, (1995).
58. Finnigan MAT: LCQ MS Detector Operator's and Service Manual.
59. Capillary electrophoresis-electrospray mass spectra of the herbicides paraquat and diquat. X Song and WL Budde. *J. Am. Soc. Mass Spectrom.* **7**, (1996), 981-986
60. On-Column Sample Concentration Using Field Amplification in CZE. Ring-Ling Chien and Dean S Burgi. *Anal. Chem.* **64**, (1992), 489A-496A

- Chapter 5 CE and CE-MS Studies by Parag and Related Techniques 115
61. Electrospray continues to evolve. Celia Henry. *Anal. Chem.* **69**, (1997), 427A-432A
 62. Analytical properties of the Nanoelectrospray Source. Matthias Wilm and Matthias Mann. *Anal. Chem.* **68**, (1996), 1-8
 63. Capillary electrochromatography/mass spectrometry – a comparison of the sensitivity of nanospray and microspray ionization techniques. Ruth N Warriner, Andy S Craze, David E Games and Stephen J Lane. *Rapid Commun. Mass Spectrom.* **12**, (1998), 1143-1149

Chapter 4

HPLC and HPLC-MS Studies of Flutriafol and Related Impurities

4.1 – OBJECTIVE

The increased emphasis on the characterisation and detection of low level impurities in commercially significant chemicals such as pharmaceuticals and agrochemicals has been previously discussed in earlier sections. As has been described in Section 1.5.2 the fungicide flutriafol is amongst the 20 most widely used pesticides in the UK and consequently its analysis and the analysis of any low level impurities present is of interest. Despite this fact, no reports describing the analysis of flutriafol and its related impurities were found when a literature search was undertaken. The techniques of HPLC and HPLC-MS are widely used in the analysis of pesticidal compounds [1,2]. The aim of this study is to assess the use of these techniques in the analysis of flutriafol and the detection and identification of any impurities present. The structures of the study compounds are shown in Table 4.1.

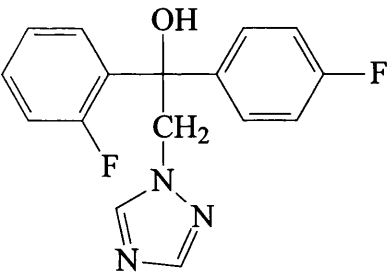
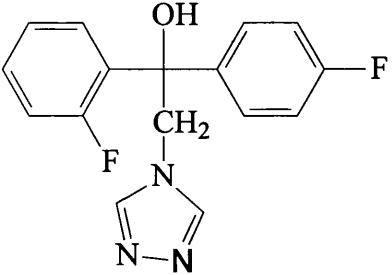
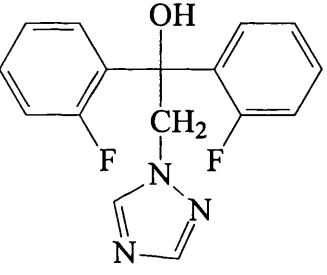
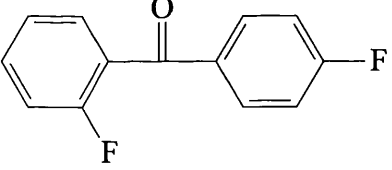
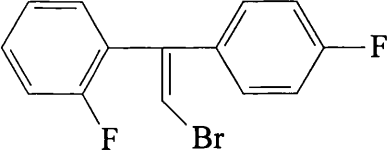
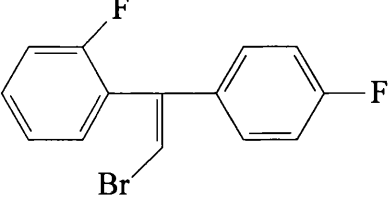
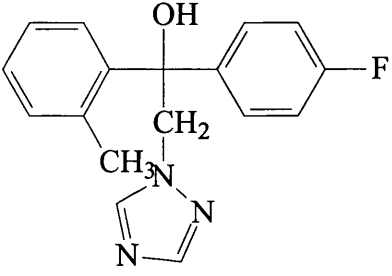
Structure	Trivial Name
	Flutriafol
	Triazol-4-yl
	2,2'-Difluoro Isomer
	2,4'-Difluorobenzophenone
	Bromoalkene (bromine cis to the p-fluorobenzene)
	Bromoalkene (bromine trans to the p-fluorobenzene)
	Methyl Tertiary Alcohol

Table 4.1 – Structures of flutriafol and related impurities studied in Chapter 4

4.2 – INTRODUCTION [3-6]

The term chromatography is used to describe a diverse range of dynamic separation methods involving two immiscible phases, one mobile the other stationary. IUPAC have defined chromatography as ‘A method used primarily for the separation of a sample, in which the components are distributed between two phases, one of which is stationary while the other moves. The stationary phase may be a solid, or a liquid supported on a solid or a gel. The stationary phase may be packed in a column, spread as a layer, or distributed as a film etc; in these definitions ‘chromatographic bed’ is used as a general term to denote any of the different forms in which the stationary phase may be used. The mobile phase may be gaseous or liquid.’

In the analysis of complex mixtures the need to separate the sample components prior to detection and quantitation is of fundamental importance. The diverse range of techniques encompassed by the term chromatography are amongst the most widely employed means of achieving the separations required.

Although the earliest record of chromatographic separation was reported in the 1900s, it was not until the 1930s and 40s that further important developments were made with the introduction of paper chromatography (PC), thin layer chromatography (TLC), ion exchange chromatography (IEC) and gel permeation chromatography (GPC). These techniques are still in use but have largely been superseded by the evolution of gas chromatography (GC) and high performance liquid chromatography (HPLC). Over the last 20 years HPLC has become established as one of the most important and widely used analytical techniques and it

- Retention Time

The retention time, t_R , of an analyte species in a chromatographic separation is the time it takes after sample injection for the analyte peak maximum to elute. The column 'dead volume', the time it takes for an unretained species to be eluted, t_0 , must also be taken into account. The actual retention time of a sample component, t'_R , can be calculated using the following equation:

$$t'_R = t_R - t_0$$

Equation 4.1

- Capacity Factor

The capacity factor, k' , is an alternative measure of analyte retention and is effectively a ratio of the number of solute molecules in the stationary phase to the number of molecules in the mobile phase.

$$k' = \frac{t_R - t_0}{t_0} = \frac{t'_R}{t_0}$$

Equation 4.2

- Efficiency

The efficiency of a chromatographic column is a measure of the effect of band broadening on a separation. Where chromatographic peaks are sharp and efficiency is high, band broadening effects are lower than in a low efficiency broad-peaked separation. Two related terms are widely used measures of efficiency, N , the number of theoretical plates and the plate height, H . The number of theoretical plates, N , can be calculated directly from the chromatographic peak using the following equations:

$$N = 5.54 \left[\frac{t_R}{W_{1/2}} \right]^2$$

Equation 4.3

$$N = 16 \left[\frac{t_R}{W} \right]^2$$

Equation 4.4

The two terms are related by Equation 4.5.

$$H = \frac{L}{N}$$

Equation 4.5

Where H = plate height
L = length of column

Comparisons of the quality of two columns of different length may be made using the plate height and for maximum efficiency, the calculated plate height should be as small as possible and band broadening should be minimised. The phenomenon of band broadening has three main contributory factors:

(i) *Eddy Diffusion*

This is the process by which solute molecules in the mobile phase move through the column via numerous different pathways. Those solute molecules following relatively straightforward, unobstructed pathways will elute more quickly than those taking more erratic pathways. The result of these multiple pathways is band broadening, the extent of which is dependent on particle size and uniformity of column packing.

(ii) *Molecular Diffusion*

Also known as longitudinal diffusion, this results from the random motion of solute molecules in the mobile and stationary phases. While this is an important factor in GC, the diffusion coefficients for liquids are significantly lower and consequently for HPLC separations this factor can be disregarded.

(iii) *Mass Transfer*

The most significant contribution to band broadening results from resistance to mass transfer at the solute–stationary phase interface. Band broadening arises because equilibrium between phases is not achieved instantaneously. The problem is exacerbated with the use of high flow rates and increases in particle size.

- Resolution

Resolution is the term used to describe the degree of separation of one sample component from another and can be determined directly from the chromatogram using the following equation:

$$R_s = \frac{2(t_{R2} - t_{R1})}{(w_1 + w_2)}$$

Equation 4.6

A resolution of 1.0 corresponds to a peak overlap of about 4% with higher R_s values representing progressively smaller overlaps. Resolution values of greater than 1.2 are desirable, with a value of 1.5 representing an almost complete separation.

4.4 – HIGH PERFORMANCE LIQUID CHROMATOGRAPHY (HPLC)

As the name suggests, liquid chromatography describes those techniques where the mobile phase is a liquid. This encompasses a variety of different methods and includes partition, ion exchange, ion-pair, size exclusion, liquid-solid adsorption and affinity chromatography. By far the most widely employed technique is High Performance Liquid Chromatography or HPLC. The versatility of the technique and its applicability to such a wide range of analytes has resulted in sales of HPLC instrumentation in the region of \$1 billion each year.

4.5 – INSTRUMENTATION [4,6,10,11]

The basic equipment required to perform HPLC is relatively simple although more sophisticated instrumentation generally allows greater versatility and precision of results which is often desirable. The schematic shown in Figure 4.2 shows a basic HPLC system and illustrates the components required, which are:

- Solvent reservoirs and mobile phase
- Pumps
- Injection system
- HPLC column
- Detector attached to data handling system

In general, commercially available instruments often have additional features such as autosamplers and thermostatted capillary compartments.

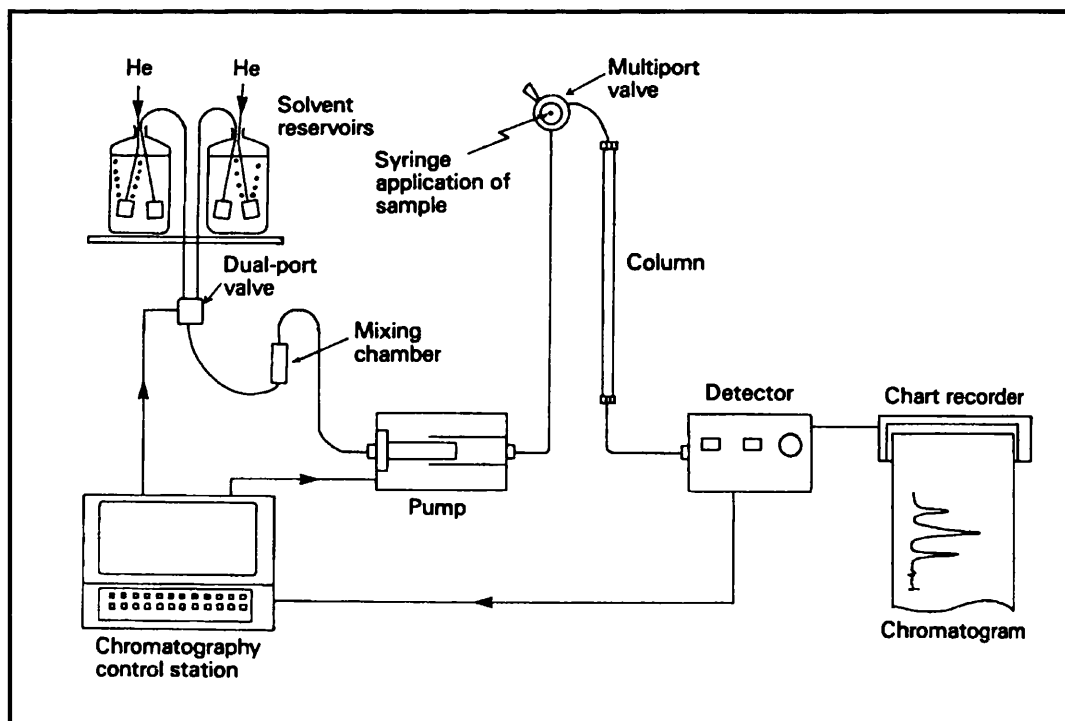


Figure 4.2 – Schematic representation of the essential components in an HPLC instrument

The following paragraph provides a brief overview and outline of basic HPLC set-up and operation. Aspects of the instrumentation will be dealt with in greater detail in the sections that follow.

The column is typically constructed from stainless steel, lined with glass, packed with a suitable stationary phase, 10-25cm in length and 4-6mm internal diameter. Mobile phase is delivered to the column via a high-pressure pump and solvent mixing system and the sample is introduced either by a syringe and septum system or via a multiport valve. Elution of sample components from the column is monitored by the detector and the response is recorded and displayed as a chromatogram.

4.5.1 - Mobile Phase

The solvents used as HPLC mobile phases are generally organic solvents such as methanol and acetonitrile, water, aqueous buffers or mixtures. Mobile phase should be filtered under vacuum prior to using nylon filters to ensure that any insoluble particles that may interfere with the flow or damage the pump are removed. Dissolved gases which may result in the formation of unwanted bubbles in the detector and pumping system can be removed by degassing the solvent. This may be performed in-situ as many of the commercially available HPLC instruments have this facility, either in the form of inert gas purge lines, vacuum pumping systems or some form of heating element. The quality of the mobile phase can also be improved by the use of commercially available HPLC grade solvents, which are of a higher quality than standard analytical grade reagents.

The selection of mobile phase when LC-MS is to be performed using an API interface is however restricted to volatile solvents and buffers. Commonly used HPLC buffers such as phosphate and borate salts are involatile and cannot be used as they crystallise and may cause blockages in the source. The Operator's Manual for the Finnigan LCQ [12] recommends that salts should be avoided where possible and that water, organic solvents and volatile buffers such as ammonium acetate should be used.

4.5.2 – Pumps

The role of the pumps is of fundamental importance. They are required to maintain a constant flow of solvent to the column and must therefore be capable of generating high pressures up to 6000psi. Any variation in flow rate must be minimal

in order that sample retention times are not affected. Pumps should be robust and should be compatible with the solvents and buffers typically used in HPLC analyses.

4.5.3 – Sample Injection

The most commonly employed methods of sample introduction in modern instrumentation are valve injectors. Previously syringe injection was used and although the technique is simple and allows variable sample loading reproducibility is poor and column blockages from fragments of septum is possible. Of the valve type injectors the Rheodyne or Valco type six port valves are the most common. These injectors employ a loop to control the amount of sample injected and give greater reproducibility. In addition, the valve injectors are easily adapted to allow automatic operation, which is highly desirable in laboratories where a large number of injections are performed.

4.5.4 – Columns

As the column is where the chromatographic separation actually occurs its selection is of fundamental importance to achieving a successful and reproducible separation. The length of the column used depends on the number of theoretical plates necessary to achieve the required resolution in any particular separation but is typically between 10 and 25cm. The majority of columns have an internal diameter of 4.6mm, although recently the use of narrow-bore and micro-bore columns has increased. These columns can be as short as 3 to 7.5cm with internal diameters of less than 2mm and have the advantage of allowing very rapid and economical analyses with increased sensitivity which is of particular use in the analysis of biological samples where sample is often limited. However the need to minimise the

Chapter 4 HPLC and HPLC-MS Studies of Plant Lipid and Related Impurities 100

extra column volume of the system necessitates the use of costly specialist injectors, flow cells and other instrumentation.

The particular packing material contained within the stainless steel casing is normally 3,5 or 10 μ m in size and is most commonly composed of silica or alumina. The various types of packing materials and their uses are described in greater detail in section 4.6.

4.5.5 – Detectors

One of the most crucial elements in a successful modern HPLC system is an effective detector. Ideally, an LC detector should encompass as many of the characteristics listed below as possible [6]:

- Good sensitivity
- Wide range of linearity of response
- Good stability and reproducibility
- Reliable and convenient
- Non-destructive
- Respond to all analytes, or have a predictable response to a limited range of groups
- No contribution to band broadening
- Rapid response independent of temperature and flow rate
- Qualitative

At present there is no ‘perfect’ detector available that fulfils all of these requirements, consequently a number of different techniques, each matching some of

the characteristics listed above, have been used as detectors in HPLC. Detectors can be classified in two groupings, bulk property detectors and solute property detectors. Bulk property detectors can also be described as general detectors as they respond to a property of the mobile phase as a whole. Detection techniques of this type include refractive index (RI) and density. Solute property detectors are also known as selective detectors and are sensitive to a property specific to the analyte species such as UV absorbance, fluorescence or electrochemical systems.

Although a wide variety of detection methods are available, by far the most widely used technique is UV-Visible Absorbance detection, and this, along with mass spectrometric detection will be discussed further in the following sections. More detailed discussion of the other detection techniques can be found in numerous publications [4,6,10,11].

4.5.5.1 – UV-Visible Absorbance Detection

As has been previously stated UV-Vis absorbance detection is the most widely used of the numerous different techniques available. This is due to a combination of factors; although sensitivity is low in comparison with other types of detector, it is adequate for the majority of HPLC analyses. It has a wide range of application as a great number of compounds are detectable by UV-Vis measurements and UV-Vis absorbance detectors are, in general, less expensive than other types of detection systems and come as standard in the majority of commercially available HPLC instruments.

The basic principles of UV-visible absorbance detection have been outlined previously in Section 3.4.2.1 and will not be discussed again here.

Three types of UV-Visible detectors are available, fixed wavelength, variable wavelength and spectrophotometric detectors and again these have been described in Chapter 3.

While the principles behind UV-visible detection and the construction of the detectors are generally the same as those used in capillary electrophoresis, in HPLC other factors must be considered. In many cases the mobile phase must be considered as several commonly used solvents or mixtures of solvent produce significant background absorbances at low UV wavelengths (200 – 215nm). This results in decreased sensitivity and has been shown to result in increased baseline noise. For these reasons the use of acetonitrile as a mobile phase solvent is particularly popular at these wavelengths as its background absorbance is very low over this range.

4.5.5.2 – Mass Spectrometric Detection [4,10,13-16]

The mass spectrometer has the potential to serve as a universal detector for HPLC [13]. Two major problems exist in achieving the successful combination of liquid chromatography and mass spectrometry. Many of the samples and the buffer systems employed in LC are involatile and in many cases are not amenable to conventional MS analysis using EI or CI. Commonly used buffers such as phosphate and borate salts are non-volatile and consequently cannot be used with the majority of LC-MS systems. Also, the relatively high flow rates, typically 0.5–5ml/min, used

in HPLC analysis translate into gas flow rates in the range 100–3000ml/min which must be removed in order to reach the vacuum (10^{-6} Torr) required for successful operation.

There are several commonly used methods of overcoming the problem of the high flow rate:

- The flow from the LC can be split so that only a fraction of the total flow is introduced into the mass spectrometer.
- The use of narrow-bore or capillary columns reduces the flow rate and eliminates the need to split the flow.
- The use of additional pumping at the source allows higher flow rates to be used.
- The solvent may be totally removed prior to introduction into the mass spectrometer.
- The use of atmospheric pressure ionisation techniques.

Since LC-MS was first performed in the early 1970s, several types of interface have been developed:

- Direct Liquid Introduction (DLI)
- Moving Belt
- Particle Beam
- Thermospray
- Continuous Flow Fast Atom Bombardment
- Atmospheric Pressure Ionisation (API)

Only the API interfaces, Electrospray (ESI) and Atmospheric Pressure Chemical Ionisation (APCI) will be discussed further, detailed accounts of the other interfaces mentioned above can be found elsewhere [4,10,13-16].

Atmospheric Pressure Ionisation (API) [17]

The use of API interfaces offers advantages over the other techniques available as any problems associated with the introduction of liquid flows directly into a high vacuum source are avoided. The mechanism of both ESI and APCI have been described previously in Section 2.2.1 as has the operation of the Finnigan API interface used throughout these studies.

Electrospray (ESI)

LC-MS using an electrospray ionisation interface was first performed by Fenn and co-workers in 1985 [18] but this early interface was only capable of introducing flows of around $10\mu\text{l}/\text{min}$ and was therefore limited to the use of capillary LC columns or required a large split. Since this time improvements to the electrospray source have been made including the inclusion of a heated capillary tube that acts as a desolvation chamber. These improvements have increased the flow capacity of the interface, enabling the use of flow rates of the order 1 - 5 ml/min. Ion suppression can however occur at such high flow rates, consequently for increased sensitivity it is recommended that the HPLC effluent is split prior to its introduction into the mass spectrometer. This may be achieved with the use of a splitting device, such as the Accurate™ splitter or using a zero dead volume T-piece.

Atmospheric Pressure Chemical Ionisation (APCI)

The combination of LC-MS with the use of APCI was first demonstrated by Carroll et al in the early 1970s [19,20], it was not, however, until the 1990s that the major breakthroughs in this technique were made with the publications by Bruins [21] and Huang et al [22]. Flow rates of up to 2.0 ml/min are readily accepted, consequently there is no need to split the HPLC flow before it is introduced into the mass spectrometer.

4.6 – COLUMN PACKINGS AND MODE OF OPERATION [4,6,10,11]

The earliest chromatographic separations were performed using columns packed with alumina or silica. Silica gel has a highly active surface layer of silanol groups onto which analyte molecules are adsorbed to varying degrees based on their polarity. Elution was achieved by washing through the column with a relatively non-polar solvent such as hexane, heptane or chloroform. This early mode of chromatography forms the basis of what is known today as Normal Phase HPLC.

4.6.1 - Normal Phase HPLC

In normal phase HPLC, as in the early forms of chromatography, the stationary phase is a polar adsorbent and the mobile phase is generally a mixture of non-aqueous solvents. It is particularly important that water is totally excluded from normal phase HPLC systems as it can significantly affect the chromatography. Interactions of the polar water molecules with the stationary phase can cause changes in retention and peak shape. This may be overcome through the addition of a polar modifier such as acetic acid to the mobile phase.

In addition to the silica gel and alumina traditionally used, bonded phases modified with cyanopropyl-, aminopropyl- and diol functional groups are also commonly used. These bonded phases provide a more homogeneous surface than unmodified silica gel and their decreased activity makes them particularly useful for the separation of moderately polar compounds. Moderately polar compounds are also well suited to separation using reversed-phase chromatography so the choice of technique is often based on the nature of the sample matrix rather than properties of the analyte.

4.6.2 – Reversed-Phase HPLC

Reversed-phase HPLC is the most popular mode of chromatography for the separation of the majority of compounds of interest in the chemical, pharmaceutical and biological sciences. The technique, as the name suggests, uses stationary and mobile phases opposite in polarity to those used in normal phase. The stationary phase is non-polar and often a hydrocarbon functional group bonded to silica gel. The most commonly used of the stationary phases is the ODS, octadecyl (C_{18}), phase, which accounts for about 75% of all applications. Other less commonly used alternatives are octyl (C_8) and phenyl packings. The mobile phase used in reversed-phase HPLC is relatively polar and in general consists of a mixture of water or aqueous buffer with a water miscible organic solvent, the most common of which are methanol, acetonitrile and tetrahydrofuran. The popularity of reversed-phase HPLC is based in part on its compatibility with aqueous samples without the need for pre-treatment and also the wide range of polarity of analyte species which may be separated.

4.6.3 – Other Modes of HPLC

While reversed-phase and normal-phase are the most widely used modes of HPLC, the term encompasses a number of other techniques with more specialised areas of application.

Ion Chromatography (IC) is an outgrowth of ion-exchange chromatography (IEC) and is useful in the analysis of inorganic and organic ions where reversed-phase and reversed-phase ion-pair chromatography are not applicable. Columns are packed with ion exchange resins and separations are based on the different levels of interaction between solute ions in the mobile phase and the fixed exchanging groups on the stationary phase.

The basis for separation in the previously described techniques of reversed-phase, normal phase and ion chromatography is the differential interactions of the solute molecules with the stationary and mobile phases. In contrast, the separations in Size Exclusion Chromatography (SEC) are based on differences in molecular size and the ability of molecules to penetrate the pores of the stationary phase. SEC is used extensively in the field of biochemistry and has proved particularly useful in the isolation of peptides and proteins and in the determination of the molecular weights of biological macromolecules.

4.7 – RESULTS AND DISCUSSION

The objective of this study was to investigate the use of HPLC in separating the impurities found in the fungicide flutriafol, see Table 4.1. The technique was also assessed in combination with mass spectrometric detection as a means of potentially identifying any unknown components.

4.7.1 – HPLC OF FLUTRIAFOL AND RELATED IMPURITIES

As discussed in Section 1.5.2.4, literature searches in the area of flutriafol and triazole fungicide analysis were unsuccessful in locating any reported work relevant to the study of HPLC analysis described here. As a consequence, initial experiments were performed using reverse-phase HPLC with a 25cm × 4.6mm column packed with the widely available Hypersil ODS stationary phase in this case with a 5 μ m particle size. Hypersil ODS is prepared with the C18 alkyl ligand monofunctionally bonded to the silica surface and is suitable for the analysis of non-polar to moderately polar compounds. 25 and 15cm × 4.6mm C8 and C18 columns are amongst the most widely used and are recommended for initial scouting work in HPLC method development [24,25].

Although the objective of the study was to separate and detect impurities present in a production sample of flutriafol, the preliminary method development work was performed using a mixture of individual reference materials for flutriafol and each of the six potential impurity compounds. The mixture was prepared purely for retention time and method development purposes and was not intended to mirror the composition of the technical sample. The composition of this mixture is detailed in Table 4.2.

Flutriafol	10 _μ g/ml
Triazol-4-yl	90 _μ g/ml
2,2'-Difluoro isomer	10 _μ g/ml
2,4'-Difluorobenzophenone	10 _μ g/ml
Bromoalkene (cis)	10 _μ g/ml
Bromoalkene (trans)	10 _μ g/ml
Methyl Tertiary Alcohol	10 _μ g/ml

Table 4.2 - Composition of flutriafol standard mixture

Initial experiments investigated the use of isocratic HPLC conditions using mixtures of methanol, water and 25mM ammonium acetate buffer (pH 4.5). The solvent systems employed are summarised in Table 4.3. The flow rate used throughout this series of analyses was 1.0 ml/min and the detection wavelength was 214 nm.

System	Composition
1	60% Ammonium acetate buffer : 40% Methanol
2	55% Ammonium acetate buffer : 45% Methanol
3	50% Ammonium acetate buffer : 50% Methanol
4	45% Ammonium acetate buffer : 55% Methanol
5	30% Ammonium acetate buffer : 70% Methanol
6	10% Water : 90% Methanol
7	20% Water : 80% Methanol
8	30% Water : 70% Methanol
9	35% Water : 65% Methanol
10	40% Water : 60% Methanol
11	45% Water : 55% Methanol
12	50% Water : 50% Methanol
13	60% Water : 40% Methanol

Table 4.3 – Summary of isocratic solvent compositions examined

While the use of aqueous buffers in HPLC separation systems is often beneficial and can improve reproducibility and peak shape, in this particular separation the use of ammonium acetate buffer was relatively unsuccessful and peak shape was poor. By comparison the use of the methanol/water mixtures was more successful and formed the basis for the work that followed. Although none of the isocratic elution systems was able to fully separate all seven study compounds the work provided valuable information. Using the 80% Methanol: 20% Water mixture all seven components were visible and analysis was complete in under 15 minutes. Unfortunately, under these conditions resolution of the first three components is poor. The use of those mixtures containing levels of methanol 65% or 60% successfully resolved the first five components in reasonable time but even after 45 minutes, the bromoalkene compounds were not eluted. The resolution data for

solvent systems 7-10 is summarised in Table 4.4 and example chromatograms are displayed in Figures 4.3 and 4.4.

		Solvent system			
		7	8	9	10
Resolution (R_s)	2,2-difluoro / triazol-4-yl	0.55	0.52	1.44	1.44
	triazol-4-yl / flutriafol		1.56	3.19	4.08
	flutriafol / me tert alcohol	2.87	4.58	8.85	9.67
	me tert alcohol / 2,4-difluoro	1.85	1.65	4.12	4.23
	2,4-difluoro / bromo trans	15.96	26.5	—	—
	bromo trans / bromo cis	6.06	8.88	—	—

Table 4.4 – Comparison of resolution data obtained for isocratic solvent systems

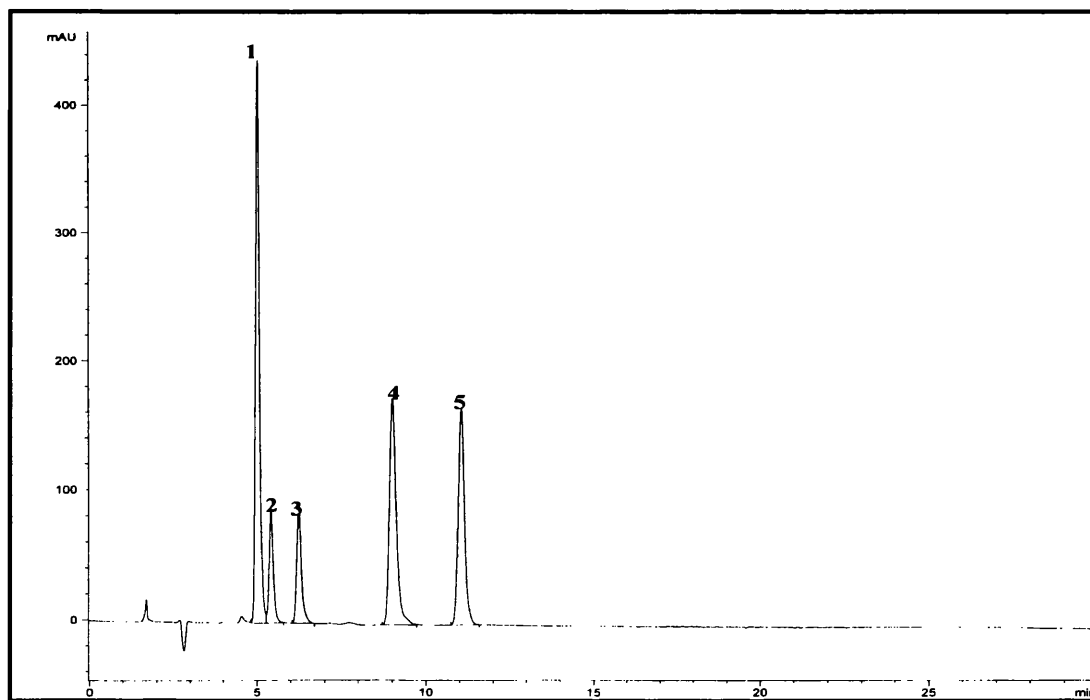


Figure 4.3 – HPLC chromatogram of a seven component flutriafol standard mixture obtained using solvent system 9

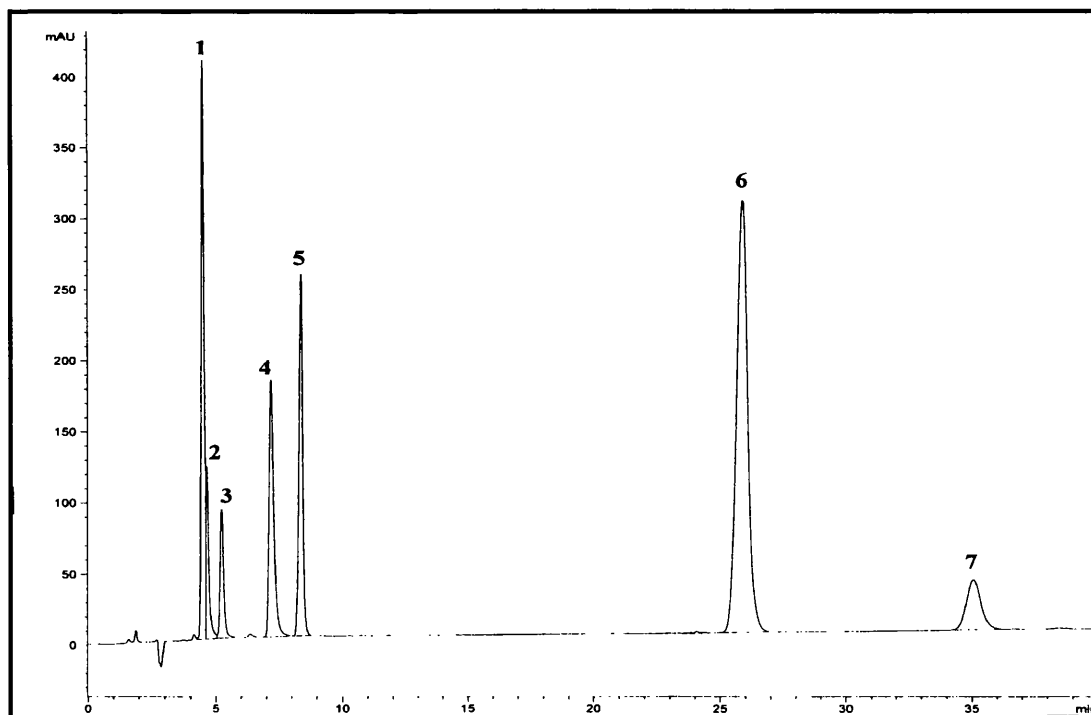


Figure 4.4 - HPLC chromatogram of a seven component flutriafol standard mixture obtained using solvent system 8

Peak No.	Sample Component
1	2,2'-Difluoro Isomer
2	Triazol-4-yl
3	Flutriafol
4	Methyl Tertiary Alcohol
5	2,4'-Difluorobenzophenone
6	Bromoalkene (trans)
7	Bromoalkene (cis)

Table 4.5 – Key to peak assignments in sample chromatograms

While isocratic elution is desirable for a number of reasons including simplicity and greater stability of baseline, in this case it is inadequate. Consequently, the use of gradient elution was investigated. Gradient elution involves varying the composition of the solvent system in a programmed way, sometimes continuously and sometimes in a series of steps. This mode of operation is frequently used in difficult separations to enhance separation efficiency and achieve

levels of resolution not possible with isocratic elution. The gradient programmes evaluated are outlined in Table 4.6 and are based primarily on the isocratic solvent systems found to be most suitable for (a) the adequate resolution of the first three sample components and (b) the elution of the bromoalkene compounds in a reasonable run time.

System	Gradient Programme	
1	Time (mins)	%Methanol
	0	60
	16	60
	19	80
	35	80
2	Time (mins)	%Methanol
	0	65
	13	65
	15	80
	30	80
3	Time (mins)	%Methanol
	0	55
	13	55
	15	80
	30	80

Table 4.6 - Summary of gradient elution programmes examined

It should also be noted that slight variations in the time programmes described were also examined with a view to further shortening the total analysis time. The resolution and efficiency of each of the three systems was assessed and the figures calculated are displayed in Table 4.7.

	1		2		3	
	Resolution (R_s)	Efficiency (plates/metre)	Resolution (R_s)	Efficiency (plates/metre)	Resolution (R_s)	Efficiency (plates/metre)
2,2-Difluoro	3.34	25158	3.13	25600	4.16	27172
Triazol-4-yl	8.32	25392	5.89	26157	10.02	25972
Flutriafol	19.66	27646	15.21	27711	25.49	29432
Me tert alcohol	9.54	27612	9.70	27907	10.69	208325
2,4-difluoro	37.74	48890	61.78	48637	32.60	311233
Bromo trans	12.84	417088	13.13	345292	12.11	352642
Bromo cis	—	325983	—	263420	—	283890

Table 4.7 – Comparison of resolution and efficiency data for gradient elution systems 1-3

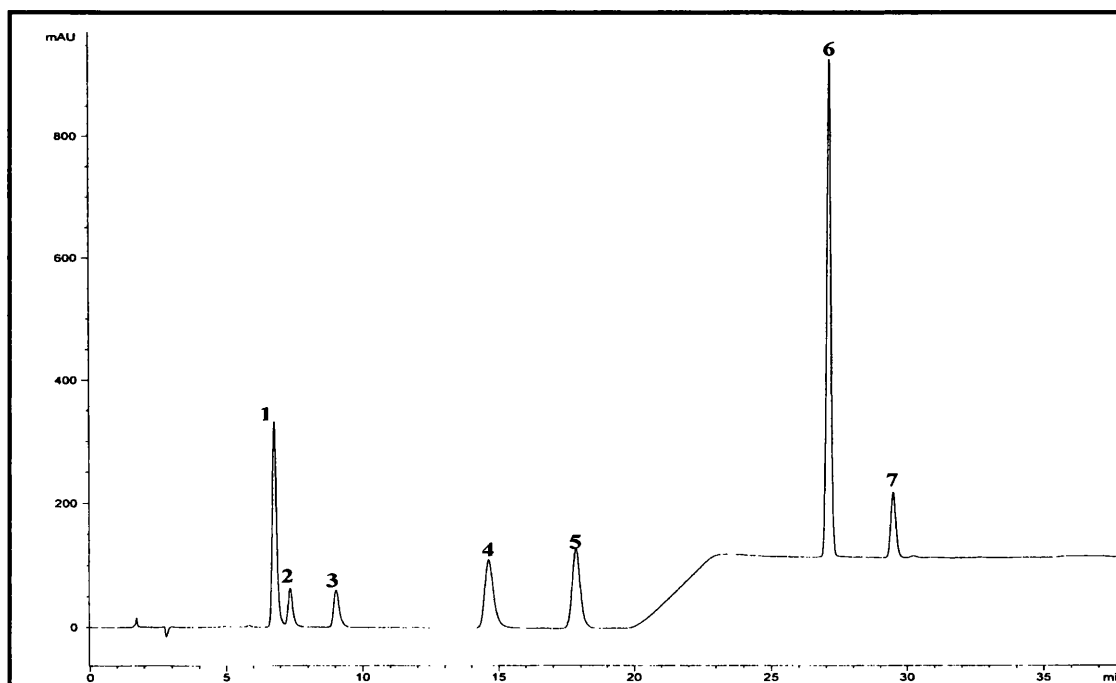


Figure 4.5(a) – HPLC chromatogram of a seven component flutriafol standard mixture obtained using gradient programme 1 (Table 4.6)

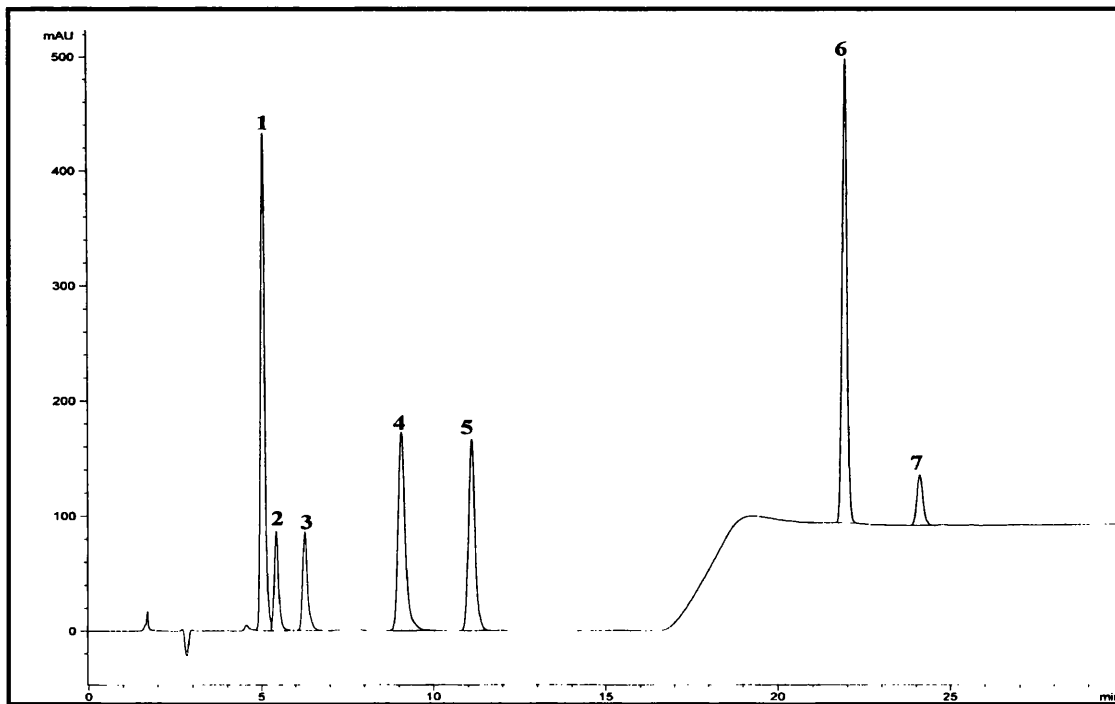


Figure 4.5(b) - HPLC chromatogram of a seven component flutriafol standard mixture obtained using gradient programme 2 (Table 4.6)

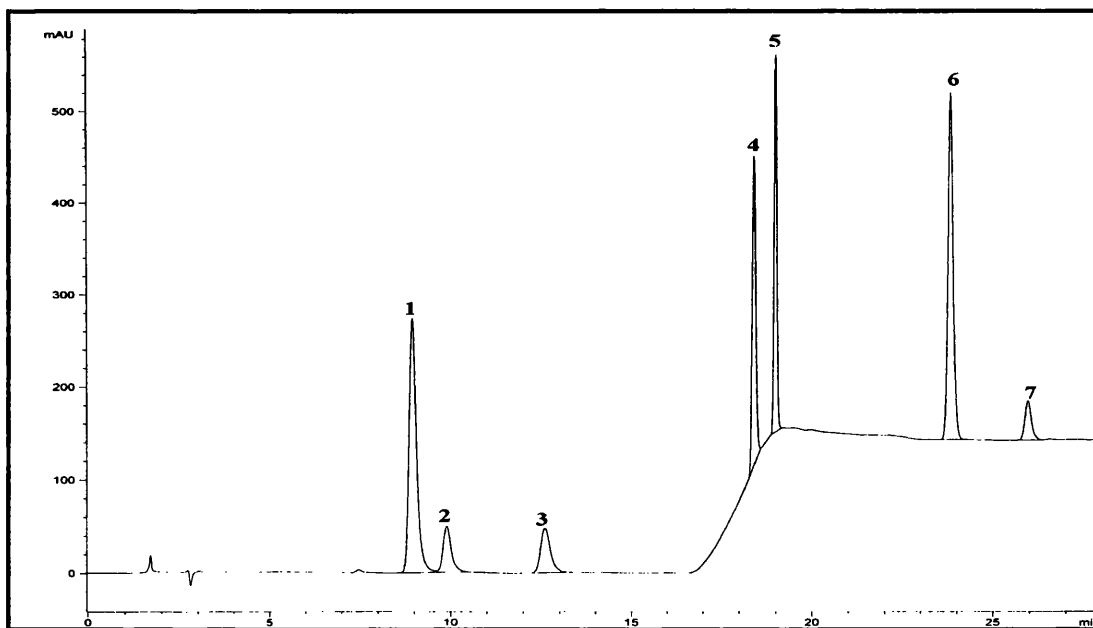


Figure 4.5(c) - HPLC chromatogram of a seven component flutriafol standard mixture obtained using gradient programme 3 (Table 4.6)

Examination of the above data in conjunction with visual examination of the chromatograms generated using each of the gradient programmes studied indicates that any of the three systems would be a suitable gradient programme. One of the main difficulties encountered in the attempts to optimise the gradient programme was that reducing the excessive resolution of one pair of components resulted in the increased resolution of other groups of components. In system 2, the resolution of flutriafol and methyl tertiary alcohol was at its lowest but the resolution of 2,4'-difluorobenzophenone and the trans bromoalkene compound was particularly high and the opposite effect was observed in system 3. Efficiencies of greater than 25000 plates/metre were achieved for all seven components with each of the three systems. These values are typical of HPLC, as manufactured columns usually possess between 40000 and 60000 plates/metre. With very little to choose between the systems it was decided to further assess the systems for use in the separation of an actual technical sample of flutriafol.

4.7.1.1 – Effect of column length and particle size

With a view to making further improvements to the separation the use of two shorter columns was investigated. The columns were both 10cm in length and again were packed with Hypersil ODS packing, one column with 5 μ m packing and the other with 3 μ m packing. The use of shorter columns can be beneficial in that analysis times can be reduced which in turn results in a lowering of the amount of solvent used. Shorter columns also have the advantage of being lower in price than the 25cm column used previously. The use of packing materials with smaller diameters can offer improvements in separation efficiency. The smaller particle size

allows more uniform column packing to be achieved and as a consequence band broadening is minimised.

The gradient programmes studied were similar to those previously examined with the 25cm column, with timings altered as appropriate for the shorter column length. While the separation was successfully transferred to the 10cm column with 3 μ m packing, the separation achieved using the 5 μ m packed column was poor by comparison. Resolution and efficiency data for separations performed on each of the two 10cm columns is displayed in Table 4.9. The gradient programmes used in each case are shown in Table 4.8.

Column 1 – 10cm, 3μm		Column 2 – 10cm, 5μm	
<u>Time (mins)</u>	<u>%Methanol</u>	<u>Time (mins)</u>	<u>%Methanol</u>
0	60	0	60
4	60	8	60
5	80	10	80
15	80	25	80

Table 4.8 – Gradient programmes used with 10cm Hypersil ODS columns

	Column 1 – 10cm, 3 μ m		Column 2 – 10cm, 5 μ m	
	Resolution (R_s)	Efficiency (plates/metre)	Resolution (R_s)	Efficiency (plates/metre)
2,2-Difluoro	3.72	19842	1.78	6218
Triazol-4-yl	9.29	21437	4.88	5725
Flutriafol	19.65	23502	13.80	6358
Me tert alcohol	3.25	75977	3.48	16283
2,4-difluoro	19.45	95176	11.43	37751
Bromo trans	6.65	100144	2.54	39242
Bromo cis	—	84183	—	12435

Table 4.9 – Comparison of resolution and efficiency data obtained for each of the 10cm columns investigated

It can be seen that while the use of the 10cm column with 3 μ m packing was beneficial and was able to successfully separate all seven components in under 12 minutes, the separation obtained using the second column was rather less successful. As expected the efficiencies achieved using the 3 μ m packed column are significantly better than those of the column with 5 μ m packing are, which accounts for the poor chromatography produced using this column. While the 25cm column packed with 5 μ m diameter material was able to fully resolve the seven study compounds, the reduction in efficiency and resolving power brought about by the shortening of column length results in the failure of the 10cm, 5 μ m column to resolve the first two components. However, the increased efficiency brought about by the decreased particle size in the 3 μ m packed column is sufficient to overcome the lowered efficiency resulting from the shortening of the column length. The efficiencies achieved using the 10cm, 3 μ m column are of similar magnitude to those obtained with the 25cm column and as a consequence the separation produced is similar in

appearance and has the advantage of a shorter run time. Examples of the chromatography produced using each of the 10cm columns are shown in Figures 4.6(a) and (b).

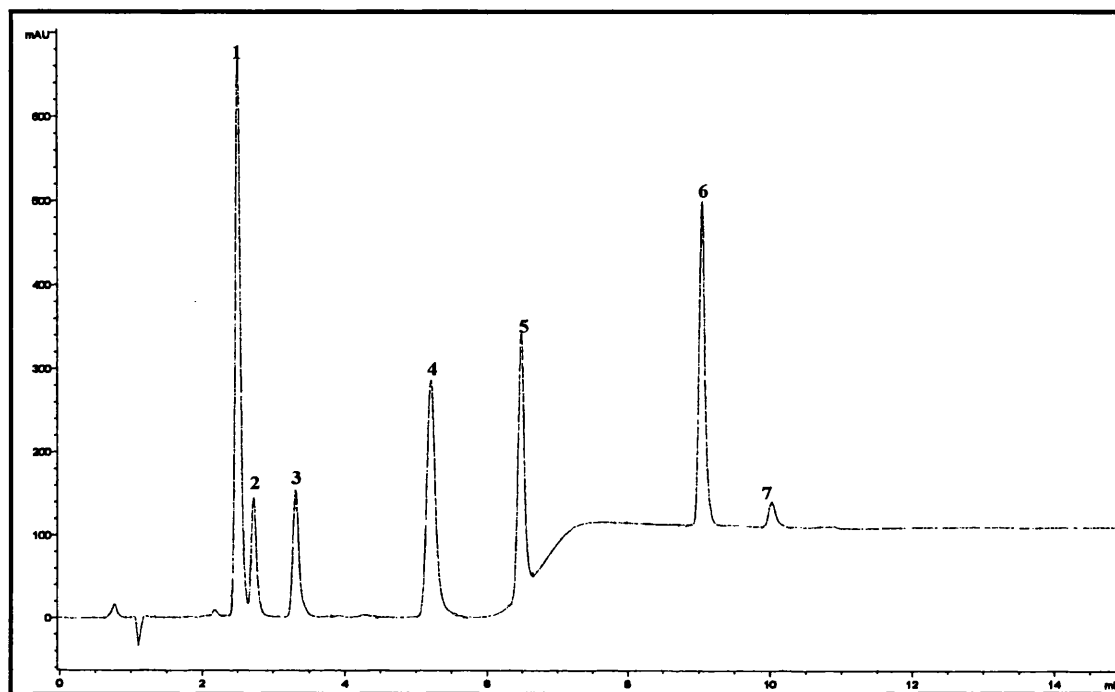


Figure 4.6(a) – HPLC chromatogram of a seven component flutriafol standard mixture obtained using a 10cm, 3 μ m Hypersil ODS column and the gradient outlined in Table 4.8

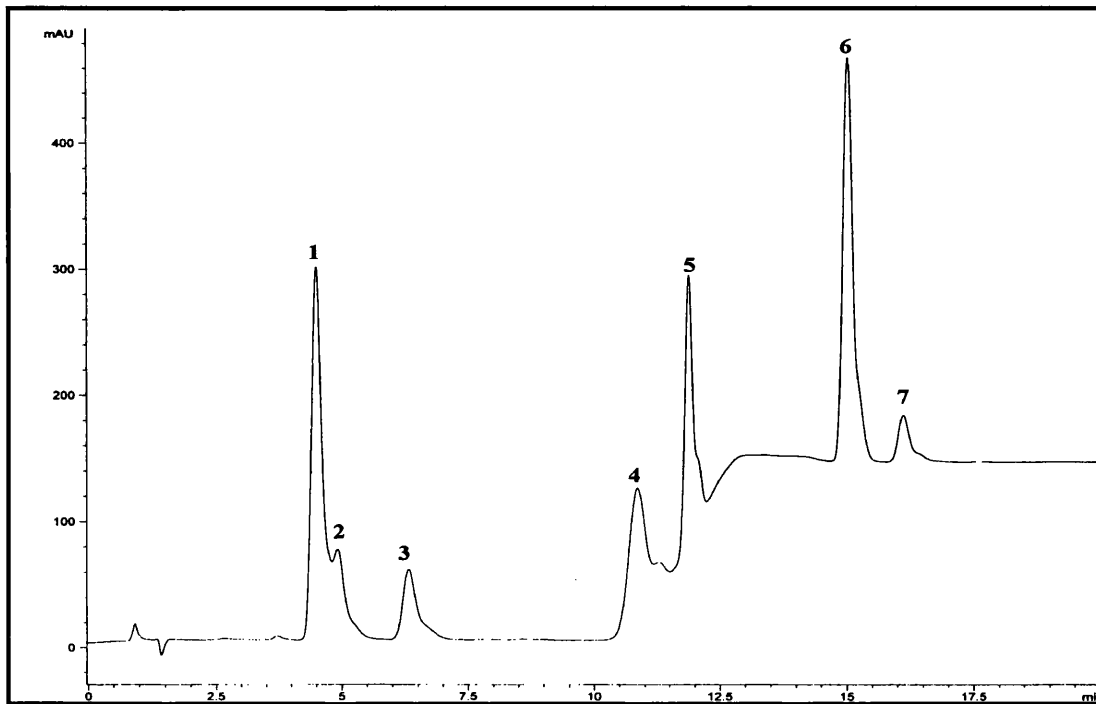


Figure 4.6(b) – HPLC chromatogram of a seven component flutriafol standard mixture obtained using a 10cm, 5 μ m Hypersil ODS column and the gradient outlined in Table 4.8

4.7.1.2 – Limit of detection (LOD) and limit of quantitation (LOQ)

The limits of detection and quantitation for each of the seven study compounds was determined under the conditions outlined below:

Column: 25cm \times 4.6mm, Hypersil ODS 5 μ m

Gradient:	Time (mins)	%Methanol
	0	65
	13	65
	15	80
	30	80

Flow Rate: 1.0 ml/min

Injection Volume: 20 μ l

Detection: UV @ 214nm

The actual amount of sample introduced onto the column was calculated for each component and as described previously in Section 3.6.1.5, the baseline noise of the chromatogram was expanded, measured and determined to be equivalent to 0.38mAU. The height of each of the sample peaks was measured and converted to mAU. The LOD and LOQ were then calculated using Equations 3.14 and 3.15, substituting the amount in nanograms for the concentration in ppm.

	LOD (ng)	LOQ (ng)
2,2'-Difluoro isomer	0.53	1.77
Triazol-4-yl	23.86	79.53
Flutriafol	2.68	8.94
Methyl tertiary alcohol	1.32	4.41
2,4'-Difluorobenzophenone	1.38	4.61
Bromoalkene (trans)	0.56	1.85
Bromoalkene (cis)	5.24	17.47

Table 4.10 - Limits of detection and quantitation for each of the seven study compounds using HPLC with UV detection

4.7.1.3 – Analysis of flutriafol technical material

Having successfully achieved the separation of flutriafol and the six related compounds using gradient elution on both the 25cm, 5 μ m and the 10cm, 3 μ m columns, the analysis of the sample of flutriafol technical material was attempted. The sample was dissolved in methanol to produce a solution equivalent to 5mg/ml (or 5000ppm). In order to prevent the massive overloading of the HPLC column and detector the solution was diluted further prior to analysis. As a number of viable gradient programmes had been identified using the standard mixture and the conditions and column had not yet been finalised each set of conditions (Table 4.6:

Systems 1-3 and Table 4.8: System1) was assessed in order to determine those most suitable for the analysis of the technical sample.

An example of the chromatography obtained for a 20 μ l injection of 2000ppm technical flutriafol under the conditions detailed in Table 4.6 – System 3, is shown in Figure 4.7.

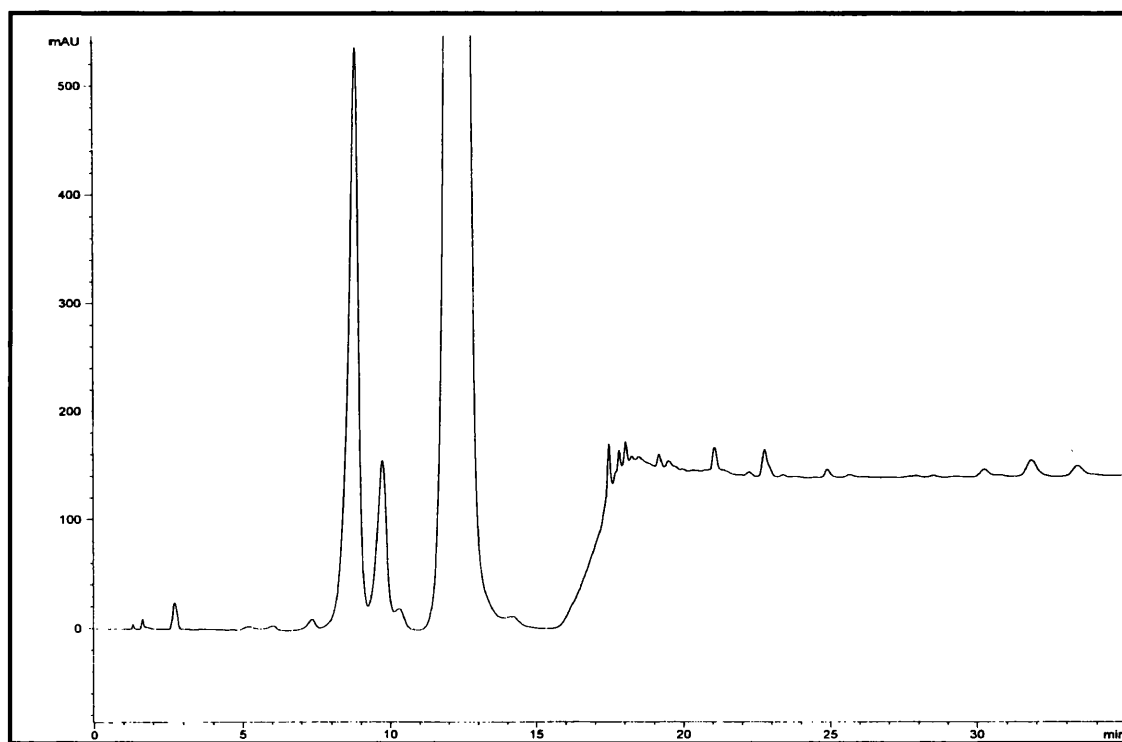


Figure 4.7 – HPLC chromatogram for a 20 μ l injection of a 2000ppm sample of technical flutriafol obtained using gradient programme 3 (Table 4.6)

It can be seen that in addition to the six impurities shown in Table 4.1 and included in the standard mixture used for method development, a significant number of other impurity peaks are present in the sample, over 3 percent by area. An area percent impurity profile is given in Table 4.11.

Peak No.	RT (mins)	RRT	%Area	Identity
1	1.3	0.10	0.02	—
2	1.6	0.13	0.07	—
3	2.7	0.22	0.26	—
4	5.2	0.42	0.09	—
5	6.1	0.49	0.09	—
6	7.4	0.59	0.23	—
7	8.9	0.71	13.27	2,2'-Difluoro Isomer
8	9.8	0.78	3.86	Triazol-4-yl
9	10.5	0.84	0.45	—
10	12.5	1.00	78.93	Flutriafol
11	14.4	1.15	0.42	—
12	17.5	1.40	0.23	Methyl Tertiary Alcohol
13	17.9	1.43	0.08	—
14	18.0	1.44	0.12	2,4'-Difluorobenzophenone
15	18.3	1.46	0.02	—
16	18.5	1.48	0.02	—
17	19.2	1.54	0.09	—
18	19.5	1.56	0.08	—
19	21.1	1.69	0.20	—
20	22.3	1.78	0.04	—
21	22.8	1.82	0.35	Bromoalkene (trans)
22	23.5	1.88	0.02	—
23	24.1	1.93	0.04	—
24	25.0	2.00	0.12	Bromoalkene (cis)
25	25.9	2.07	0.09	—
26	30.6	2.45	0.18	—
27	32.2	2.58	0.36	—
28	33.8	2.70	0.27	—

Table 4.11 – Area percent impurity profile of a sample of technical flutriafol

As each of the three gradient programmes run on the 25cm column were successful in providing a separation of the sample of flutriafol production material the selection of the final experimental conditions for use in the HPLC-MS work was not clear-cut. The lower efficiency 10cm, 3 μ m column was unable to cope with the higher concentrations of impurities present in the sample and the gradient programme used was unable to adequately resolve the 2,2'-difluoro isomer and triazol-4-yl. In each of the analyses run on the 25cm column the run time had been extended in order to include the numerous impurities eluting after the bromoalkene (cis). Had the efficiency and resolution provided by the 10cm column been adequate the shorter column would have been preferred as the analysis times offered were significantly shorter than those achieved using the 25cm column. As this was not the case, it was decided to use the system offering the shortest run time on the 25cm column, system 3 (Table 4.6), extended to accommodate the additional components. The final conditions are outlined below:

Column: 25cm \times 4.6mm Hypersil ODS 5 μ m

Gradient:	<u>Time (mins)</u>	<u>%Methanol</u>
	0	55
	13	55
	15	80
	40	80

Flow Rate: 1.0 ml/min

Detection: UV @ 214nm

4.7.2 – HPLC-MS OF FLUTRIAFOL AND RELATED IMPURITIES

While HPLC has successfully detected a number of impurity peaks, it should be noted that the area percent profile does not provide a true reflection of the sample composition and is included for information only. The impurity profile shown includes only those components detectable at a UV wavelength of 214nm and does not take into account any differences in response factors. It was hoped that the HPLC-MS experiments would provide structural information to assist in the identification of the unknowns detected as well as detecting any compounds not visible by UV detection.

4.7.2.1 – HPLC-APCI-MS

The LCQ was tuned and calibrated as has been previously described in Section 3.6.3 and further optimised with the infusion of a solution of flutriafol dissolved in methanol. The instrumental settings were adjusted manually to optimise the signal for the fungicide. A capillary temperature of 150°C and an APCI vaporiser temperature of 500°C were used together with a sheath gas flow rate of 65 unit and an auxiliary gas flow rate of 30 units. The capillary voltage was set at +40V for the positive mode analyses. The APCI source can accommodate liquid flows of 200 μ l/min to 2ml/min, consequently the column eluent was introduced into the source in its entirety and without the need for splitting.

4.7.2.2 – HPLC-ESI-MS

The ESI probe on the LCQ is capable of accommodating liquid flow rates of between 1.0 μ l/min and 1.0ml/min without the need for splitting. Although the flow rate employed was within this range, the eluent was split using a zero dead volume

tee-piece for the purposes of these experiments as this mode of operation offers increased sensitivity. The tee-piece arrangement used gave an approximate split ratio of 25:75 (MS: waste) with a resultant flow rate of 250 μ l/min being delivered to the ESI source. The split was checked before and after use by measuring the volume of liquid delivered to waste over a measured period of time to ensure the split was maintained at the same level throughout.

4.7.2.3 – Comparison of ionisation modes

Preliminary experiments concentrated on introducing each of the seven study compounds in turn in order to establish the on-line retention time and to acquire mass spectral data for each component. The signal intensities for the major species observed for each of the seven study compounds using both ESI and APCI are shown in Table 4.12.

	ESI		APCI		APCI	
	m/z	Positive ion	Positive ion	m/z	Negative ion	
2,2'-Difluoro Isomer	302	4.55×10^6	9.61×10^6	300	2.42×10^5	
				360	5.92×10^5	
Triazol-4-yl	302	1.74×10^6	1.32×10^8	300	7.04×10^4	
				360	2.95×10^5	
Flutriafol	302	1.09×10^6	1.38×10^7	300	1.99×10^6	
Methyl Tertiary Alcohol	298	4.41×10^6	1.13×10^7	356	8.93×10^5	
				166	4.72×10^4	
2,4'-Difluorobenzophenone	219	2.39×10^5	3.26×10^4	249	4.05×10^5	
				166	6.02×10^4	
Bromoalkene (trans)	295	7.90×10^4	—	111	8.62×10^5	
	296	1.67×10^5	—	113	8.22×10^5	
				99	1.26×10^6	
				97	2.48×10^5	
				81	2.17×10^6	
				79	2.28×10^6	
Bromoalkene (cis)	—	—	—	—	—	

Table 4.12 – Comparison of HPLC-APCI-MS and HPLC-ESI-MS

In the case of 2,2'-difluoro isomer, triazol-4-yl, flutriafol and methyl tertiary alcohol, while both positive mode APCI and ESI produced good signal intensities the positive mode APCI was in each case the most sensitive. The signal intensities obtained for these compounds in negative mode APCI while generally not as strong as in the positive mode were still relatively good. The results of each of the remaining three compounds were, however, more variable, signal responses were, on the whole, poor and ionisation was unreliable. The analysis of the bromoalkene compounds was particularly unsuccessful with very little data obtained for each of

the two compounds in either APCI or ESI in positive mode. The experiments performed in negative mode were slightly more successful; signal intensities were relatively good and spectra provided useful structural information for the trans bromoalkene compound, the cis bromoalkene, however, again failed to generate any consistent results. Figure 4.8(f) shows the mass spectrum for the trans bromoalkene compound acquired in negative mode APCI, the signals observed and the ratios they are in are indicative of a monobrominated compound. Bromine consists of ^{79}Br and ^{81}Br with approximately 50 percent of each present. Ions corresponding to each of these isotopes are present in the mass spectrum in addition to pairs of signals corresponding with $[\text{Br}_+18]^-$ and $[\text{Br}_+32]^-$ and each pair is present in an approximately 1:1 ratio.

The majority of the subsequent work was performed in APCI mode as it had provided the most successful results in the majority of cases.

The major peaks observed in the mass spectra obtained for each of the study compounds are summarised in Table 4.13 together with tentative peak assignments. The data refers to the positive mode experiments except in the case of the trans bromoalkene compound where the negative mode was more successful. Examples of the mass spectra for each compound are shown in Figures 4.8(a)-(f), no data is included for the cis bromoalkene compound as the results produced were consistently poor and no reproducible data was obtained.

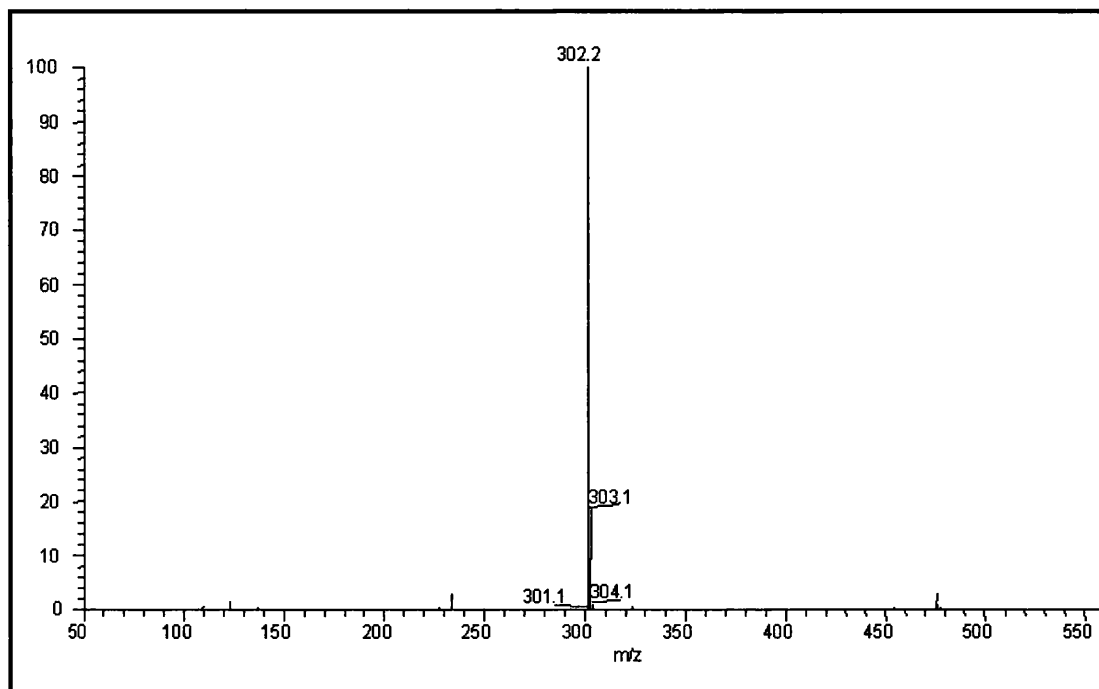


Figure 4.8(a) – Mass spectrum of 2,2'-difluoro isomer obtained under HPLC-MS conditions in positive mode APCI

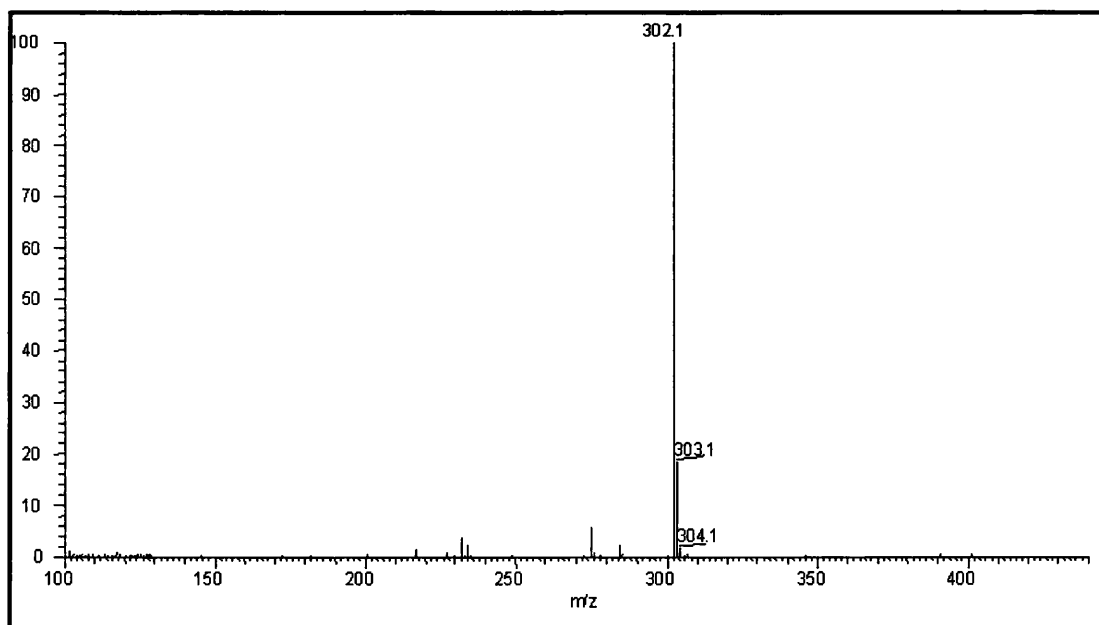


Figure 4.8(b) – Mass spectrum of triazol-4-yl isomer obtained under HPLC-MS conditions in positive mode APCI

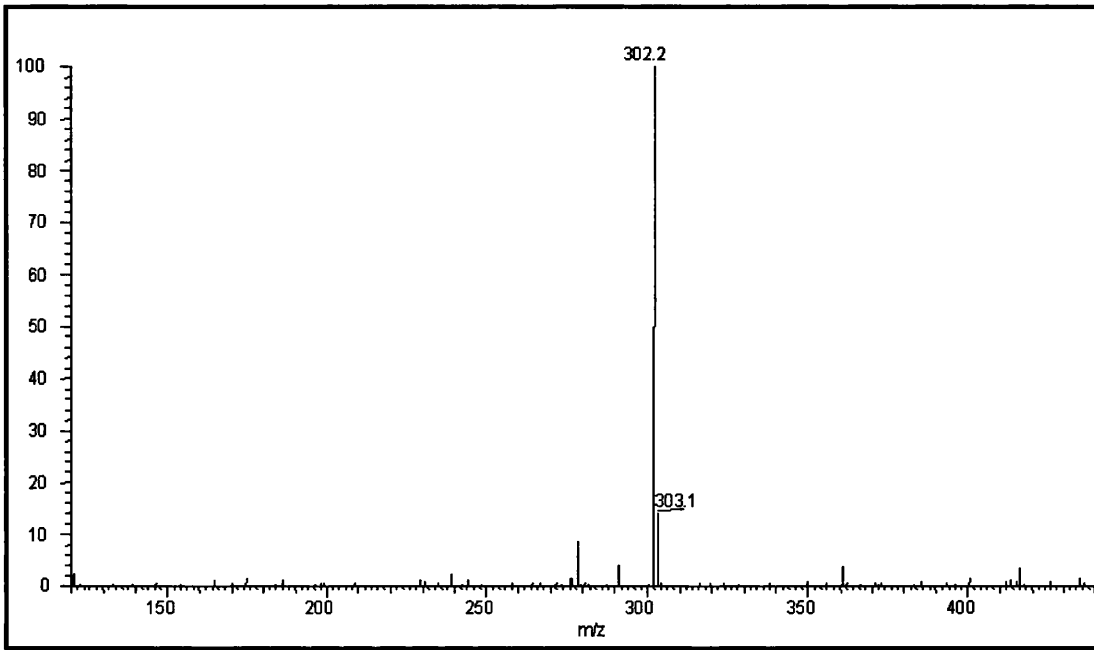


Figure 4.8(c) – Mass spectrum of flutriafol obtained under HPLC-MS conditions in positive mode APCI

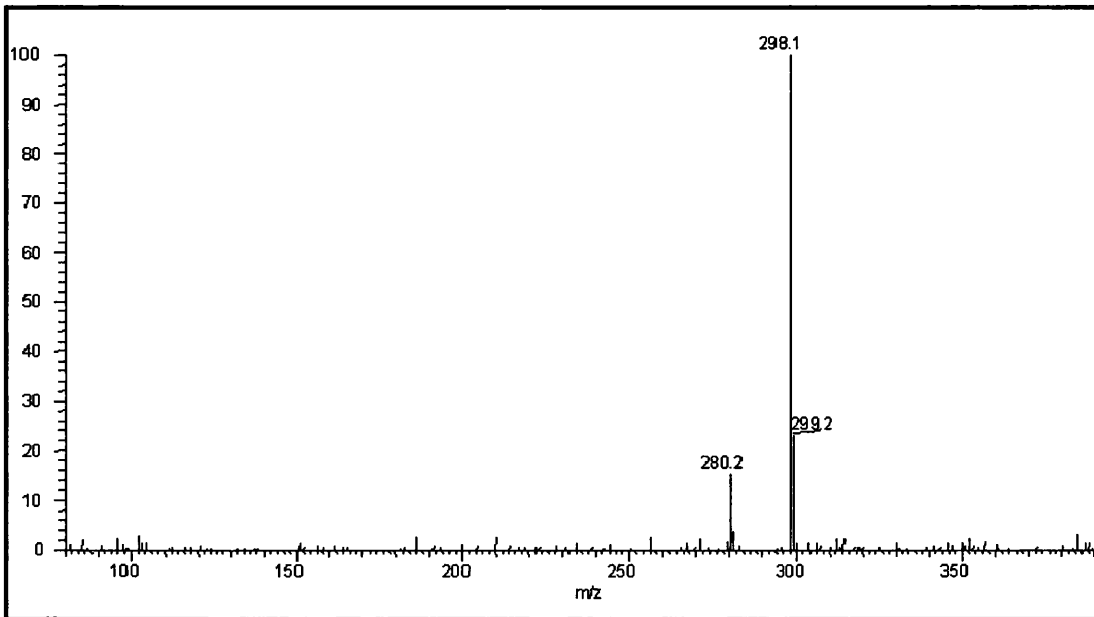


Figure 4.8(d) – Mass spectrum of methyl tertiary alcohol obtained under HPLC-MS conditions in positive mode APCI

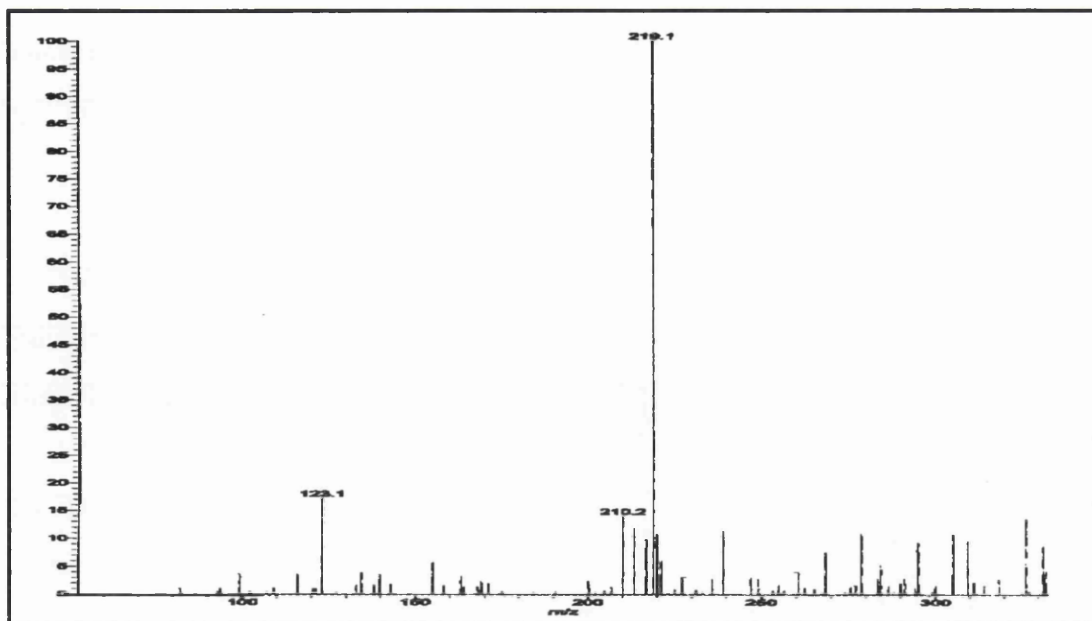


Figure 4.8(e) – Mass spectrum of 2,4'-difluorobenzophenone obtained under HPLC-MS conditions in positive mode APCI

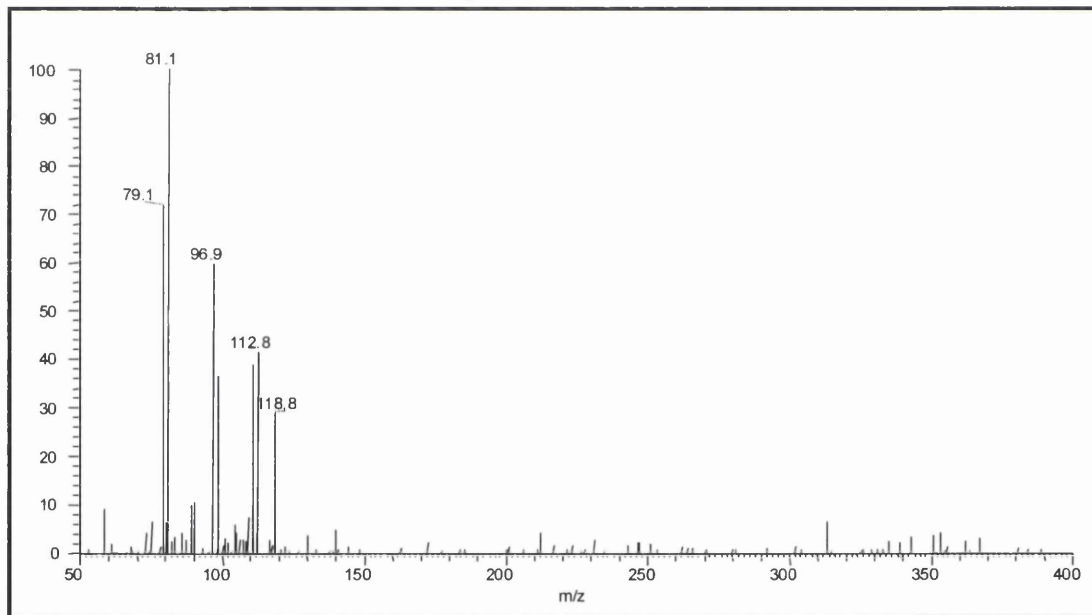


Figure 4.8(f) – Mass spectrum of bromoalkene (trans) obtained under HPLC-MS conditions in negative mode APCI

Analyte	M _r	Ion Observed	Species
2,2'-Difluoro isomer	301	302 ₍₁₀₀₎ 284 ₍₂₂₎ 234 ₍₁₉₎	[M+H] ⁺ [MH-H ₂ O] ⁺ [M-C ₂ N ₃ H] ⁺
Triazol-4-yl	301	302 ₍₁₀₀₎	[M+H] ⁺
Flutriafol	301	302 ₍₁₀₀₎	[M+H] ⁺
Methyl tertiary alcohol	297	298 ₍₁₀₀₎ 280 ₍₁₅₎	[M+H] ⁺ [MH-H ₂ O] ⁺
2,4'-Difluorobenzophenone	218	219 ₍₁₀₀₎	[M+H] ⁺
Bromoalkene (trans) (-ve)	295 (294/ 296)	111 ₍₃₈₎ 113 ₍₄₀₎ 99 ₍₃₇₎ 97 ₍₆₂₎ 81 ₍₁₀₀₎ 79 ₍₇₂₎	⁸¹ Br ⁻ ⁷⁹ Br ⁻
Bromoalkene (cis)	295	—	—

Table 4.13 - Summary of HPLC-MS data for each of the study compounds

4.7.2.4 – Limits of detection (LOD) for flutriafol and related impurities

Using Equation 3.14, the LOD for each of the seven study compounds was determined based on a signal-to-noise ratio of 3:1.

	APCI Positive Ion		APCI Negative Ion		ESI Positive Ion
	Full Scan	SIM	Full Scan	SIM	Full Scan
2,2'-Difluoro isomer	0.48ng	88pg	0.31ng	—	19.7ng
Triazol-4-yl	4.69ng	56pg	0.66ng	—	—
Flutriafol	12ng	0.17ng	2.59ng	—	10ng
Methyl tertiary alcohol	17.4ng	0.52ng	9.54ng	0.17ng	70.6ng
2,4'-Difluorobenzophenone	129ng	11.7ng	188ng	—	51.2ng
Bromoalkene (trans)	54.5ng	—	50ng	—	—
Bromoalkene (cis)	25ng	—	—	—	278ng

Table 4.14 – Limits of detection (LOD) for flutriafol and related impurities by HPLC-MS

It can be seen that in full scan mode mass spectrometric detection offers little or no improvement in limits of detection when compared with those obtained for the study compounds in the off-line experiments with UV detection. Indeed, the limits of detection obtained for three of the components were significantly worse in the HPLC-MS study as a result of their poor ionisation. As expected, the greater selectivity offered with the use of single ion monitoring (SIM), resulted in improvements in detection limits.

Where possible, the linearity of response was determined with a series of injections of varying volumes, again this was not possible for either of the bromoalkene compounds or the 2,4'-difluorobenzophenone as the response was consistently poor and unreliable. Response was plotted against the on-column sample amount, using Microsoft Excel, to produce a series of linearity graphs and the R² correlation coefficient was determined. The R² values for each of the compounds are summarised in Table 4.15 and the linearity graphs are shown in Figures 4.9(a)-(d).

	R²
2,2'-Difluoro Isomer	0.995
Triazol-4-yl	0.990
Flutriafol	0.997
2,4'-Difluorobenzophenone	1.000

Table 4.15 – Linear regression coefficients for data in Figures 4.9(a)-(d)

For each of the four compounds the response was reasonably linear over the plotted range with R² values greater than 0.99 in each case.

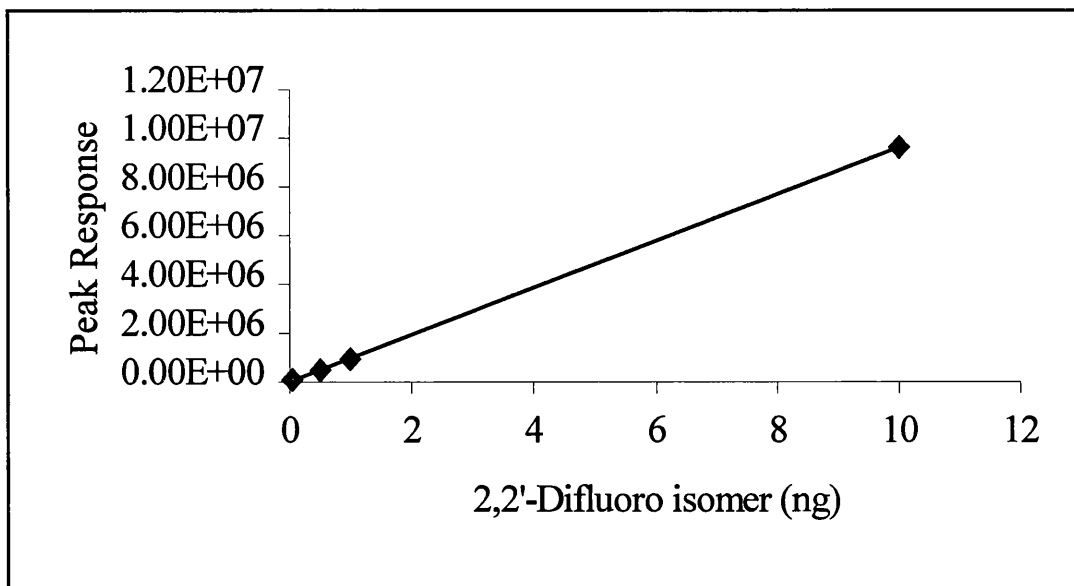


Figure 4.9(a) – Linearity of response for 2,2'-Difluoro Isomer in APCI positive mode

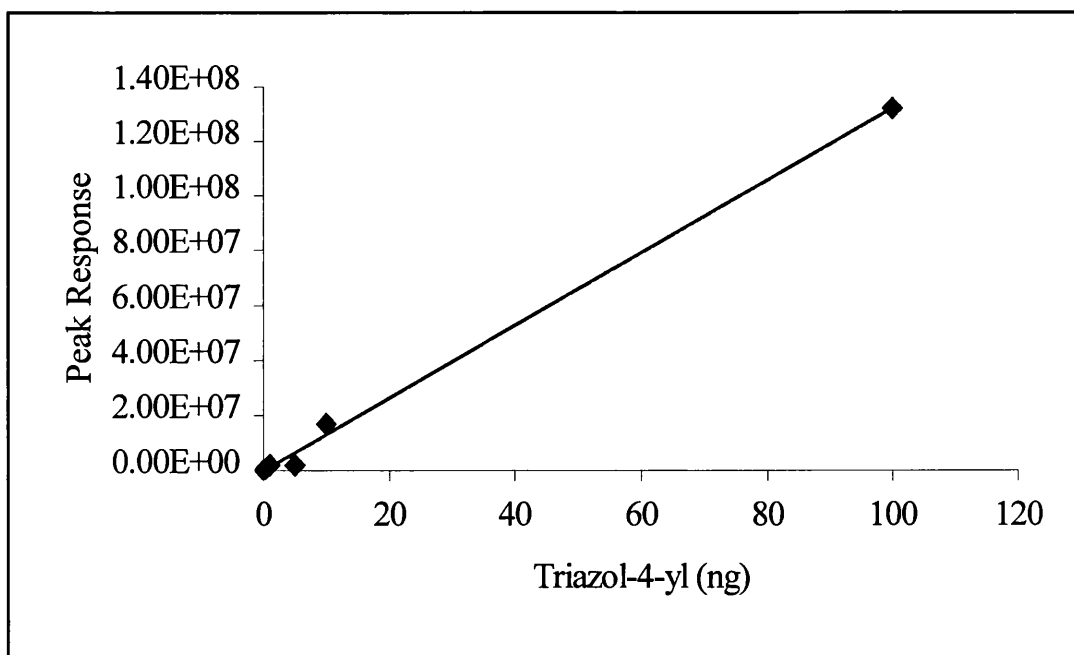


Figure 4.9(b) - Linearity of response for Triazol-4-yl in APCI positive mode

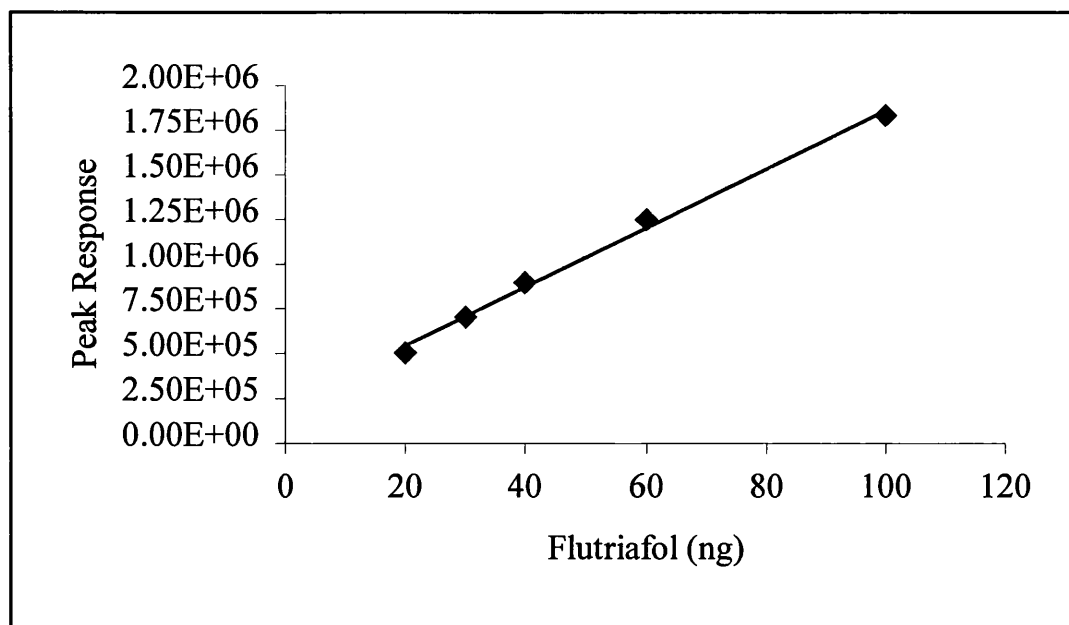


Figure 4.9(c) - Linearity of response for Flutriafol in APCI positive mode

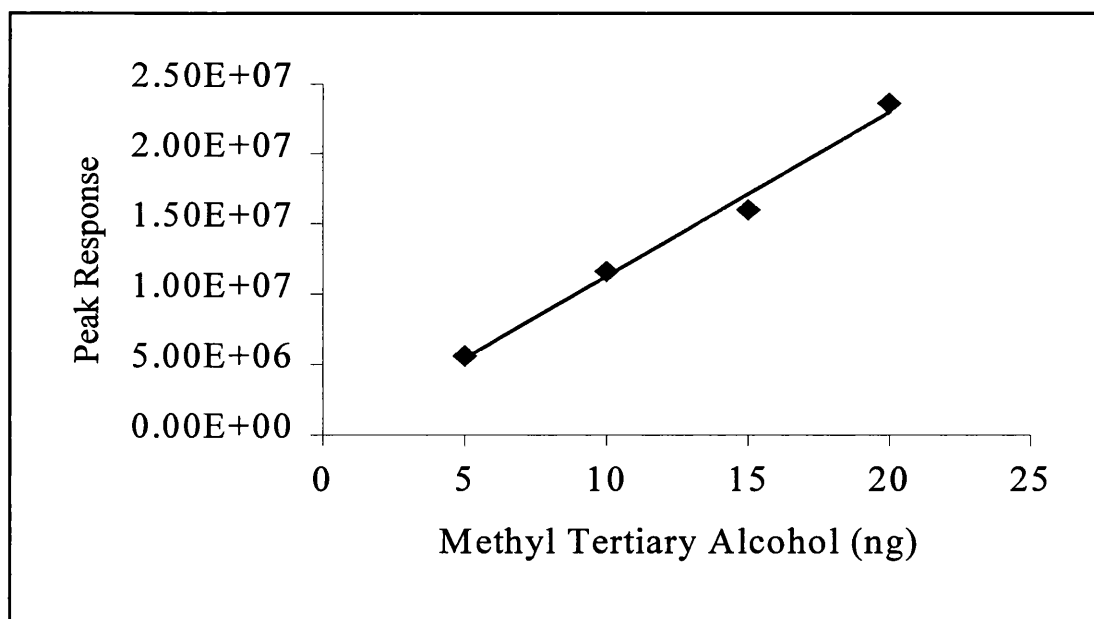


Figure 4.9(d) - Linearity of response for Methyl Tertiary Alcohol in APCI positive mode

4.7.2.5 – Tandem Mass Spectrometry (MSⁿ)

The technique of tandem mass spectrometry was used to obtain additional information relating to the structure and fragmentation of each of the seven study compounds. The information was used, where possible, to perform selected reaction monitoring (SRM) and consecutive reaction monitoring (CRM) experiments in order to further improve sensitivity and detection limits.

The data obtained in the initial MSⁿ experiments is summarised in Table 4.16 and proposed fragmentation pathways are outlined in Figures 4.10(a)-(d).

	Precursor Ion	%ce	MS ² Ions	%ce	MS ³ Ions	%ce	MS ⁴ Ions
2,2'-Difluoro isomer	302	15	233	13	109	—	—
					123	—	—
					137	12	109
Triazol-4-yl	302	14	233	15	109	—	—
					123	—	—
					137	12	109
Flutriafol	302	15	233	15	109	—	—
					123	—	—
					137	—	—
Methyl tertiary alcohol	298	14	229	15	105	—	—
					109	—	—
					133	—	—
					137	—	—
2,4'-Difluorobenzophenone	219	13	123	—	—	—	—
Bromoalkene (trans)	—	—	—	—	—	—	—
Bromoalkene (cis)	—	—	—	—	—	—	—

Table 4.16 – Summary of collision energies required and fragments generated in MSⁿ experiments

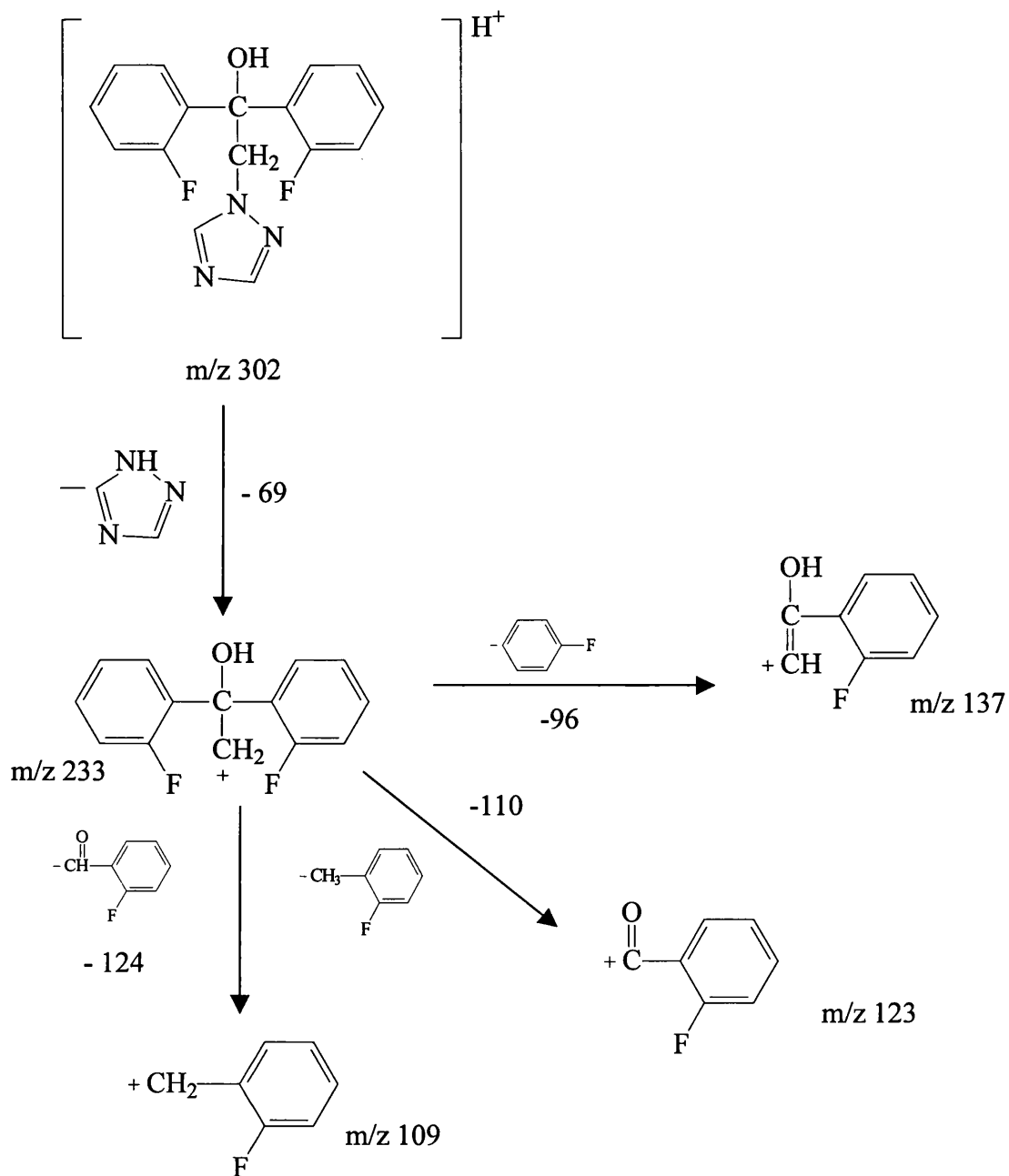


Figure 4.10(a) - Proposed mechanism for the fragmentation of 2,2'-difluoro isomer

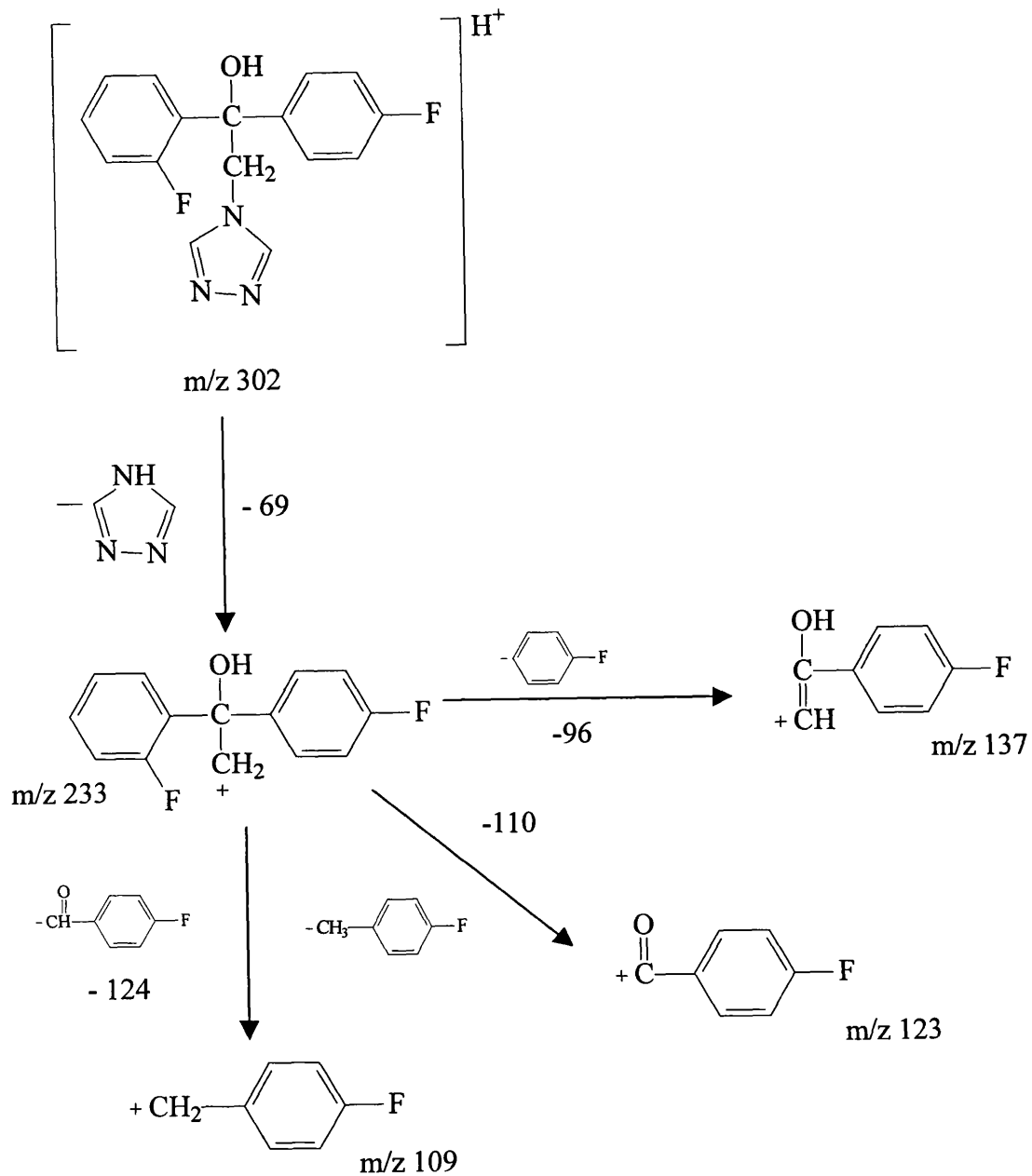


Figure 4.10(b) - Proposed mechanism for the fragmentation of triazol-4-yl

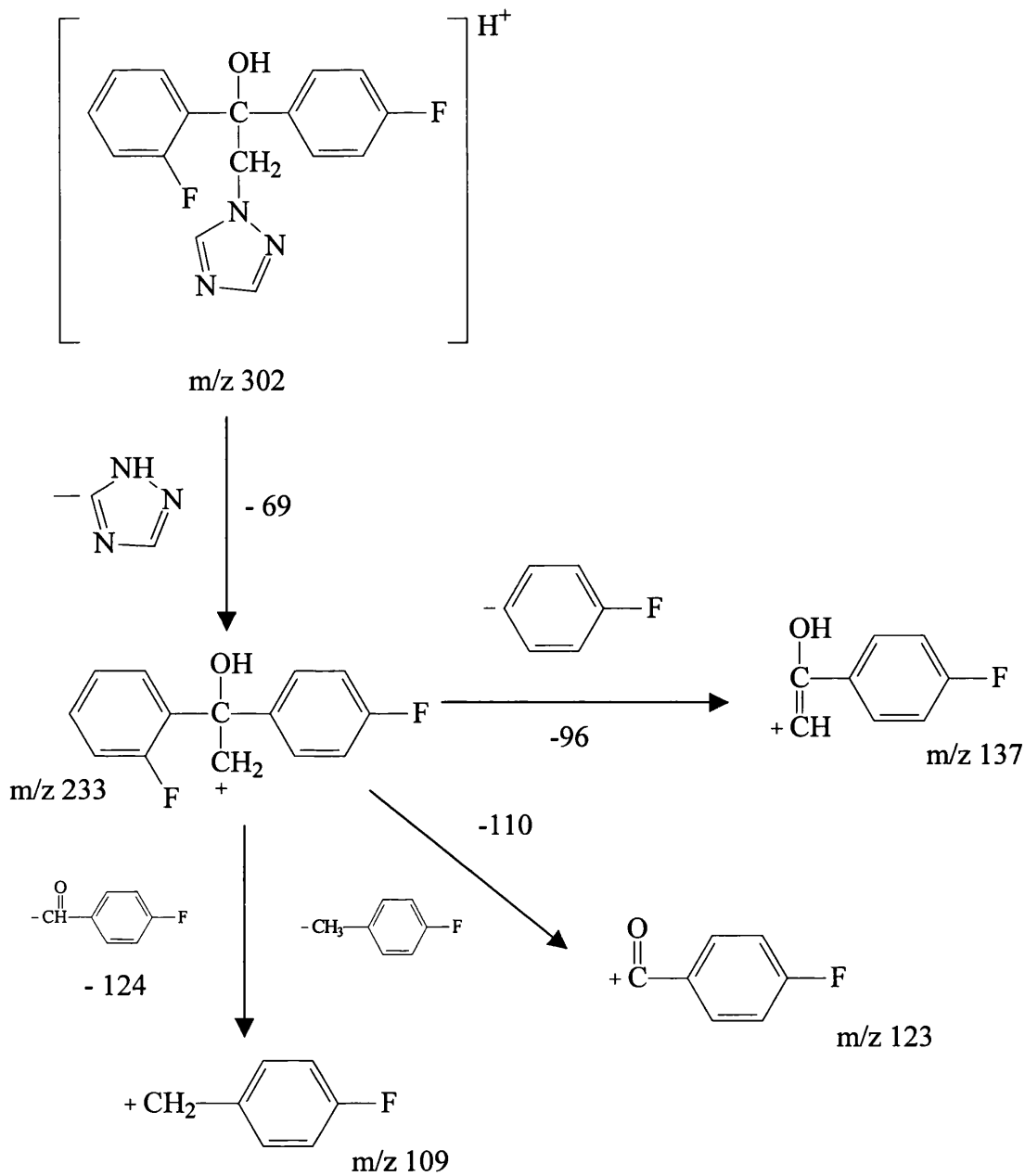


Figure 4.10(c) - Proposed mechanism for the fragmentation of flutriafol

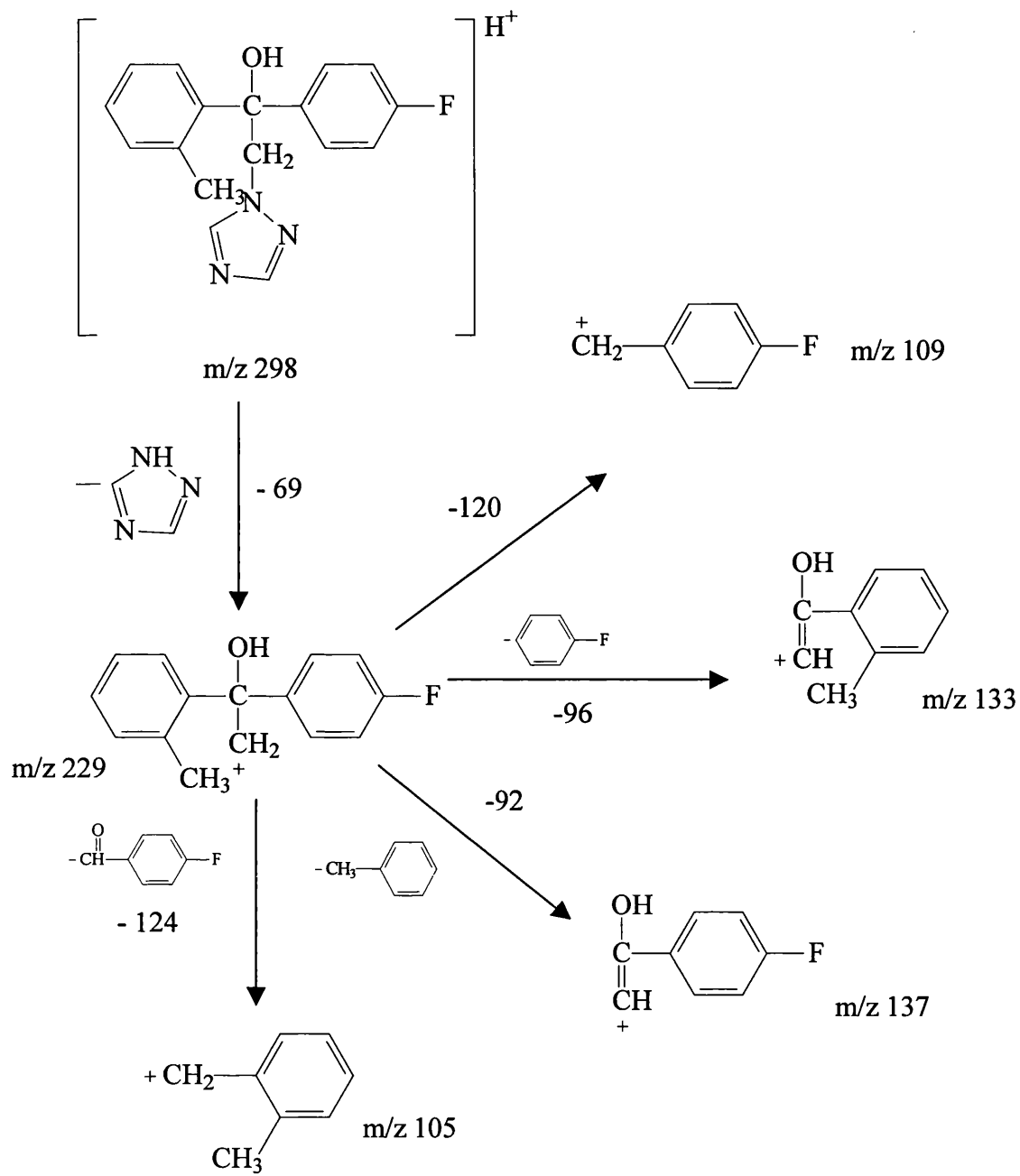


Figure 4.10(d) - Proposed mechanism for the fragmentation of methyl tertiary alcohol

As has been previously mentioned the information generated in the MSⁿ experiments was used to investigate the use of SRM and CRM. These modes of operation have been outlined in Sections 2.6.5 and 2.6.6 and are useful techniques for improving limits of detection. The detection limits obtained in this series of experiments are summarised in Table 4.17.

	SRM		CRM	
	Reaction Path	LOD	Reaction Path	LOD
2,2'-Difluoro Isomer	302 → 233	17.6pg	302 → 233 → 109/123 /137	14.7pg
Triazol-4-yl	302 → 233	8.1pg	302 → 233 → 109/123 /137	4.1pg
Flutriafol	302 → 233	38.9pg	—	—
Methyl Tertiary Alcohol	298 → 229	0.39ng	298 → 229 → 109	0.28ng
			298 → 229 → 105	0.26ng
			298 → 229 → 105/109 /133/137	0.12ng
2,4'-Difluorobenzophenone	—	—	—	—
Bromoalkene (trans)	—	—	—	—
Bromoalkene (cis)	—	—	—	—

Table 4.17 - Limits of detection (LOD) for flutriafol and related impurities by HPLC-MS using SRM and CRM

The data displayed in Table 4.17 demonstrates that both SRM and CRM were successful in improving the detection limits for each of the compounds analysed using these techniques. Although the signal intensity was observed to decrease with the increased number of reactions (i.e. increased n value), the accompanying increase in selectivity resulted in improved detection limits. The failure of the bromoalkene compounds and the 2,4'-difluorobenzophenone to produce consistent results in the original MS experiments meant that attempts to perform MSⁿ and subsequent SRM

and CRM experiments were unsuccessful. MSⁿ was attempted in the negative mode for the two bromoalkene compounds, as this mode of operation had previously proved more reliable, but again this was unsuccessful and no useful data was obtained.

4.7.2.6 – HPLC-MS of the seven component standard mixture

Having established the on-line retention times and determined mass spectral information for the majority of the seven study compounds the on-line separation of the seven component standard mixture was performed as a precursor to performing HPLC-MS of the technical sample. Figures 4.11(a) and (b) show the total ion chromatogram and mass chromatograms acquired in positive mode APCI using the instrumental conditions outlined previously in sections 4.7.1.3 and 4.7.2.1.

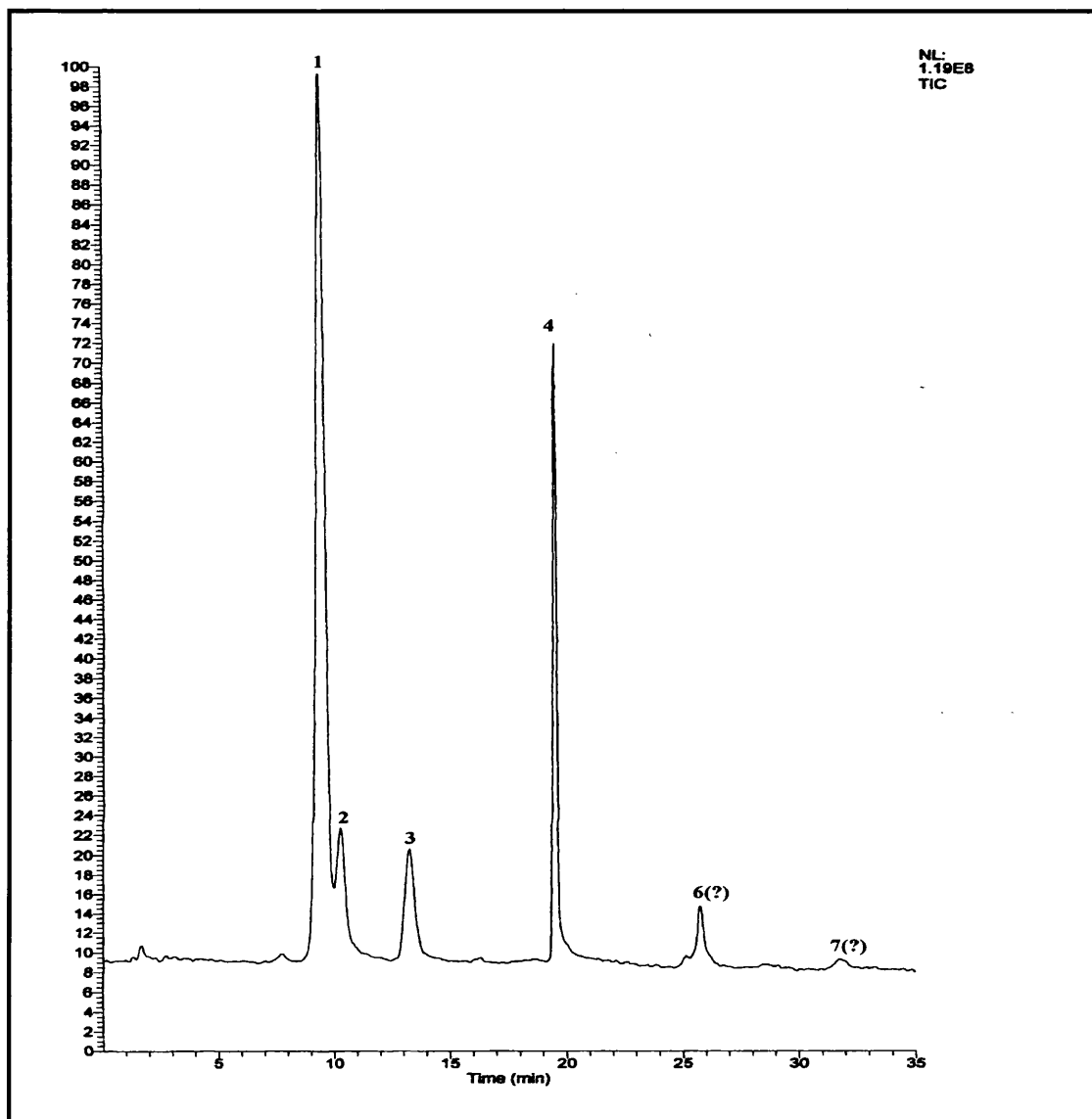


Figure 4.11(a) - TIC for a seven component flutriafol standard mixture obtained under HPLC-MS conditions in positive mode APCI

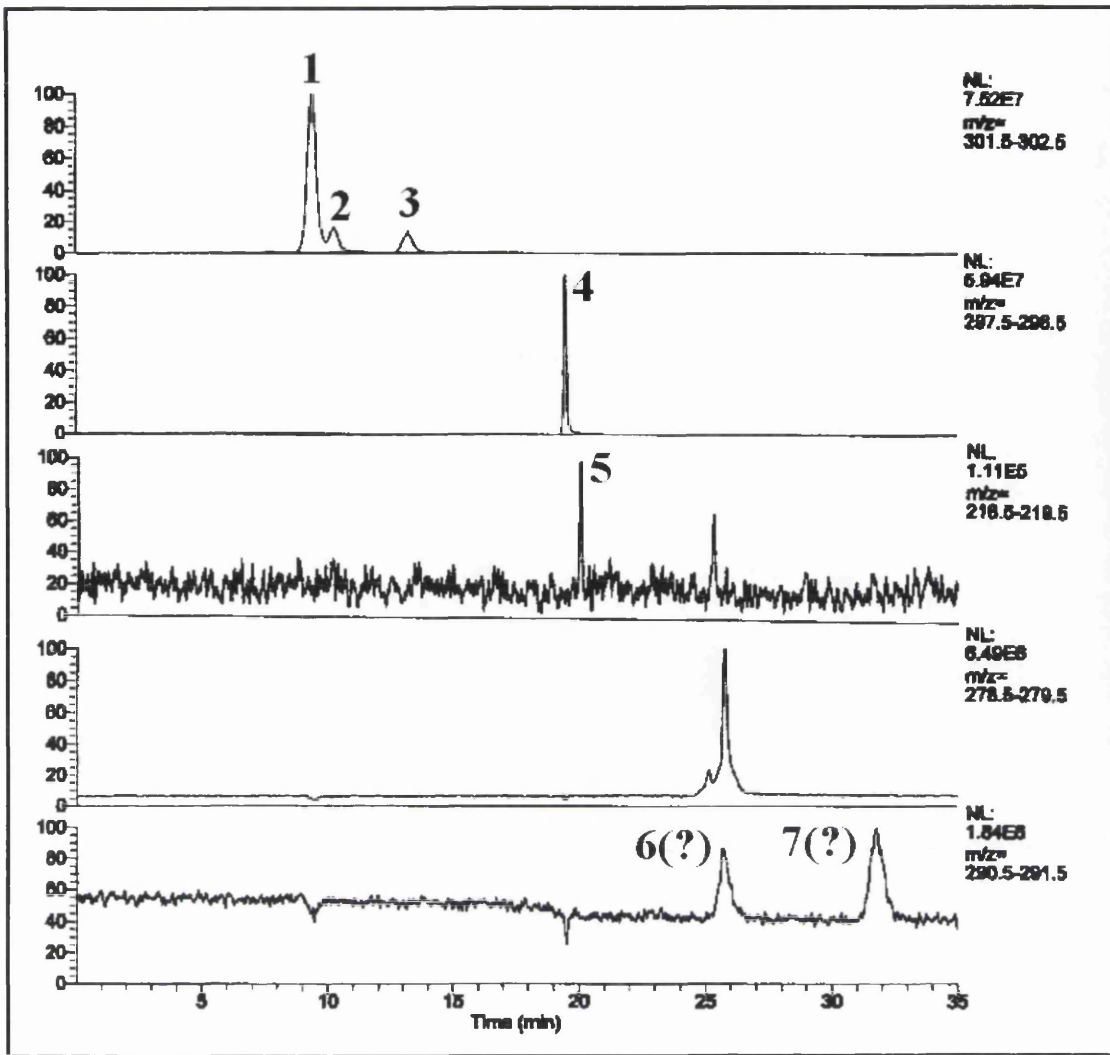


Figure 4.11(b) - Mass chromatograms for a seven component flutriafol standard mixture obtained under HPLC-MS conditions in positive mode APCI

It can be seen that six peaks are clearly visible in the TIC. The four most prominent peaks were found to correspond with the offline retention times and with the mass spectral data previously obtained for 2,2'-difluoro isomer, triazol-4-yl, flutriafol and methyl tertiary alcohol. No peak corresponding to 2,4'-difluorobenzophenone was observed in the TIC and the signal in the m/z 219 mass chromatogram is very weak. Although two peaks were observed in the TIC and in mass chromatograms for m/z 291 which corresponded approximately with the retention times of the two bromoalkene compounds, the mass spectra produced were not comparable with the previously obtained results. The low sensitivity for the bromoalkene compounds and 2,4'-difluorobenzophenone was as expected given the poor results obtained for the three components in the studies performed using the individual standards.

It was also observed that in comparison with the off-line HPLC chromatograms some resolution was lost, particularly in the separation of 2,2'-difluoro isomer and triazol-4-yl. In the UV chromatograms the components are baseline resolved whereas in the MS total ion chromatogram the triazol-4-yl peak is present as a shoulder on the 2,2'-difluoro isomer peak.

A limited amount of work was carried out using negative mode APCI with some success. In addition to the four peaks previously seen in the positive ion TIC, a fifth peak corresponding to 2,4'-difluorobenzophenone was also visible in the negative ion TIC. In line with the experiments performed using individual standards of the study compounds, the signal intensities achieved in negative mode for

flutriafol, triazol-4-yl, 2,2-difluoro isomer and methyl tertiary alcohol were lower than those obtained in positive mode APCI.

4.7.2.7 – HPLC-MS of flutriafol technical material

Having assessed the utility of HPLC-MS for the separation and analysis of the seven component standard mixture and previously used the off-line HPLC methodology for analysis of the flutriafol technical material, the HPLC-MS conditions were applied to the separation of the technical sample. In order to maximise the quantities of the trace impurities introduced into the mass spectrometer the LCQ's divert valve facility was employed. Rather than introducing the HPLC eluent directly into the source the flow was first introduced into the divert valve located on the front of the LCQ. The valve was configured to enable the switching of flow between the MS detector and waste following the procedure in the LCQ manual [28]. This facility can be controlled via the data system, but in this series of experiments, it was decided to operate the valve manually via a button on the front of the instrument as this mode of operation offered greater flexibility.

The technical flutriafol material was dissolved in methanol to produce a sample equivalent to 1mg/ml with respect to flutriafol. Injection volumes of up to 50 μ l were introduced onto the HPLC column and as the hugely overloaded flutriafol peak was eluted the divert valve was switched to waste. When elution was complete the valve was switched back so that the flow was again introduced into the mass spectrometer. This mode of operation minimises the risk of source contamination while increasing the quantities of trace components able to be introduced into the MS detector.

Initial experiments were performed using the gradient programme outlined in Section 4.7.1.3 but it was observed that on completion of the gradient peaks still appeared to be eluting. Consequently, the final time in the gradient programme was removed to allow analysis to continue until no further peaks were observed. Although these conditions had successfully separated the standard mixture in a reasonable time, the increased time of up to 60 minutes required for the analysis of the technical material was rather prohibitive. Consequently, the decision was made to revert to the use of the 10cm, 3 μ m column using the gradient programme outlined in Table 4.8. Again, this was modified to lengthen the analysis time and allow the elution and detection of the numerous late eluting impurities. However, the massive overloading of the flutriafol peak as a result of the high sample concentration and large injection volume resulted in the loss of resolution at the beginning of the separation which again necessitated adjustment of the gradient programme. The revised gradient programme is outlined below.

<u>Time (minutes)</u>	<u>%Methanol</u>
0	60
5	60
6	80
15	80
30	100
45	100

Figures 4.12(a) and (b) show the TIC and mass electropherograms obtained for a 30 μ l injection of the 1mg/ml sample in positive ion mode APCI and using the 10cm, 3 μ m Hypersil ODS column. The flow was diverted to waste from approximately 4 minutes to 9.5 minutes while elution of the flutriafol peak took

place. The mass spectral data for each of the peaks observed in the TIC is summarised in Table 4.18.

Peak No.	Retention Time (mins)	Ions observed
1	3.9	302 ₍₁₀₀₎ 232 ₍₁₈₎ 303 ₍₁₇₎ 284 ₍₁₀₎
2	9.4	302 ₍₁₀₀₎ 284 ₍₃₃₎ 303 ₍₁₈₎
3	14.1	302 ₍₁₀₀₎ 298 ₍₅₇₎ 280 ₍₃₉₎ 303 ₍₁₈₎ 284 ₍₃₅₎ 316 ₍₁₃₎
4	15.0	302 ₍₁₀₀₎ 303 ₍₁₆₎ 284 ₍₆₈₎ 244 ₍₄₆₎ 391 ₍₁₀₎
5	16.7	314 ₍₁₀₀₎ 316 ₍₇₀₎ 302 ₍₉₅₎ 502 ₍₆₇₎
6	17.5	314 ₍₁₀₀₎ 316 ₍₇₁₎ 302 ₍₂₃₎
7	18.3	279 ₍₁₀₀₎ 507 ₍₃₈₎ 302 ₍₂₄₎ 232 ₍₁₇₎
8	19.7	302 ₍₁₀₀₎ 279 ₍₆₇₎ 491 ₍₅₅₎ 391 ₍₂₇₎ 490 ₍₂₅₎ 492 ₍₂₁₎
9	22.2	489 ₍₁₀₀₎ 232 ₍₇₈₎ 490 ₍₂₈₎ 233 ₍₁₁₎
10	23.0	489 ₍₁₀₀₎ 232 ₍₇₇₎ 490 ₍₃₂₎ 233 ₍₁₃₎
11	23.8	489 ₍₁₀₀₎ 232 ₍₈₀₎ 490 ₍₃₉₎ 233 ₍₁₂₎
12	26.2	485 ₍₁₀₀₎ 232 ₍₅₃₎ 486 ₍₃₅₎ 228 ₍₃₄₎
13	27.7	485 ₍₁₀₀₎ 232 ₍₂₉₎ 486 ₍₃₅₎ 228 ₍₃₉₎
14	28.6	315 ₍₁₀₀₎ 332 ₍₄₄₎
15	29.6	256 ₍₁₀₀₎ 279 ₍₅₇₎
16	30.1	282 ₍₁₀₀₎ 283 ₍₂₁₎ 279 ₍₁₃₎ 256 ₍₁₁₎
17	31.5	391 ₍₁₀₀₎ 392 ₍₂₄₎ 371 ₍₁₀₎
18	32.2	391 ₍₁₀₀₎ 419 ₍₉₆₎ 401 ₍₃₂₎ 420 ₍₂₉₎ 338 ₍₂₁₎
19	32.7	447 ₍₁₀₀₎ 448 ₍₃₄₎ 391 ₍₃₄₎ 385 ₍₂₃₎ 367 ₍₁₃₎
20	34.1	391 ₍₁₀₀₎ 427 ₍₉₇₎ 409 ₍₄₃₎ 428 ₍₃₈₎ 312 ₍₂₉₎
21	35.1	391 ₍₁₀₀₎ 369 ₍₅₇₎
22	35.4	391 ₍₁₀₀₎ 490 ₍₆₅₎ 473 ₍₄₇₎
23	36.5	391 ₍₁₀₀₎ 584 ₍₆₀₎ 549 ₍₅₂₎
24	38.1	411 ₍₁₀₀₎ 391 ₍₃₈₎ 412 ₍₃₂₎ 440 ₍₂₅₎

Table 4.18 – Summary of mass spectral data obtained for flutriafol technical material in positive mode APCI

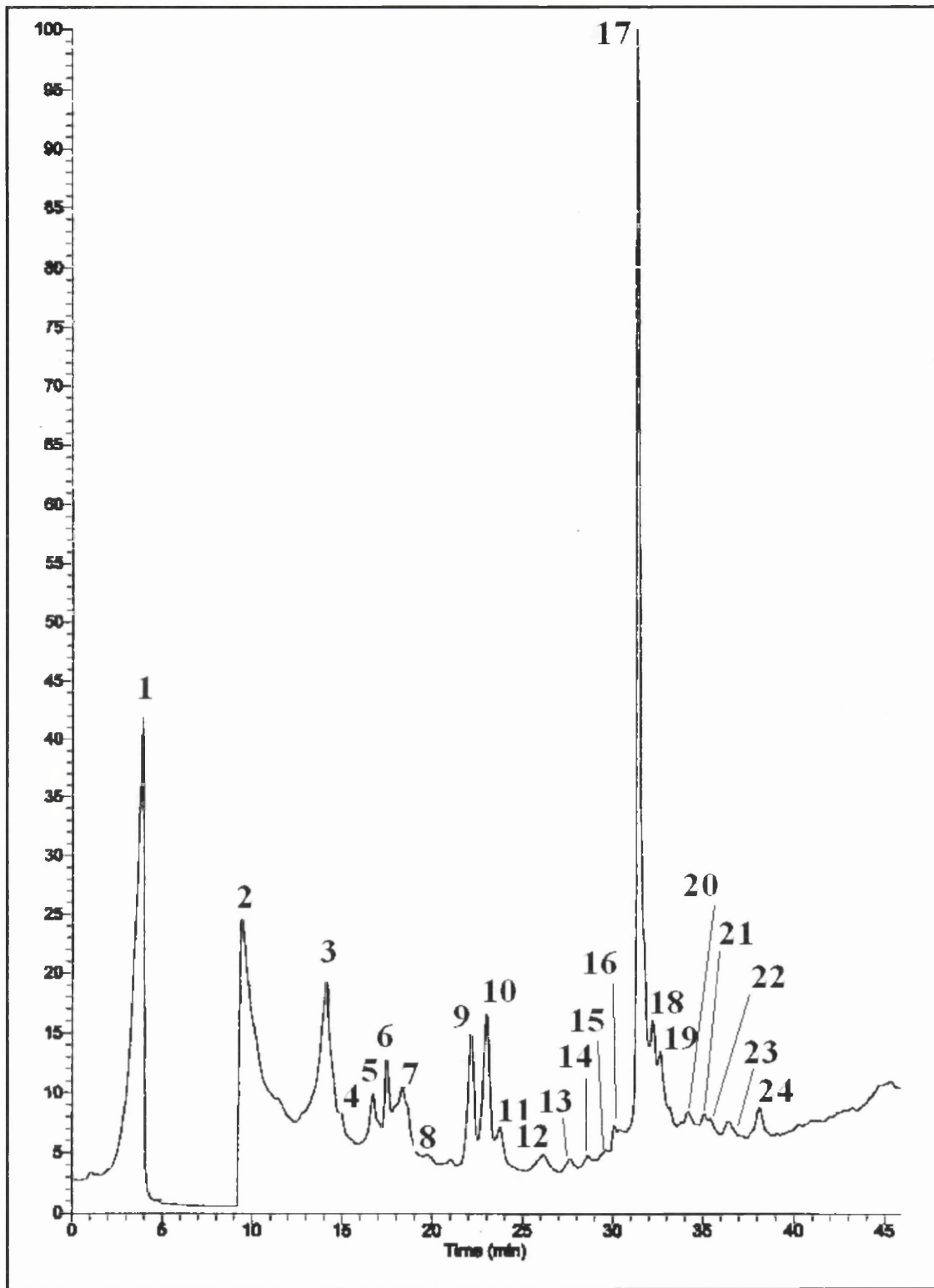


Figure 4.12(a) - TIC for sample of flutriafol technical material obtained under HPLC-MS conditions in positive mode APCI

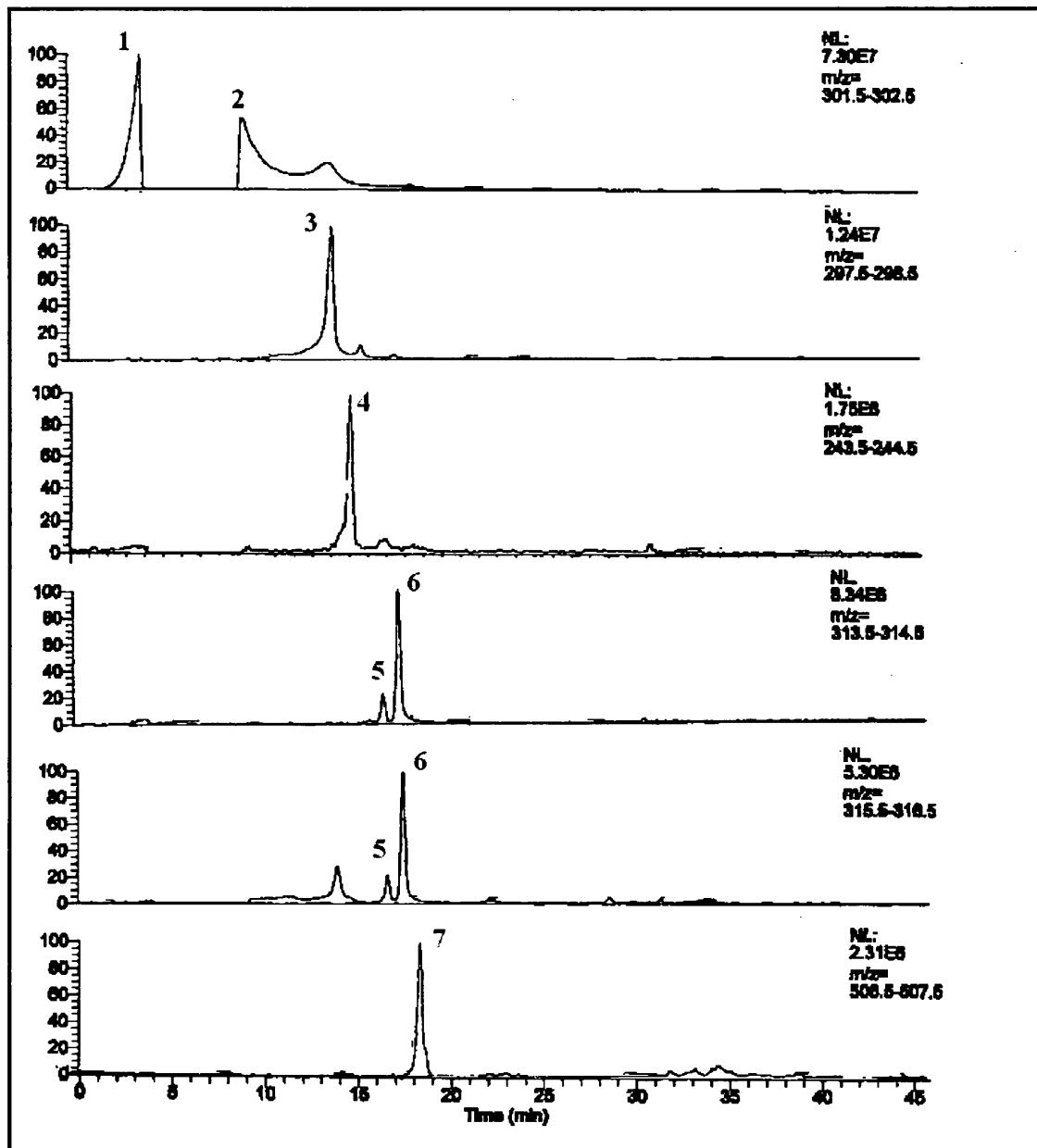


Figure 4.12(b) - Mass chromatograms for a sample of flutriafol technical material obtained under HPLC-MS conditions in positive mode APCI

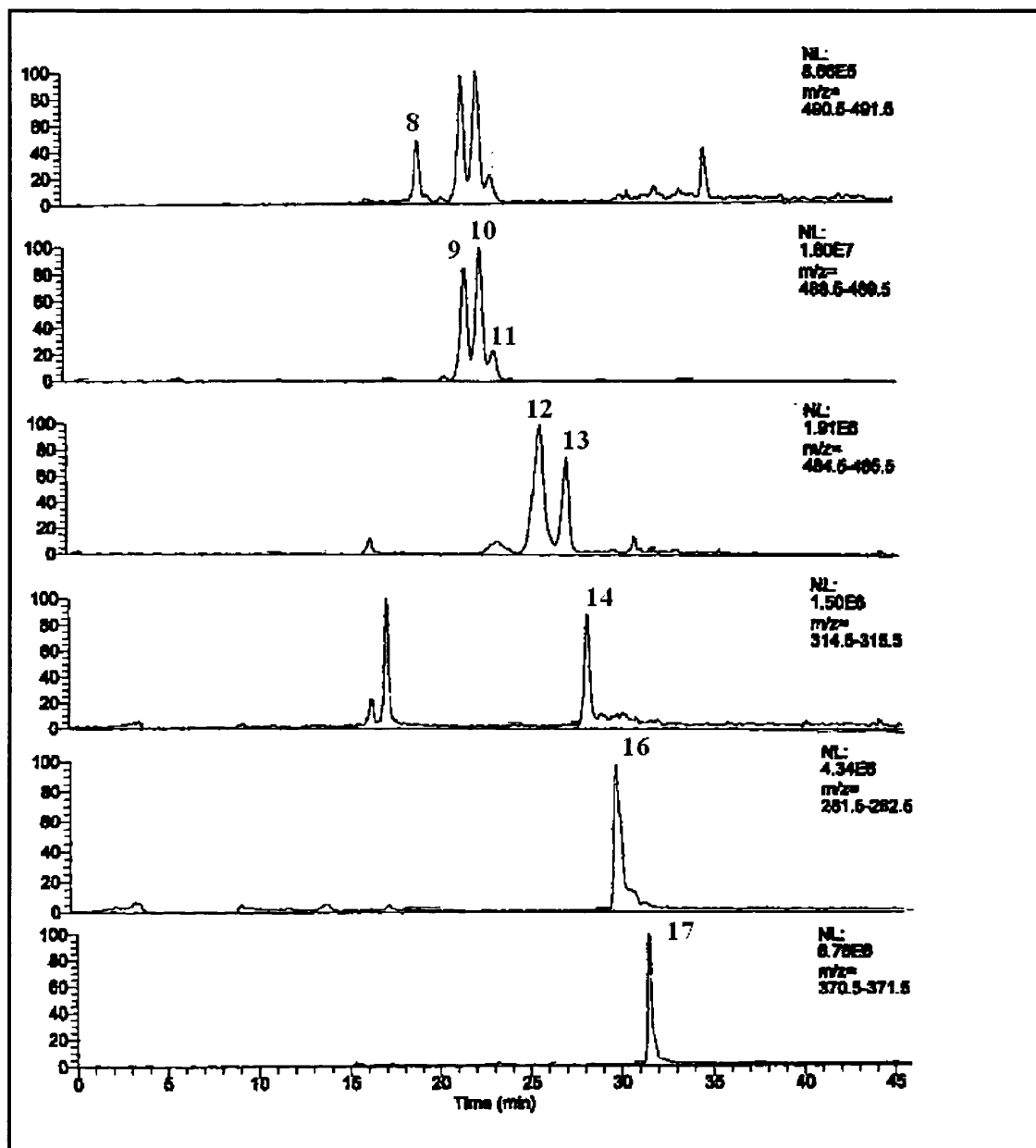


Figure 4.12(b) (continued) - Mass chromatograms for a sample of flutriafol technical material obtained under HPLC-MS conditions in positive mode APCI

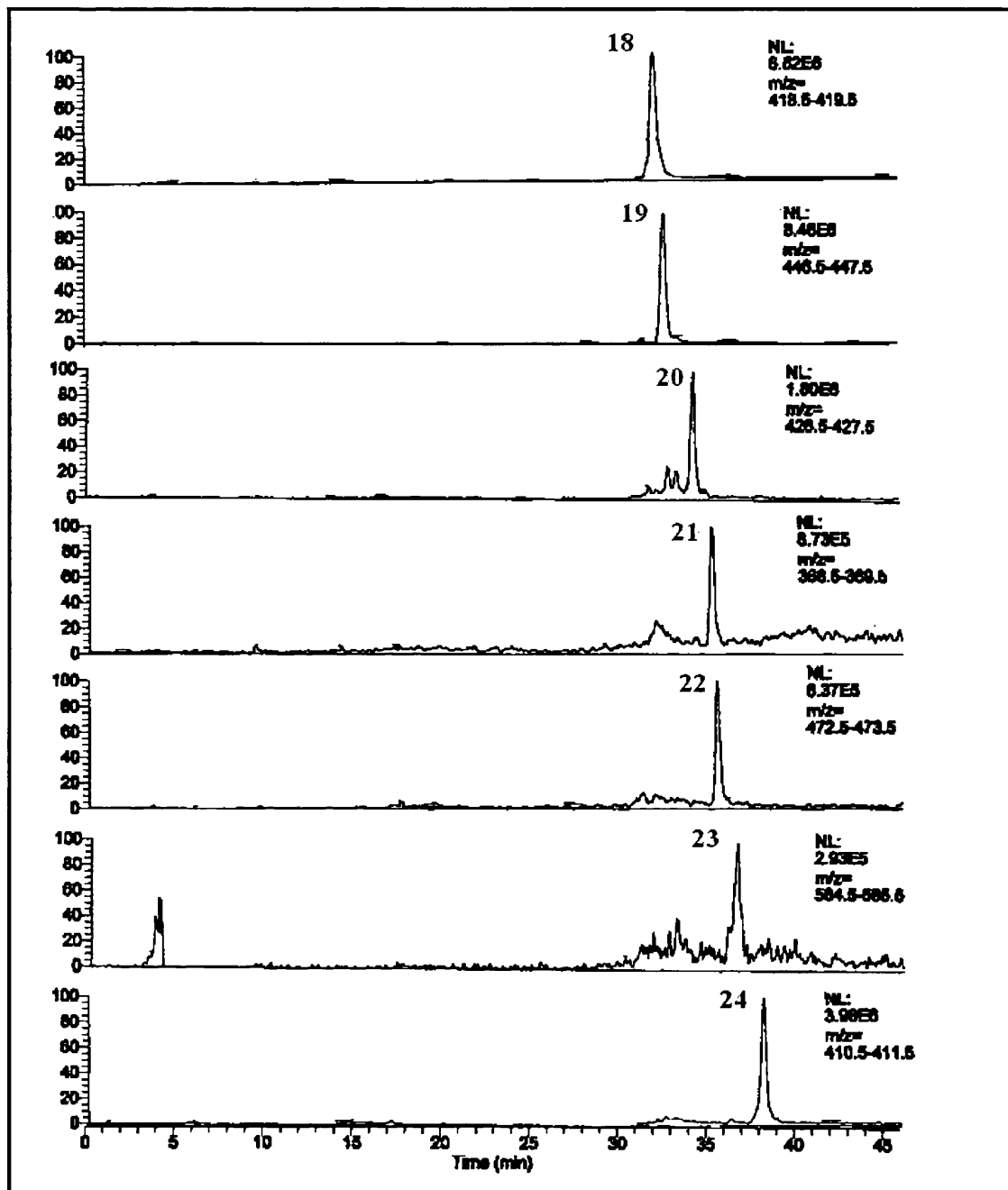


Figure 4.12(b) (continued) - Mass chromatograms for a sample of flutriafol technical material obtained under HPLC-MS conditions in positive mode APCI

In order to obtain further structural information for the numerous unidentified impurities, tandem MS was attempted. The Experimental Method facility on the LCQ operating system was used to set up a series of scan events over appropriate intervals. Unfortunately the number of peaks detected and the lengthy run time meant that the method was rather complex. Consequently, no useful information was obtained as it was difficult to find the appropriate collision energy setting as the lengthy run time was not conducive to the rapid turnaround of required when attempting to develop and optimise the MSⁿ experimental conditions. Based on the limited mass spectral information available some peaks were tentatively identified and in other cases some structural information was ascertained.

- Peaks 1 and 2

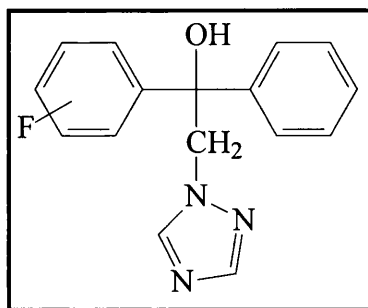
The presence of peaks at m/z 302 and the retention times obtained correspond with 2,2'-difluoro isomer, flutriafol and triazol-4-yl. Because the flutriafol peak was so overloaded resolution of these peaks was lost and it is probable that all three components were diverted to waste and the 'peaks' observed are merely the front and the tail of this unresolved mixture.

- Peak 3

Although the most abundant ion at this time is m/z 302 it is suspected that this is carried over from the flutriafol and therefore the next most abundant ion is m/z 298. This presence of this ion and the relative retention time of the peak correspond with methyl tertiary alcohol.

- Peak 4

Again it is thought that the intense signal at m/z 302 is the result of flutriafol carry over and that the m/z 284 peak corresponds to the $[M+H]^+$ ion. Based on these assumptions the peak has been tentatively assigned as being due to the monofluorinated compound shown below.



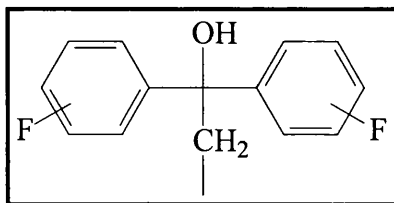
- Peaks 5 and 6

The mass spectra obtained for each of these peaks contain signals typical of brominated compounds. As has been previously described, the mass spectra of bromine containing compounds typically contain two signals separated by two mass units in an approximately 1:1 ratio. These peaks have been tentatively identified as trifluorinated bromoalkene compounds.

- Peaks 9-13

Although it has not been possible to identify any possible structures for these components the similarities in the mass spectra for each of these peaks would appear to indicate that there are also similarities in the structures of the compounds. The components producing peaks 9,10 and 11 are assumed to be isomers as are the components resulting in peaks 12 and 13. It is suspected that the difference of 4 mass units between each set of isomers is due to the presence of a fluorine atom in the first set of compounds where a methyl group is present

in the second. The presence of signals at m/z 232 and 233 would appear to indicate the presence of the structure shown below.



- Peaks 17-19

Although no definite similarities were noted in the mass spectra corresponding to peaks 17, 18 and 19, it was noted that there was a difference of 28 mass units between the assumed $[M+H]^+$ ion for each component. This may indicate that these components are part of a series.

The identification of the remaining components was more difficult as no similarities with the spectra of the known impurities were observed and without the additional information provided by tandem mass spectrometry little or no structural information was available.

It was noted that although peaks corresponding to 2,4'-difluorobenzophenone and the two bromoalkene compounds had been observed in the UV trace for the technical flutriafol material no signals corresponding to these impurities were observed in the TIC. This was predictable given the poor results achieved for these compounds in the previous positive ion experiments.

4.8 – CONCLUSION

HPLC is a widely available technique which has proved to be invaluable in the analysis of industrially significant substances such as pharmaceuticals and agrochemicals. Modern instrumentation offers reliable and automated analysis and coupled with mass spectrometric detection it is potentially a highly sensitive and selective technique useful for the detection and characterisation of polar, ionic, thermally unstable, non-volatile compounds.

The technique of HPLC has been demonstrated to provide a suitable means of separating the fungicide flutriafol from a standard mixture of related impurity compounds. While, isocratic solvent systems were unable to provide adequate resolution of all seven study compounds in a reasonable analysis time, gradient elution was able to fully resolve each of the standard components in under 30 minutes. Limits of detection for each of the seven study compounds were determined and generally found to be in the low nanogram range for each component.

With a view to reducing analysis times, the use of shorter columns was investigated. It was found that while reducing the column length resulted in shorter run times the resulting decrease in efficiency was detrimental to the separation and resolution was lost. It was observed that a smaller particle size, offering increased efficiency, was necessary to maintain the separation in the shorter length columns. Separation of the seven study compounds was achieved in around 12 minutes using a 10cm column with 3 μ m packing, less than half the time required with the 25cm, 5 μ m column.

The methodology developed was successfully used in the analysis of a production sample of flutriafol. In addition to the six known related impurities, which were detected at levels of up to 13 percent (by area), about twenty other peaks were observed, the majority of which were present at lower levels than the named components.

Following the success of the off-line HPLC analysis the instrument was interfaced with the LCQ quadrupole ion trap mass spectrometer and work was performed in both APCI and ESI modes to determine the most suitable method of ionisation. Initial experiments demonstrated that for flutriafol, 2,2'-difluoro isomer, triazol-4-yl and methyl tertiary alcohol the signal intensities achieved were good in both ESI and APCI in positive ion mode, with the most abundant ion in each case corresponding to $[M+H]^+$. The ionisation of the three remaining study compounds was poor by comparison, although the use of negative ionisation appeared to be more promising.

Tandem mass spectrometry was performed to determine fragmentation, and where possible SRM and CRM were carried out. The increased selectivity resulting from the use of these modes of operation resulted in improved detection limits despite the decreased signal intensity.

Use of the divert valve facility on the LCQ allowed relatively large injection volumes of high concentration solutions of technical sample to be introduced into the mass spectrometer. Flow from the HPLC instrument was diverted to waste as the flutriafol peak was eluted and so minimising any potential problems associated with

introducing extremely high concentration levels of sample into the mass spectrometer, such as contamination of the source. This enabled greater concentrations of the low level impurities to be introduced, thereby improving their chances of detection and possible identification. Over twenty peaks were detected in the TIC and the mass spectral information obtained was used to tentatively identify a number of these components. Attempts to perform MSⁿ using the Experiment Method facility on the LCQ were unsuccessful and consequently the structural information available for many of the components was minimal and peak identification was not possible.

Further work should be performed, initially, to further validate the off-line HPLC method, which should be adapted to take into account the increased run time required for elution of the numerous impurities present in the technical material. Having determined the instrumental conditions capable of separating the mixture of flutriafol and related impurities the methodology should be assessed to determine its fitness for use. This procedure should take into account the linearity, repeatability, reproducibility and robustness of the method in order to obtain confidence in the results of the analysis. Successful validation of the method and some additional work could enable the method to be used quantitatively.

Further investigation of the use of different lengths, internal diameters and internal diameters of column should be investigated. The use of 10cm columns has already been investigated briefly and found to offer reduced analysis times. Shorter columns, between 3 and 10cm in length, are now widely available [30] and are used in the technique of Fast LC, which, as the name suggests, offers rapid analysis. It is

also reported that Fast LC offers greater sensitivity and better LC-MS compatibility [31]. These factors in combination with the additional benefits of low solvent consumption and rapid method development would appear to offer a promising area of investigation. The use of narrow bore columns in the technique of capillary liquid chromatography (CLC) also offers a potential area for further work. This technique employs columns between with internal diameters of less than 1mm and is reported to offer good sensitivity when operated with mass spectrometric detection [32].

The use of preparative HPLC or column chromatography may be useful as a means of isolating the numerous trace impurities detected in the flutriafol technical material. This would simplify the characterisation and identification of these compounds, enabling a more thorough examination of each by tandem mass spectrometry. The availability of further impurity standards would also enable further optimisation of the HPLC method.

Although a significant amount of work was performed using tandem mass spectrometric methods and the SIM, SRM and CRM modes of operation in positive mode APCI the work carried out in negative ion mode was minimal. Negative mode has already been demonstrated to be potentially useful in the detection of the bromoalkene compounds and 2,4'-difluorobenzophenone and it is likely that there are additional impurity components more amenable to negative ionisation present in the technical sample. It would therefore be beneficial to perform further work in this area and to optimise the conditions to enhance the reliability of ionisation of the three previously mentioned compounds.

Although tandem mass spectrometry was attempted for the flutriafol technical material it was largely unsuccessful. This is an obvious area for further work and the success of the previously mentioned areas of additional investigation would simplify this greatly. The shorter analysis times potentially available with the use of shorter columns would allow more rapid turnaround of analyses which would be beneficial in the development of experimental method conditions as would the availability of additional isolated impurity standards.

REFERENCES CITED IN CHAPTER 4

1. Pesticides. Joseph Sherma. *Anal. Chem.* **65**, (1993), 40R-54R
2. Pesticides. Joseph Sherma. *Anal. Chem.* **67**, (1995), 1R-20R
3. Chromatographic Methods. A Braithwaite and FJ Smith. Chapman and Hall. (1992). 1-10
4. High Performance Liquid Chromatography Fundamental Principles and Practice. Ed. WJ Lough and IW Wainer. Chapman and Hall. (1996)
5. Principles of Instrumental Analysis. Douglas A Skoog and James J Leary. Saunders College Publishing. (1992). 579-604
6. Introduction to Modern Liquid Chromatography. LR Snyder and JJ Kirkland. John Wiley and Sons Inc. (1979)
7. Instrumental Analysis. Charles K Mann, Thomas J Vickers and Wilson M Gulick. Harper and Row. (1974). 637-665
8. Instrumental Methods of Chemical Analysis. Galen W Ewing. McGraw Hill Book Company. (1985). 340-347
9. Chromatographic Methods. A Braithwaite and FJ Smith. Chapman and Hall. (1992). 11-23
10. Principles of Instrumental Analysis. Douglas A Skoog and James J Leary. Saunders College Publishing. (1992). 628-669
11. Chromatographic Methods. A Braithwaite and FJ Smith. Chapman and Hall. (1992). 212-290
12. Finnigan MAT: LCQ MS Detector Operator's and Service Manual
13. Introduction to Mass Spectrometry. J Throck Watson. Lippincott-Raven. (1997). 399-413

14. Mass Spectrometry for Chemists and Biochemists. Robert AW Johnstone and Malcolm E Rose. Cambridge University Press. (1996). 158-172
15. Mass Spectrometry: Analytical Chemistry by Open Learning. James Barker. John Wiley and Sons. (1999). 320-333
16. LC/MS Chapter G1.2. Back To Basics CD-ROM. Micromass UK Limited. (1999)
17. Atmospheric-pressure-ionization mass spectrometry, II. Applications in pharmacy, biochemistry and general chemistry. AP Bruins. *Trends Anal. Chem.* **13**, (1994), 81-90
18. Electrospray interface for LC-MS. CM Whitehouse, RN Dreyer, M Yamashita and JB Fenn. *Anal. Chem.* **57**, (1985), 675-679
19. Atmospheric Pressure Ionization (API) Mass Spectrometry. Solvent-Mediated Ionization of Samples Introduced in Solution and in a Liquid Chromatograph Effluent Stream. EC Horning, DI Carroll, I Dzidic, KD Haegele, MD Horning and RN Stillwell. *J. Chromatogr. Sci.* **12**, (1974), 725-729.
20. Atmospheric Pressure Ionization Mass Spectrometry: Corona Discharge Ion Source for use in Liquid Chromatography-Mass Spectrometer-Computer Analytical System. DI Carroll, I Dzidic, RN Stillwell, KD Haegele and EC Horning. *Anal. Chem.* **47**, (1975), 2369-2373
21. Mass Spectrometry with Ion Sources Operating at Atmospheric Pressure. AP Bruins. *Mass Spectrom. Rev.* **10**, (1991), 53-77
22. Atmospheric pressure ionisation mass spectrometry: detection for the separation sciences. EC Huang, JJ Conboy, T Wachs and JD Henion. *Anal. Chem.* **62**, (1990), 713A-725A

23. Using A Gradient Scouting Run To Get Started. John W Dolan. *LC.GC Int.* **9**, (1996), 130-136
24. Starting Out Right, Part 1 – Selecting the Tools. John W Dolan. *LC.GC Int.* **13**, (2000), 12-15
25. Spectroscopic methods in organic chemistry. Dudley H Williams and Ian Fleming. McGraw-Hill Book Company. (1989)
26. Interpretation of Mass Spectra. Fred W McLafferty and Frantisek Turecek. University Science Books. (1993)
27. Finnigan MAT: LCQ Getting Started With Your Applications Manual
28. ICH Harmonised Tripartite Guidance. Notes for guidance on the validation of analytical procedures: methodology (CPMP/ICH/281/95). The European Agency for the Evaluation of Medicinal Products, ICH, UK (1996)
29. Thermo Hypersil Product Catalogue
30. The Time Is Now For Fast LC. Michael Dong. *Today's Chemist at Work* **9**, (2000), 46-51
31. The Analysis of β -Blockers by Capillary Liquid Chromatography/Atmospheric Pressure Chemical Ionization Mass Spectrometry. Kathryn A Hutton and David E Games. *Rapid Commun. Mass Spectrom.* **11**, (1997), 735-744

Chapter 5

Experimental Details

This chapter provides details of the reagents, instrumentation and other experimental detail relating to the procedures and data presented in the preceding chapters of this thesis.

5.1 – CHAPTER 3

Samples and Standards

Individual standards of paraquat dichloride, 2,2-paraquat di-iodide, monoquat iodide, 2,2-bipyridyl, 4,4-bipyridyl and n-methyl pyridinium iodide were provided by Zeneca Agrochemicals, Bracknell, Berkshire, UK, as was a sample of technical paraquat.

Sample and Standard Preparation

Samples and standards were prepared by dissolution of an appropriate amount of material in either HPLC grade water or CE buffer solution depending on the application. Subsequent dilutions were performed using Gilson Pipetman dispensers. All samples and standards were filtered through 0.2 μ m nylon syringe filters from Phenomenex, Torrance, CA, USA.

Analytical Reagents

HPLC grade water and methanol were supplied by Fisher Scientific, Loughborough, Leicestershire, UK.

AnalaR grade ammonium acetate, sodium chloride and sodium acetate were purchased from BDH, Poole, Dorset, UK.

Glacial acetic acid (99.99+ %) and β -alanine were purchased from Aldrich.

Buffer Preparation

All CE buffers were prepared by dissolving appropriate amounts of the relevant salts in HPLC grade water (and methanol where appropriate). The pH of the buffers was adjusted with the addition of glacial acetic acid using a Beckman Φ 20 pH meter. All CE buffers were filtered using 0.2 μ m nylon syringe filters available from Phenomenex.

Capillaries

Fused silica capillaries (50 μ m id, 365 μ m od) were obtained from Composite Metal Services Ltd, Hallow, Worcestershire, UK.

Hydrophilic CElect P150 capillaries (50 μ m id, 363 μ m od) were purchased from Supelco, Poole, Dorset, UK.

MicroSolv CE Deactivated fused silica capillaries (50 μ m id, 330 μ m od) were supplied by AECS, Bridgend, UK.

The standard fused silica capillaries were conditioned prior to use, between analyses and before storage with 0.1M sodium hydroxide followed by HPLC grade water (and CE buffer where necessary).

Instrumentation – CE

A Beckman P/ACE 2200 CE system incorporating a multi-wavelength UV detector from Beckman Instruments, High Wycombe, Buckinghamshire, UK was used throughout. A cylinder of compressed air from BOC, Guildford, Surrey, UK was connected to the instrument and regulated at a pressure of 85psi to facilitate the filling and flushing of the capillary.

Samples, standards, buffers and rinsing solutions were contained in 4.5ml vials.

Sample introduction was performed either by application of 0.5psi pressure, or by applying a voltage of up to 5kV across the capillary.

The separation capillary is coiled around a spool and held in a sealed, temperature controlled cartridge through which Fluorinert FC-77 electronic liquid coolant (3M, Manchester, UK) flows in order to maintain a steady temperature.

The data handling system used to control the instrument and record data was Beckman System Gold version 8.1 which was installed on an IBM PS/2 PC.

Instrumentation – MS

CE-MS was performed using the Beckman P/ACE system coupled to a Finnigan LCQ quadrupole ion trap mass spectrometer (Finnigan, Hemel Hempstead, Hertfordshire, UK).

Oxygen-free nitrogen was used as the sheath and auxiliary gas and helium was used as the damping/collision gas, both were supplied by BOC.

Modifications were made to the standard Finnigan ESI interface to accommodate the CE capillary; these modifications are covered in detail in section 3.6.3.

A sheath liquid composed of 90% HPLC grade methanol (Fisher) and 10% 0.01M acetic acid (Aldrich) was contained within a Hamilton syringe and delivered via a length of Teflon tubing to the electrospray source by the LCQ's integrated syringe pump.

The instrument was controlled by the Navigator data system using the Microsoft Windows NT operating system installed on a Gateway 2000 P5-120 PC.

5.2– CHAPTER 4

Samples and Standards

Individual standards of flutriafol, triazol-4-yl, 2,4-difluorobenzophenone, 2,2-difluoro isomer, methyl tertiary alcohol, bromoalkene (cis) and bromoalkene (trans) were provided by Zeneca Agrochemicals, Bracknell, Berkshire, UK, as was a sample of technical flutriafol.

Sample and Standard Preparation

Samples and standards were prepared by dissolution of an appropriate amount of material in either HPLC grade methanol. Subsequent dilutions were performed using Gilson Pipetman dispensers. All samples and standards were filtered through 0.2 μ m nylon syringe filters (Phenomenex).

Analytical Reagents

HPLC grade water and methanol were supplied by Fisher Scientific, Loughborough, Leicestershire, UK.

Mobile Phase Preparation

HPLC eluent was prepared using HPLC grade solvents and filtered through 0.45 μ m nylon filters purchased from Alltech, Carnforth, Lancashire, UK, using a Millipore filter apparatus.

Columns

The LC columns used throughout were a Hypersil ODS, 5 μ m, 4.6mm \times 250mm, a Hypersil ODS, 5 μ m, 4.6mm \times 100mm and a Hypersil ODS, 3 μ m, 4.6mm \times 100mm,

all of which were purchased from Jones Chromatography, Hengoed, Mid Glamorgan, UK.

Instrumentation – HPLC

An HP1100 series LC system from Hewlett Packard, Wilmington, DE, USA, was used. This instrument comprises a vacuum degasser unit, quaternary pump, autosampler, thermostatted column compartment and a diode array detector. The data system used to control the instrument and record the data was the Hewlett Packard Chemstation version 04.01.

Instrumentation – MS

As in Chapter 3 the mass spectrometer used was the Finnigan LCQ ion trap. The ESI and APCI interfaces used were also supplied by Finnigan these are described in greater detail in Section 2.5.